DOCTOR OF PHILOSOPHY

Deep soil: investigating carbon sequestration potential and greenhouse gas behaviour in agricultural subsoil

Button, Erik

Award date:
2022

Awarding institution:
Bangor University

DOCTOR OF PHILOSOPHY

Deep soil: investigating carbon sequestration potential and greenhouse gas behaviour in agricultural subsoil

Button, Erik

Award date:
2022

Deep soil: investigating carbon sequestration potential and greenhouse gas behaviour in agricultural subsoil

PRIFYSGOL BANGOR UNIVERSITY

Erik Sebastian Button, 2022

School of Natural Sciences, Bangor University

A thesis submitted to Bangor University in candidature for the Philosophiae degree

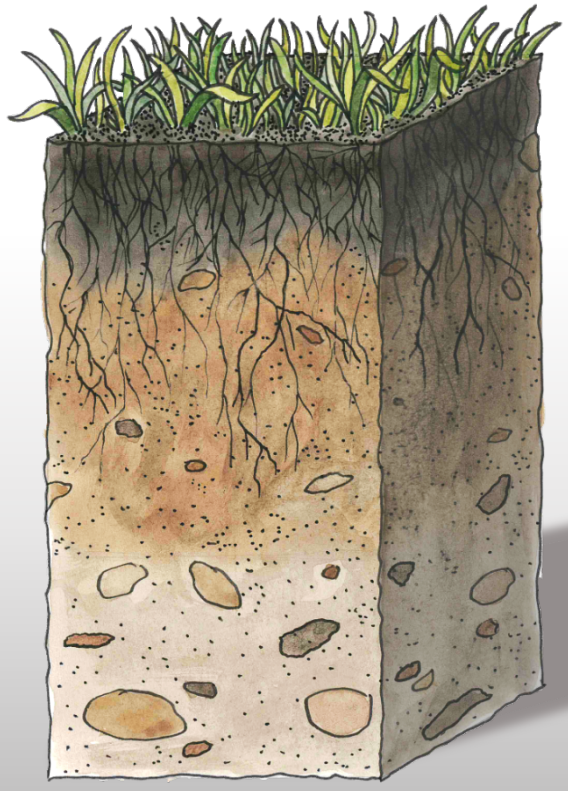

FLEXIS
SMART ENERGY FOR OUR FUTURE
YNNI CALL AR GYFER EIN DYFODOL

UNDEB EWROPEAIDD EUROPEAN UNION
Llywodraeth Cymru Welsh Government
Cronfa Datblygu Rhanbarthol Ewrop
European Regional Development Fund

I hereby declare that this thesis is the result of my own investigations, except where otherwise stated. All other sources are acknowledged by bibliographic references. This work has not previously been accepted in substance for any degree and is not being currently submitted in candidature for any degree unless, as agreed by the University, for approved dual awards.

I confirm that I am submitting this work with the agreement of my supervisors.

Signed	**15th July 2022** Date

Soil profile artwork on front cover created by Erik Button, 2022.

Thesis Summary

The release of carbon (C) emissions into the atmosphere is the primary driver of global climate change. Addressing this is the biggest environmental challenge faced by humankind. To overcome the challenge, a growing focus has been on the largest terrestrial C store, soil, for its ability to sequester further C from the atmosphere. Due to the intensity of agricultural soil management, agricultural soils have a large C deficit that can be filled yielding various co-benefits. The scale and feasibility of enhancing this C sink, however, is much debated. Recently, soil beneath the topsoil (i.e. subsoil) has been proposed as a better potential target than topsoil. This is because the conditions, soil characteristics and low disturbance allows C in agricultural subsoils to reach thousands of years of age. The overall aims of this thesis were to 1) evaluate and investigate subsoil-targeted C sequestration strategies; and 2) investigate the mechanisms underpinning subsoil greenhouse gas (GHG) dynamics (production and consumption) to understand how these impact C sequestration success. Firstly, I conducted an extensive review and meta-analysis of the literature describing mechanisms of subsoil C stabilisation to better evaluate subsoil-targeted C sequestration strategies and explore opportunities and limitations of this field, concluding that the strategies can offer more potential to sequester C in the long-term, but this is highly context dependent. Secondly, a series of laboratory incubations was conducted to test an approach to enhance subsoil C sequestration via the addition of iron to enhance C stabilisation. Despite the reduction in microbial C respiration of specific C forms, bulk soil C was not protected in the soil tested, so the method was not deemed an effective strategy for this soil. Next, a deep rooting grass field trial with or without root excluding mesh buried at different depths was established. Measuring GHGs above and below the mesh and using the concentration gradient method (CGM), more C was respired from root-accessible soil though this made no difference at the soil surface. This suggests that more C is gained than is lost from deeper rooting. To address the second aim, GHGs were measured at different depths across 2 growing seasons. The CGM was tested for gas flux estimation of carbon dioxide (CO_2) to assess the method across different conditions and understand the movement and contribution of the gas to the surface-atmosphere flux. The CGM performed poorly in drought conditions and evidence of depth-dependent GHG consumption was found. Finally, an incubation study in a precision-controlled environment with added $^{15}N_2O$ was conducted to disentangle the biological and physical mechanisms underpinning N_2O production and consumption in soil. The diffusion rates did not differ with depth, but deeper soil consumed more N_2O when drier due to aerobic denitrification, suggesting subsoils have high denitrification potential despite the low microbial biomass. Together, this research provides a valuable contribution to the understanding of the behaviour of C and GHGs in the subsoil environment, which is essential to pursuing subsoil C sequestration – a useful tool for aiding climate change mitigation. Going forward, greater evidence and policy support is required for large-scale adoption of subsoil-targeted C sequestration strategies.

Table of Contents

Acknowledgements

Firstly, I would like to thank my supervisors, Davey Jones and Dave Chadwick for their support and guidance over the years. I've had an unforgettable time at Bangor and am grateful you believed in me and gave me this opportunity all those years ago.

Thanks to Laura Cardenás and all those at North Wyke who welcomed me and supported me with my challenging experiment through the very uncertain times of early 2020. Also, a big thanks to Kara for the many head-scratching meetings figuring out how to solve all the complex pool dilution equations.

A big thank you to the Environment Centre Wales 2nd floor lab group, especially, Lucy, Joe, John, Kara, Miles, Danielle, Megan, Maria, Jeewani and David for your valuable help, advice, and welcome distractions. The many and often lengthy tea breaks and chats sustained me!

Whilst not directly relevant to my PhD, I'd like to thank Jacqueline Hannam and the Soil and Land Use Team at Welsh Government, with whom I had the opportunity to do a 6-month placement during my PhD. It was a hugely insightful and valuable experience that gave me confidence and pride in my experience and insight into different career paths available to me.

The biggest of all thanks must go to you, Lucy. What a journey it's been! With big highs, big lows, and everything in between. We had our very own lockdown office, an unforgettable conference trip to Australia and countless adventures that made my time in Bangor so memorable. You've absolutely made my PhD experience and I can't thank you enough for all your patient support and advice over the years. Here's to a new chapter and many more adventures in New Zealand!

A thanks to all my friends from North Wales and beyond who've offered welcome distractions with chats and outdoor adventures that reset the mind and nourished the soul!

Finally, a huge thank you to my parents, Diana and Norbert, for their everlasting support and for believing in me no matter what I choose to pursue. Thank you for all your listening, patience and engaging with my PhD-related wins and woes. I am so grateful to you both!

Abbreviations

AFPS, ε	Air-filled Pore Space	**GHG(s)**	Greenhouse gas(es)
Al	Aluminium	**M**	Molar
ANOVA	Analysis of Variance	**MBC**	Microbial Biomass Carbon
BD, B_d	Bulk Density	**MRP**	Molybdate Reactive Phosphorus
C	Carbon	**N**	Nitrogen
$CaCO_3$	Calcium carbonate	**N_2**	Nitrogen Molecule
CEC	Cation Exchange Capacity	**NDVI**	Normalized Difference Vegetation Index
CGM	Concentration Gradient Method	**NH_4^+**	Ammonium
CH_4	Methane	**NO_3^-**	Nitrate
CO_2	Carbon Dioxide	**N_2O**	Nitrous Oxide
CM	Chamber Method	**O, O_2**	Oxygen
DOC	Dissolved Organic Carbon	**P**	Phosphorus
DOM	Dissolved Organic Matter	**PLFA**	Phospholipid-derived Fatty Acids
DON	Dissolved Organic Nitrogen	**POM**	Particulate Organic Matter
DW	Dry Weight	**SEM**	Standard Error of the Mean
D_s	Diffusion Coefficient	**SF_6**	Sulphur Hexafluoride
D_s/D_0	Relative Diffusivity	**SIC**	Soil Inorganic Carbon
EC	Electrical Conductivity	**SOC**	Soil Organic Carbon
ECD	Electron Capture Device	**SOM**	Soil Organic Matter
Fe	Iron	**UK**	United Kingdom
FID	Flame Ionisation Detector	**VOC**	Volatile Organic Compound
GC	Gas chromatograph	**WFPS**	Water-filled Pore Space

List of Tables

List of Figures

are oxalate-extractable. See Appendix 1 for the search term strategy, selection criteria, data exclusion and conversion and PRISMA diagram.

Fig. 2.2 Measured soil properties of A (ca. 0-30 cm) and B (ca. 30-100+ cm) horizons of agricultural (Inceptisol, Alfisol, Mollisol, Ultisol and Oxisol) soil profiles, ordered by least to most weathered. Data was collected from studies (N = 188) via a systematic literature search conducted in October 2020. See the Appendix 1 for the search term strategy, selection criteria, data exclusion and conversion and PRISMA diagram. The *n* in the plots refers to the number of soil profile measurements included in the boxplot. Significance at p >0.05 (n.s.); p <0.05 (*); 0.01 (**); and 0.001 (***). Where there is no sign the sample size was too small to perform a test. For more information see Appendix 1. BD is dry bulk density; SOC is soil organic carbon; MBC is microbial biomass-C; CEC is cation exchange capacity; and Fe and Al are oxalate-extractable.

Fig. 2.3 Conceptual diagram of the top- and sub-soil C cycles, demonstrating the major SOM (soil organic matter) inputs (in green boxes); the primary components determining soil OM persistence (in cyan); agricultural management (in grey box); and losses (in orange boxes and teal arrows) in an arable system. POM is particulate organic matter and DOM is dissolved organic matter. Dashed arrows represent mechanisms that depend on certain soil characteristics to occur or that they occur at very low rates. *The specific balance between physical disturbance and OM inputs from agricultural management determines the impact on topsoil OM.

Fig. 2.4 Means (±SEM) of the carbon storage rate in the A and B horizons and the combined A and B horizons (A+B) following different subsoil-targeted C sequestration strategies. The number of studies included (N) is shown in the individual plots and the number of measurements included are in parentheses. Different letters correspond to significant differences between means (p <0.05 Tukey). See Appendix 1 for the search term strategy and specific inclusion criteria. *Transfer of exogenous C is not the same as C sequestration in terms of C removal from the atmosphere. **Infrequent deep ploughing (every >10 years).

Fig. 2.5 Schematic representation of how mineral subsoils (i.e. Mollisol, Alfisol) will likely change in response to different climate change scenarios with potential feedbacks in the C and N cycles. Elevated CO_2 will induce plant growth, deeper rooting and more rhizodeposition in the subsoil. This will promote enhanced subsoil microbial activity and may induce subsoil priming of old SOM. The drying in combination with more microbial activity will stimulate more mesofaunal activity and bioturbation at depth. The greater formation of macropores (represented by the white vertical lines extending from the soil surface into the soil) due to greater topsoil drying will promote greater gas exchange and aeration of the subsoil. This will reduce the plant available water wet zone in the soil. Elevated CO_2 in combination with freshwater waterlogging will decrease C turnover and force mesofauna closer to the soil surface. The dashed lines are dependent on water availability, which are in low supply during droughts. This model assumes there are no constraints to deep rooting (e.g. due to excess acidity, salinity or compaction).

Fig. 3.1 Cumulative soil CO_2 efflux from top- and subsoil (mean ± SEM) incubations (n = 4) over 45 days with the addition of different rates of Fe(III) or Fe(II). Values correspond to the g dry weight equivalent. Note different y-axis range for Fe(III) and Fe(II).

Fig. 3.2 Effect of the addition of different rates of Fe(III) or Fe(II) on soil water chemistry: (a) dissolved organic carbon (DOC), (b) soil pH, and (c) electrical conductivity (EC) and molybdate reactive phosphorus (MRP) from top- and subsoil over 45 days (mean ± SEM, *n* = 4). The highest Fe(II) rate is not displayed in panel (d) as the concentrations exceeded detectable limits of the methodology used. Values correspond to the g dry weight equivalent. Note different y-axis range for Fe(III) and Fe(II).

Fig. 3.3 Cumulative ^{14}C-CO_2 evolved after the addition of ^{14}C-labelled a) glucose, b) citrate, and c) *Zea mays* shoot residues incubated in top- and subsoil with different added rates of Fe(III) or Fe(II). Values are mean ± SEM (*n* = 4). Incubations were 72 h for a) and b), while c) was incubated for 336 h, before the soil was extracted.

Fig. 4.1 Schematic 3D diagram of an example plot (40 cm mesh) used in this study. Plots with a buried mesh at 20, 40 or 60 cm have gas pipes at 10 cm above and below the

mesh depth. The control plots (no mesh) have gas pipes at all depths (i.e. 10, 30, 50 and 70 cm). The buried end 50 cm of the gas pipes have holes in them for soil air sampling of the centre of the plot. All plots have surface gas sampling chambers on the top of plots and liners on the walls surrounding the plots. The dimensions of the plots were not all exactly 200 x 200 cm. Diagram not to scale.

Fig. 4.2 a) Daily average air and soil temperature, b) hourly barometric pressure, and c) average volumetric soil water content (θ) and total daily rainfall for the experimental period 1st Jan – 31st Dec 2021. N.B the weather station was not operational from the 1st Jan – 23rd March due to a technical issue.

Fig. 4.3 Mean (± SEM) aboveground fresh biomass in plots (*n* = 4) with root-excluding mesh installed at 20, 40, 60 cm or without mesh (No mesh) at different harvesting times in 2021 and 2022. N.B. the grass was wet in the August harvest resulting in higher biomass.

Fig. 4.4 Mean (± SEM) cumulative surface a) CO_2 and b) N_2O fluxes from deep rooting grass plots (*n* = 4) with or without root-excluding mesh buried at 20, 40, 60 cm depths.

Fig. 4.5 Depth profiles of mean (± SEM) gas concentrations of a) CO_2 and b) N_2O from biweekly sampling of gas collectors installed at different soil depths (*n* = 4) between April and September 2021. Colours reflect the depth or absence of a buried root-excluding mesh.

Fig. 4.6 The CGM modelled versus the chamber measured surface a) CO_2 and b) N_2O flux between April and September 2021. The straight lines are the x = y and the dashed lines are the linear fit of the data. The equation, R^2 and *p* values correspond to the fitted line of the data.

Fig. 4.7 Soil CO_2 fluxes modelled by the CGM from soil at 30, 50 and 70 cm with or without root access. In plots with no root access ('-Roots'), the gas sampling pipes were 10 cm below a root-excluding mesh installed at either 20, 40 or 60 cm. There was no mesh present in the '+Roots' plots that could limit rooting access. Asterisks represent statistical difference between soil CO_2 with root access status at $p < 0.001$ (***); $p < 0.01$ (**); $p < 0.05$ (*) and $p > 0.05$ (-).

Fig. 5.1 Daily average a) air and soil temperature; b) total daily precipitation and average volumetric water content (θ); c) estimated diffusivity of SF_6 through the soil of different depths; and d) mean (± SEM) crop height (*n* = 10) and NDVI (*n* = 4) during the 2018 and 2019 growing seasons (1st May – 20th Sep). Colours reflect different measurement depths. The vertical dotted lines are the dates when ammonium nitrate fertilizer was applied in 2019, where 40 kg ha^{-1} was applied on the 7th May and 110 kg ha^{-1} on the 30th May.

Fig. 5.2 Depth profiles of mean (± SEM) gas concentrations of a) CO_2; b) N_2O; and c) CH_4 from weekly sampling of gas collectors installed at different soil depths (*n* = 8) in a field under maize in 2018 (22 Jun 2018 – 19 Sep 2018; *N* = 644) and wheat in 2019 (22 May 2019 – 5 Sep 2019; *N* = 533). Colours reflect different sampling depths. Solid and dotted lines represent the maize and wheat, respectively. The 'X' at 0 cm depth represents the approximate ambient levels of the respective gases (CO_2, 420 ppm; N_2O, 330 ppb; CH_4, 1.85 ppm, respectively). The curves were forced to intercept the x-axis (0 cm) at the aforementioned concentrations.

Fig. 5.3 The a) mean (± SEM) CO_2 concentrations from the gas collectors installed at different depths (*n* = 8); b) measured (CM) and modelled estimates (GM) of CO_2 fluxes (mean ± SEM) at different depths in the soil profile (*n* = 8); and c) cumulative CO_2 flux of the mean measured and estimated fluxes from different depths. 'CM Surface Daily' is the mean 24 h surface CO_2 flux, while 'CM Surface' is the mean surface flux between 1000 and 1300 h - the same sampling times and days as for the gas collector sampling. The 3 sampling times in 2019 (7th, 14th and 19th Aug) in b) had no surface CO_2 flux measurements, so these were estimated from 58 CO_2 flux sampling points before and after the missing dates via the best fit (exponential; R^2 = 0.76).

Fig. 5.4 The mean surface measured (CM) versus modelled (GM) CO_2 flux (± SEM) in a field under maize (*n* = 12) or wheat (*n* = 16) production. The grey symbols points represent the raw data while the transparent dashed line is the linear correlation for maize ($y = 0.62x$, $R^2 = 0.10$) and the transparent dotted line is the corresponding correlation for wheat ($y = 1.02x$, $R^2 = 0.46$). The trend lines are forced through 0 at the y-intercept. The solid line is the 1:1 line ($y = x$).

Fig 5.5 Net fluxes (means ± SEM) of CO_2, CH_4, and N_2O of destructively sampled (n = 4) soil of different depths incubated for 72 h with added headspace gas concentrations: Ambient (490 ppm CO_2; 2 ppm CH_4; 310 ppb of N_2O) and High (2800 ppm CO_2; 32 ppm CH_4; 5500 ppb N_2O). Different letters indicate significant differences between the gas concentrations of the soil depths and headspace concentrations for each GHG at p <0.05 (Tukey). Positive values indicate production and negative values indicate consumption.

Fig. 6.1 The dual-headspace system used for incubating the soil cores in this study. The system can be placed in 2 different modes, 'flush' and 'flow over'. The former is where air flow from the gas cylinders is directed to enter via the headspace below the core, while the latter directs this air via the headspace above the soil core. Specific dimensions and materials can be found in the Appendix 5 (S1).

Fig. 6.2 The fluxes of SF_6 (means ± SEM) from the small versus the large headspace from the 0-10 and 50-60 cm soil depths at 50 and 70% WFPS (n = 6). The dashed line represents the best fit for the flux data (R^2 = 0.96; y = 1.26x – 0.29) and the solid line represents the y = x. The axes are logarithmic.

Fig. 6.3 The mean (± SEM) relative diffusivity (D_s/D_0) of intact top- and subsoil cores at 2 different levels of air-filled pore space (ε; cm^3 cm^{-3}). Different letters represent statistical difference of means between soil depths (upper-case) and between soil depth and WFPS (lower-case) at p <0.05. Asterisks represent statistical difference in overall WFPS means at p <0.001 (***); p <0.01 (**); p <0.05 (*) and p >0.05 (-).

Fig. 6.4 Gross N_2O emission a); gross N_2O uptake b); Net N_2O emission c); and the ratio between the net and gross N_2O emission d) (means ± SEM; n = 6) in intact 0-10 and 50-60 cm soil cores at 50 and 70% WFPS. Measured by the ^{15}N-N_2O pool dilution method. Different letters represent statistical difference of means between soil depths (upper-case) and between soil depth and WFPS (lower-case) at p < 0.05. Asterisks represent statistical difference in overall WFPS means at p <0.001 (***); p <0.01 (**); p <0.05 (*) and p >0.05 (-).

Chapter 1

Introduction

1.1 Soil carbon

Carbon (C) is the 4th most abundant element in the universe. It is the primary component of biological compounds in organic form and in many minerals in inorganic form. These various C forms are exchanged between three main planetary reservoirs, the oceanic, atmospheric, and terrestrial. This biogeochemical cycling, the global C cycle, is vital to all life on the planet (Canadell et al., 2022; Friedlingstein et al., 2019). The cycle is a closed system meaning that the amount of C does not change, but the location of the C in different reservoirs does. Importantly, the amount of C that is released into the atmosphere is predominantly in balance with that taken up by sinks under natural circumstances (Canadell et al., 2022). However, since the onset of fossil fuel burning for energy during the Industrial Revolution (ca. 1760), this cycle has started to become unbalanced by more C entering and remaining in the atmosphere than is naturally cycled (Fig. 1.1; Friedlingstein et al., 2019). A build-up of greenhouse gases (GHGs) in the atmosphere over more than 260 years of this burning has enhanced the 'greenhouse effect' which is warming and destabilising the climate. This is causing greatest environmental threat to the planet experienced in human history (Canadell et al., 2022).

Understanding the global C cycle is key to understanding and addressing climate change. This is because small relative changes in C reservoirs can have large impacts on GHG emissions and the balancing of the C cycle (Köchy et al., 2015). The oceans are the greatest C reservoirs on the planet and, together with global vegetation, the biggest sinks of atmospheric C (Fig.1.1). The increase of C in the atmosphere has enhanced the strength of these sinks in response, though their future growth is uncertain (Huntzinger et al., 2017; McKinley et al., 2017), with the saturation of sinks possible (Le Quéré et al., 2007). On land, however, soil is the largest C reservoir, greater than the atmospheric and vegetation reservoirs combined (Fig. 1.1; Canadell et al., 2022; Friedlingstein et al., 2019). Not only is soil a valuable C reservoir, but they also provide us with over 94% of our food (FAO, 2022) and other vital ecosystem services, such as biodiversity, water regulation and nutrient cycling (Jónsson and Davídsdóttir, 2016), for which soil C is crucial (Milne et al., 2015). While soil is naturally formed, it is considered non-renewable over human timescales due to slow rates of formation, high rates of soil loss and high demands on the resource (Lal, 2009). As such, the fate of our species is contingent on how we manage this crucial resource (Amundson et al., 2015).

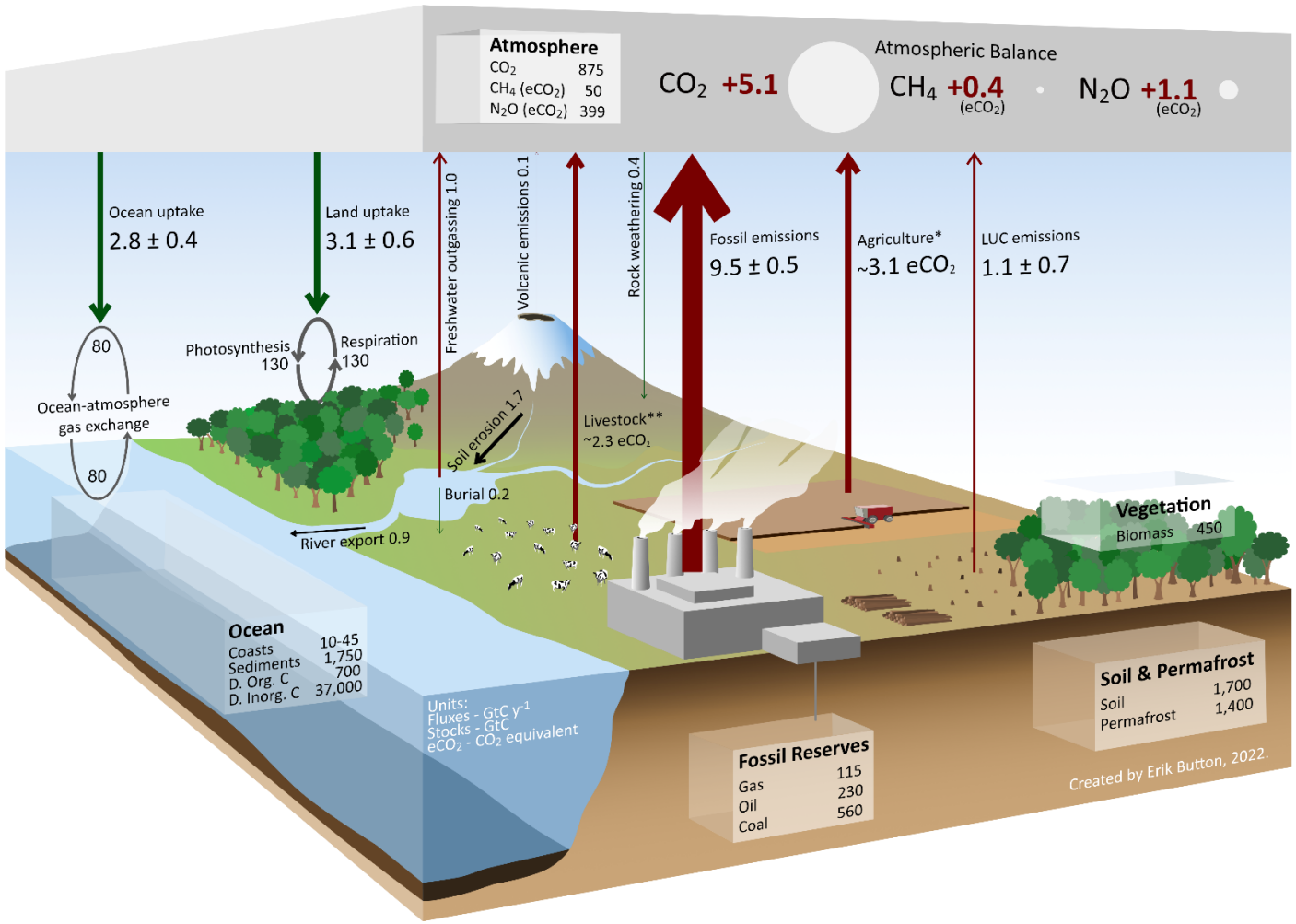

Fig. 1.1 Schematic diagram of the global soil C cycle with inclusion of agriculture-related CO_2 equivalent fluxes (Gt eCO_2-C y^{-1}) and atmospheric balances. Data from Canadell et al. (2022). Arrow width is relative to magnitude of flux. Values are estimates. LUC is land use change; D. Org. C and D. Inorg. C are dissolved organic and inorganic C, respectively. *refers to N_2O emissions from agricultural land, including rice cultivation. **refers to CH_4 emissions from livestock rearing.

As soil C is gaining recognition for its importance in the environment, food security, and the climate, interest from both the public and scientific communities grows (Fig. 1.2). Soil C is present in the soil as soil organic C (SOC) and soil inorganic C (SIC). It is estimated that

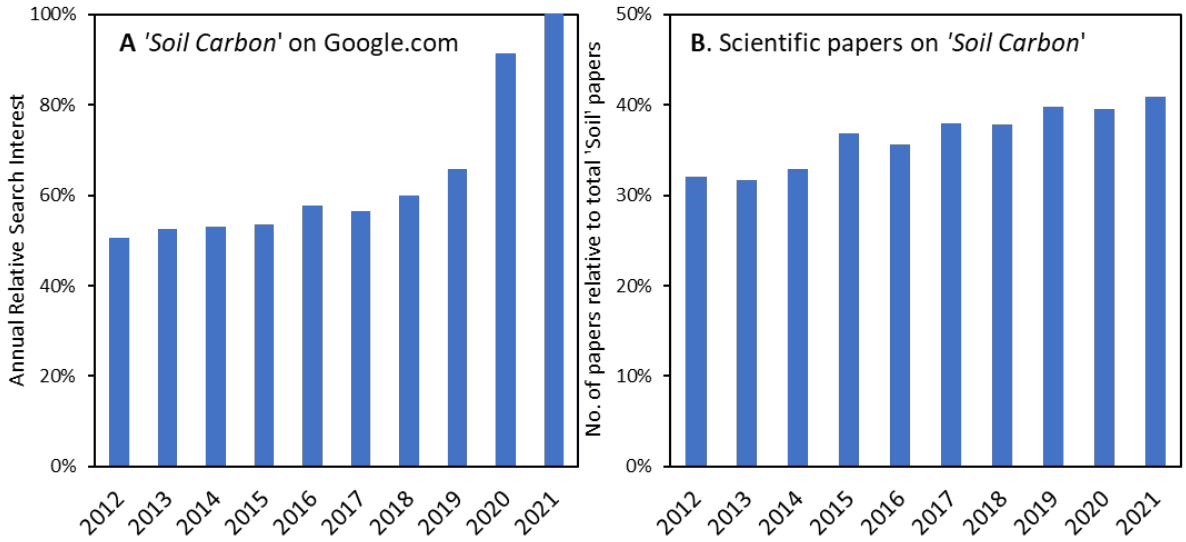

Fig. 1.2 A) 'Soil carbon' annual search interest (relative to year with the highest searches for the period; from trends.google.com) and B) the proportion of papers published in the Soil Science category under 'Soil' (*N* = 50,937; data from webofscience.com) containing 'Soil Carbon' search terms (*N* = 18,786) since 2012.

the SOC stock in the upper meter of soil ranges between 1450-1550 Gt C and the SIC stock between 700-750 Gt C (Batjes, 1996), the majority of which is present underneath the topsoil (A horizon, ca. 0-30 cm; Jobbágy and Jackson, 2000). The balance between the forms of C in the soil depends on the ecosystem, where forest soil C can be close to 100% SOC and desert soil C can be >80% SIC across the whole soil profile (Wang et al., 2010). It is SOC, however, that is present in all soils; the most important form for providing soil services (Milne et al., 2015); and the more susceptible to loss and degradation (Sanderman, 2012; Sanderman et al., 2017).

While SOC in topsoil turns over at a fast rate (Salomé et al., 2010), SOC in deep soil is much older (Schöning and Kögel-Knabner, 2006; Shi et al., 2020; Torn et al., 1997). Though the study of subsoils is developing, gaps in the knowledge of the mechanisms, behaviour and dynamics of subsoil C remain (Bernal et al., 2016; Inagaki et al., 2020; Stockmann et al., 2013). This is not helped by a recent trend of shallower sampling (Yost and Hartemink, 2020), likely due to the extra samples or challenges of deeper soil study. Nevertheless, the old age of deep

soil C is thought to be due to the oligotrophic conditions; low microbial biomass and access to C substrates (Dove et al., 2020; Salomé et al., 2010); higher relative abundance of reactive surfaces for C stabilisation (Rumpel and Kögel-Knabner, 2011); and lower disturbance (Lal et al., 2015) in deeper soils. Even in managed agricultural (crop- and grassland) soils, which cover 38% of global land area (FAO, 2020), SOC can reach thousands of years in age in deeper layers (30-100 cm; Shi et al., 2020). However, agricultural topsoils have lost an estimated 133 Gt C due to agricultural management practices over the last 2 centuries (Sanderman et al., 2017). Loss of SOC leads to the release of GHGs and impairs the ability of soils to provide ecosystem services, which we rely on (Don et al., 2011; Tsiafouli et al., 2015). Yet, an opportunity to restore and even enhance the long-term storage of C in agricultural soils with atmospheric C exists (Lal et al., 2015), which can contribute to offsetting agricultural and fossil fuel GHG emissions (Fig. 1.1).

1.2 Carbon sequestration

By adapting agricultural management practices, it is thought possible for atmospheric C to be incorporated into agricultural soil for long-term storage (i.e. soil C sequestration; Lal, 2004a; Lal et al., 2015; Lorenz et al., 2007; Minasny et al., 2017; Powlson et al., 2011). The most popular of current methods for achieving this are the reduction of tillage intensity, use of cover crops, agroforestry, biochar application and other similar methods (Das et al., 2014; Fornara et al., 2018; Hübner et al., 2021; Lugato et al., 2014; Mondal et al., 2020; Rodrigues et al., 2021). Some of these practices form the basis for conservation and regenerative agriculture. Conservation agriculture is an established farming system based on the principles of minimising soil disturbance (i.e. reduced/no tillage), maintaining permanent soil cover and rotating crops (Hobbs et al., 2008). While regenerative agriculture lacks a scientific definition, it is generally based on soil conservation as the starting point for the contribution to and regeneration of ecosystem services to enhance the environmental, social and economic aspects of sustainable food production (Schreefel et al., 2020). It is believed that these systems will play an increasingly important role in meeting the higher demands for food in the future and sequestering more C in the soil (Giller et al., 2021; Hobbs et al., 2008; Schreefel et al., 2020). However, accurate quantification of realistic sequestration rates is currently difficult and estimations vary greatly (Chen et al., 2018; Minasny et al., 2017; Zomer et al.,

2017). However, this strategy for climate change mitigation has received substantial public and scientific attention, especially since the announcement of the COP21 '4 per mille' initiative in 2015 (www.4p1000.org). This initiative aims to encourage the sequestration of 4‰ (i.e. 0.4%) of additional C per year, which can completely offset anthropogenic C emissions (relative to 2015 levels). Whether this rate is possible is hotly debated in the scientific community (Baveye et al., 2018; de Vries, 2018; Minasny et al., 2017; Poulton et al., 2018), but is generally agreed to be an aspirational target to aim for. While the initiative is a bold and positive step in the right direction that should be supported by the public, policy and scientists, it has also highlighted the importance for the scientific community to be clear and consistent with the meaning and context of C sequestration to maximise its uptake and success.

As is evident from the scale of the issue in figure 1.1, fossil fuel emissions are central to driving climate imbalance and reducing these are fundamental to climate change mitigation. Therefore, directly or indirectly framing soil C sequestration as the 'solution' to the climate crisis is dangerous as it may hamper efforts to address the root of the cause - reducing fossil fuel emissions. This is especially important as soil is a relatively small sink with finite capacity compared to the large oceanic C sink (Fig. 1.1; Lal, 2004b). Soil C sequestration can, however, complement the necessary shift towards a low or carbon neutral society with multiple co-benefits (Baker et al., 2020; Sykes et al., 2020).

It is also crucial to emphasize that C sequestration is *not* a one-way process. C sequestered can rapidly be lost to the atmosphere nullifying any climate or soil function benefits, if management practices change (Smith, 2008). This loss is more likely to occur in topsoils where C turnover is higher due to decomposition favouring conditions and greater microbial activity and biomass (Salomé et al., 2010). As a result, there has been a growing interest in the potential of targeting deeper soil for C sequestration, where the inherent characteristics are thought to be concomitant with long-term C storage (Chabbi et al., 2009; Chen et al., 2018; Kautz et al., 2013). Examples of these are, infrequent deep inversion tillage (Alcántara et al., 2016; Schiedung et al., 2019), deep rooting crops (Kell, 2011; Lynch and Wojciechowski, 2015) and burial or injection of various products (e.g. mineral or clay; Churchman et al., 2014; Porras et al., 2018). Evaluation and experimental evidence of current

and emerging subsoil-targeted C sequestration strategies are lacking. These gaps need to be addressed to assess the potential of pursuing deep soil C sequestration.

1.3 Greenhouse gases

The behaviour and fate of CO_2 and other GHGs (CH_4 and N_2O) play an important role in the success of C sequestration and global GHG budgeting (Almaraz et al., 2020; Blagodatsky and Smith, 2012; Boyer et al., 2006). If a sequestration approach induces the release of substantial GHGs, then any C gained could be outweighed by the release of CO_2 or other more powerful GHGs. This is especially important in the case of subsoils, where CO_2 and N_2O concentrations increase with depth (Fig. 1.3; Davidson et al., 2004; Dong et al., 2013; Wang et al., 2018). If disturbed, this reservoir of gas can quickly diffuse to the soil surface (Mencuccini and Hölttä, 2010). Though how large this affect is largely unknown.

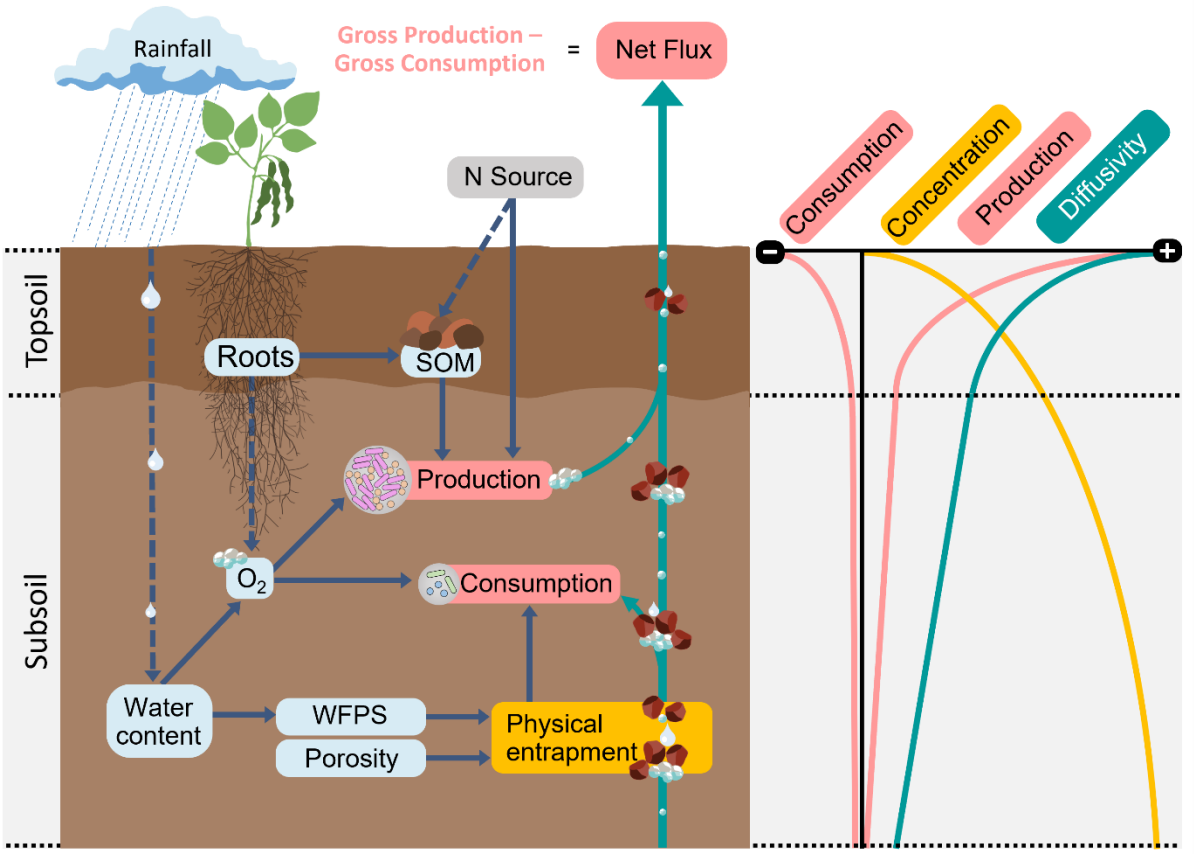

Fig. 1.3 Schematic diagram of the mechanisms and soil properties underpinning N_2O behaviour and fate in an agricultural soil. An increased soil water content from percolating

rainwater increases water-filled pore space which decreases the O_2 content of the soil and increases the physical entrapment of gas in the soil by restricting diffusivity. This is the primary reason for the observed high concentrations of N_2O at depth, despite low N_2O production at depth. N_2O production and consumption rely on anaerobic conditions which can occur in microsites even when the soil is freely draining. Root respiration and microbial respiration of root products can cause local O_2 depletion. Fertiliser application increases N supply and the production of N_2O. All these processes impact the net flux, which is a balance between the gross production and consumption rates of N_2O. The lines in the panel on the right demonstrate the expected trends of these major processes with depth. Dashed lines represent transient or dependent effects.

It is of particular importance to limit the emission of the GHG, N_2O, as it depletes ozone and has a global warming potential almost 300 times that of CO_2. Agriculture is the greatest source of N_2O, contributing significantly to atmospheric imbalance (Fig. 1.1). As such, understanding the fate and behaviour of this gas in the soil profile is of great importance when considering subsoil targeted C sequestration strategies. The behaviour of this gas is more complex than CO_2 as it is dependent on several factors and can be both microbially produced and consumed in the soil profile (Fig. 1.3; Clough et al., 2005), the balance of which determine the surface-atmosphere flux.

While the study of N_2O has been extensive, focus has predominantly been on surface-atmosphere gas exchange, via chamber (Oertel et al., 2016; Vangeli et al., 2022) and eddy-covariance methods (Baldocchi, 2003; Rachael M. Murphy et al., 2022). While of great use, these methods do not gain insight into the dynamics and processes underpinning GHGs at depth (Wang et al., 2018). This is in part due to the difficulty of measuring fluxes *in situ* and the challenge of disentangling physical and biological processes that can occur simultaneously (Fig. 1.3; Wen et al., 2016). Other techniques, including the concentration gradient method (CGM) and isotope enrichment have allowed progress at different spatial and temporal ranges (Clough et al., 2006; Maier and Schack-Kirchner, 2014; von Fischer and Hedin, 2002; Yang and Silver, 2016). Yet, further testing and validation of these are necessary to understand the limitations and application for accurate GHGs budgeting and ensuring successful subsoil C sequestration strategies.

1.4 Methodological approaches

To investigate scientific questions, different repeatable measurement and analysis methods are required. Common methods differ in their application, cost, reliability, and scope, among other factors. Therefore, choosing an appropriate method requires consideration of their individual advantages and disadvantages.

1.4.1 Gas flux measurement methods

Various methods to quantify the gas exchange between the soil surface and the atmosphere exist. The most important field methods in the context of GHG soil-atmosphere gas exchange are the chamber, eddy covariance and concentration gradient methods (as suggested by Maier and Schack-Kirchner, 2014). The advantages and disadvantages of these are summarised in Table 1.2.

Chamber methods

The static (closed, non-flow-through, steady-state) open-bottom chamber method is the most common technique for measuring soil-atmosphere fluxes and has been in use for 95 years (Lundegårdh, 1927). Chambers placed over the soil are temporarily sealed creating a closed headspace that is sampled over time by chemically trapping gas or taking gas samples (Charteris et al., 2020) or using automated closure and direct measurement of the headspaces gas concentration in the field (Grace et al., 2020; Marsden et al., 2019). Another version of this method is with dynamic (flow-through, non-steady-state) chambers (Maier et al., 2022). These have a known flow of air in and out of a soil chamber headspace, where the flow rate and the difference in concentration between the in and out flow of gas is used to calculate the flux. These chambers are part of automated systems which can produce higher temporal resolution data with less labour, but are more expensive, are limited by number of chambers and need skilled operation and maintenance (Yu et al., 2013).

The reason for the popularity of the static chamber approach for GHG measurements is due to its low cost, ease of use and local and versatile applicability. Due to the prolific use of chambers, an extensive database exists that can be used for comparison of various gas fluxes in different contexts (e.g. Jian et al., 2021). The greatest consequence of the chamber method, however, is that it affects the microclimate (temperature, soil moisture, pressure) and physical characteristics (gas transport; rainfall, litter fall and wind exclusion or modification) of the chamber environment. This can cause over- and underestimates of soil

fluxes (Chaichana et al., 2018; Maier and Schack-Kirchner, 2014; Rochette et al., 1992), though reliably validating this is a challenge (Yu et al., 2013). In addition, due to the heterogeneity of soil fluxes, extrapolation of gas exchange from a few chambers to greater areas can introduce large error and a high number of chambers may be needed to best represent the field.

Eddy covariance method

A method that avoids the aforementioned chamber-related problems, is the eddy covariance method. This is an atmospheric micrometeorological measurement technique which can produce net gas exchange measurements across soil/canopy-atmosphere interfaces by interpreting the covariance between wind velocity and scalar concentration fluctuations (Baldocchi, 2003). As fluxes are averaged over time, sampling error can be relatively low (Baldocchi, 2003). Automated eddy covariance towers are best used for longer-term ecosystem scale studies (e.g. Cowan et al., 2020), as spatial heterogeneity is integrated. However, this method is limited by requiring flat land and no/low wind velocities for best results. Nevertheless, agreement between eddy covariance and closed chamber GHG measurements has generally been observed to be very good for N_2O (Murphy et al., 2022a, 2022b); good for CO_2 (Balogh et al., 2007; Reth et al., 2005; Riederer et al., 2014), and adequate for CH_4 (Chaichana et al., 2018; Yu et al., 2013). However, the challenging issue of knowing which method is more accurate when they do not agree remains (Yu et al., 2013).

Concentration gradient method

The concentration gradient method (CGM) calculates fluxes based on the gradient of soil concentrations and the effective gas diffusivity in soil, assuming molecular diffusion is the dominant transport of gas in soil (Jong and Schappert, 1972; Maier and Schack-Kirchner, 2014). Compared to the chamber and eddy covariance methods, which only measure soil-atmosphere fluxes, the CGM can gain additional information regarding the production and consumption of GHGs in the soil profile. In addition, the method avoids chamber-related effects by use of various soil profile gas sampling approaches (see examples in Maier and Schack-Kirchner, 2014). As a result of this and recent technological advances, this method has been gaining attention and been applied in various gas exchange studies (Maier and Schack-Kirchner, 2014).

By extrapolating the fluxes at depths to the soil surface, the CGM can produce good

estimates of soil-atmosphere gas exchange, as validated by chamber based measurements (Li and Kelliher, 2005; Maier and Schack-Kirchner, 2014; Wang et al., 2018; Xiao et al., 2015). The accuracy of the CGM estimates are, however, largely determined by the soil diffusion coefficient (D_s), which is often modelled and rarely measured (Li and Kelliher, 2005). In general, the CGM is most successful when i) the D_s is measured (methods described by Allaire et al. 2008); ii) data input is at high temporal resolution; and iii) it is used for CO_2, in particular. This is because CO_2 uptake processes are negligible, compared to N_2O and CH_4 where consumption and oxidation processes occur heterogeneously throughout the soil profile (Maier and Schack-Kirchner, 2014). Continuous assessment of the CGM is important to identify its strengths and limitations in different climates, vegetation and soil types and depths.

Table 1.1 Summary of the advantages and disadvantages of chamber, eddy covariance and concentration gradient methods for soil-atmosphere gas flux calculation.

Method	Advantages	Disadvantages
Chamber	• Low cost and easy to use in a range of conditions and areas. • Lots of studies to compare results with. • Can be measured continuously (i.e. automated system)	• Local chamber effects can bias data (e.g. temperature, moisture, pressure, air movement) • Measurements are localised and may not accurately represent the fluxes from a larger area. • High variation due to spatial heterogeneity in soil gas fluxes.
Eddy covariance	• Range of timescales possible (hours to years). • Ecosystem scale measurements. • Ideal for building long-term datasets. • Avoids issues of spatial heterogeneity and chamber effects. • Useful for model validation. • Low random sampling error.	• Expensive. • Exact location of the source of fluxes cannot be determined. • Measurements yield a mean meaning homogeneity is assumed. • Requires reliable power source. • Best results with atmospheric-steady conditions. • Can require gap filling when flux measurements drop out.

		• Most applicable on flat and homogenous land. • Poor results in low wind.
Concentration gradient	• Low cost and easy to use in a range of conditions and areas. • Provides insight into subsurface processes and dynamics. • Can be measured continuously. • Avoids chamber effects.	• Does not work as well for N_2O and CH_4 due to consumptive processes. • Dependent on accurate measurement or modelling of D_s. • Best to validate against surface measurements. • Can cause soil disturbance at depth.

1.4.2 Isotope tracing

Stable and radioactive isotopes are extremely useful tools for tracing the fate of a particular compound in a complex system with high degrees of accuracy and specificity. For example, using C isotopes can gain valuable insight into C cycling processes and can be used as constraints for C models (Torn et al., 2002). Tracing can be done with radioactive or stable isotopes; the advantages and disadvantages of which are summarised in Table 1.2. Depending on the isotopes, radio and stable isotopes can be used simultaneously.

Stable isotopes

Stable isotopes have been used extensively to trace compounds since first being applied in soils around 80 years ago. The most popular stable isotopes for studying C and N related soil and greenhouse gases processes are ^{12}C, ^{13}C, ^{14}N, ^{15}N, ^{16}O and ^{18}O (Zhu et al., 2019), with ^{15}N most popular (International Atomic Energy Agency, 2001). Light element stable isotopes (e.g. H, C, N, O, S) are most commonly measured by isotope ratio mass spectrometry, which passes a gas containing the isotopes through a strong magnetic field that deflects the isotopes depending on their mass and records them (International Atomic Energy Agency, 2001). This method is highly precise and so can also be used for natural abundance

analysis, but is expensive, requires high operator skill and reliable power source as it runs continuously. The advantages and disadvantages of stable isotopes is summarised in table 1.2.

The original assumptions in stable isotope studies were that the isotopic composition of an element does not change and that the behaviour of light and heavy isotopes in reactions is the same (Xing et al., 1997). However, it was later discovered that these are not true, with variation in natural abundance of elemental isotopes and differences in the behaviours of light and heavy isotopes in reactions observed (Xing et al., 1997), which resulted in the development of different isotope study approaches. The main approaches of stable isotope use are natural abundance and enrichment studies.

The variation in natural abundance of an isotope relies on isotopic fractionation, which is caused by the biological, chemical or physical preference for the light (e.g. ^{14}N) over the heavy isotope (^{15}N) in a reaction (Werth and Kuzyakov, 2010). This means that reaction products will be enriched in the lighter isotope and the reaction substrate will be enriched in the heavy isotope. The deviation of the heavy isotope abundance from that of the respective isotope standard is expressed as a ratio using the ∂-notation. The established standards are Pee Dee Belemnite for C, atmospheric N_2 for N and Standard Mean Ocean Water for O (Zhu et al., 2019). Natural abundance studies allow for quantification of C and N balances and cycling processes (Werth and Kuzyakov, 2010). For example, due to the differential use of isotopes in C_3 and C_4 photosynthesis, the contribution of plant-derived C to bulk soil C can be traced (Rasse et al., 2006).

Isotope pool dilution is an isotope enrichment method by which heavy isotope-enriched compounds are added to a solid, gas or liquid volume and the dilution of the enriched isotope pool is measured via the flux of unlabelled compound into the pool. Initially, this method was used in solid phases (Davidson et al., 1991), but has since been applied to the study of CH_4 (von Fischer and Hedin, 2002) and N_2O (Wen et al., 2016; Yang et al., 2011) gases. The latter being developed to address a need for better N_2O consumption methodologies (Almaraz et al., 2020; Groffman et al., 2006). Being able to trace different molecules, this method is thought to gain more insight into the processes occurring in the soil (Yang et al., 2011). However, its accuracy has been questioned, as N_2O produced and consumed within microsites would not interact with the pool and, therefore, N_2O

consumption would be underestimated by this method (Well and Butterbach-Bahl, 2013). However, as concluded by Almaraz et al. (2020), the ^{15}N-N_2O pool dilution method does not capture all N_2, but is the only method that can measure N_2O uptake and emission and be used with undisturbed soil that can be applied to the field.

Radioactive isotopes

Radioactive isotopes behave in the same way as their stable counterparts, but have certain advantages over stable isotopes (International Atomic Energy Agency, 2001), summarised in table 1.2. The practicality and use of individual radioisotopes depend on the half-life, mode (α-, β-, γ-decay) and energy of decay. The radioisotope of C, ^{14}C, is the most used radioisotope in environmental science due to its study relevance and the safety and practicality of its long half-life of 5,730 years. The principle of measurement is the same as for the stable isotope pool dilution method, whereby the radioactively labelled compound that is added to a system is the equivalent of the enriched stable isotope. However, radioactive isotope analysis is faster. Radioisotope particles are chemically trapped in alkaline solution and measured by liquid scintillation counting which quantifies scintillations (emitted light flashes) from the reaction of released isotope β-particles and chemiluminescent reactive organic solvents. This method has recently been criticised for underestimating ^{14}C radioactivity, as the chemically trapped ^{14}C-CO_2 was found to be outgassed by the certain organic scintillation solvent (Boos et al., 2022). They suggest more efficient solvents (e.g. Optiphase HiSafe 3) and recommend molarity, volume and base saturation (1 M, ≥ 1 ml, 50%; respectively) of alkaline solution for the best results.

Most common radioactive isotope studies in soil involve the addition of ^{14}C-labelled compounds and the consequent measurement of ^{14}C-CO_2 microbial respiration. This approach allows for the measurement and partitioning of microbial metabolism of organic C into both growth and respiration pathways (Jones et al., 2019). This is important to understand the mechanisms underpinning the fate of C that is added to the soil. Another application of radioisotope study is to use the natural decay of the radioactive isotope to determine the age of an element, as done for estimating the centurial to millennial age of C in the soil by Shi et al. (2020).

Table 1.2 Summary of the advantages and disadvantages of radio and stable isotopes for tracing studies.

Isotope	Advantages	Disadvantages
Stable	• Can be studied without tracer (i.e. natural abundance studies). • Multiple stable isotopes exist for most elements. • Can remain in system indefinitely.	• Expensive, technical, and slow analysis. • Requires quantification of natural abundance and fractionation pools.
Radio	• Easily traced • Analysis time is rapid, approximately 1 min sample^{-1}. • Studies can be short (<1 week).	• Exposure to radioisotopes can have health risks. • Strict guidelines must be observed when working with radioisotopes. • Many elements of interest* do not have practical radioactive isotopes. • Purchasing radioisotopes can be expensive as they require nuclear reactors for production.

*to common C-related soil studies.

1.5 Conclusions

C and its sequestration in soil has been studied extensively, but focus has predominantly been on topsoils. Yet, there is reason to believe that C sequestration efforts are better targeted to deeper soil layers. While the importance of studying deeper soil is being recognised, knowledge gaps need to be addressed to unlock the potential of subsoil C sequestration. In addition, C sequestration studies must consider GHG emissions as these can counteract any C gains made. The following experimental work addresses the key knowledge gaps identified through this review:

- Soil C sequestration strategies that target topsoils have been well documented and while subsoil specific strategies exist, they have not been evaluated or compared. This is needed to determine the methods that have potential and to understand how and which soil types they are best applied to for maximum sequestration success. Therefore, Chapter 2, aims to assess emerging subsoil-targeted strategies in the context of the subsoil C sources, mechanisms of stabilisation and soil via a systematic search of the literature.

- Many of the subsoil-targeted C sequestration strategies are based on theory, *ex situ* evidence and/or are highly context dependent. Therefore, further insight and evidence of their mechanisms and outcomes are needed to build the full picture of this approach to C sequestration. Chapters 3 and 4, assess the C sequestration potential of 2 emerging subsoil-specific strategies from novel perspectives.
- The behaviour and fate of GHGs in the soil are not fully understood. In the context of deep C sequestration, understanding how disturbance of the subsoil may impact these is essential for sequestration success. The CGM is a valuable tool for doing this, which also requires further validation. Chapters 4 and 5 aim to test the CGM in a variety of contexts and gain insight into the behaviour and dynamics of subsoil GHGs.
- Understanding the balance between N_2O production and consumption in the soil profile is important for accurate determination of the soil-atmosphere flux. How this varies with depth is difficult to measure and so in Chapter 6 the aim is to apply the pool dilution method to study this and improve our understanding of the physical and biological factors in soil N_2O processes.

1.6 Thesis aims and objectives

This thesis has been motivated by the need for further research to address the knowledge gaps presented above. This section details the aims and objectives of the thesis, followed by a brief description of the relevant chapters and experimental work referring to each objective. The thesis is divided into 7 chapters with a meta-analysis and a series of 4 experimental chapters. A list of the experimental chapter titles is presented in section 1.7. Individual hypotheses and objectives are described in detail within each chapter.

Thesis aims

The work presented in this PhD thesis primarily aims to evaluate and investigate subsoil-targeted C sequestration strategies. In addition, the behaviour and fate of soil GHGs in deep soil is investigated to understand how these may impact C sequestration success from a climate change mitigation perspective.

Objective 1 – *Evaluate the current potential and strategies for sequestering C in agricultural subsoils*

In Chapter 2, the sources and stabilisation mechanisms of C in the subsoil are reviewed to understand how and why subsoils can be targeted for C sequestration. A meta-analysis was conducted to collect data from the literature to characterise top- and subsoils by important biological, chemical, and physical soil properties for C sequestration and to evaluate the current evidence of subsoil-targeted C sequestration strategies.

Objective 2 – *Determine whether the addition of iron to agricultural soils is an effective C sequestration strategy*

In Chapter 3, a series of laboratory incubations were conducted to determine the potential of adding Fe to agricultural soils. Different forms of Fe were added to agricultural top- and subsoils with native or ^{14}C-labelled substrates and the impact on soil chemistry and CO_2 fluxes were determined.

Objective 3 – *Quantify the contribution of deep-rooting grass to deep soil organic carbon*

In Chapter 6, a field trial was set up with deep rooting grass and root-excluding mesh installed at different depths to determine whether deep rooting was at the expense of aboveground and higher surface-atmosphere fluxes.

Objective 4 – *Investigate the dynamics of soil greenhouse gases at depth*

In Chapter 4, soil GHGs were measured at different depths across multiple growing seasons to understand how environmental conditions influence the dynamics of GHGs with depth and to further evaluate the concentration gradient method.

Objective 5 – *Disentangle the physical and biological components of N_2O mechanisms in intact agricultural soil*

In Chapter 5, a series of laboratory incubations with intact top- and subsoil cores were conducted to determine the diffusion coefficient and gross N_2O production and consumption rates applying the ^{15}N-N_2O pool dilution method in a novel way.

1.7 Chapter information

The chapters herein have been prepared in the style of journal article manuscripts. Each experimental chapter starts with a title page detailing the authors, their contributions to the work, and the journal publication status. For consistency and clarity, the experimental

chapters will be referred to as they appear in the thesis. The chapter titles and publication statuses are as follows:

Chapter	Title	Status
1	Introduction.	
2	Deep-C storage: Biological, chemical and physical strategies to enhance carbon stocks in agricultural subsoils.	Published in Soil *Biology and Biochemistry*
3	Addition of iron to agricultural topsoil and subsoil is not an effective C sequestration strategy.	Published in *Geoderma*
4	Impact of deep-rooting grass root exclusion on aboveground biomass and soil greenhouse gas fluxes.	Not to be submitted
5	Greenhouse gas production, diffusion and consumption in a soil profile under maize and wheat production.	Under review in *Geoderma*
6	Separating production and consumption of N_2O in intact agricultural soil cores at different depths and moisture contents using the ^{15}N-N_2O pool dilution method.	Under review in *European Journal of Soil Science*
7	Discussion and conclusions.	

1.8 References

Alcántara, V., Don, A., Well, R., Nieder, R., 2016. Deep ploughing increases agricultural soil organic matter stocks. Global Change Biology 22, 2939–2956.

Allaire, S.E., Lafond, J.A., Cabral, A.R., Lange, S.F., 2008. Measurement of gas diffusion through soils: Comparison of laboratory methods. Journal of Environmental Monitoring 10, 1326–1336.

Almaraz, M., Wong, M.Y., Yang, W.H., 2020. Looking back to look ahead: a vision for soil denitrification research. Ecology 101, 1–10.

Amundson, R., Berhe, A.A., Hopmans, J.W., Olson, C., Sztein, A.E., Sparks, D.L., 2015. Soil and human security in the 21st century. Science 348.

Baker, S.E., Stolaroff, J.K., Peridas, G., Pang, S.H., Goldstein, H.M., Lucci, F.R., Li, W., Slessarev, E.W., Pett-Ridge, J., Ryerson, F.J., Wagoner, J.L., Kirkendall, W., Aines, R.D., Sanchez, D.L., Cabiyo, B., Baker, J., McCoy, S., Uden, S., Runnebaum, R., Wilcox, J., Psarras, P.C., Pilorgé, H., McQueen, N., Maynard, D., McCormick, C., 2020. Getting to neutral: options for negative carbon emissions in California. Lawrence Livermore National Laboratory.

Baldocchi, D.D., 2003. Assessing the eddy covariance technique for evaluating carbon dioxide exchange rates of ecosystems: Past, present and future. Global Change Biology 9, 479–492.

Balogh, J., Nagy, Z., Fóti, S., Pintér, K., Czóbel, S., Péli, E.R., Acosta, M., Marek, M. V., Csintalan, Z., Tuba, Z., 2007. Comparison of CO_2 and H_2O fluxes over grassland vegetations measured by the eddy-covariance technique and by open system chamber. Photosynthetica 45, 288–292.

Batjes, N.H., 1996. Total carbon and nitrogen in the soils of the world. European Journal of Soil Science 65, 10–21.

Baveye, P.C., Berthelin, J., Tessier, D., Lemaire, G., 2018. The “4 per 1000” initiative: A credibility issue for the soil science community? Geoderma 309, 118–123.

Bernal, B., McKinley, D.C., Hungate, B.A., White, P.M., Mozdzer, T.J., Megonigal, J.P., 2016. Limits to soil carbon stability; Deep, ancient soil carbon decomposition stimulated by new labile organic inputs. Soil Biology and Biochemistry 98, 85–94.

Blagodatsky, S., Smith, P., 2012. Soil physics meets soil biology: Towards better mechanistic prediction of greenhouse gas emissions from soil. Soil Biology and Biochemistry 47, 78–92.

Boos, E.F., Magid, J., Bruun, S., Jørgensen, N.O.G., 2022. Liquid scintillation counting can underestimate ^{14}C-activity of $^{14}CO_2$ trapped in NaOH. Soil Biology and Biochemistry 166.

Boyer, E.W., Alexander, R.B., Parton, W.J., Li, C., Butterbach-Bahl, K., Donner, S.D., Skaggs, R.W., Del Grosso, S.J., 2006. Modelling denitrification in terrestrial and aquatic ecosystems at regional scales. Ecological Applications 16, 2123–2142.

Canadell, J.G., Monteiro, P.M.S., Costa, M.H., Cunha, C. da L., Cox, P.M., Eliseev, A. V., Henson, S., Ishii, M., Jaccard, S., Koven, C., Lohila, A., Patra, P.K., Piao, S., Rogelj, J., S., S., Zaehle, S., Zickfeld, K., 2022. Global Carbon and other Biogeochemical Cycles and Feedbacks, in: Climate Change 2021: The Physical Science Basis, Contribution of Working Group I to the Sixth Assessment Report of the Intergovernmental Panel on Climate Change. Cambridge University Press, Cambridge, United Kingdom and New York, NY, USA.

Chabbi, A., Kögel-Knabner, I., Rumpel, C., 2009. Stabilised carbon in subsoil horizons is located in spatially distinct parts of the soil profile. Soil Biology and Biochemistry 41, 256–261.

Chaichana, N., Bellingrath-Kimura, S.D., Komiya, S., Fujii, Y., Noborio, K., Dietrich, O., Pakoktom, T., 2018. Comparison of closed chamber and eddy covariance methods to improve the understanding of methane fluxes from rice paddy fields in Japan. Atmosphere 9.

Charteris, A.F., Chadwick, D.R., Thorman, R.E., Vallejo, A., de Klein, C.A.M., Rochette, P., Cárdenas, L.M., 2020. Global Research Alliance N_2O chamber methodology guidelines: Recommendations for deployment and accounting for sources of variability. Journal of Environmental Quality 49, 1092–1109.

Chen, S., Martin, M.P., Saby, N.P.A., Walter, C., Angers, D.A., Arrouays, D., 2018. Fine resolution map of top- and subsoil carbon sequestration potential in France. Science of the Total Environment 630, 389–400.

Churchman, G.J., Noble, A., Bailey, G., Chittleborough, D., Harper, R., 2014. Clay Addition and Redistribution to Enhance Carbon Sequestration in Soils, in: Soil Carbon. Switzerland, 327–335.

Clough, T.J., Kelliher, F.M., Wang, Y.P., Sherlock, R.R., 2006. Diffusion of ^{15}N-labelled N_2O into soil columns: a promising method to examine the fate of N_2O in subsoils. Soil Biology and Biochemistry 38, 1462–1468.

Clough, T.J., Sherlock, R.R., Rolston, D.E., 2005. A review of the movement and fate of N_2O in the subsoil. Nutrient Cycling in Agroecosystems 72, 3–11.

Cowan, N., Levy, P., Maire, J., Coyle, M., Leeson, S.R., Famulari, D., Carozzi, M., Nemitz, E., Skiba, U., 2020. An evaluation of four years of nitrous oxide fluxes after application of ammonium nitrate and urea fertilisers measured using the eddy covariance method. Agricultural and Forest Meteorology 280, 107812.

Das, S.K., Avasthe, R.K., Singh, R., Babu, S., 2014. Biochar as carbon negative in carbon credit under changing climate. Current Science 107, 1090–1091.

Davidson, E.A., Hart, S.C., Shanks, C.A., Firestone, M.K., 1991. Measuring gross nitrogen mineralization, and nitrification by ^{15}N isotopic pool dilution in intact soil cores. Journal of Soil Science 42, 335–349.

Davidson, E.A., Ishida, F.Y., Nepstad, D.C., 2004. Effects of an experimental drought on soil emissions of carbon dioxide, methane, nitrous oxide, and nitric oxide in a moist tropical forest. Global Change Biology 10, 718–730.

de Vries, W., 2018. Soil carbon 4 per mille: a good initiative but let's manage not only the soil but also the expectations: Comment on Minasny et al. (2017) Geoderma 292: 59–86. Geoderma 309, 111–112.

Don, A., Schumacher, J., Freibauer, A., 2011. Impact of tropical land use change on soil organic carbon stocks – a meta-analysis. Global Change Biology, 17, 1658-1670.

Dong, W., Wang, Y., Hu, C., 2013. Concentration profiles of CH_4, CO_2 and N_2O in soils of a wheat–maize rotation ecosystem in North China Plain, measured weekly over a whole year. Agriculture, Ecosystems and Environment 1, 260–272.

Dove, N.C., Arogyaswamy, K., Billings, S.A., Botthoff, J.K., Carey, C.J., Cisco, C., Deforest, J.L., Fairbanks, D., Fierer, N., Gallery, R.E., Kaye, J.P., Lohse, K.A., Maltz, M.R., Mayorga, E., Pett-Ridge, J., Yang, W.H., Hart, S.C., Aronson, E.L., 2020. Continental-scale patterns of extracellular enzyme activity in the subsoil: An overlooked reservoir of microbial activity. Environmental Research Letters 15.

FAO, 2022. Food balances 2010–2019: global, regional and country trends. FAOSTAT Analytical Brief Series No. 40. Rome, FAO.

FAO, 2020. Land use in agriculture by the numbers. Food and Agriculture Organisation of the United Nations. FAOSTAT. Rome, Italy.

Fornara, D.A., Olave, R., Burgess, P., Delmer, A., Upson, M., McAdam, J., 2018. Land use change and soil carbon pools: evidence from a long-term silvopastoral experiment. Agroforestry Systems 92, 1035–1046.

Friedlingstein, P., Jones, M.W., O'Sullivan, M., Andrew, R.M., Hauck, J., Peters, G.P., Peters, W., Pongratz, J., Sitch, S., Quéré, C. Le, Bakker, D.C.E., Canadell, J.G., Ciais, P., Jackson, R.B., Anthoni, P., Leticia, B., Bastos, A., Bastrikov, V., Becker, M., Bopp, L., Buitenhuis, E., Chandra, N., Chevallier, F., Chini, L.P., Currie, K.I., Feely, R.A., Gehlen, M., Gilfillan, D., Gkritzalis, T., Goll, D.S., Gruber, N., G, S., Zaehle, and S., 2019. Global Carbon Budget 2019 1–4.

Giller, K. E., Hijbeek, R., Andersson, J. A., & Sumberg, J. (2021). Regenerative Agriculture: An agronomic perspective. Outlook on Agriculture, 50, 13–25

Grace, P.R., van der Weerden, T.J., Rowlings, D.W., Scheer, C., Brunk, C., Kiese, R., Butterbach-Bahl, K., Rees, R.M., Robertson, G.P., Skiba, U.M., 2020. Global Research Alliance N_2O chamber methodology guidelines: Considerations for automated flux measurement. Journal of Environmental Quality 49, 1126–1140.

Groffman, P.M., Altabet, M. a., Bohlke, J.K., Butterbach-Bahl, K., David, M.B., Firestone, M.K., Giblin, A.E., Kana, T.M., Nielsen, L.P., Voyteck, M. a., 2006. Methods for Measuring Denitrification: Diverse approaches to a difficult problem. Ecological Applications 16, 2091–2122.

Hobbs, P.R., Sayre, K. and Gupta, R., 2008. The role of conservation agriculture in sustainable agriculture. Philosophical Transactions of the Royal Society B: Biological Sciences, 363, 543-555.

Hübner, R., Kühnel, A., Lu, J., Dettmann, H., Wang, W., Wiesmeier, M., 2021. Soil carbon sequestration by agroforestry systems in China: A meta-analysis. Agriculture, Ecosystems and Environment 315, 107437.

Huntzinger, D.N., Michalak, A.M., Schwalm, C., Ciais, P., King, A.W., Fang, Y., Schaefer, K., Wei, Y., Cook, R.B., Fisher, J.B., Hayes, D., Huang, M., Ito, A., Jain, A.K., Lei, H., Lu, C., Maignan, F., Mao, J., Parazoo, N., Peng, S., Poulter, B., Ricciuto, D., Shi, X., Tian, H., Wang, W., Zeng, N., Zhao, F., 2017. Uncertainty in the response of terrestrial carbon

sink to environmental drivers undermines carbon-climate feedback predictions. Scientific Reports 7, 1–8.

Inagaki, T.M., Possinger, A.R., Grant, K.E., Schweizer, S.A., Mueller, C.W., Derry, L.A., Lehmann, J., Kögel-Knabner, I., 2020. Subsoil organo-mineral associations under contrasting climate conditions. Geochimica et Cosmochimica Acta 270, 244–263.

International Atomic Energy Agency, 2001. Use of isotope and radiation methods in soil and water management and crop nutrition. Vienna, Austria.

Jian, J., Vargas, R., Anderson-Teixeira, K.J., Stell, E., Herrmann, V., Horn, M., Kholod, N., Manzon, J., Marchesi, R., Paredes, D., Bond-Lamberty, B.P., 2021. A Global Database of Soil Respiration Data. Version 5.0. ORNL DAAC, Oak Ridge, Tennessee, USA.

Jobbágy, E.G., Jackson, R.B., 2000. The vertical distribution of soil organic carbon and its relation to climate and vegetation. Ecological Applications 10, 423–436.

Jones, D.L., Cooledge, E.C., Hoyle, F.C., Griffiths, R.I., Murphy, D. V., 2019. pH and exchangeable aluminum are major regulators of microbial energy flow and carbon use efficiency in soil microbial communities. Soil Biology and Biochemistry 138, 0–4.

Jong, E. De, Schappert, H.J., 1972. Calculation of soil respiration and activity from CO_2 profiles in the soil. Soil Science 113, 328–333.

Jónsson, J.Ö.G., Davídsdóttir, B., 2016. Classification and valuation of soil ecosystem services. Agricultural Systems 145, 24–38.

Kautz, T., Amelung, W., Ewert, F., Gaiser, T., Horn, R., Jahn, R., Javaux, M., Kemna, A., Kuzyakov, Y., Munch, J.C., Pätzold, S., Peth, S., Scherer, H.W., Schloter, M., Schneider, H., Vanderborght, J., Vetterlein, D., Walter, A., Wiesenberg, G.L.B., Köpke, U., 2013. Nutrient acquisition from arable subsoils in temperate climates: A review. Soil Biology and Biochemistry 57, 1003–1022.

Kell, D.B., 2011. Breeding crop plants with deep roots: Their role in sustainable carbon, nutrient and water sequestration. Annals of Botany 108, 407–418.

Köchy, M., Hiederer, R., Freibauer, A., 2015. Global distribution of soil organic carbon – Part 1: Masses and frequency distributions of SOC stocks for the tropics, permafrost regions, wetlands, and the world. Soil 1, 351–365.

Lal, R., 2009. Laws of sustainable soil management. Sustainable Agriculture 29, 9–12.

Lal, R., 2004a. Soil Carbon Sequestration Impacts on Global Climate Change and Food Security. American Association for the Advancement of Science 304, 1623–7.

Lal, R., 2004b. Soil carbon sequestration to mitigate climate change. Geoderma 123, 1–22.

Lal, R., Negassa, W., Lorenz, K., 2015. Carbon sequestration in soil. Current Opinion in Environmental Sustainability 15, 79–86.

Le Quéré, C., Rödenbeck, C., Buitenhuis, E.T., Conway, T.J., Langenfelds, R., Gomez, A., Labuschagne, C., Ramonet, M., Nakazawa, T., Metzl, N., Gillett, N., Heimann, M., 2007. Saturation of the southern ocean CO_2 sink due to recent climate change. Science 316, 1735–1738. doi:10.1126/science.1136188

Li, Z., Kelliher, F.M., 2005. Determining nitrous oxide emissions from subsurface measurements in grazed pasture: A field trial of alternative technology. Australian Journal of Soil Research 43, 677–687.

Lorenz, K., Lal, R., Preston, C.M., Nierop, K.G.J., 2007. Strengthening the soil organic carbon pool by increasing contributions from recalcitrant aliphatic bio(macro)molecules. Geoderma 142, 1–10.

Lugato, E., Bampa, F., Panagos, P., Montanarella, L., Jones, A., 2014. Potential carbon sequestration of European arable soils estimated by modelling a comprehensive set of management practices. Global Change Biology 20, 3557–3567.

Lundegårdh, H., 1927. Carbon Dioxide Evolution of Soil and Crop Growth. Soil Science 23, 417–453.

Lynch, J.P., Wojciechowski, T., 2015. Opportunities and challenges in the subsoil: Pathways to deeper rooted crops. Journal of Experimental Botany 66, 2199–2210.

Maier, M., Glatzel, S., Kutzbach, L., Weber, T.K.D., Huth, V., Schäfer, K., Fiedler, J., Jordan, S., Weymann, D., Fuß, R., Jurasinski, G., Hagemann, U., 2022. Introduction of a guideline for measurements of greenhouse gas fluxes from soils using non-steady-state chambers 1–15.

Maier, M., Schack-Kirchner, H., 2014. Using the gradient method to determine soil gas flux: A review. Agricultural and Forest Meteorology 192–193, 78–95.

Marsden, K.A., Holmberg, J.A., Jones, D.L., Charteris, A.F., Cárdenas, L.M., Chadwick, D.R., 2019. Nitrification represents the bottle-neck of sheep urine patch N_2O emissions from extensively grazed organic soils. Science of the Total Environment 695, 133786.

McKinley, G.A., Fay, A.R., Lovenduski, N.S., Pilcher, D.J., 2017. Natural Variability and Anthropogenic Trends in the Ocean Carbon Sink. Annual Review of Marine Science 9, 125–150.

Mencuccini, M., Hölttä, T., 2010. The significance of phloem transport for the speed with which canopy photosynthesis and belowground respiration are linked. New Phytologist 185, 189–203.

Milne, E., Banwart, S.A., Noellemeyer, E., Abson, D.J., Ballabio, C., Bampa, F., Bationo, A., Batjes, N.H., Bernoux, M., Bhattacharyya, T., Black, H., Buschiazzo, D.E., Cai, Z., Cerri, C.E., Cheng, K., Compagnone, C., Conant, R., Coutinho, H.L.C., de Brogniez, D., Balieiro, F. de C., Duffy, C., Feller, C., Fidalgo, E.C.C., da Silva, C.F., Funk, R., Gaudig, G., Gicheru, P.T., Goldhaber, M., Gottschalk, P., Goulet, F., Goverse, T., Grathwohl, P., Joosten, H., Kamoni, P.T., Kihara, J., Krawczynski, R., La Scala, N., Lemanceau, P., Li, L., Li, Z., Lugato, E., Maron, P.A., Martius, C., Melillo, J., Montanarella, L., Nikolaidis, N., Nziguheba, G., Pan, G., Pascual, U., Paustian, K., Piñeiro, G., Powlson, D., Quiroga, A., Richter, D., Sigwalt, A., Six, J., Smith, J., Smith, P., Stocking, M., Tanneberger, F., Termansen, M., van Noordwijk, M., van Wesemael, B., Vargas, R., Victoria, R.L., Waswa, B., Werner, D., Wichmann, S., Wichtmann, W., Zhang, X., Zhao, Y., Zheng, Jinwei, Zheng, Jufeng, 2015. Soil carbon, multiple benefits. Environmental Development 13, 33–38.

Minasny, B., Malone, B.P., McBratney, A.B., Angers, D.A., Arrouays, D., Chambers, A., Chaplot, V., Chen, Z.S., Cheng, K., Das, B.S., Field, D.J., Gimona, A., Hedley, C.B., Hong, S.Y., Mandal, B., Marchant, B.P., Martin, M., McConkey, B.G., Mulder, V.L., O'Rourke, S., Richer-de-Forges, A.C., Odeh, I., Padarian, J., Paustian, K., Pan, G., Poggio, L., Savin, I., Stolbovoy, V., Stockmann, U., Sulaeman, Y., Tsui, C.C., Vï¿½gen, T.G., van Wesemael, B., Winowiecki, L., 2017. Soil carbon 4 per mille. Geoderma 292, 59–86.

Mondal, S., Chakraborty, D., Bandyopadhyay, K., Aggarwal, P., Rana, D.S., 2020. A global analysis of the impact of zero-tillage on soil physical condition, organic carbon content, and plant root response. Land Degradation and Development 31, 557–567.

Murphy, R.M., Richards, K.G., Krol, D.J., Gebremichael, A.W., Lopez-Sangil, L., Rambaud, J., Cowan, N., Lanigan, G.J., Saunders, M., 2022a. Assessing nitrous oxide emissions in time and space with minimal uncertainty using static chambers and eddy covariance from a temperate grassland. Agricultural and Forest Meteorology 313, 108743.

Murphy, Rachael M., Saunders, M., Richards, K.G., Krol, D.J., Gebremichael, A.W., Rambaud, J., Cowan, N., Lanigan, G.J., 2022. Nitrous oxide emission factors from an intensively grazed temperate grassland: A comparison of cumulative emissions determined by eddy covariance and static chamber methods. Agriculture, Ecosystems and Environment 324, 107725.

Murphy, R.M., Saunders, M., Richards, K.G., Krol, D.J., Gebremichael, A.W., Rambaud, J., Cowan, N., Lanigan, G.J., 2022b. Nitrous oxide emission factors from an intensively grazed temperate grassland: A comparison of cumulative emissions determined by eddy covariance and static chamber methods. Agriculture, Ecosystems and Environment 324, 107725.

Oertel, C., Matschullat, J., Zurba, K., Zimmermann, F., Erasmi, S., 2016. Greenhouse gas emissions from soils—A review. Chemie Der Erde 76, 327–352.

Porras, R.C., Hicks Pries, C.E., Torn, M.S., Nico, P.S., 2018. Synthetic iron (hydr)oxide-glucose associations in subsurface soil: Effects on decomposability of mineral associated carbon. Science of the Total Environment 613–614, 342–351.

Poulton, P., Johnston, J., Macdonald, A., White, R., Powlson, D., 2018. Major limitations to achieving “4 per 1000” increases in soil organic carbon stock in temperate regions: Evidence from long-term experiments at Rothamsted Research, United Kingdom. Global Change Biology 24, 2563–2584.

Powlson, D.S., Whitmore, A.P., Goulding, K.W.T., 2011. Soil carbon sequestration to mitigate climate change: A critical re-examination to identify the true and the false. European Journal of Soil Science 62, 42–55.

Rasse, D.P., Mulder, J., Moni, C., Chenu, C., 2006. Carbon Turnover Kinetics with Depth in a French Loamy Soil. Soil Science Society of America Journal 70, 2097.

Reth, S., Göckede, M., Falge, E., 2005. CO2 efflux from agricultural soils in Eastern Germany - Comparison of a closed chamber system with eddy covariance measurements. Theoretical and Applied Climatology 80, 105–120.

Riederer, M., Serafimovich, A., Foken, T., 2014. Net ecosystem CO_2 exchange measurements by the closed chamber method and the eddy covariance technique and their dependence on atmospheric conditions. Atmospheric Measurement Techniques 7, 1057–1064.

Rochette, P., Gregorich, E.G., Desjardins, R.L., 1992. Comparison of static and dynamic closed chambers for measurement of soil respiration under field conditions. Canadian Journal of Soil Science 72, 605–609.

Rodrigues, L., Hardy, B., Huyghebeart, B., Fohrafellner, J., Fornara, D., Barančíková, G., Bárcena, T.G., De Boever, M., Di Bene, C., Feizienė, D., Kätterer, T., Laszlo, P., O'Sullivan, L., Seitz, D., Leifeld, J., 2021. Achievable agricultural soil carbon sequestration across Europe from country-specific estimates. Global Change Biology 27, 6363–6380.

Rumpel, C., Kögel-Knabner, I., 2011. Deep soil organic matter-a key but poorly understood component of terrestrial C cycle. Plant and Soil 338, 143–158.

Salomé, C., Nunan, N., Pouteau, V., Lerch, T.Z., Chenu, C., 2010. Carbon dynamics in topsoil and in subsoil may be controlled by different regulatory mechanisms. Global Change Biology 16, 416–426.

Sanderman, J., 2012. Can management induced changes in the carbonate system drive soil carbon sequestration? A review with particular focus on Australia. Agriculture, Ecosystems and Environment 155, 70–77.

Sanderman, J., Hengl, T., Fiske, G.J., 2017. Soil carbon debt of 12,000 years of human land use. Proceedings of the National Academy of Sciences 115, 201800925.

Schiedung, M., Tregurtha, C.S., Beare, M.H., Thomas, S.M., Don, A., 2019. Deep soil flipping increases carbon stocks of New Zealand grasslands. Global Change Biology 25, 2296–2309.

Schöning, I., Kögel-Knabner, I., 2006. Chemical composition of young and old carbon pools throughout Cambisol and Luvisol profiles under forests. Soil Biology and Biochemistry 38, 2411–2424.

Shi, Z., Allison, S.D., He, Y., Levine, P.A., Hoyt, A.M., Beem-Miller, J., Zhu, Q., Wieder, W.R., Trumbore, S., Randerson, J.T., 2020. The age distribution of global soil carbon inferred from radiocarbon measurements. Nature Geoscience 13, 555-559.

Schreefel, L., Schulte, R.P.O., De Boer, I.J.M., Schrijver, A.P. and Van Zanten, H.H.E., 2020. Regenerative agriculture–the soil is the base. Global Food Security, 26, 100404.

Smith, P., 2008. Land use change and soil organic carbon dynamics. Nutrient Cycling in Agroecosystems 81, 169–178.

Stockmann, U., Adams, M.A., Crawford, J.W., Field, D.J., Henakaarchchi, N., Jenkins, M., Minasny, B., McBratney, A.B., Courcelles, V. de R. de, Singh, K., Wheeler, I., Abbott, L., Angers, D.A., Baldock, J., Bird, M., Brookes, P.C., Chenu, C., Jastrow, J.D., Lal, R., Lehmann, J., O'Donnell, A.G., Parton, W.J., Whitehead, D., Zimmermann, M., 2013. The knowns, known unknowns and unknowns of sequestration of soil organic carbon. Agriculture, Ecosystems and Environment 164, 80–99.

Sykes, A.J., Macleod, M., Eory, V., Rees, R.M., Payen, F., Myrgiotis, V., Williams, M., Sohi, S., Hillier, J., Moran, D., Manning, D.A.C., Goglio, P., Seghetta, M., Williams, A., Harris, J., Dondini, M., Walton, J., House, J., Smith, P., 2020. Characterising the biophysical, economic and social impacts of soil carbon sequestration as a greenhouse gas removal technology. Global Change Biology 26, 1085–1108.

Torn, M.S., Lapenis, a G., Timofeev, a, Fischer, M.L., Babikov, B. V, Harden, J.W., 2002. Organic carbon and carbon isotopes in modern and 100-year- old-soil archives of the Russian steppe. Global Change Biology 8, 941–953.

Torn, M.S., Trumbore, S.E., Chadwick, O.A., Vitousek, P.M., Hendricks, D.M., 1997. Mineral control of soil organic carbon storage and turnover. Nature 389, 170–173.

Tsiafouli, M.A., Thébault, E., Sgardelis, S.P., de Ruiter, P.C., van der Putten, W.H., Birkhofer, K., Hemerik, L., de Vries, F.T., Bardgett, R.D., Brady, M.V., Bjornlund, L., Jørgensen, H.B., Christensen, S., Hertefeldt, T.D., Hotes, S., Gera Hol, W.H., Frouz, J., Liiri, M., Mortimer,

S.R., Setälä, H., Tzanopoulos, J., Uteseny, K., Pižl, V., Stary, J., Wolters, V., Hedlund, K., 2015. Intensive agriculture reduces soil biodiversity across Europe. Global Change Biology 21, 973–985.

Vangeli, S., Posse, G., Beget, M.E., Otero Estrada, E., Valdettaro, R.A., Oricchio, P., Kandus, M., Di Bella, C.M., 2022. Effects of fertilizer type on nitrous oxide emission and ammonia volatilization in wheat and maize crops. Soil Use and Management 1–13.

von Fischer, J.C., Hedin, L.O., 2002. Separating methane production and consumption with a field-based isotope pool dilution technique. Global Biogeochemical Cycles 16, 8-1-8–13.

Wang, Y., Li, X., Dong, W., Wu, D., Hu, C., Zhang, Y., Luo, Y., 2018. Depth-dependent greenhouse gas production and consumption in an upland cropping system in northern China. Geoderma 319, 100–112.

Wang, Y., Li, Y., Ye, X., Chu, Y., Wang, X., 2010. Profile storage of organic/inorganic carbon in soil: From forest to desert. Science of the Total Environment 408, 1925–1931.

Well, R., Butterbach-Bahl, K., 2013. Comments on "A test of a field-based ^{15}N-nitrous oxide pool dilution technique to measure gross N_2O production in soil" by Yang et al. (2011), Global Change Biology, 17, 3577-3588. Global Change Biology 19, 133–135.

Wen, Y., Chen, Z., Dannenmann, M., Carminati, A., Willibald, G., Kiese, R., Wolf, B., Veldkamp, E., Butterbach-Bahl, K., Corre, M.D., 2016. Disentangling gross N_2O production and consumption in soil. Scientific Reports 6, 1–8.

Werth, M., Kuzyakov, Y., 2010. 13C fractionation at the root-microorganisms-soil interface: A review and outlook for partitioning studies. Soil Biology and Biochemistry 42, 1372–1384.

Xiao, X., Kuang, X., Sauer, T.J., Heitman, J.L., Horton, R., 2015. Bare Soil Carbon Dioxide Fluxes with Time and Depth Determined by High-Resolution Gradient-Based Measurements and Surface Chambers. Soil Science Society of America Journal 79, 1073.

Xing, G., Cao, Y., Sun, G., 1997. Natural ^{15}N abundance in soils, in: Nitrogen in Soils of China. Developments in Plant and Soil Sciences.

Yang, W.H., Silver, W.L., 2016. Gross nitrous oxide production drives net nitrous oxide fluxes across a salt marsh landscape. Global Change Biology 22, 2228–2237.

Yang, W.H., Teh, Y.A., Silver, W.L., 2011. A test of a field-based ^{15}N-nitrous oxide pool dilution technique to measure gross N_2O production in soil. Global Change Biology 17, 3577–3588.

Yost, J.L., Hartemink, A.E., 2020. How deep is the soil studied – an analysis of four soil science journals. Plant and Soil.

Yu, L., Wang, H., Wang, G., Song, W., Huang, Y., Li, S.G., Liang, N., Tang, Y., He, J.S., 2013. A comparison of methane emission measurements using eddy covariance and manual and automated chamber-based techniques in Tibetan Plateau alpine wetland. Environmental Pollution 181, 81–90.

Zhu, X.C., Di, D.R., Ma, M.G., Shi, W.Y., 2019. Stable isotopes in greenhouse gases from soil: A review of theory and application. Atmosphere 10, 1–14.

Zomer, R.J., Bossio, D.A., Sommer, R., Verchot, L. V., 2017. Global Sequestration Potential of Increased Organic Carbon in Cropland Soils. Scientific Reports 7, 1–8.

Chapter 2

Deep-C storage: Biological, chemical and physical strategies to enhance carbon stocks in agricultural subsoils

Authors

Erik S. Button, Jennifer Pett-Ridge, Daniel V. Murphy, Yakov Kuzyakov, David R. Chadwick, Davey L. Jones.

Publication status

This manuscript has been published in *Soil Biology and Biochemistry*.

Citation

Button, E.S., Pett-Ridge, J., Murphy, D.V., Kuzyakov, Y., Chadwick, D.R. and Jones, D.L., 2022. Deep-C storage: Biological, chemical and physical strategies to enhance carbon stocks in agricultural subsoils. *Soil Biology and Biochemistry* 170, 108697.

Author contributions

ESB conceived the structure, wrote the majority of the manuscript, conducted all meta-analysis work, created the figures and graphics and revised the manuscript following peer-review. JPR, DVM, YK, DRC and DLJ contributed writing to certain sections and edited and advised on the manuscript.

Abstract

Due to their substantial volume, subsoils contain more of the total soil carbon (C) pool than topsoils. Much of this C is thousands of years old, suggesting that subsoils offer considerable potential for long-term C sequestration. However, knowledge of subsoil C behaviour and manageability remains incomplete, and subsoil C storage potential has yet to be realised at a large scale, particularly in agricultural systems. A range of biological (e.g. deep-rooting), chemical (e.g. biochar burial) and physical (e.g. deep ploughing) C sequestration strategies have been proposed, but are yet to be assessed. In this review, we identify the main factors that regulate subsoil C cycling and critically evaluate the evidence and mechanistic basis of subsoil strategies designed to promote greater C storage, with particular emphasis on agroecosystems. We assess the barriers and opportunities for the implementation of strategies to enhance subsoil C sequestration and identify 5 key current gaps in scientific understanding. We conclude that subsoils, while highly heterogeneous, are in many cases more suited to long-term C sequestration than topsoils. The proposed strategies may also bring other tangible benefits to cropping systems (e.g. enhanced water holding capacity and nutrient use efficiency). Furthermore, while the subsoil C sequestration strategies we reviewed have large potential, more long-term studies are needed across a diverse range of soils and climates, in conjunction with chronosequence and space-for-time substitutions. Also, it is vital that subsoils are more consistently included in modelled estimations of soil C stocks and C sequestration potential, and that subsoil-explicit C models are developed to specifically reflect subsoil processes. Finally, further mapping of subsoil C is needed in specific regions (e.g. in the Middle East, Eastern Europe, South and Central America, South Asia and Africa). Conducting both immediate and long-term subsoil C studies will fill the knowledge gaps to devise appropriate soil C sequestration strategies and policies to help in the global fight against climate change and decline in soil quality. In conclusion, our evidence-based analysis reveals that subsoils offer an untapped potential to enhance global C storage in terrestrial ecosystems.

Keywords: Chemical stabilization; Greenhouse gas emissions; Organic matter priming; Physical protection; Regenerative agriculture; subsoil carbon.

2.1 Introduction

Soil, a global reservoir of 3000 Pg carbon (C) (Köchy et al., 2015) with a mean age of 3100 years (He et al., 2016), has a significant capacity for long-term C storage. However, the extent to which this terrestrial C sink will continue to grow as atmospheric CO_2 concentrations increase remains unclear. Most C in agricultural soils (cropland and pasture) is held in an organic form (soil organic carbon, SOC), which is susceptible to destabilization as a result of changes in land use, management practices and environmental conditions (Guo and Gifford, 2002; Davidson and Janssens, 2006). Due to agriculture alone, 133 Gt of SOC has already been lost to the atmosphere in the past two centuries, and the rate of loss is increasing (Sanderman et al., 2017). SOC loss severely impacts soil functions, including water infiltration, nutrient supply and biodiversity, leading to erosion, a decline in soil fertility and a release of greenhouse gases (GHGs - CO_2, CH_4, N_2O) (Don et al., 2011; Tsiafouli et al., 2015). Due to the projected growing demand for food production from already degraded land, intensive agriculture is putting soils at further risk of SOC loss (Johnson et al., 2014; Sanderman et al., 2017). Still, enhanced soil C sequestration of ~1000 additional Pg C is thought to be possible (Lorenz and Lal, 2005).

Sequestering organic C in the soil can have multiple benefits, including i) offsetting of anthropogenic C emissions, ii) restoring soil function, iii) improved soil resilience (to erosion, pollution, diseases and drought), iv) increased agricultural productivity and sustainability, and v) greater food security (Lal et al., 2015). Due to these expected benefits, promoting SOC sequestration is of keen interest to both the scientific and policymaking communities. A number of recent analyses suggest that 'natural solutions' like sequestering C in soil are economical and 'no-regrets options' that could achieve a substantial portion of the negative emissions needed to achieve carbon neutrality (Baker et al., 2020; Sykes et al., 2020). While the recent '4 per 1000' soil C sequestration initiative has drawn both support (Minasny et al., 2017; Rumpel et al., 2020) and criticism (Baveye et al., 2018; de Vries, 2018; Poulton et al., 2018) from the scientific community, this initiative: i) has been an aspiration and definitive step in the direction of direct action to mitigate climate change via soil C sequestration, ii) brought soil C sequestration to extensive scientific, public and political attention, and iii) considers soil below the topsoil, albeit to a maximum depth of 40 cm, in the context of C sequestration.

Currently, the practiced measures to limit C loss and/or maximise C retention in agricultural soils are largely targeted to topsoils (Ap horizon; ca. 0-30 cm). This predisposition towards topsoils is confirmed by Yost and Hartemink, (2020) who found the mean soil depth studied in 4 primary soil science journals to be 24 cm between 2004 and 2019. Topsoil C retention strategies include reducing tillage intensity, the addition of organic amendments, growing cover crops, using leys with grazing livestock, agroforestry and restoring of natural vegetation (Smith, 2008), along with a variety of regenerative agriculture practices still being tested.

However, topsoil, despite being rich in SOC (per volume of soil), has a relatively low potential to sequester further C (Rumpel and Kögel-Knabner, 2011; Hobley et al., 2017). Due to favourable soil conditions for decomposition, high microbial activity, aeration, large inputs of labile organic matter, and high soil disturbance; topsoils experience high rates of C mineralization and short C residence times (Schlesinger and Andrews, 2000; Fontaine et al., 2007; Salomé et al., 2010). As a result, C retention strategies have had varying results in improving soil C stocks and decreasing soil GHG emissions in the long term (Kirkby et al., 2014; Smith et al., 2014a). In addition, as topsoil C sequestration is reversible, changes in land use and management can lead to rapid C loss (Smith, 2008).

While deep soil horizons (ca. ≥ 30 cm) are often considered biologically quiescent, deep soil C is responsive to environmental change (Bernal et al., 2016; Hobley et al., 2017; Slessarev et al., 2020) and comprises the majority of the global soil C pool (Jobbágy and Jackson, 2000). Therefore, to limit C losses and increase C stocks over longer timescales (i.e. 50-1000 years; Piccolo et al., 2018), approaches targeting deeper, low disturbance soil may have the potential to be more successful. The residence time of subsoil (B horizon; ca. ~30-100+ cm) C increases with depth, with C here commonly attaining millenial age (Torn et al., 1997, 2002; Rumpel et al., 2002; Schöning and Kögel-Knabner, 2006). This is confirmed by Shi et al., (2020) who determined the global mean of deep cropland and grassland soil (30-100 cm) to be 3700 and 5400 years old by radiocarbon measurements, which is 3.8- and 3.5-fold older than measured in the topsoil (0-30 cm), respectively. As awareness of the potential for subsoils to promote SOC sequestration grows, interest in C dynamics and strategies of sequestration in subsoils have developed (Chabbi et al., 2009; Kautz et al., 2013; Chen et al., 2018). However, how subsoil C is stabilised, enabling this long-term persistence is still not

fully understood (Fontaine et al., 2007; Jones et al., 2018) and specific subsoil C sequestration strategies are lacking sufficient evidence and comparative assessment.

In this review, we explore the potential of C sequestration in non-waterlogged subsoils with a specific focus on agricultural lands (cropland and pasture). Firstly, we explore the nature and properties of subsoils and the forms and amounts of C present within them. Subsequently, we review the evidence and different approaches of current subsoil C sequestration strategies and identify knowledge gaps in the literature. Finally, the challenges facing C sequestration in subsoils are addressed, alongside suggestions of how progress can be made.

2.2 Subsoil carbon

2.2.1 Subsoil biological, chemical and physical properties

In the past, and in early subsoil C models (e.g. RothPC-1, Jenkinson and Coleman, 2008), subsoils were essentially thought of and treated as 'less concentrated' topsoils, but this general assumption has more recently been dismantled (Salome et al., 2010). Indeed, the differences between the environmental, physico-chemical and biological characteristics of topsoils and subsoils (Rumpel and Koegel-Knabner, 2011) are such that a sound understanding of subsoil processes cannot be directly inferred from our current understanding of topsoils.

Because of their high spatial variability at a range of scales (i.e. field, landscape, regional), driven in part by pedology, environment and climate, subsoils are difficult to generalise (Chabbi et al., 2009). To better characterise the diversity, similarities, and differences of top and subsoil horizons, we collected soil profile data of 203 studies across different climates and soil types around the world (Fig. 2.1, Fig. 2.2). Details on the search term strategy, selection criteria and spread of soil orders and study locations are presented in the Appendix 1 (Table S1-S2, Fig. S1-S2). We used a topsoil-subsoil boundary of 30 cm when categorising the measurements. A numerical boundary was used because studies predominantly sample soil by soil depth intervals (Yost and Hartemink, 2020). This particular depth was chosen as it is commonly the boundary of soil disturbance (reflecting a historical 12-inch plough; Davis et al., 2018) in ploughed soils, which was a key criterion in the definition of subsoils in this review. However, this boundary does not well represent all soils. For

example, in lower production rain-limited environments where no-tillage practices are often used, the topsoil may be functionally defined as <10 cm deep (Hoyle et al., 2013). To avoid falsely categorising soil horizons and better determine whether measurements belonged to the A or B horizon, we used the authors defined boundaries within the individual studies (see Appendix 1 for more detail).

As is evident from Figure 2.1, subsoil (ca. 30-100+ cm) physical, chemical and biological properties significantly differ to those of topsoils. Physical soil properties, bulk density and clay content, were on average 10 and 22% higher in B horizons, while most biochemical properties were greater in the A horizon. Overall, SOC, Total N and MBC were 64, 58 and 48% lower in the B horizon. Importantly, how much properties differ between depths changes when these are split into some of the most agriculturally important soil orders (Fig. 2.2). The Inceptisol, Alfisol and Mollisol A and B horizons soil property measurements are relatively consistent with each other, apart from a lack of difference in Inceptisol clay content with depth. Ultisol and Oxisols profiles, on the other hand, are more distinct. Bulk density did not differ between soil horizons and CEC was significantly lower in the B horizon of Ultisol and Oxisols.

While the search term strategy was not exhaustive (Appendix 1, Table S1), Figure 2.1 shows that although several key soil properties involved in C stabilization in subsoils are frequently reported (e.g. pH, SOC, texture, bulk density), other important properties are not (e.g. MBC, CEC, Fe and Al oxyhydroxide content). This lack of reporting of soil quality indicators for subsoils limits our ability to determine the key regulators of deep C storage. Generally, the rates of C input to the subsoil are much lower than topsoils, and rates of release back to the atmosphere are also slow, as evidenced by the older age of C at depth (Shi et al., 2020). Why C turnover is slower in the subsoil, then, is likely due to: i) low disturbance from agricultural practices (Lal et al., 2015); ii) proportionally lower SOC and microbial biomass (Fontaine et al., 2007; Salome et al., 2010; Liu et al., 2018b), iii) the physical (in)accessibility of microbes to C substrates outside of hotspots (Heitkötter and Marschner, 2018; Dove et al., 2020; Salomé et al., 2010); iv) high abundance of available mineral surfaces (e.g. clay and Fe/Al in the Bw horizon) and Ca^{2+} for adsorption and chemical stabilization of C (Mikutta et al., 2006; Rumpel and Kögel-Knabner, 2011); and, v) the prevailing oligotrophic conditions (i.e. low O_2, N availability, pH etc.) which limit enzyme synthesis (e.g. O_2-dependent phenol

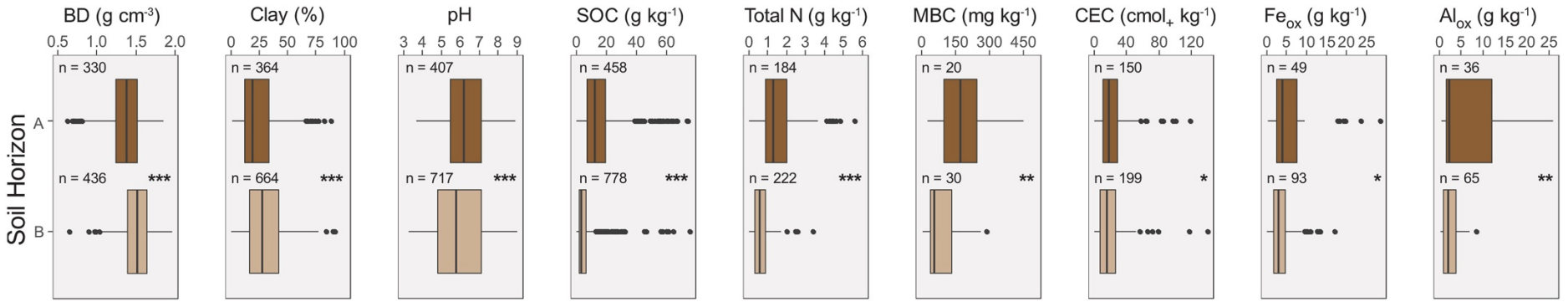

Fig. 2.1 Measured soil properties of A (*ca*. 0-30 cm) and B (*ca*. 30-100+ cm) horizons of agricultural soil profiles. Data was collected from studies (n = 203) via a systematic literature search conducted in October 2020. The n in the plots refers to the number of soil profile measurements included in the boxplot. Significance at p< 0.05 (*); 0.01 (**); and 0.001 (***). BD is dry bulk density; SOC is soil organic carbon; MBC is microbial biomass-C; CEC is cation exchange capacity; and Fe and Al are oxalate-extractable. See Apendix 1 for the search term strategy, selection criteria, data exclusion and conversion and PRISMA diagram.

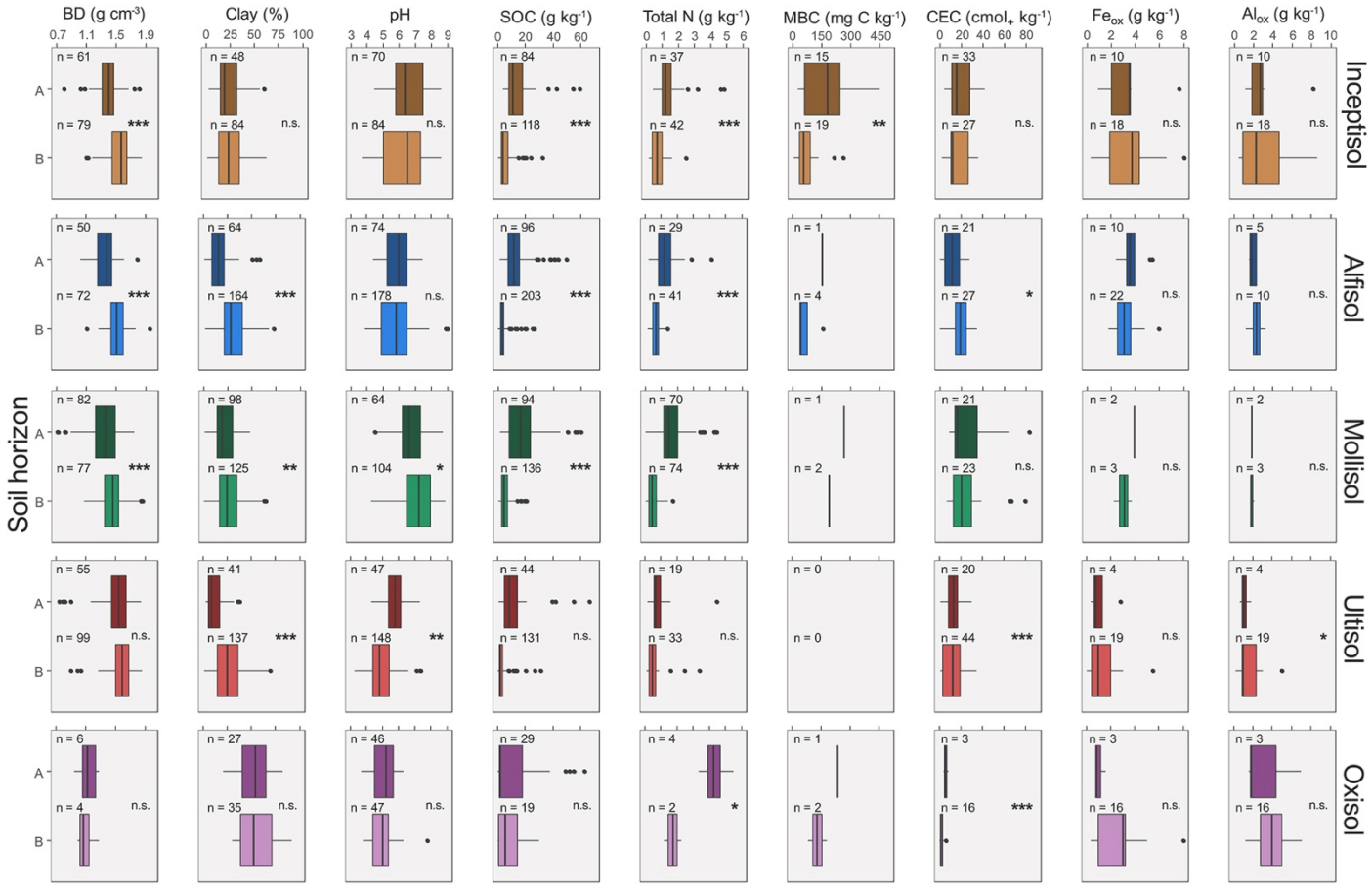

Fig. 2.2 Measured soil properties of A (ca. 0-30 cm) and B (ca. 30-100+ cm) horizons of agricultural (Inceptisol, Alfisol, Mollisol, Ultisol and Oxisol) soil profiles, ordered by least to most weathered. Data was collected from studies (*N* = 188) via a systematic literature search conducted in October 2020. See the Appendix 1 for the search term strategy, selection criteria, data exclusion and conversion and PRISMA diagram. The *n* in the plots refers to the number of soil profile measurements included in the boxplot. Significance at $p > 0.05$ (n.s.); $p < 0.05$ (*); 0.01 (**); and 0.001 (***). Where there is no sign the sample size was too small to perform a test. For more information see Appendix 1. BD is dry bulk density; SOC is soil organic carbon; MBC is microbial biomass-C; CEC is cation exchange capacity; and Fe and Al are oxalate-extractable.

oxidases) and activity (Xiang et al., 2008; Salomé et al., 2010; Shahzad et al., 2018a; Dove et al. 2020) and so microbial activity.These mechanisms underpin the mean residence times of SOC in subsoils, which are typically on the scale of millennia as compared to centuries in topsoils (Shi et al., 2020).

At the field scale, subsoils can be characterised by a high degree of spatial heterogeneity due to the presence of larger aggregate structures (e.g. prisms), preferential water flow pathways and root proliferation (White and Kirkegaard, 2010). This can lead to the creation of biological hotspots in subsoils (e.g. biopores; Chabbi et al., 2009; Kautz et al., 2013; Kuzyakov and Blagodatskaya, 2015). These hotspots of degradable substrates and associated microbial activity play an important role in C, N and P transformations in the subsoil (Hoang et al., 2016). Outside of these microsites, the inactivity of microbes may explain the measured long-term stability of SOC (Heitkötter and Marschner, 2018).

Understanding the influence of microorganisms on deep soil C is crucial because microbial products – including exo-enzymes, extracellular polymeric substances (EPS), and cell wall materials – contribute increasingly to long-lived soil organic matter in deeper soil horizons (Dove et al., 2020; Peixoto et al., 2020; Dwivedi et al., 2017; Sher et al., 2020). Recently, the number of soil microbiology studies focused on subsoils has expanded (e.g. Eilers et al., 2012; Kramer et al., 2013; Li et al., 2014; Brewer et al., 2019; Diamond et al., 2019; Polain et al., 2020). Microbial community composition, biosynthetic potential and metabolic pathways change significantly with depth, with relatively more copiotrophs present in the topsoil and oligotrophs in the subsoil (Fierer et al., 2003; Uksa et al., 2015; Jones et al., 2018; Brewer et al., 2019; Sharrar et al., 2020). The vertical distribution of these microbial groups has been found to be predominantly determined by the availability and forms of C (Fierer et al., 2003; Stone et al., 2014; Fanin et al., 2019). Deep soils are enriched in autotrophic archaea implicated in ammonia oxidation (Brewer et al., 2019) and symbiotrophic fungi (Schlatter et al., 2018) with enzymatic capacities that are distinct from their saprotrophic counterparts. Indications of methylotrophy and “dark autotrophy” (CO_2 fixation) have also been uncovered in subsoil bacterial genomes (particularly in Chloroflexi) (Brewer et el., 2019; Butterfield et al., 2016). Shifts from protozoa, fungi and Gram-negative bacteria in the topsoil to Gram-positive bacteria (and actinomycetes) with greater depth (Fierer et al., 2003; Stone et al.,

2014; Fanin et al., 2019) reflect the required adaptations for survival in deeper soil. Gram-positive bacteria, for instance, are well adapted to subsoils by their ability to sporulate, resilience to harsh environments (i.e. water limited) and preference for older more complex C derived from soil organic matter (SOM; Setlow, 2007; Kramer and Gleixner, 2008). Other strategies, such as storage of internal resources, dormancy and trophic flexibility, found in *Dormibacteraeota* which are particularly abundant in subsoils across the US (Brewer et al., 2019; Lennon, 2020), highlight the range of strategies used by microbial groups to overcome the limitations of subsoils.

Agricultural practices have been shown to strongly affect the size, structure and activity of microbial communities in topsoil, however, they appear to have less effect in subsoils where disturbance is lower, and communities seems more resilient. For example, crop type (cotton vs. maize and wheat vs. maize) and time in the cropping cycle has been shown to have relatively little impact on subsoil communities (Polain et al., 2020; Kramer et al., 2013). Inorganic fertilisation, however, can change the microbial community structure throughout the soil profile by topsoil -derived leachates altering the availability of C in the subsoil (Li et al., 2014).

Despite clear differences in microbial communities, microbial competition for C and N can be as intense in the subsoil as in the topsoil (Jones et al., 2018; Diamond et al., 2019). Findings by Jones et al. (2018) suggest that subsoil microbes are more C limited but can rapidly become active and grow upon organic C addition. This is supported by the short lag phase in CO_2 production after the addition of C substrates to subsoils particularly when high amounts of labile C are added (Cressey et al., 2018; de Sosa et al., 2018). Soil N supply also typically decreases with depth (Murphy et al., 1998; Ekelund et al., 2001; Kemmitt et al., 2008; Uksa et al., 2014; Banning et al., 2015) and inorganic N is heterogeneously distributed in the subsoil compared to the topsoil (Taylor et al., 2002; Kuzyakov and Blagodatskaya, 2015). Therefore, limited microbial access to spatially distributed substrates in the subsoil is likely an important factor for SOC accumulation and stabilization (Preusser et al., 2019).

2.2.2 Subsoil priming of SOM

Soil priming, the short-term mineralization of SOC through the introduction of labile C (Kuzyakov et al., 2000), has different controls in topsoils versus subsoils. These are driven by

differences in labile C availability (De Graaff et al., 2014), co-location of decomposers and substrates (Salomé et al., 2010), microbial responses to C inputs (Sanaullah et al., 2011), and the frequency of the inputs. However, the occurrence of priming does not mean there is no net SOC storage — in most cases where C is inputted, the resulting net C stock is higher even if some is lost to priming. In addition, due to stimulated microbial growth from priming, microbial products and necromass may accumulate and stabilise in the longer term ('entombing effect'; Liang et al., 2017) reducing the extent of C loss from priming.

Higher priming C losses have been measured in subsoil compared to topsoil (relative to native soil C content) (Salomé et al., 2010; Hoang et al., 2017; Jia et al., 2017; Meyer et al., 2018), but the opposite response has also been reported (De Graaff et al., 2014). When OM is added to the subsoil, the strength of priming is likely to be dependent on the C:N ratio of the OM being introduced and the intrinsic nutrient status of the soil (e.g. N and P status; Kuzyakov et al., 2000). If a high C:N material is incorporated, this may temporarily satisfy short-term C demand causing reduced C respiration, however, it is also likely to stimulate microbial growth and induce N mining from native SOM (Jones et al., 2018; Meyer et al., 2018).

A concern for many subsoil priming studies is that experiments are commonly conducted in laboratory conditions that poorly mimic those in the field (e.g. on sieved soil at ambient O_2 concentration) and are known to often overestimate net losses. Physical subsoil disturbance can increase C mineralization by up to 75%, as found in a laboratory incubation study by Salomé et al. (2010). This increase in SOM turnover has been ascribed to (i) improved aeration, (ii) greater physical access to C substrates previously inaccessible or held within aggregates, and (iii) the mining of nutrients from SOM. Many studies also use highly labile C substrates (e.g. glucose) at high dose rates that can drive excessive nutrient limitation. Consequently, the net C loss (priming effects) can be overestimated. Overall, our understanding of the mechanisms and factors involved in subsoil priming remains poor. It is likely that the relative balance between net C losses versus gains may vary on seasonal versus decadal timescales and in response to agronomic management regimes (e.g. subsoil C input, crop nutrient and water use) (Wang et al., 2016). To gain further insight into subsoil C dynamics, the different sources of C that reach the subsoil, mechanisms by which they are stabilised, and realistic *in situ* tests need to be considered in future studies. This will allow

interventions to enhance C sequestration in subsoils to be more effectively designed (e.g. timing, placement in the subsoil, frequency of intervention, links to root architecture).

2.2.3 Subsoil gas emissions

The behaviour and fate of GHGs in subsoils play an important role in subsoil C sequestration (Blagodatsky and Smith, 2012), and overall system C balance. Here we focus on C containing gases, CH_4 CO_2, in the context of C sequestration, although we note that N_2O fluxes (reviewed by Clough et al. (2005)) should also be considered in a holistic analysis of deep soil C sequestration strategies.

Soil CO_2 concentrations are known to increase with depth, despite fluxes decreasing with depth and not contributing substantially to surface fluxes (Davidson et al. 2004; Xiao et al. 2015; Wang et al. 2019). This suggests that CO_2 in the subsoil does not move rapidly to the soil surface and if undisturbed may be entrapped in soil pores and solution or used by subsoil autotrophs. However, this 'trapped' CO_2 is vulnerable; along a subsoil-to-surface CO_2 gradient of >10,000 ppm to atmospheric concentrations, it may only take a few hours to days for CO_2 to diffuse to the atmosphere (e.g. when CO_2 is produced near subsoil macropores or when the water-filled pore space is low; Mencuccini and Hölttä, 2010). Thus, subsoil disturbance could disturb the deep dynamic reservoir of subsoil CO_2.

Wang et al. (2019) found that while CO_2 concentrations increased with depth following a full inversion of forest subsoil to 60 cm, the soil surface CO_2 flux remained largely unaffected by the highly invasive subsoil disturbances. In the case of enhanced subsoil rooting for C sequestration, plant root uptake of water from the subsoil can lead to increased aeration, greater gas diffusivity, soil shrinkage and the formation of macropores which facilitate migration to the surface (Shaw et al., 2014). Roots can also take up dissolved inorganic C (CO_2, HCO_3^-) from soil and rapidly transport it through the xylem to the leaves where it can be refixed or released back to the atmosphere (Bloemen et al., 2016). Although the uptake rate of HCO_3^- from soil is generally low, the direct recycling of HCO_3^- produced inside the roots (i.e. from respiration) back to the shoots via the xylem may be significant in reducing CO_2 concentration in soil (Rao et al., 2019). Still, these CO_2 loss effects maybe counterbalanced by the accrual of deep root C inputs; studies of deep-rooted perennial grasses planted in low C soils found no effect of these crops on surface CO_2 fluxes and increases in total soil profile C

stocks in some soil types (Bates et al., 2021; Slessarev et al., 2020). Therefore, it is important to consider that different sequestration strategies, such as deep tillage and planting of deeper rooting varieties, may influence the soil-atmosphere flux and the soil CO_2 budget in different ways.

Over a recent decade (2008-2017), global CH_4 emissions from agricultural systems were estimated at 206 Tg y^{-1}; this represented 56% of the total anthropogenic emissions (Saunois et al., 2020; Jackson et al., 2020). To our knowledge, the fraction of this total contributed by agricultural subsoils has not been estimated. In many well-drained systems, CH_4 produced by methanogens in anaerobic microsites can be consumed by methanotrophs in oxic regions during transit to the surface (Le Mer and Roger, 2001; Wang et al., 2018), suggesting CH_4 dynamics in the soil have limited bearing on any C sequestration outcome.

Very little is known about microbial volatile organic compound (VOC) production and consumption rates in subsoils. VOCs have low-molecular-weights (typically <250 MW) with high vapor pressures. They can be produced in soil by both microorganisms and plant roots (Peneulas et al., 2014). Like CH_4, VOCs are both produced and consumed *in situ* (Tassi et al., 2009), suggesting they are unlikely to be relevant to C sequestration.

2.2.4 Subsoil carbon sources and stabilization

The primary inputs of C to subsoils include: i) root-derived C (both dead roots and living root rhizodeposition); ii) leaching of dissolved organic C (DOC) from the topsoil; iii) delivery of particulate organic matter via bioturbation or leaching, and iv) microbially-derived C (immobilization of CH_4 or volatile organic-C, dark fixation of CO_2). The primary C sources and their stabilization mechanisms in the top- and subsoil are presented in figure 3. Roots in the subsoil decompose relatively slowly, whereas topsoil and detritusphere leachates and root exudates with high C:N ratios and C availability are more easily mineralised. Subsoil microbial biomass has a slower turnover time (Spohn et al., 2016). The C:N ratio declines with soil depth in most agricultural soils (Rumpel and Kögel-Knabner, 2011; Lou et al., 2012), demonstrating that C in the subsoil cycles slower compared to soil nearer the surface.

2.2.4.1 Root-derived carbon

Plants may direct up to half of photosynthetically fixed C to roots (Jones et al., 2009) and most subsoil organic carbon (OC) is plant root-derived (Rasse et al., 2005; Suseela et al., 2017). For plants with deep rooting architecture, roots and their products (i.e. exudates and cell sloughing) have substantial potential to enter stabilised subsoil OC pools (Rasse et al., 2006; Kätterer et al., 2011; Suseela et al., 2017), and root litter decomposes more slowly in deep soils (Pries et al., 2018). While this stabilization depends on the soil environment and root physiology (Farrar et al., 2003), three primary root-derived C sources are thought to contribute to stable OC by different mechanisms (Fig. 2.3): aggregation, root biochemistry and association.

Due to the major role of biotic processes in soil aggregation, it is often thought less relevant as a C stabilization mechanism in subsoils (Lorenz and Lal, 2005). However, recent studies have revealed aggregation may be as important in the subsoil as it is at the surface (Moni et al., 2010; Sanaullah et al., 2011; Baumert et al., 2018). For example, Moni et al. (2010), found up to 40% of SOC was occluded within aggregates throughout the whole soil profile (>100 cm depth). Sher et al. (2020) found enhanced microbial production of soil-binding extracellular polysaccharides throughout a 1 m soil profile following conversion from annuals to deeper-rooting perennials, and suggest that aggregation is likely an important mechanism in subsoil C protection.

The biochemical composition of primary roots can contribute to their stabilization in soil, particularly those with significant amounts of lignin, tannin or suberin (Rasse et al., 2005). The decomposition of lignin may be slowed through protection via mineral association (Rumpel et al., 2015; Hall et al., 2016; Huang et al., 2019), accelerated by short-term fluctuations in redox states, or gut processing within earthworms (Le Mer et al., 2020). In addition, extracellular enzymes (e.g. those that decompose lignin - phenol oxidase) have been found to largely be stabilised via sorption onto mineral surfaces in subsoils (Dove et al., 2020). While tannin residence time in soil is similar to non-associated lignin (Meier et al., 2008), suberin is a major contributor to SOC with a high potential for long-term stabilization (Rasse et al., 2005; Suseela et al., 2017). In subsoils, Rumpel et al. (2004) found suberin-derived hydroxyalkanoic acids to be preferentially preserved (over lignin) in clay particle fractions. However, despite its important role in root chemistry and SOC stabilization (Suseela et al., 2017), the behaviour and persistence of suberin in subsoils remains poorly understood

(McCormack et al., 2015).

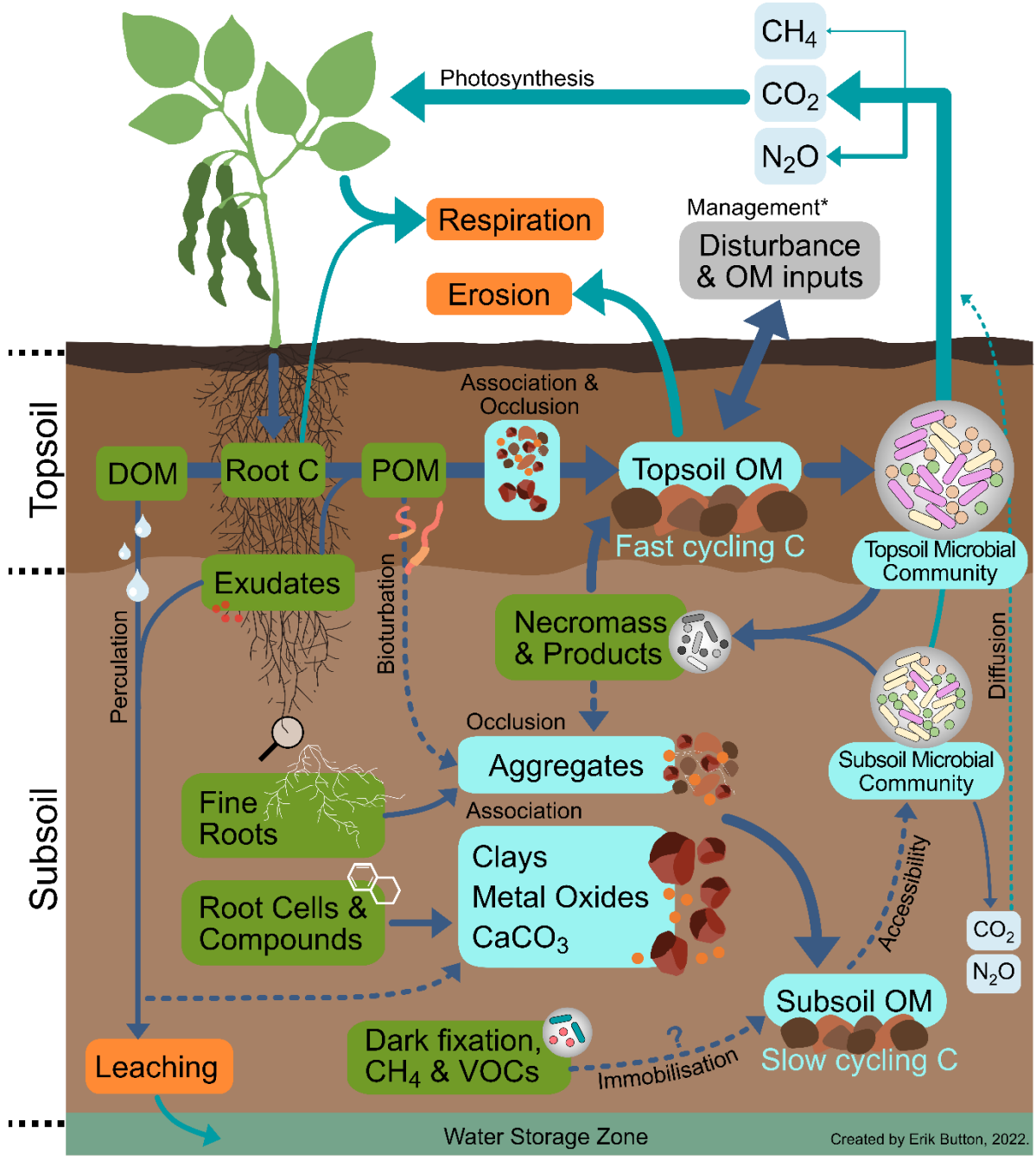

Fig. 2.3 Conceptual diagram of the top- and sub-soil C cycles, demonstrating the major SOM (soil organic matter) inputs (in green boxes); the primary components determining soil OM persistence (in cyan); agricultural management (in grey box); and losses (in orange boxes and teal arrows) in an arable system. POM is particulate organic matter and DOM is dissolved organic matter. Dashed arrows represent mechanisms that depend on certain soil characteristics to occur or that they occur at very low rates.

*The specific balance between physical disturbance and OM inputs from agricultural management determines the impact on topsoil OM.

Root exudates, organic compounds passively released from roots, can have a multitude of interactions with soil minerals (Farrar et al., 2003). For example, Keiluweit et al. (2015) showed that oxalic acid (a common root exudate) liberates C previously protected by minerals, thus promoting C loss via increased microbial availability. Although exudation varies with plant age and species, measurements of exudation and rhizodeposition suggest up to 7% of net fixed C can be deposited in croplands and 11% in grasslands (Pausch and Kuzyakov, 2018; Jones et al., 2009). Exudates contain sugars, organic acids, amino acids, fatty acids and plant hormones; these are primarily C sources that can be mineralised within hours by the soil microbial community (Rasse et al., 2005; Salomé et al., 2010, Zhalnina et al., 2018). Yet, negatively charged organic acid anions can become fixed on the surface of positively charged Fe and Al (hydr)oxides, protecting them from short-term mineralization (Jones and Edwards, 1998; Oburger et al., 2011). Other root deposits, such as mucilage and EPS, also play an important role as binding agents for aggregate formation (Baumert et al., 2018, Sher et al. 2020). Mucilage is reactive and high in hydroxy groups and can adsorb to clay particles and organic molecules (Gaume et al., 2000).

Physical separation of decomposers from exudates in subsoils may be one of the key drivers of exudate-C stabilization (Salomé et al., 2010), although very little is known about rhizosphere and root detritusphere microbial communities in subsoils. It is possible that roots also deliver C into subsoils via arbuscular mycorrhizal associations (Sosa-Hernandez et al., 2019). Subsoil arbuscular mycorrhizas are different taxonomically from those in topsoils (Sosa-Hernandez et al., 2018); however, whether they differ functionally requires further research (Wang et al., 2017).

2.2.4.2 Leaching of dissolved organic C from the topsoil

Dissolved organic carbon (DOC) represents another primary C input to subsoils. During the decomposition of SOM and plant litter, microbes produce nanoparticulate C (nPOC) and DOC) (Solinger et al., 2000; van den Berg et al., 2012). DOC consists of a complex array of organic compounds, each with distinct properties, structures, sizes, and sorptive characteristics, and play a significant role in C dynamics, soil formation and pollutant

transport (Kaiser and Guggenberger, 2000; Kothawala et al., 2012; Jagadamma et al., 2014). Organic molecules can—depending on the soil hydrology, texture and structure—enter the subsoil and become stabilised in organo-mineral complexes, mineralised, or leached into groundwater or aquatic systems (Fig. 2.3; Whitmore et al., 2015). Because DOC can be leached to great soil depths and become sorbed to form organo-mineral complexes, DOC is an important source of stabilised C in subsoils (Mikutta et al., 2006; Kramer et al., 2012); multiple studies have observed greater adsorption with increased depth, possibly due to a greater amount of unfilled sorption sites or clay in some soil types (Kaiser and Zech, 2000; Solinger et al., 2000; Jastrow et al., 2007; Moni et al., 2010).

Various stabilization reactions bind DOC to the solid phase (Solinger et al., 2000; Dignac et al., 2017), including van der Waals forces, anion exchange, cation bridging, ligand exchange, hydrogen bonding and physical adsorption, which vary in their importance depending on the functional groups of DOC and the sorbent. Clay particles and Fe and Al (hydr)oxides in the fine fraction (<53 μm) of subsoils are the primary substrates for DOC sorption (Torn et al., 1997; Jobbágy and Jackson 2000; Kaiser and Zech 2000), protecting C for thousands of years (Schöning and Kögel-Knabner, 2006; Shi et al., 2020). Some of these sorption sites can bind C very strongly (through bi- or tri-dentate ligand binding), while others are much weaker (mono-dentate binding or cation bridging). More recent microscopy studies (Müller et al., 2013; Schweizer et al., 2017) reveal that the majority of mineral particles are not colonised by microbes and are largely devoid of OC, which contrasts with older refuted studies (e.g. Guggenberger and Kaiser (2003)).

2.2.4.3 Delivery of particulate organic matter via faunal bioturbation and leaching

Faunal bioturbation may be an important aspect of subsoil C dynamics (Fig. 2.3; Wilkinson et al., 2009; Rumpel and Kögel-Knabner, 2011). Soil macro-organisms, such as earthworms, ground-dwelling rodents and termites, directly and indirectly drive both C inputs into and outputs from the top- and subsoil (Bossuyt et al., 2005; Wilkinson et al., 2009; Rumpel and Kögel-Knabner, 2011). By moving, burying and mixing vast quantities of soil and fresh OM, bioturbators have an important role in soil formation, C and N dynamics and shaping the soil environment (Wilkinson et al., 2009).

Anecic earthworms can burrow to soil depths of 1-2 m, occasionally reaching up to 5

m (Lee, 1985). By transporting fresh particulate OM into the subsoil and mixing it with mineral soil, earthworms can contribute to the heterogeneous distribution of subsoil SOC (Don et al., 2008; Rumpel and Kögel-Knabner, 2011), and mediate soil aggregate formation which is associated with SOC stabilization (Six et al., 2004). However, field and lab studies frequently find anecic earthworms induce SOM loss from increased respiration. This is likely due to stimulation of microbial activity within biopores (Banfield et al., 2017) with C-rich labile earthworm mucus and higher O_2 levels (Hoang et al., 2016, 2017). Earthworms and their casts are known to be hotpsots of N_2O emission, as they also contain high mineral N concentrations (Elliott et al. 1991; Lubbers et al 2013; Nieminen et al., 2015). Finally, Lubbers et al. (2017) found that the topsoil (0 - 25 cm) SOC content was lower after 2 years in the presence of epigeic and endogeic earthworms, suggesting faunal bioturbation diluted SOC in the topsoil by mixing it with C depleted subsoil. Termites and ants may also increase C transfer to depth either through deposition of necromass, food stores and exudates but also indirectly by creating channels in the soil that fill with water and thus move DOC and POM to depth (Jouquet et al., 2011). These channels may also stimulate aeration and rooting at depth (Banfield et al., 2018) leading to crop yield increases and thus greater C inputs (Kautz et al., 2013).

In addition to faunal bioturbation, particulate organic C (POC) can also be transported downwards in the soil profile by water. In the case of large fragments of SOM, this can occur via macropores while smaller nanoparticulate fragments can be transported through the soil matrix (Li et al., 2019). For example, viruses (ca. 20-100 nm in size) and bacteria (ca. 1-3 µm in size) applied to the soil surface in livestock manure have been measured in subsoils (Krog et al., 2017) and similarly, particles of black C have been shown to move downward in soil profiles (Leifeld et al., 2007; Major et al., 2010).

2.2.4.4 Microbially derived C

Soil microbial community structure, genomic capacity, and ecophysiology are strongly depth-dependent (Brewer et al., 2019). Understanding the influence of depth on microbial traits is crucial because microbial products – including exo-enzymes, EPS, and cell wall materials – may contribute increasingly to long-lived SOM in deeper soil horizons (Dove et al., 2020; Peizoto et al., 2020; Dwivedi et al., 2017; Sher et al., 2020). While we do not currently

have enough data to speculate too much on the persistence of root-derived vs microbe-derived SOM in deep soils, recent evidence suggests that microbially derived necromass is a major contributor to SOC (Zhang et al., 2020; Wang et al., 2021). Wang et al. (2021) estimated that half of SOC under cropland and grasslands is derived from microbial necromass and that it predominantly originates from fungi. In addition, they found that the contribution of microbial necromass to SOC increased with depth in grasslands while the opposite was true in croplands. Overall, the organisms, biosynthetic potential and metabolic pathways of deep soils differ from better-studied shallow soils (Butterfield et al., 2016; Sharrar et al., 2020; Diamond et al., 2019). For example, deep soils are enriched in autotrophic archaea implicated in ammonia oxidation (Brewer et al., 2019) and symbiotrophic fungi (Schlatter et al., 2018) with distinct enzymatic capacities from their saprotrophic counterparts (Miyauchi et al., 2020). In addition, deep soil microbes may play a particularly unique role in subsoil C accumulation through immobilization of methane (CH_4) and volatile organic carbon (VOC) or via dark autotrophy (CO_2 fixation).

Apart from surface photosynthetic CO_2 fixation and chemoautotrophic fixation, dark anaplerotic (i.e. non-photosynthetic) heterotrophic fixation of CO_2 occurs in a wide range of soils and is linked to the provision of C-skeletons for amino acid synthesis (Yang et al., 2017; Nel and Cramer, 2019). A wide range of soil archaea and bacteria are capable of dark anaplerotic CO_2 fixation in both aerobic and anaerobic conditions (Saini et al., 2011), and produce organic acids. Although the overall contribution of dark fixation is extremely small in topsoils (Ge et al., 2013), dark fixation may be proportionally more important in subsoils, presumably due to C limitations with depth (Šantrůčková et al., 2018), and higher CO_2 concentrations. As yet, there are no *in situ* studies of dark CO_2 fixation in agricultural subsoils and it is difficult to critically assess the significance of this process in the overall net C balance of subsoils. In arctic soils, Šantrůčková et al. (2018) found that long term microbial dark fixation of CO_2 corresponded to between 0.016 and 38% of plant C fixation, highlighting the uncertainties regarding the importance of CO_2 fixation in the net soil C balance. The preferred microhabitats and edaphic conditions of microorganisms responsible for dark CO_2 fixation in subsoils are also unknown.

While chemoautotrophy (i.e. C fixation from the oxidation of reduced forms of inorganic N and S; NH_4^+, S^{2-}) can be very important in extreme ecosystems (e.g. hydrothermal

vents), it is thought to be a relatively minor C fixation process in soil due to the relatively low growth yields of chemoautotrophic organisms and their inability to compete against heterotrophic bacteria. Despite this, chemoautotrophic ammonia-oxidizers and nitrite-oxidizers can be abundant in subsoils (10^5-10^8 g^{-1}) suggesting that their role in C fixation should not be discounted (Jones et al., 2018; Tao et al., 2018).

2.3 Enhancing C sequestration in subsoils

Capturing CO_2 from the atmosphere and submitting this to long-term storage in the subsoil as organic C has potential to offset substantial anthropogenic CO_2 emissions and bring a range of other ecosystem service co-benefits. Various approaches to increasing SOC in soils exist, but here we discuss strategies that aim to: i) increase C inputs; ii) reduce C losses; and/or iii) increase C residence time in soil. However, we agree with Olson et al. (2014) that 'true' sequestration is not a transfer of C, but increased C fixation from the atmosphere. The depth of the subsoil that is considered in this review for strategies to have the greatest effect is the soil to approximately 1 meter depth (i.e. an 'impressionable zone'). The volume of this zone is different at each site due to the depth of the B and C horizons, the watertable and presence/absence of a hardpan.

2.3.1 Deeper-rooting phenotypes and perennials

Use of plants with deep rooting systems, particularly perennials, has been proposed as a method to increase SOC stocks, particularly in subsoils (Paustian et al., 2016). A common concern is that increasing plant C allocation to roots decreases harvestable aboveground biomass (Powlson et al., 2011), however, a review by Kell (2012) concluded that deep roots are unlikely to limit, but may instead promote harvestable biomass. Breeding deeper rooting grass and crop varieties is a less invasive strategy (compared to those discussed above) that has substantial potential in sequestring C in the subsoil of some soil types (Smith, 2004; Kell, 2011, 2012). Deeper roots can yield co-benefits for plant productivity and drought tolerance, including improved plant capture of nutrients (e.g. N, P) and water (Kell, 2012; Lynch and Wojciechowski, 2015; Pierret et al., 2016), as well as higher crop yields (Lilley and Kirkegaard, 2011) and greater resistance to, for example, slope erosion (Dignac et al., 2017). The use of deep-rooting crops can also be readily combined with mechanical interventions to promote

access to previously compacted subsoil layers (He et al., 2019) or to the deep placement of fetilisers to promote root proliferation at depth (McEwan and Johnston, 1979).

By adopting crops that grow an extra 100 cm in depth, Kell (2012) calculates an additional 100 t C ha^{-1} could be sequestered, corresponding to a 118 ppmv reduction in atmospheric CO_2. Whether these values are accurate is difficult to determine, yet, deeper-rooting undoubtedly increases C entering the subsoil (Liebig, 2005; Omonode and Vyn, 2006; Follett et al., 2012; Ledo et al., 2020), but the benefits thereof may only be apparent in the longer-term (7-10 years), as found by Ma et al. (2000) and Carter and Gregorich (2010). This is because net SOC stock increase is a balance between enhanced root C supply to the subsoil and greater soil respiration (Schmidt et al., 2011; Shahzad et al., 2018b). This is exemplified by the relatively low increase in C in the soil profile (0.07 ± 0.02 g C kg^{-1} y^{1}) with time (Fig. 2.4). Figure 2.4 also demonstrates that higher C gains are more likely in the topsoil (0.13 ± 0.06 g C kg^{-1} y^{1}) where root density is greater, and the volume of soil is lower relative to many subsoils (0.04 ± 0.02 g C kg^{-1} y^{1}).

Perennialisation of annual crops and conversion of annual to perennial crops can enhance rooting depth and architecture, which increases C input into the subsoil (Liebig et al., 2005; Kell, 2011; Powlson et al., 2011). In addition, perennialization means less tillage and the associated C losses, allowing for more C accrual. Slessarev et al. (2020) showed that the increased rooting depths offered by perennial grasses added appreciable soil carbon in sandy and loam soil (although no SOC increase was measurable in clay-rich sites), and deep roots may also lead to changes in site hydrology and the responsiveness of deep soil microbes (Oerter et al., 2021; Min et al., 2021). Aggregation may also increase as a result of greater root biomass found by Sher et al. (2020). A meta-analysis by Ledo (2020) found an 11% increase in the 0-100 cm soil depth following conversion to perennial crops from annuals over a 20-year period. Similarly, Follett et al., (2012) found a 2 t C y^{-1} increase in the 0-150 cm depth following 9 years of maize cultivation, where the majority of the increase was below 30 cm. These results are echoed by other studies (Liebig, 2005; Omonode and Vyn, 2006) that found SOC stock gains in the whole soil profile following conversion of annual crops to perennial grasses. However, as Johnston et al. (2016) found, N_2O emissions can increase with perennials and SOC increases in the subsoil can be limited (Ma et al., 2000; Chimento et al., 2014).

Apart from breeding deeper rooting varieties, there are several potential avenues for

breeding C sequestration desirable traits in crops. For example, enhancing the root release of low molecular weight exudates and extracellular polymeric substances may promote C retention when they become sorbed to mineral surfaces or physically protected (Salomé et al., 2010; Sher et al., 2019). Furthermore, fungi, such as arbuscular mycorrhizal fungi (AMF), can reduce C mineralization by i) their complex C-containing mycelium being less mineralisable, ii) improving root lifespan, iii) enhancing root-derived C protection

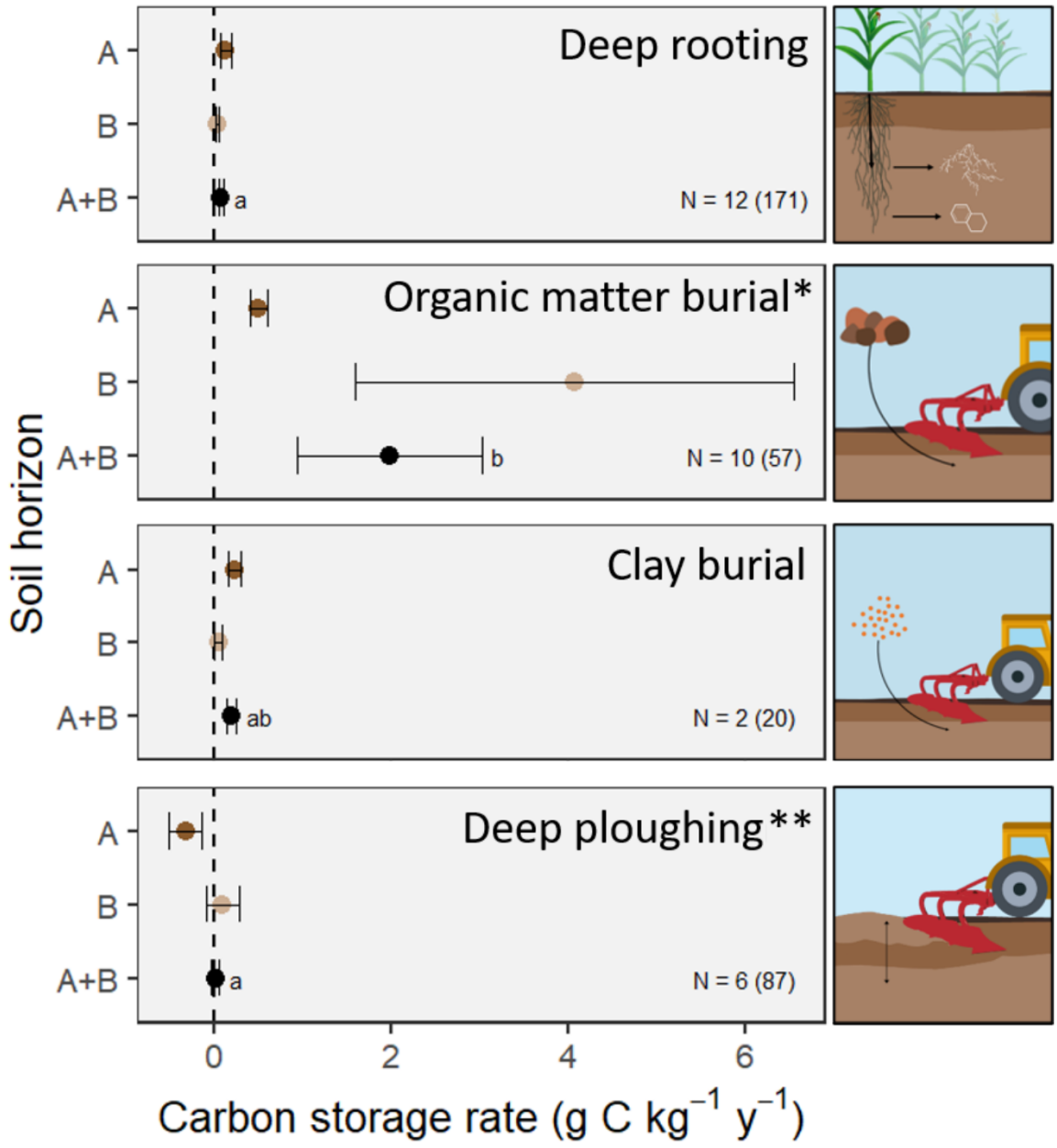

Fig. 2.4 Means (±SEM) of the carbon storage rate in the A and B horizons and the combined A and B horizons (A+B) following different subsoil-targeted C sequestration strategies. The number of studies included (N) is shown in the individual plots and the number of

measurements included are in parentheses. Different letters correspond to significant differences between means ($p < 0.05$, Tukey). See Appendix 1 (S2 and Table S4) for the search term strategy and specific inclusion criteria. *Transfer of exogenous C is not the same as C sequestration in terms of C removal from the atmosphere. **Infrequent deep ploughing (every >10 years).

in aggregates, and iv) outcompeting microbes (mostly bacteria) for N (De Deyn et al., 2008; Bardgett et al., 2014). While AMF colonisation typically decreases with depth (Bardgett et al., 2014; Lynch and Wojciechowski, 2015), it can be promoted by decreasing the N and increasing the suberin contents in roots (Bardgett et al., 2014). Increasing fine root density promotes the physical occlusion of root C within aggregates (Lynch and Wojciechowski, 2015; Dignac et al., 2017). Also, including traits associated with overcoming subsoil limitations, such as acidity (by e.g. organic acid release) would prove useful in highly weathered tropical soils. While of substantial potential, these breeding avenues are based on theory and are currently experimentally untested.

2.3.2 Organic matter burial in the subsoil

Burial of OM, such as straw, in the subsoil by deep ripping or DP (see 2.3.6) is a strategy used primarily for ameiloration of subsoil compaction, yet it can increase the subsoil C stock. This is supported by data collected from 10 studies (Fig. 2.4), which show large C gains in both topsoil (0.5 ± 0.1 g C kg^{-1} y^{1}) and subsoil horizons (4.1 ± 2.5 g C kg^{-1} y^{1}). Burial of large amounts of plant residue or animal waste adds large amount of C to the soil stock (2.0 ± 1.1 g C kg^{-1} y^{1} across the soil profile). While these are remarkable numbers, it is important to remember that a transfer of exogenous C is not the same as C sequestration in terms of C removal from the atmosphere (as defined by Olson et al., 2014). Therefore, amending the soil with large amounts of C will lead to greater C stock. Yet, it is both unlikely that all of the introduced C will remain (Leskiw et al., 2012; Liu et al., 2018b) or that it increases C fixation of atmospheric C, meaning the gains in figure 4 are not 'true' C sequestration. In addition, the physical disturbance required to input labile OM at depth may promote access to previously unavailable C (Salomé et al., 2010). This response is confirmed by Shahzad et al. (2018a) who observed increased respiration rates of buried C4 maize litter in C3 subsoil (55-75 cm) compared to the topsoil (0-15 cm). This was attributed to a i) growth in the biomass of subsoil

microbes which are more limited by the availability of labile C than in the topsoil; ii) improved co-location of decomposers and substrate, and finally; iii) microbial N mining, as the litter introduced is nutrient-poor (C:N of 21:1) compared to native subsoil OM (C:N of 8.5:1). Therefore, if this is to be pursued as a C sequestration strategy, it is important to ensure additions are driving 'true' accrual of C.

2.3.3 Biochar burial

Due to its aromatic structure, biochar is extremely resistant to breakdown (Farrell et al., 2013; Naisse et al., 2015), with commonly <3% of biochar-C decomposing in the first 1-2 years (Major et al., 2010; Jones et al., 2011; Naisse et al., 2015; Wang et al., 2016). This recalcitrance has stimulated interest in its use to store C for climate change mitigation (Das et al., 2014; Smith, 2016). The application of biochar to topsoils has been extensively researched (Song et al., 2016) and surface-applied biochar has limited downward movement potential (Major et al., 2010) To date, there have been relatively few studies on biochar burial in subsoils, particularly at the field scale, however, the limited evidence suggests that it can have positive agronomic benefits when buried at or below 30 cm (Bruun et al., 2014; Iijima et al., 2015). In many cases, however, its C sequestration potential and practicality have been exaggerated. Similar to OM burial, it typically does not cause a truly 'additive' C effect, nor net removal of CO_2 from the atmosphere (Chenu et al., 2019) at the landscape scale, and the negative impacts have often been ignored (Jones et al., 2011; Hilber et al., 2017; Baveye et al., 2018). Further agronomic trials are therefore required to critically evaluate subsoil biochar burial as a mechanism to promote long-term C storage.

2.3.4 Iron (hydr)oxide additions

The most important control of C persistence in the soil is believed to be its association with minerals via sorption (Torn et al., 1997; Lehmann and Kleber, 2015). Of these minerals, Fe and Al (hydr)oxides are widespread in most soils at varying concentrations and have been consistently found to adsorb SOC and increase in concentration with weathering (Kaiser and Guggenberger, 2000; Mikutta et al., 2006; Lalonde et al., 2012). In this review, we focus on Fe (hydr)oxides, due to the large production of iron-containing sludge from the wastewater treatment process (Chen et al., 2015), which could be used for the chemical modification of

subsoils.

Lab-based experiments investigating the association of OC with Fe (hydr)oxides report substantially decreased decomposition from Fe-associated SOC (Jones and Edwards, 1998; Mikutta et al., 2007; Wen et al., 2019a). In forest soils, a high proportion of stable OC is bound to iron (Mikutta et al., 2006; Zhao et al., 2016). Furthermore, Porras et al. (2018), found that <0.5% of Fe-associated glucose added to a subsoil decomposed compared to non-associated glucose, with the effect strongest at 50-60 cm depth. As glucose is neutrally charged and does not associate with sorption surfaces, it suggests that an indirect mechanism is involved in suppressing C turnover (e.g. availability of nutrients such P, or mobility of microbes and exoenzymes). Also, this Fe-associated SOC was found to be more resistant than native SOC to increased temperatures (Porras et al., 2018). These promising results, albeit from a handful of lab-based studies, suggest that adding iron or iron-associated OM into subsoils may be an effective strategy for stabilising and sequestering subsoil SOC, respectively. However, a limited evidence base (especially at the field scale) means further research is needed before this strategy can be meaningfully evaluated.

The degree of soil C that is saved from mineralization from Fe addition in the field is likely to be dependent on several factors, including the method of subsoil application, the mineral makeup of the soil, the native subsoil C content, soil pH as well as texture and parent material (Button et al., 2022). This method may be particularly relevant in sandy soils where little chemical protection potential exists in the subsoil but of limited relevance to highly weathered soils already rich in Fe. Building a greater evidence base, especially with field studies, will allow for better evaluation of the potential of this strategy.

2.3.5 Clay addition to subsoil

Similar to the discussion above for Fe, clay addition also has the potential to bind large amounts of SOC. While clay addition has been used to improve SOM and nutrient retention in sandy topsoils (Cann, 2000; Shapel et al., 2019), its addition to sandy subsoils has received less attention. In this scenario, the clay would be added to the soil surface and then incorporated by mechanical soil inversion. While this approach shows promise (Hall et al., 2010; Churchman et al., 2014; Fig. 2.4), evidence is limited and the practicality and long-term impacts on C storage are not yet known.

2.3.6 Deep ploughing

Natural instances of soil burial demonstrate that SOC can be stabilised for millennia (Chaopricha and Marín-Spiotta, 2014; Wang et al., 2014a). Mechanical soil inversion techniques, such as deep ploughing (DP), rotary hoe or spading of agricultural land (i.e. mechanical inversion of the soil >30 cm depth), buries more C-rich topsoil and plant residues at depth allowing C accumulation in a 'new' unsaturated C-poor topsoil (Nieder et al., 1995; Alcántara et al., 2017, 2016). However, many disregard DP as a soil management option and suggest that any C input from DP is outweighed by the C lost to respiration (Freibauer et al., 2004; Fontaine et al., 2007; Powlson et al., 2011). Studies that claim this, however, rarely match the timescales at which DP is deemed effective (>10 years), do not fully balance C inputs and CO_2 lost by respiration, lack experimental evidence, or often focus only on CO_2 fluxes and not changes in the C stock.

Alcántara et al. (2017) found that 36-48 years after DP (to a depth of 55-90 cm) arable land, SOC stocks increased by 67% compared to a reference subsoil and resulted in substantially lower GHG emissions compared to conventional and zero-tillage management. The specific mechanisms driving the stabilization of the buried topsoil are untested, but lower microbial activity, a physical disconnect between decomposer and substrate and access to unsaturated mineral surfaces deeper in the soil are likely primary drivers (Salomé et al., 2010; Schiedung et al., 2019). More recently, Schiedung et al. (2019) found that 20 years after DP (100-300 cm) total SOC stocks (0-150 cm) increased by 69%, a marked annual C sequestration rate of almost 9 t C ha^{-1} y^{-1}, but interestingly the 'new' topsoil had 36% less SOC than the original topsoil, possibly due to a lower C sequestration capacity. This is supported by Alcantara et al. (2016), who found that 'new' topsoils contained 15% less SOC even 3-5 decades after DP, suggesting that the capacity of the 'new' topsoils to sequester C was low in their study; we expect this is highly context dependent.

The results from 6 studies of different soils where SOC was measured in the A and B horizons before DP and 12-48 years after are presented in figure 2.4 (methods in Appendix 1). These results demonstrate that i) buried topsoil drives a C increase in the subsoil (0.09 ± 0.2 g C kg^{-1} y^{1}); and ii) DP had an overall limited effect on the net C stock (0.004 ± 0.05 g C kg^{-1} y^{1}). Based solely on this data, DP is the least effective of the strategies for which sufficient

data was available. However, 2 important factors were determined for the success of DP. Firstly, the timespan between DP and SOC stock measurement is important (i.e. more time allows for greater accumulation of C in the 'new' topsoil). Secondly, the location and soil type are crucial to the DP sequestration outcome. DP should not be done when i) soil has high contents of very old SOC, ii) the topsoil is low in C, iii) the soil has a high stone content, iii) steep slopes are present where erosion will be high, or v) subsoils are unfavourable for plant growth (e.g. Al^{3+} and Mn^{2+} toxicity at low pH or Na^{+} toxicity in alkaline soils). Subsoils with <70% silt content that restrict root growth could benefit from DP (Schneider et al., 2017) and sequester SOC (FAO, 2017). Duplex soils (sand over clay; often with a perched water table at the interface) could also benefit from DP where the new surface soil layer has increased clay content while the subsoil has better drainage. Increased plant production and deeper rooting depth on such soils could lead to greater C sequestration.

Mapping the areas with potential for soil inversion and establishing longer-term field studies will be essential to underpin any widespread DP implementation as a management practice for C sequestration. While DP is an expensive process if only used to change SOC profiles, the machinery and additional fuel costs could be offset through increased plant yield in soils where ameliorating subsoil constraints can occur at the same time (e.g. mixing with lime; uplift of subsoil $CaCO_3$; improved aeration, compaction alleviation), or where existing surface soil problems (e.g. herbicide-resistant weed seeds) become buried at sufficient depth to remove this constraint to crop production.

2.3.7 Subsoil water table management

In most cropping soils, a low water table depth is desirable to promote effective rooting. If the field is not free draining, then subsoil artificial drainage is installed to lower the water table and improve aeration. From a limited number of studies, this physical disturbance and change in conditions has not been shown to have a major effect on GHG emissions (Dobbie and Smith, 2006; Valbuena-Parralejo et al., 2019) and C storage in mineral soils (Mayer et al., 2018). This suggests that artificial drainage may indirectly provide an effective way to deliver C deeper into the soil profile.

In contrast to mineral soils, the drainage of agricultural peatlands has resulted in very large net SOM loss rates (equivalent to 12 t C ha^{-1} y^{-1}; Taft et al., 2017). This breakdown of SOM

also leads to the release of plant-available nutrients making these soils some of the most productive in the world. In many cases these C stores have taken tens of thousands of years to accumulate, however, they are being lost within decades in some cases. This rapid loss of natural capital is fuelled by the removal of anoxic constraints on native SOM decomposition by microbes and mesofauna (Wu et al., 2017). However, at soil loss rates of 1-2 cm y^{-1}, this practice is clearly unsustainable and mitigation strategies are required to preserve the remaining SOM. Raising the water table, therefore, offers an opportunity in these peat soils to re-establish anoxic conditions and prevent SOM loss from deeper peat layers. If the water table is raised, however, care must be taken not to negatively affect root growth (and thus yields) and also not to create conditions that would be conducive to N_2O and CH_4 release. An experiment where the water table was raised to 30 cm of the soil surface was found to reduce total GHG emissions from 80 to 25 kg CO_2-e ha^{-1} d^{-1} (Taft et al., 2018). Wen et al (2019b) showed the importance of the C/N ratio of cover crop residues on total GHG emissions when raising the water table from 50 to 30cm; with vetch (low C/N ratio) resulting increased N_2O and total GHG emissions, and rye (high C/N ratio) resulting in reduced N_2O and total GHG emissions. While proving effective at reducing C losses, raising the water table makes the soil physically unstable, unsuitable for vehicle trafficking and also prone to flooding. This highlights the trade-offs between the effectiveness and practicality of C mitigation options.

2.4 Challenges and opportunities – looking to the future

2.4.1 Genetic engineering - can we modify subsoil rooting?

The demand for food to feed an increasing world population, in a future of climate instability, limited supply of P-rich ore (van Vuuren et al., 2010), and a global imbalance of N fertilizer availability (Springmann et al., 2018), will place additional pressure on agricultural land, with new land clearings causing further SOC loss. At the same time, climate change is affecting food staples variably (Peñuelas et al., 2017, Ray et al., 2019). Accelerated improvement to crops to tackle food security is possible with technologies such as gene editing (e.g. CRISPR cas9; Chen et al., 2019) being applied to improve traits, such as yield, disease and salt tolerance, and plant architecture (Energy Futures Initiative, 2020; Lian et al., 2020). The advantage of gene editing is that the genome of a species can be targeted to suppress undesirable traits or turn on and over-express desirable traits (there is no foreign

DNA added). This technology is now permitted for application within the agricultural sector in some countries (e.g. USA, Australia) with others still debating its use. In the context of this review, we foresee an opportunity for gene editing to alter root systems (e.g. targeted root exudates) and to change the lignin lattice (composition and structure) to form a less biodegradable plant residue. This potential has already been highlighted in rice and tomato plants using CRIPR cas9 where the production and exudation of strigolactones has been successfully modified to promote plant growth (Butt et al., 2018; Lian et al., 2020). It has also been used as gene editing tool to alter root branching frequency and branching angle in tobacco and rice (Bettembourg et al., 2017; Gao et al., 2018; Kitomi et al., 2020). Lignin is a major component of plant cell walls accounting for 30% of the organic C in the biosphere (Ralph et al., 2004). Its metabolic pathways and function in plants are well characterised; Liu et al. (2018a) review the basis for genetic improvement of lignin. Xu et al. (2019) have also demonstrated how CRISPR cas9 can be used to change the secondary metabolite composition in roots while Gasparis et al. (2019) have shown how it can be used to alter a range of root morphology traits. As yet, these technologies have not been harnessed to alter rhizosphere C flow or promote C storage in soil (Energy Futures Initiative, 2020).

2.4.2 Climate change - what are the consequences for subsoil SOC stocks?

Rising atmospheric CO_2 can increase the growth and grain production of C_3 crops and benefit C_4 crops experiencing drought stress (Fig. 2.5). Kimball (2016) reviewed 27 years of free -air CO_2 enrichment experiments and found biomass and yield were increased by eCO_2 in all C_3 crop species by 19%, but not in C_4 species except when water was limiting (30%). Conversely, drought stress and rising atmospheric O_3 cause negative impacts on plant production. How climate change will impact subsoil SOC stocks and microbial C utilisation rates is less clear. Elevated atmospheric CO_2 is projected to increase the quantity of C flow to root exudates (Phillips et al., 2011; Fig. 2.5); however, this may not necessarily translate into an increase in SOC due to a concomitant increase in microbial activity (Keiluweit et al., 2015; Kuzyakov et al., 2019). Pries et al., (2017) found that warming forest soil to 100 cm by 4°C increased respiration of the whole soil profile by 34-37%. Subsoils contributed the majority to this (20-25%) with millennial old C respired. This is echoed by a recent meta-analysis of over 100 eCO_2 studies suggesting soil carbon storage declines when plant biomass is strongly

stimulated by eCO_2 in forests, however, grassland soils have a large capacity to drawdown CO_2 and have increased SOC stocks (Terrer et al. 2021). As well, Baumert et al. (2018) found that increased subsoil exudation caused a 10% increase in SOC, due to a stimulation of fungi. Research is currently lacking to answer the key question - *are subsoil SOC stocks in mineral and organic soils secure from climate change?*

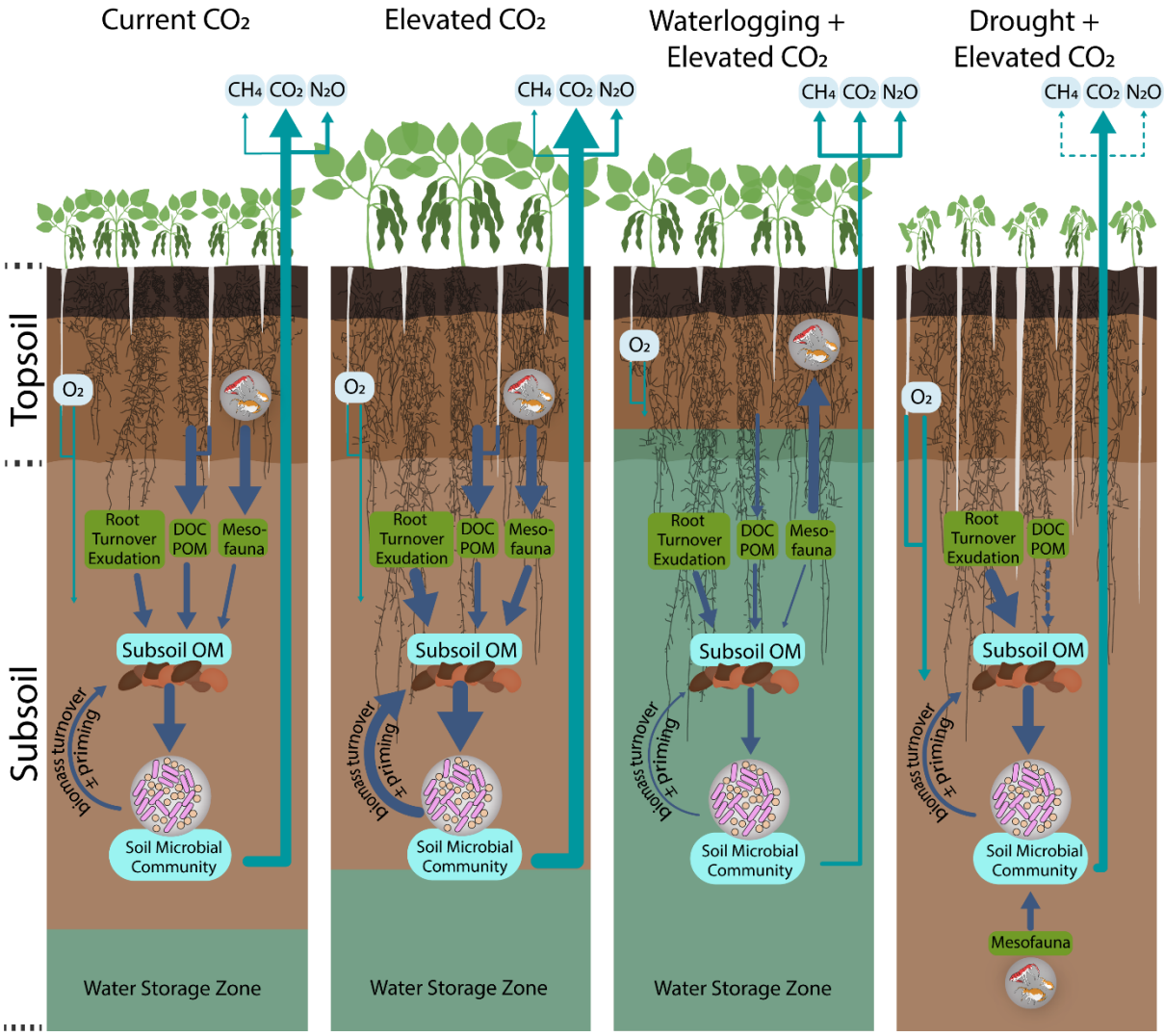

Fig. 2.5 Schematic representation of how mineral subsoils (i.e. Mollisol, Alfisol) will likely change in response to different climate change scenarios with potential feedbacks in the C and N cycles. Elevated CO_2 will induce plant growth, deeper rooting and more rhizodeposition in the subsoil. This will promote enhanced subsoil microbial activity and may induce subsoil priming of old SOM. The drying in combination with more microbial activity will stimulate more mesofaunal activity and bioturbation at depth. The greater formation of macropores (represented by the white vertical lines extending from the soil surface into the soil) due to greater topsoil drying will promote greater gas exchange and aeration of the subsoil. This will reduce the plant available water wet zone in the soil. Elevated CO_2 in combination with

freshwater waterlogging will decrease C turnover and force mesofauna closer to the soil surface. The dashed lines are dependent on water availability, which are in low supply during droughts. This model assumes there are no constraints to deep rooting (e.g. due to excess acidity, salinity or compaction).

Extremes in climate events will increase with global warming causing increased frequency of wet-dry cycles (Meehl et al., 2007; Fig. 2.5). To some extent, subsoils will be buffered from extremes in temperature and moisture due to the overlying topsoil (Wordell-Dietrich et al., 2017; Qin et al., 2019). Gobel et al. (2011) proposed that the soil C balance is sensitive to climate extremes that decrease the wettability of soil and thus increase water repellence. This would increase surface water run-off and cause heterogeneous preferential flow pathways through the subsoil (Fig. 2.5); causing potentially less plant growth and more spatially variable root growth leading to less subsoil plant root C inputs. Water repellence in both surface and subsoils will also cause the water inside soil pores to form as droplets instead of continuous water films (Goebel et al., 2007). Disconnect in water films, as a consequence of water repellence, will restrict the diffusion of DOC (Or et al., 2007) and nutrients which will limit microbial uptake. This disconnect in water films is likely to also increase the stability of existing SOM against biological enzymatic decomposition thus increasing SOC residence time (Goebel et al., 2007). Water repellence is already widespread globally (Goebel et al., 2011) and is expected to become more frequent. How this alters the SOC balance is uncertain and highlights the need for SOC models to take account of differences in SOM turnover rates in water repellent soils.

2.4.3 Microbial survival in subsoils - are there unknown metabolic pathways?

Microbial cells exist in both metabolically active and dormant states. Jones and Lennon (2010) proposed that dormancy contributes to the maintenance of microbial diversity; fast-growing species use energy sources to grow competitively, whereas slow-growing species use greatly reduced metabolism (i.e. anabiosis) to outcompete other species during periods of energy starvation. This enables slower-growing organisms to exist without direct competition with fast-growing species. It is expected that in C-limited subsoils microbial competition for SOC sources required for energy-generation (i.e. electron donors) will be

intense. This poses the question - *Do we fully understand microbial metabolic pathways in slow-growing (oligotrophic) species within subsoils and does this impact on C storage?*

The discovery of alternative microbial energy pathways in surface soils suggests more understanding is needed. Research by Greening et al. (2015) highlights that an aerobic heterotrophic acidobacterium uses H_2 oxidation from atmospheric scavenging when organic electron donors are scarce. Hydrogenase-encoding genes were subsequently identified in 51 bacterial and archaeal phyla (Greening et al., 2016). Furthermore, Ji et al. (2017) found atmospheric H_2, CO_2 and CO gases to be energy sources for Antarctic surface soil communities. Atmospheric CO oxidation enables the survival of aerobic heterotrophic bacteria in energy-limited environments and has been found in many species of soil bacteria and archaea (Cordero et al., 2019). These findings highlight that trace gas oxidation may be a general mechanism for microbial persistence in topsoils (Greening et al., 2016). Such exploratory genomic studies warrant investigation in both oxic and anoxic subsoil layers.

2.4.4 What are the key challenges in studying subsoils and can they be overcome?

Soil sampling depth has largely been driven by interest, practicality, and cost. This is reflected by a majority of C studies focusing on shallow soil layers (<30 cm; Yost and Hartemink, 2020). However, sampling below this in agricultural systems is not that difficult with use of sharpshooter, hammer and semi-mechanical soil corers, while hydraulic probes can be rented cost-effectively for deeper sampling. Indeed, deeper sampling used to be more common (Yost and Hartemink, 2020), so why is sampling becoming shallower? Although there is no current explanation, it could simply be because sampling deeper creates more samples to collect, process and analyse. We would like to argue that sampling deeper is worthwhile and to urge the soil science community not to stop sampling deeper. This is especially important as subsoils are different (Fig. 2.1 and 2.2) and changes in SOC stock may be vary through the soil profile (e.g. Tautges et al., 2019) which topsoil sampling would miss, resulting in potentially misleading results and interpretation. In the case of *in situ* studies, there are different ways to take samples actively or passively (e.g. subsoil gas sampling systems; see Maier and Shack-Kirchner, 2014), with relative ease and limited soil disturbance which can greatly improve our understanding of the deep soil environment. Nevertheless, *ex situ* studies remain the more common practice (Rumpel and Kögel-Knabner, 2011), however, adequately

simulating subsoil environmental conditions (e.g. lack of disturbance, lower O_2 concentrations, different temperature and moisture contents, etc.) is difficult, making these more variable and less appropriate for extrapolation to field conditions.

Both SOC content and bulk density variability contribute to C stock uncertainty, in turn affecting how large a change in stock can be observed through time or space. In the Western Australian SOC Audit, for example, Holmes et al. (2012) determined that variability in SOC (%) contributed to 84-99% of the uncertainty in C stocks compared to <5% from bulk density. They illustrated that the rapid indirect measurement of bulk density using a gamma-neutron density meter could be used in place of labour-intensive traditional volumetric rings or clod measurements. Scanlan et al. (2018) have since developed a hand-held 3-dimensional scanning system based on a time-of-flight camera to measure the volume of the void created when using any excavation method (ring, auger, or shovel). This system was shown to measure bulk density accurately and rapidly in soils tested (35-71% gravel content; 0-40 cm depth).

Both near- and mid-infra-red (NIR, MIR) scanning of soil has been shown to provide accurate estimates of SOC content (%) once properly calibrated (Hutengs et al., 2019). In-field scanning of intact soil cores collected to depth provides a rapid means of determining SOC content with the added advantage of also having IR predict SOM fractions required for SOC model initialisation as well as a range of soil properties (e.g. clay %) which are required for C models. These soil layers can then be recovered for additional chemical and biological analysis.

2.4.5 What is the size of the subsoil C reservoir and how much more can be stored?

To determine how much additional C can be sequestered globally requires that we know how much C is currently present in the soil (Smith et al., 2020). A consensus on the size of the global SOC stock, however, is lacking, with estimates ranging from 500 to 3000 Gt C (Todd-Brown et al., 2013; Scharlemann et al., 2014). This variation in estimates occurs due to variations in model parameters and different soil depths considered in each study (Harrison et al., 2011; James et al., 2014). The alternative, mapping of soils by extensive geochemical sampling projects, has covered the majority of Europe (FOREGS; Salminen et al., 2005), the USA (NASGLP; Smith et al., 2014b), China (GCB; Wang et al., 2014b) and Australia (NGSA;

Caritat and Cooper, 2011), often also including deep soil samples. While time and resource intensive, this is the best way to get high quality fine-scale data to quantify the global C stock and identify areas where sequestration can be most successful. We encourage colleagues from the Middle East, Eastern Europe, South and Central America, South Asia and Africa to pursue extensive mapping programs.

Smith et al. (2020) argue that to implement C sequestration initiatives, we need more reliable SOC change monitoring, reporting and verification platforms for policymaker support and gaining investments. Similar to the uncertainties of the soil C stock, consensus on how much more C can be sequestered in soil has not been achieved (Minasny et al., 2017; Zomer et al., 2017). This is due to the mentioned issues with stock estimates and differences in the sequestration strategies, land type and how SOC change is measured (Smith et al., 2020). Frequently, the depth of soil C estimation is not stated. As a result, over- or underestimation of the sequestration potential may occur. Current evidence for topsoils suggests that the soil C sink will eventually reach saturation (Solinger et al., 2000; Hoyle et al., 2013; Smith, 2016; Wiesmeier et al., 2015) after approximately 20 to 80 y of positive C sequestration management (Lal and Bruce, 1999; Minasny et al., 2017; Poulton et al., 2018). As the rate of accumulation is non-linear and decreases soon after it begins, estimated annual C sequestration rates can only realistically be achieved within the short-term. Many studies do not indicate a time within which this rate can be achieved, so their accuracy remains unknown. Furthermore, when management practices targeting greater C accrual in subsoils are discontinued, it is important to consider whether the C sequestered will be susceptible to being lost, and if so at what rate. The recent UN FAO program for the global assessment of C sequestration potential (GSOCseq; FAO, 2019) is a promising new vision that aims to build the international capacity of SOC change monitoring, reporting and verifying which will be essential in moving C sequestration forwards.

2.4.6 What are the limitations of existing subsoil C simulation models?

Soil C models are essential for predicting SOC sequestration over long timescales (> 50 years; Chenu et al., 2018), however, they are only useful if parameterised properly (Dignac et al., 2017). Currently, the majority of C models (e.g. RothC, Century) are only designed to describe topsoil C dynamics (Smith et al., 1997; Stockmann et al., 2013). Also, the depth of

soil that the C stock is estimated to is often not reported in these models, making comparisons between the results of models challenging (Stockmann et al., 2013; Todd-Brown et al., 2013). As surface and subsoil C characteristics and dynamics are substantially different (as demonstrated by Salomé et al., 2010; Sanaullah et al., 2011; Hoyle et al., 2013; Zieger et al., 2018; Qin et al., 2019), model parameterisation must be different for subsoils. While subsoil models exist (Table 1), they are relatively recently developed, vary in their description of C, their accuracy and the depth of C they measure. This is mostly because (reliable) estimates for C supply and subsequent transformation rates do not exist for multiple soil layers (Keyvanshokouhi et al., 2019) or are not linked with other factors that affect subsoil C storage (e.g. N availability, carbonate content). While progress in subsoil C models has been made, a greater mechanistic understanding of the specific subsoil C inputs as well as more extensive field-derived data will be required to further optimise existing models (Taghizadeh-Toosi et al., 2014) and be able to reflect potential strategies to increase subsoil C content.

Another aspect that needs consideration in soil C forecasting models is better climate projections for agricultural subsoils (i.e. frequency of wettability). For example, in regions that receive less rainfall, subsoils will become progressively drier, microbial activity will slow and more C may accumulate. This drying may promote feedbacks such as deeper rooting, leading to greater removal of water, changes in nutrient availability which will affect subsoil C dynamics (Fig. 4). In contrast, saturated subsoils may dry out and shift from being anoxic to oxic and thus SOM may decompose faster. As for topsoils (Jiang et al., 2014), there is a clear need to link climate forecast models to C models, preferably with climate models that also incorporate extreme weather events.

Table 2.1 Models that address different C-related processes in topsoils and subsoils.

Model name	Function	Additional Information	Reference
-	C estimation	Non-linear mixed effect model for estimation of forest soil (to 2.5 m) C.	James et al. (2014)
-	C estimation	Linear function for topsoil and power function for subsoil (to 0.75 m).	Beem-Miller and Lehmann (2017)
RothPC-1	C turnover estimation	Subsoil (to 1 m) version of topsoil RothC model with 2 new parameters.	Jenkinson and Coleman (2008)
ECOSSE	C turnover estimation	Evaluation of model in predicting SOC dynamics (to 1 m).	Dondini et al. (2016)
ECOSSE	C sequestration estimation	8 year simulation of C and N dynamics (to 0.3 m).	Khalil et al. (2013)
DailyDayCent	C sequestration estimation	Simulation of long-term C storage (to 0.2 m) in agricultural soils with different additions.	Begum et al. (2017)
C-Tool	C sequestration estimation	Simulation of medium - long-term C storage (to 1 m) in agricultural soils.	Taghizadeh-Toosi et al. (2014)
OC-VGEN	C sequestration estimation	Simulation of long-term C storage (to 1.2 m) in agricultural soils with different management scenarios.	Keyvanshokouhi et al. (2019)

2.4.7 What factors will affect the likely success of subsoil interventions?

The overall success of different interventions to promote subsoil C storage depends on (i) their effectiveness to store C in the long term and the evidence to support this, (ii) their impact on other ecosystem services (including agricultural productivity), (iii) cost of implementation, (iv) practicality, (v) social acceptability, (vi) legislative barriers, and (vii) overall C cost of interventions (i.e. is more C stored than released in the process?). The importance of these is likely to be highly context-specific varying from farm-to-farm and country-to-country. For example, mechanical interventions may not be cost-effective or feasible by smallholder farms, whereas plant-based solutions may be implemented by all landowners. Strategies promoting higher subsoil C storage (e.g. DP, OM burial, deep rooting

crops) are likely to improve nutrient cycling and water-holding capacities, leading to increases in crop yield (Gregorich et al., 1994). These win-win-win scenarios (i.e. more C, greater water use efficiency, higher yields) should help promote the adoption of subsoil technologies by farmers. In the case of OM, biochar and Fe additions to the subsoil, mechanical intervention is required. Although not mainstream, most of this equipment is commercially available to allow wide-scale adoption of subsoil technologies should these options gain support. One barrier to overcome in some countries is the legalities surrounding the addition of C-rich wastes to agricultural land. This will need a strong scientific evidence base and may take a long time for legislation to be passed. Lastly, it is known that some farmers can be resistant to change (cultural inertia; Hyland et al., 2016) and that there is resistance to geoengineering approaches to tackle climate change in both the public and scientific community (Robock et al., 2015). In addition, costs, practicalities and training needs may need addressing. Realistically, financial incentives for farmers (e.g. via the carbon market or agri-environment schemes) could be used to promote subsoil C technologies (Siedenburg et al., 2012). There is also a need for policymakers and extension agencies to focus on knowledge exchange and awareness programs, making use of the multiple co-benefits related to adopting pro-subsoil C behaviour (van de Ven et al., 2018).

2.5 Concluding remarks

Due to their favourable characteristics and conditions, subsoils have a large potential to offset CO_2 emissions by sequestering C. A growing body of evidence suggests that, due to their large volume, less disturbance and more static nature, subsoils have the potential to sequester more C than topsoils, highlighting the importance of undertaking further studies on deep soils. Nevertheless, based on the evidence herein we suggest the best current strategies for enhancing full profile C sequestration success are:

- Use of deeper rooting varieties is a cheap and easy way to enhance the C supply to the subsoil. While tangible benefits may take years to establish, it is likely to be more effective in lighter soils and those not with old C-rich subsoils.
- While additions of OM and biochar to subsoils increase the C stock and can be beneficial, these are unlikely to lead to ‘true’ C sequestration.

- Addition of iron and clay to subsoils may be effective in very specific soils, but current evidence is not sufficient to recommend their widespread adoption.
- Deep ploughing (DP) can be effective when >10 years apart and in soil that does not have high contents of very old SOC; C-poor topsoil; a high stone content; steep slopes; or unfavourable subsoils for plant growth. Silty and Duplex soils could particularly benefit from DP.
- Water table management can be highly effective in enhancing C sequestration. In mineral soils lowering the water table can allow for greater C delivery in the subsoil, while in organic soils raising it is beneficial to C sequestration – but not for agricultural capability.

Based on the evidence presented, we have also identified 5 key knowledge gaps and priority areas for future research:

1. Improve our understanding of the mechanisms that regulate C stabilization in subsoils and the factors driving long C residence times (e.g. rates of subsoil C supply and loss; stabilization mechanisms of suberin and DOC; sorption of SOC to minerals; role of Ca^{2+} and $CaCO_3$ in C stabilization, role of microbes in SOC residence time; persistence of microbial necromass; spatial organisation of roots, microbial communities and SOC).
2. Undertake studies that take advantage of space-for-time substitutions, long-term field and chronosequence studies of subsoil sequestration technologies (in isolation or combination). These studies also need to consider the trade-offs between different ecosystem services and the overall effects on soil health as well as their practicality and economic viability.
3. Perennialisation and improvement of deep-rooting traits in crops and grasses that promote greater subsoil C storage (e.g. by harnessing gene-editing technologies; better selection of rhizosphere communities; better *in situ* techniques for studying subsoil root dynamics).
4. Investigations into how climate change, especially changes in moisture status and extreme weather events, will affect subsoil C storage.
5. Use the information gathered above to improve the parameterization of soil profile- and landscape-level models of subsoil C dynamics that allow us to simulate the impact

of different land management and future climate scenarios on subsoil C, but also improve global climate models.

2.6 Acknowledgements

This work was supported by the FLEXIS (Flexible Integrated Energy Systems) programme funded by Welsh Government and the Australian Grains Research and Development Corporation's project (DAW1801-001RTX) titled "Nutrient re-distribution and availability in ameliorated and cultivated soils in the Western Region". J. Pett-Ridge's contribution was supported by the LLNL Soil Microbiome SFA, #SCW1632 and performed under the auspices of the U. S. DOE by Lawrence Livermore National Laboratory under Contract DE-AC52-07NA27344. The authors would also like to thank the anonymous reviewers for their valuable comments and suggestions to improve the manuscript.

2.7 References

Alcántara, V., Don, A., Vesterdal, L., Well, R., Nieder, R., 2017. Stability of buried carbon in deep-ploughed forest and cropland soils - Implications for carbon stocks. Scientific Reports 7, 1-12.

Alcántara, V., Don, A., Well, R., Nieder, R., 2016. Deep ploughing increases agricultural soil organic matter stocks. Global Change Biology 22, 2939-2956.

Banfield, C.C., Dippold, M.A., Pausch, J., Hoang, D.T.T., Kuzyakov, Y., 2017. Biopore history determines the microbial community composition in subsoil hotspots. Biology and Fertility of Soils 53, 573-588.

Banfield, C.C., Pausch, J., Kuzyakov, Y., Dippold, M.A., 2018. Microbial processing of plant residues in the subsoil - The role of biopores. Soil Biology and Biochemistry 125, 309-318.

Banning, N.C., Maccarone, L.D., Fisk, L.M., Murphy, D.V., 2015. Ammonia-oxidising bacteria not archaea dominate nitrification activity in semi-arid agricultural soil. Scientific Reports 5, 11146.

Bardgett, R.D., Mommer, L., De Vries, F.T., 2014. Going underground: Root traits as drivers of ecosystem processes. Trends in Ecology and Evolution 29, 692-699.

Barrett, M., Jahangir, M., Lee, C., Smith, C., Bhreathnach, N., Collins, G., Richards, K., O'Flaherty, V., 2013. Abundance of denitrification genes under different piezometer depths in four Irish agricultural groundwater sites. Environmental Science and Pollution Research 20, 6646-6657.

Bates, C.T., Escalas, A., Kuang, J., Hale, L., Wang, Y., Herman, D., Nuccio, E.E., Wan, X., Bhattacharyya, A., Fu, Y. and Tian, R., 2021. Conversion of marginal land into switchgrass conditionally accrues soil carbon but reduces methane consumption. The ISME Journal,1-16.

Baumert, V.L., Vasilyeva, N.A., Vladimirov, A.A., Meier, I.C., Kögel-Knabner, I. and Mueller, C.W., 2018. Root exudates induce soil macroaggregation facilitated by fungi in subsoil. Frontiers in Environmental Science, 6.

Baveye, P.C., Berthelin, J., Tessier, D., Lemaire, G., 2018. The “4 per 1000” initiative: A credibility issue for the soil science community? Geoderma 309, 118-123.

Beem-Miller, J., Lehmann, J., 2017. Subsoil carbon accumulation on an arable Mollisol is retention dominated, in contrast to input driven carbon dynamics in topsoil. 11321, 19th EGU General Assembly, EGU2017, Vienna, Austria.

Begum, K., Kuhnert, M., Yeluripati, J., Glendining, M. and Smith, P., 2017. Simulating soil carbon sequestration from long term fertilizer and manure additions under continuous wheat using the DailyDayCent model. Nutrient Cycling in Agroecosystems, 109, 291-302.

Blagodatsky, S., Smith, P., 2012. Soil physics meets soil biology: Towards better mechanistic prediction of greenhouse gas emissions from soil. Soil Biology and Biochemistry 47, 78-92.

Bloemen, J., Teskey, R.O., McGuire, M.A., Aubrey, D,P., Steppe, K., 2016. Root xylem CO_2 flux: an important but unaccounted-for component of root respiration. Trees-Structure and Function 30, 343-52.

Bossuyt, H., Six, J., Hendrix, P.F., 2005. Protection of soil carbon by microaggregates within earthworm casts. Soil Biology and Biochemistry 37, 251-258.

Brewer, T.E., Aronson, E.L., Arogyaswamy, K., Billings, S.A., Botthoff, J.K., Campbell, A.N., Dove, N.C., Fairbanks, D., Gallery, R.E., Hart, S.C. and Kaye, J., 2019. Ecological and genomic attributes of novel bacterial taxa that thrive in subsurface soil horizons. mBio 10, 1318-1319.

Bruun, E.W., Petersen, C.T., Hansen, E., Holm, J.K., Hauggaard-Nielsen, H., 2014. Biochar amendment to coarse sandy subsoil improves root growth and increases water retention. Soil Use and Management 30, 109-118.

Butterfield, C.N., Z. Li, P.F. Andeer, S. Spaulding, B.C. Thomas, A. Singh, R.L. Hettich, K.B. Suttle, A.J. Probst, S.G. Tringe, T. Northen, C.P., Banfield J.F., 2016. Proteogenomic analyses indicate bacterial methylotrophy and archaeal heterotrophy are prevalent below the grass root zone. PeerJ . 4: p. e2687.

Button, E.S., Chadwick, D.R. and Jones, D.L., 2022. Addition of iron to agricultural topsoil and subsoil is not an effective C sequestration strategy. Geoderma, 409, 115646.

Cann, M.A., 2000. Clay spreading on water repellent sands in the south east of South Australia - promoting sustainable agriculture. Journal of Hydrology 231, 333-341.

de Caritat, P. and Cooper, M., 2011. National Geochemical Survey of Australia: Executive summary. Introduction. Background to the project. The Geochemical atlas of Australia. Total content maps. Geoscience Australia.

Carter, M.R., Gregorich, E.G., 2010. Carbon and nitrogen storage by deep-rooted tall fescue (*Lolium arundinaceum*) in the surface and subsurface soil of a fine sandy loam in eastern Canada. Agriculture, Ecosystems and Environment 136, 125-132.

Chabbi, A., Kögel-Knabner, I., Rumpel, C., 2009. Stabilised carbon in subsoil horizons is located in spatially distinct parts of the soil profile. Soil Biology and Biochemistry 41, 256-261.

Chacon, N., Silver, W.L., Dubinsky, E.A., Cusack, D.F., 2006. Iron reduction and soil phosphorus solubilization in humid tropical forests soils: The roles of labile carbon pools and an electron shuttle compound. Biogeochemistry 78, 67-84.

Chaopricha, N.T., Marin-Spiotta, E., 2014. Soil burial contributes to deep soil organic carbon storage. Soil Biology and Biochemistry 69, 251-264.

Chen, K., Wang, Y., Zhang, R., Zhang, H., Gao, C., 2019. CRISPR/Cas genome editing and precision plant breeding in agriculture. Annual Review Plant Biology 70, 667-697.

Chen, S., Martin, M.P., Saby, N.P.A., Walter, C., Angers, D.A., Arrouays, D., 2018. Fine resolution map of top- and subsoil carbon sequestration potential in France. Science of the Total Environment 630, 389-400.

Chen, Z., Wang, X., Ge, Q., Guo, G., 2015. Iron oxide red wastewater treatment and recycling of iron-containing Sludge. Journal of Cleaner Production 87, 558-566.

Chenu, C., Angers, D.A., Barré, P., Derrien, D., Arrouays, D., Balesdent, J., 2018. Increasing organic stocks in agricultural soils: Knowledge gaps and potential innovations. Soil and Tillage Research 188, 41-52.

Chimento, C., Almagro, M. and Amaducci, S., 2014. Carbon sequestration potential in perennial bioenergy crops: the importance of organic matter inputs and its physical protection. Gcb Bioenergy 8, 111-121.

Churchman, G.J., Noble, A., Bailey, G., Chittleborough, D., Harper, R., 2014. Clay addition and redistribution to enhance carbon sequestration in soils. In: Soil Carbon (Eds. Hartemink, A.E., McSweeney, K.). Progress in Soil Science, pp. 327-335. Springer, Switzerland.

Clough, T.J., Sherlock, R.R. and Rolston, D.E., 2005. A review of the movement and fate of N_2O in the subsoil. Nutrient Cycling in Agroecosystems 72, 3-11.

Cordero, P.R.F., Bayly, K., Leung, P.M., Huang, C., Islam, Z.F., Schittenhelm, R.B., King, G.M., Greening, C. 2019. Atmospheric carbon monoxide oxidation is a widespread mechanism supporting microbial survival. The ISME Journal 13, 2868-2881.

Das, S.K., Avasthe, R.K., Singh, R., Babu, S., 2014. Biochar as carbon negative in carbon credit under changing climate. Current Science 107, 1090-1091.

Davidson, E.A., Janssens, I.A., 2006. Temperature sensitivity of soil carbon decomposition and feedbacks to climate change. Nature 440, 165-173.

Davis, M.R., Alves, B.J.R., Karlen, D.L., Kline, K.L., Galdos, M., Abulebdeh, D., 2018. Review of soil organic carbon measurement protocols: A US and Brazil comparison and recommendation. Sustainability 10, 53.

De Deyn, G.B., Cornelissen, J.H.C., Bardgett, R.D., 2008. Plant functional traits and soil carbon sequestration in contrasting biomes. Ecology Letters 11, 516-531.

De Graaff, M.A., Jastrow, J.D., Gillette, S., Johns, A., Wullschleger, S.D., 2014. Differential priming of soil carbon driven by soil depth and root impacts on carbon availability. Soil Biology and Biochemistry 69, 147-156.

de Sosa, L.L., Glanville, H.C., Marshall, M.R., Schnepf, A., Cooper, D.M., Hill, P.W., Binley, A., Jones, D.L., 2016. Stoichiometric constraints on the microbial processing of carbon with soil depth along a riparian hillslope. Biology and Fertility of Soils 54, 949-963,

de Vries, W., 2018. Soil carbon 4 per mille: a good initiative but let's manage not only the soil but also the expectations: Comment on Minasny et al. (2017) Geoderma 292: 59-86.

Geoderma 309, 111-112.

Diamond, S., Andeer, P.F., Li, Z., Crits-Christoph, A., Burstein, D., Anantharaman, K., Lane, K.R., Thomas, B.C., Pan, C., Northen, T.R. and Banfield, J.F., 2019. Mediterranean grassland soil C–N compound turnover is dependent on rainfall and depth, and is mediated by genomically divergent microorganisms. Nature microbiology 4, 1356-1367.

Dignac, M.-F., Derrien, D., Barré, P., Barot, S., Cécillon, L., Chenu, C., Chevallier, T., Freschet, G.T., Garnier, P., Guenet, B., Hedde, M., Klumpp, K., Lashermes, G., Maron, P.-A., Nunan, N., Roumet, C., Basile-Doelsch, I., 2017. Increasing soil carbon storage: mechanisms, effects of agricultural practices and proxies. A review. Agronomy for Sustainable Development 37, 14.

Dwivedi, D., Riley, W.J., Torn, M.S., Spycher, N., Maggi, F. and Tang, J.Y., 2017. Mineral properties, microbes, transport, and plant-input profiles control vertical distribution and age of soil carbon stocks. Soil Biology and Biochemistry, 107, 244-259.

Dobbie, K.E. and Smith, K.A., 2006. The effect of water table depth on emissions of N_2O from a grassland soil. Soil Use and Management, 22, 22-28.

Don, A., Schumacher, J., Freibauer, A., 2011. Impact of tropical land use change on soil organic carbon stocks - a meta-analysis. Global Change Biology 17, 1658-1670.

Don, A., Steinberg, B., Schöning, I., Pritsch, K., Joschko, M., Gleixner, G., Schulze, E.D., 2008. Organic carbon sequestration in earthworm burrows. Soil Biology and Biochemistry 40, 1803-1812.

Dondini, M., Richards, M., Pogson, M., Jones, E.O., Rowe, R.L., Keith, A.M., McNamara, N.P., Smith, J.U. and Smith, P., 2016. Evaluation of the ECOSSE model for simulating soil organic carbon under Miscanthus and short rotation coppice-willow crops in Britain. Gcb Bioenergy, 8, 790-804.

Dove, N.C., Arogyaswamy, K., Billings, S.A., Botthoff, J.K., Carey, C.J., Cisco, C., DeForest, J.L., Fairbanks, D., Fierer, N., Gallery, R.E. and Kaye, J.P., 2020. Continental-scale patterns of extracellular enzyme activity in the subsoil: an overlooked reservoir of microbial activity. Environmental Research Letters, 15, 1040.Eilers, K.G., Debenport, S., Anderson, S., Fierer, N., 2012. Digging deeper to find unique microbial communities: The strong effect of depth on the structure of bacterial and archaeal communities in soil. Soil Biology and Biochemistry 50, 58-65.

Ekelund, F., Ronn, R., Christensen, S., 2001. Distribution with depth of protozoa, bacteria and fungi in soil profiles from three Danish forest sites. Soil Biology and Biochemistry 33, 475-481.

Elliott, P.W., Knight, D., Anderson, J.M., 1991. Variables controlling denitrification from earthworm casts and soil in permanent pastures. Biology and Fertility of Soils, 11, 24-29.

Energy Futures Initiative, 2020. From the Ground Up: Cutting-Edge Approaches for Land-Based Carbon Dioxide Removal.

Fanin, N., Kardol, P., Farrell, M., Nilsson, M.C., Gundale, M.J., Wardle, D.A., 2019. The ratio of Gram-positive to Gram-negative bacterial PLFA markers as an indicator of carbon availability in organic soils. Soil Biology and Biochemistry 128, 111-114.

FAO, 2017. Proceedings of the Global Symposium on Soil Organic Carbon 2017. Food and Agriculture Organization of the United Nations, Rome, Italy.

FAO, 2019. Submission by the Food and Agriculture Organization of the United Nations (FAO) to the United Nations Framework Convention on Climate Change (UNFCCC) in relation to the Koronivia joint work on agriculture (4/CP.23) on Topics 2(b) and 2(c).

Farrar, J., Hawes, M., Jones, D., Lindow, S., 2003. How roots control the flux of carbon to the rhizosphere. Ecology 84, 827-837.

Farrell, M., Kuhn, T. K., Macdonald, L. M., Maddern, T. M., Murphy, D. V., Hall, P. A., Singh, B. P., Baumann, K., Krull, E. S., Baldock, J. A. 2013. Microbial utilisation of biochar-derived carbon. Science of the Total Environment 465, 288-297.

Fierer, N., Schimel, J.P., Holden, P.A., 2003. Variations in microbial community composition through two soil depth profiles. Soil Biology and Biochemistry 35, 167-176.

Follett, R.F., Vogel, K.P., Varvel, G.E., Mitchell, R.B. and Kimble, J., 2012. Soil carbon sequestration by switchgrass and no-till maize grown for bioenergy. BioEnergy Research 5, 866-875.

Fontaine, S., Barot, S., Barré, P., Bdioui, N., Mary, B., Rumpel, C., 2007. Stability of organic carbon in deep soil layers controlled by fresh carbon supply. Nature 450, 277-280.

Freibauer, A., Rounsevell, M.D.A., Smith, P., Verhagen, J., 2004. Carbon sequestration in the agricultural soils of Europe. Geoderma 122, 1-23.

Gao, J., Zhang, T., Xu, B., Jia, L., Xiao, B., Liu, H., Liu, L., Yan, H. and Xia, Q., 2018. CRISPR/Cas9-mediated mutagenesis of carotenoid cleavage dioxygenase 8 (CCD8) in tobacco affects shoot and root architecture. International journal of molecular sciences, 19, 1062.

Gasparis, S., Przyborowski, M., Kala, M., Nadolska-Orczyk, A., 2019. Knockout of the HvCKX1 or HvCKX3 gene in barley (Hordeum vulgare L.) by RNA-guided Cas9 nuclease affects the regulation of cytokinin metabolism and root morphology. Cells 8, 782.

Gaume, A., Weidler, P.G., Frossard, E., 2000. Effect of maize root mucilage on phosphate adsorption and exchangeability on a synthetic ferrihydrite. Biology and Fertility of Soils 31, 525-532.

Ge, T.D., Wu, X.H., Chen, X.J., Yuan, H.Z., Zou, Z.Y., Li, B.Z., Zhou, P., Liu, S.L., Tong, C.L., Brookes, P., 2013. Microbial phototrophic fixation of atmospheric CO_2 in China subtropical upland and paddy soils. Geochimica et Cosmochimica Acta 113, 70-78.

Goebel, M-O., Woche, S.K., Bachmann, J., Lamparter A., Fischer, W.R., 2007. Significance of wettability-induced changes in microscopic water distribution for soil organic matter decomposition. Soil Science Society of America Journal 71, 1593-1599.

Goebel, M-O., Bachmann, J., Reichstein, M., Janssens, I.A., Guggenberger, G., 2011. Soil water repellency and its implications for organic matter decomposition - is there a link to extreme climatic events? Global Change Biology 17, 2640-2656.

Greening, C., Carere, C., R., Rushton-Green, R., Harold, L., K., Hards, K., Taylor, M., C., Morales, S.E., Stott, M.B., Cook, G.M., 2015. Persistence of the dominant soil phylum Acidobacteria by trace gas scavenging. Proceedings of the National Academy of Sciences 112, 10497-10502.

Greening, C., Biswas, A., Carere, C.R., Jackson, C.J., Taylor, M.,C., Stott, M.B., Cook, G.M., Morales, S.E., 2016. Genomic and metagenomic surveys of hydrogenase distribution indicate H2 is a widely utilised energy source for microbial growth and survival. ISME Journal 10, 761-777.

Gregorich, E.G., Monreal, C.M., Carter, M.R., Angers, D.A., Ellert, B.H., 1994. Towards a minimum data set to assess soil organic matter quality in agricultural soils. Canadian Journal of Soil Sceince 74, 367-385.

Guggenberger, G., Kaiser, K., 2003. Dissolved organic matter in soil: Challenging the paradigm of sorptive preservation. Geoderma 113, 293-310.

Guo, L.B., Gifford, R.M., 2002. Soil carbon stocks and land use change: A meta analysis. Global Change Biology 8, 345-360.

Hall, D.J.M., Jones, H.R., Crabtree, W.L. and Daniels, T.L., 2010. Claying and deep ripping can increase crop yields and profits on water repellent sands with marginal fertility in southern Western Australia. Soil Research, 48, 178-187.

Hall, S.J., Silver, W.L., Timokhin, V.I., Hammel, K.E., 2016. Iron addition to soil specifically stabilized lignin. Soil Biology and Biochemistry 98, 95-98.

Harrison, R., Footen, P., Strahm, B., 2011. Deep soil horizons: contribution and importance to soil carbon pools and in assessing whole-ecosystem response to management and global change. Forest Science 57, 67-76.

He, Y., Trumbore, S.E., Torn, M.S., Harden, J.W., Vaughn, L.J., Allison, S.D. and Randerson, J.T., 2016. Radiocarbon constraints imply reduced carbon uptake by soils during the 21st century. Science, 353, 1419-1424.

He, J.N., Shi, Y., Zhao, J.Y., Yu, Z.W., 2019. Strip rotary tillage with a two-year subsoiling interval enhances root growth and yield in wheat. Scientific Reports 9, 11678.

Heitkötter, J. and Marschner, B., 2018. Soil zymography as a powerful tool for exploring hotspots and substrate limitation in undisturbed subsoil. *Soil Biology and Biochemistry*, 124, 210-217.

Hilber, I., Bastos, A.C., Loureiro, S., Soja, G., Marsz, A., Cornelissen, G., Bucheli, T.D., 2017. The different faces of biochar: contamination risk versus remediation tool. Journal of Environmental Engineering and Landscape Management 25, 86-104.

Hoang, D.T.T., Bauke, S.L., Kuzyakov, Y., Pausch, J., 2017. Rolling in the deep: Priming effects in earthworm biopores in topsoil and subsoil. Soil Biology and Biochemistry 114, 59-71.

Hoang, D.T.T., Pausch, J., Razavi, B.S., Kuzyakova, I., Banfield, C.C., Kuzyakov, Y., 2016. Hotspots of microbial activity induced by earthworm burrows, old root channels, and their combination in subsoil. Biology and Fertility of Soils 52, 1105-1119.

Hobley, E., Baldock, J., Hua, Q., Wilson, B., 2017. Land-use contrasts reveal instability of subsoil organic carbon. Global Change Biology 23, 955-965.

Holmes, K.W., Wherrett, A., Keating, A., Murphy, D.V., 2012. Meeting bulk density sampling requirements efficiently to estimate soil carbon stocks. Soil Research 49, 680-695.

Hoyle, F.C., D'Antuono, D., Overheu, T., Murphy, D.V. 2013. Capacity for increasing soil organic carbon stocks in dryland agricultural systems. Soil Research, 51, 657-667.

Huang, C., Shi, X., Wang, C., Guo, L., Dong, M., Hu, G., Lin, J., Ding, T. and Guo, Z., 2019. Boosted selectivity and enhanced capacity of As (V) removal from polluted water by triethylenetetramine activated lignin-based adsorbents. International journal of biological macromolecules 140, 1167-1174.

Hutengs, C., Seidel, M., Oertel, F., Ludwig, B. and Vohland, M., 2019. In situ and laboratory soil spectroscopy with portable visible-to-near-infrared and mid-infrared instruments for the assessment of organic carbon in soils. Geoderma, 355, 113900.

Hyland, J.J., Jones, D.L., Parkhill, K.A., Barnes, A.P., Williams, A.P., 2016. Farmers' perceptions of climate change: identifying types. Agriculture and Human Values 33, 323-339.

Iijima, M., Yamane, K., Izumi, Y., Daimon, H., Motonaga, T., 2015. Continuous application of biochar inoculated with root nodule bacteria to subsoil enhances yield of soybean by the nodulation control using crack fertilization technique. Plant Production Science 18, 197-208.

Jackson, R.B., Saunois, M., Bousquet, P., Canadell, J.G., Poulter, B., Stavert, A.R., Bergamaschi, P., Niwa, Y., Segers, A. and Tsuruta, A., 2020. Increasing anthropogenic methane emissions arise equally from agricultural and fossil fuel sources. Environmental Research Letters, 15, 071002.

James, J., Devine, W., Harrison, R., Terry, T., 2014. Deep soil carbon: Quantification and modeling in subsurface layers. Soil Science Society of America Journal 78, S1-S10.

Jastrow, J.D., Amonette, J.E., Bailey, V.L., 2007. Mechanisms controlling soil carbon turnover and their potential application for enhancing carbon sequestration. Climatic Change 80, 5-23.

Jenkinson, D.S. and Coleman, K., 2008. The turnover of organic carbon in subsoils. Part 2. Modelling carbon turnover. European Journal of Soil Science, 59, 400-413.

Ji, M., Greening, C., Vanwonterghem, I., Carere, C.R., Bay, S.K., Steen, J.A., Montgomery, K., Lines, T., Beardall, J., van Dorst, J., Snape, I., Stott, M.B., Hugenholtz, P., Ferrari, B.C., 2017. Atmospheric trace gases support primary production in Antarctic desert surface soil. Nature 552, 400-403.

Jia, J., Feng, X., He, J.S., He, H., Lin, L., Liu, Z., 2017. Comparing microbial carbon sequestration

and priming in the subsoil versus topsoil of a Qinghai-Tibetan alpine grassland. Soil Biology and Biochemistry 104, 141-151.

Jiang, G.Y., Xu, M.G., He, X.H., Zhang, W.J., Huang, S.M., Yang, X.Y., Liu, H., Peng, C., Shirato, Y., Iizumi, T., Wang, J.Z., Murphy, D.V., 2014. Soil organic carbon sequestration in upland soils of northern China under variable fertilizer management and climate change scenarios. Global Biogeochemical Cycles 28, 319-333

Jobbágy, E.G., Jackson, R.B., 2000. The vertical distribution of soil organic carbon and its relation to climate and vegetation. Ecological Applications 10, 423-436.

Johnson, J.A., Runge, C.F., Senauer, B., Foley, J., Polasky, S., 2014. Global agriculture and carbon trade-offs. Proceedings of the National Academy of Sciences 111, 12342-12347.

Jones, D.L., Edwards, A.C., 1998. Influence of sorption on the biological utilization of two simple carbon substrates. Soil Biology and Biochemistry 30, 1895-1902.

Jones, D.L., Nguyen, C., Finlay, R.D., 2009. Carbon flow in the rhizosphere: carbon trading at the soil-root interface. Plant and Soil 321, 5-33.

Jones, D.L., Edwards-Jones, G., Murphy, D.V., 2011. Biochar mediated alterations in herbicide breakdown and leaching in soil. Soil Biology and Biochemistry 43, 804-813.

Jones, D.L., Magthab, E.A., Gleeson, D.B., Hill, P.W., Sánchez-Rodríguez, A.R., Roberts, P., Ge, T., Murphy, D. V., 2018. Microbial competition for nitrogen and carbon is as intense in the subsoil as in the topsoil. Soil Biology and Biochemistry 117, 72-82.

Jones, S.E., Lennon, J.T., 2010. Dormancy contributes to the maintenance of microbial diversity. Proceedings of the National Academy of Sciences 107, 5881-5886.

Jouquet, P., Traore, S., Choosai, C., Hartmann, C., Bignell, D., 2011. Influence of termites on ecosystem functioning. Ecosystem services provided by termites. European Journal of Soil Biology 47, 215-222.

Kaiser, K., Guggenberger, G., 2000. The role of DOM sorption to mineral surfaces in the preservation of organic matter in soils. Organic Geochemistry 31, 711-725.

Kaiser, K., Zech, W., 2000. Dissolved organic matter sorption by mineral constituents of subsoil clay fractions. Journal of Plant Nutrition and Soil Science 163, 531-535.

Kätterer, T., Bolinder, M.A., Andrén, O., Kirchmann, H., Menichetti, L., 2011. Roots contribute more to refractory soil organic matter than above-ground crop residues, as revealed by a long-term field experiment. Agriculture, Ecosystems and Environment 141, 184-192.

Kautz, T., Amelung, W., Ewert, E., Gaiser, T., Horn, R., Jahn, R., Javaux, M., Kuzyakov, Y., Munch, J.C., Pätzold, S., Peth, S., Scherer, H.W., Schloter, M., Schneider, H., Vanderborght, J., Vetterlein, D., Wiesenberg, G., Köpke, U., 2013. Nutrient acquisition from the arable subsoil in temperate climates: A review. Soil Biology and Biochemistry 57, 1003-1022.

Keiluweit, M., Bougoure, J.J., Nico, P.S., Pett-Ridge, J., Weber, P.K., Kleber, M., 2015. Mineral protection of soil carbon counteracted by root exudates. Nature Climate Change 5, 588-595.

Kell, D.B., 2012. Large-scale sequestration of atmospheric carbon via plant roots in natural and agricultural ecosystems: why and how. Philosophical Transactions of the Royal Society B 367, 1589-1597.

Kell, D.B., 2011. Breeding crop plants with deep roots: Their role in sustainable carbon, nutrient and water sequestration. Annals of Botany 108, 407-418.

Kemmitt, S.J., Wright, D., Murphy D.V., Jones, D.L., 2008. Regulation of amino acid biodegradation in soil as affected by depth. Biology and Fertility of Soils,44, 933-941.

Keyvanshokouhi, S., Cornu, S., Lafolie, F., Balesdent, J., Guenet, B., Moitrier, N., Moitrier, N., Nougier, C., Finke, P., 2019. Effects of soil process formalisms and forcing factors on simulated organic carbon depth-distributions in soils. Science of the Total Environment 652, 523-537.

Khalil, M.I., Richards, M., Osborne, B., Williams, M., Müller, C., 2013. Simulation and validation of greenhouse gas emissions and SOC stock changes in arable land using the ECOSSE model. Atmospheric Environment 81, 616-624.

Kimball, B.A., 2016. Crop responses to elevated CO_2 and interactions with H_2O, N, and temperature. Current opinion in plant biology, 31, 36-43.

Kirkby, C.A., Richardson, A.E., Wade, L.J., Passioura, J.B., Batten, G.D., Blanchard, C., Kirkegaard, J.A., 2014. Nutrient availability limits carbon sequestration in arable soils. Soil Biology and Biochemistry 68, 402-409.

Kitomi, Y., Hanzawa, E., Kuya, N., Inoue, H., Hara, N., Kawai, S., Kanno, N., Endo, M., Sugimoto, K., Yamazaki, T. and Sakamoto, S., 2020. Root angle modifications by the DRO1 homolog improve rice yields in saline paddy fields. Proceedings of the National Academy of Sciences, 117, 21242-21250.

Kothawala, D.N., Roehm, C., Blodau, C., Moore, T.R., 2012. Selective adsorption of dissolved organic matter to mineral soils. Geoderma 189-190, 334-342.

Kramer, C. and Gleixner, G., 2008. Soil organic matter in soil depth profiles: distinct carbon preferences of microbial groups during carbon transformation. Soil Biology and Biochemistry 40, 425-433.

Kramer, M.G., Sanderman, J., Chadwick, O.A., Chorover, J., Vitousek, P.M., 2012. Long-term carbon storage through retention of dissolved aromatic acids by reactive particles in soil. Global Change Biology 18, 2594-2605.

Kramer, S., Marhan, S., Haslwimmer, H., Ruess, L. and Kandeler, E., 2013. Temporal variation in surface and subsoil abundance and function of the soil microbial community in an arable soil. Soil Biology and Biochemistry, 61, 76-85.

Krog, J.S., Forslund, A., Larsen, L.E., Dalsgaard, A., Kjaer, J., Olsen, P., Schultz, A.C., 2017. Leaching of viruses and other microorganisms naturally occurring in pig slurry to tile drains on a well-structured loamy field in Denmark. Hydrogeology Journal 25, 1045-1062.

Kuzyakov, Y., Friedel, J.K., Stahr, K., 2000. Review of mechanisms and quantification of priming effects. Soil Biology and Biochemistry 32, 1485-1498.

Kuzyakov, Y. and Blagodatskaya, E., 2015. Microbial hotspots and hot moments in soil: concept and review. Soil Biology and Biochemistry, 83, 184-199.

Kuzyakov, Y., Horwath, W.R., Dorodnikov, M., Blagodatskaya, E., 2019. Review and synthesis of the effects of elevated atmospheric CO_2 on soil processes: No changes in pools, but increased fluxes and accelerated cycles. Soil Biology and Biochemistry 128, 66-78.

Lal, R., Bruce, J.P., 1999. The potential of world cropland soils to sequester C and mitigate the greenhouse effect. Environmental Science and Policy 2, 177-185.

Lal, R., Negassa, W., Lorenz, K., 2015. Carbon sequestration in soil. Current Opinions in Environmental Sustainability 15, 79-86.

Lalonde, K., Mucci, A., Ouellet, A., Gélinas, Y., 2012. Preservation of organic matter in sediments promoted by iron. Nature 483, 198-200.

Le Mer, J., Roger, P., 2001. Production, oxidation, emission and consumption of methane by soils: A review. European Journal of Soil Biology 37, 25-50.

Le Mer, G., Barthod, J., Dignac, M.F., Barré, P., Baudin, F. and Rumpel, C., 2020. Inferring earthworms' impact on the stability of organo-mineral associations by Rock-Eval pyrolysis and 13C NMR spectroscopy. Organic Geochemistry 144, 104016.

Ledo, A., Smith, P., Zerihun, A., Whitaker, J., Vicente-Vicente, J.L., Qin, Z., McNamara, N.P., Zinn, Y.L., Llorente, M., Liebig, M. and Kuhnert, M., 2020. Changes in soil organic carbon under perennial crops. Global Change Biology 26, 4158-4168.

Lee, K.E., 1985. Earthworms: their ecology and relationships with soils and land use. Academic Press Inc., London.

Lehmann, J., Kleber, M., 2015. The contentious nature of soil organic matter. Nature 528, 60-68.

Leifeld, J., Fenner, S., Muller, M., 2007. Mobility of black carbon in drained peatland soils. Biogeosciences 4, 425-432.

Lennon, J.T., 2020. Microbial Life Deep Underfoot. mBio 11.Leskiw, L.A., Welsh, C.M., Zeleke, T.B., 2012. Effect of subsoiling and injection of pelletized organic matter on soil quality and productivity. Canadian Journal of Soil Science 92, 269-276.

Leskiw, L.A., Welsh, C.M. and Zeleke, T.B., 2012. Effect of subsoiling and injection of pelletized organic matter on soil quality and productivity. Canadian Journal of Soil Science, 92, 269-276.

Li, C., Yan, K., Tang, L., Jia, Z. and Li, Y., 2014. Change in deep soil microbial communities due to long-term fertilization. Soil Biology and Biochemistry, 75, 264-272.

Li, Y., Jones, D.L., Chen, Q. and Chadwick, D.R., 2019. Slurry acidification and anaerobic digestion affects the speciation and vertical movement of particulate and nanoparticulate phosphorus in soil after cattle slurry application. Soil and Tillage Research, 189, 199-206.

Lian, T., Huang, Y., Xie, X., Huo, X., Shahid, M.Q., Tian, L., Lan, T. and Jin, J., 2020. Rice SST Variation Shapes the Rhizosphere Bacterial Community, Conferring Tolerance to Salt Stress through Regulating Soil Metabolites. Msystems, 5, 00721-20.

Liang, C., Schimel, J.P. and Jastrow, J.D., 2017. The importance of anabolism in microbial control over soil carbon storage. Nature microbiology 2, 1-6.

Liebig, M.A., Johnson, H.A., Hanson, J.D. and Frank, A.B., 2005. Soil carbon under switchgrass stands and cultivated cropland. Biomass and Bioenergy 28, 347-354.

Lilley, J.M., Kirkegaard, J.A., 2011. Benefits of increased soil exploration by wheat roots. F. Crop. Res. 122, 118-130.

Liu, K., Luo, L., Zheng, L. 2018a. Lignins: biosynthesis and biological functions in plants. International Journal of Molecular Sciences 19, 335.

Liu, X., Rezaei Rashti, M., Dougall, A., Esfandbod, M., Van Zwieten, L., Chen, C., 2018b. Subsoil application of compost improved sugarcane yield through enhanced supply and cycling of soil labile organic carbon and nitrogen in an acidic soil at tropical Australia. Soil and Tillage Research 180, 73-81.

Lorenz, K., Lal, R., 2005. The depth distribution of soil organic carbon in relation to land use and management and the potential of carbon sequestration in subsoil horizons. Advances in agronomy, 88, 35-66.

Lou, Y.L., Xu, M.G., Chen, X.N., He, X.H., Zhao, K., 2012. Stratification of soil organic C, N and C:N ratio as affected by conservation tillage in two maize fields of China. Catena 95, 124-130.

Lubbers, I.M., Van Groenigen, K.J., Fonte, S.J., Six, J., Brussaard, L. and Van Groenigen, J.W., 2013. Greenhouse-gas emissions from soils increased by earthworms. Nature Climate Change, 3, 187-194.

Lubbers, I.M., Pulleman, M.M., Van Groenigen, J.W., 2017. Can earthworms simultaneously enhance decomposition and stabilization of plant residue carbon? Soil Biology and Biochemistry 105, 12-24.

Lynch, J.P., Wojciechowski, T., 2015. Opportunities and challenges in the subsoil: Pathways to deeper rooted crops. Journal of Experimental Botany 66, 2199-2210.

Ma, Z., Wood, C.W., Bransby, D.I., 2000. Soil management impacts on soil carbon sequestration by switchgrass. Biomass and Bioenergy 18, 469-477.

Maier, M., Schack-Kirchner, H., 2014. Using the gradient method to determine soil gas flux: A review. Agricultural and Forest Meteorology 192-193, 78-95.

Major, J., Lehmann, J., Rondon, M., Goodale, C., 2010. Fate of soil-applied black carbon: Downward migration, leaching and soil respiration. Global Change Biology 16, 1366-1379.

Mayer, S., Schwindt, D., Steffens, M., Volkel, J., Kogel-Knabner, I., 2018. Drivers of organic carbon allocation in a temperate slope-floodplain catena under agricultural use. Geoderma 327, 63-72.

McCormack, M.L., Dickie, I.A., Eissenstat, D.M., Fahey, T.J., Fernandez, C.W., Guo, D., Helmisaari, H.S., Hobbie, E.A., Iversen, C.M., Jackson, R.B., Leppälammi-Kujansuu, J., Norby, R.J., Phillips, R.P., Pregitzer, K.S., Pritchard, S.G., Rewald, B., Zadworny, M., 2015. Redefining fine roots improves understanding of below-ground contributions to terrestrial biosphere processes. New Phytologist 207, 505-518.

Meehl, G.A., Stocker, T.F., Collins, W.D., Friedlingstein, P., Gaye, A.T., Gregory, J.M. Kitoh, A., Knutti, R., Murphy, J.M., Noda, A., Raper, S.C.B., Watterson, I.G., Weaver, A.J., Zhao, Z., 2007. Global climate projections. In: Climate Change 2007: The Physical Science Basis. Contribution of Working Group I to the Fourth Assessment Report of the Intergovernmental Panel on Climate Change, Cambridge University Press, Cambridge. pp. 747-845.

Meier, C.L., Suding, K.N., Bowman, W.D., 2008. Carbon flux from plants to soil: Roots are a below-ground source of phenolic secondary compounds in an alpine ecosystem. Journal of Ecology 96, 421-430.

Mencuccini M., Hölttä T., 2010. The significance of phloem transport for the speed with which canopy photosynthesis and belowground respiration are linked. New Phytologist 185, 189-203

Meyer, N., Welp, G., Rodionov, A., Borchard, N., Martius, C., Amelung, W., 2018. Nitrogen and phosphorus supply controls soil organic carbon mineralization in tropical topsoil and subsoil. Soil Biology and Biochemistry 119, 152-161.

Mikutta, R., Kleber, M., Torn, M.S., Jahn, R., 2006. Stabilization of soil organic matter: Association with minerals or chemical recalcitrance? Biogeochemistry 77, 25-56.

Mikutta, R., Mikutta, C., Kalbitz, K., Scheel, T., Kaiser, K., Jahn, R., 2007. Biodegradation of forest floor organic matter bound to minerals via different binding mechanisms. Geochimica Cosmochimica Acta 71, 2569-2590.

Min, K., Slessarev, E., Kan, M.P., Mcfarlane, K., Oerter, E., Pett-Ridge, J., Nuccio, E.E. and Berhe, A.A., 2021. Soil depth gradients in microbial growth kinetics under deeply-vs. shallow-rooted plants. bioRxiv.

Minasny, B., Malone, B.P., McBratney, A.B., Angers, D.A., Arrouays, D., Chambers, A., Chaplot, V., Chen, Z.S., Cheng, K., Das, B.S., Field, D.J., Gimona, A., Hedley, C.B., Hong, S.Y., Mandal, B., Marchant, B.P., Martin, M., McConkey, B.G., Mulder, V.L., O'Rourke, S., Richer-de-Forges, A.C., Odeh, I., Padarian, J., Paustian, K., Pan, G., Poggio, L., Savin, I., Stolbovoy, V., Stockmann, U., Sulaeman, Y., Tsui, C.C., Vågen, T.G., van Wesemael, B., Winowiecki, L., 2017. Soil carbon 4 per mille. Geoderma 292, 59-86.

Miyauchi, S., Kiss, E., Kuo, A., Drula, E., Kohler, A., Sánchez-García, M., Morin, E., Andreopoulos, B., Barry, K.W., Bonito, G. and Buée, M., 2020. Large-scale genome sequencing of mycorrhizal fungi provides insights into the early evolution of symbiotic traits. Nature communications, 11, 1-17.

Moni, C., Rumpel, C., Virto, I., Chabbi, A., Chenu, C., 2010. Relative importance of sorption versus aggregation for organic matter storage in subsoil horizons of two contrasting soils. European Journal of Soil Science 61, 958-969.

Murphy, D.V., Sparling, G.P., Fillery, I.R.P., 1998. Stratification of microbial biomass C and N and gross N mineralisation with soil depth in two contrasting Western Australian agricultural soils. Soil Research 36, 45-56.

Naisse, C., Girardin, C., Davasse, B., Chabbi, A., Rumpel, C., 2015. Effect of biochar addition on C mineralisation and soil organic matter priming in two subsoil horizons. Journal of Soils and Sediments 15, 825-832.

Nel, J.A., Cramer, M.D., 2019. Soil microbial anaplerotic CO_2 fixation in temperate soils. Geoderma 335, 170-178.

Nieder, R., Kersebaum, K.C., Richter, J., 1995. Significance of nitrate leaching and long term N immobilization after deepening the plough layers for the N regime of arable soils in N.W. Germany. Plant and Soil 173, 167-175.

Nieminen, M., Hurme, T., Mikola, J., Regina, K., Nuutinen, V., 2015. Impact of earthworm *Lumbricus terrestris* living sites on the greenhouse gas balance of no-till arable soil. Biogeosciences 12, 5481-5493.

Müller, C.W., Weber, P.K., Kilburn, M.R., Hoeschen, C., Kleber, M. and Pett-Ridge, J., 2013. Advances in the analysis of biogeochemical interfaces: NanoSIMS to investigate soil microenvironments. Advances in agronomy, 121, 1-46.

Oburger, E., Leitner, D., Jones, D.L., Zygalakis, K.C., Schnepf, A., Roose, T., 2011. Adsorption and desorption dynamics of citric acid anions in soil. European Journal of Soil Science 62, 733-742.

Oerter, E., Slessarev, E., Visser, A., Min, K., Kan, M., McFarlane, K.J., Saha, M.C., Berhe, A.A., Pett-Ridge, J. and Nuccio, E., 2021. Hydraulic redistribution by deeply rooted grasses and its ecohydrologic implications in the southern Great Plains of North America. Hydrological Processes, 35.

Olson, K.R., Al-Kaisi, M.M., Lal, R. and Lowery, B., 2014. Experimental consideration, treatments, and methods in determining soil organic carbon sequestration rates. Soil Science Society of America Journal, 78, 348-360.

Omonode, R.A. and Vyn, T.J., 2006. Vertical distribution of soil organic carbon and nitrogen under warm-season native grasses relative to croplands in west-central Indiana, USA. Agriculture, Ecosystems and Environment 117, 159-170.

Or, D., Smets, B.F., Wraith, J.M., Dechesne, A., Friedman, S.P., 2007. Physical constraints affecting bacterial habitats and activity in unsaturated porous media - a review. Advances in Water Resources 30, 1505-1527.

Pausch, J., Kuzyakov, Y., 2018. Carbon input by roots into the soil: Quantification of rhizodeposition from root to ecosystem scales. Global Change Biology 24, 1-12.

Paustian, K., Lehmann, J., Ogle, S., Reay, D., Robertson, G.P. and Smith, P., 2016. Climate-smart soils. Nature, 532, 49-57.

Peñuelas, J., Ciais, P., Canadell, J.G., Janssens, I.A., Fernández-Martínez, M., Carnicer, J., Obersteiner, M., Piao, S., Vautard, R. and Sardans, J., 2017. Shifting from a fertilization-dominated to a warming-dominated period. Nature ecology and evolution, 1, 1438-1445.

Peixoto, L., Elsgaard, L., Rasmussen, J., Kuzyakov, Y., Banfield, C.C., Dippold, M.A. and Olesen, J.E., 2020. Decreased rhizodeposition, but increased microbial carbon stabilization with soil depth down to 3.6 m. Soil Biology and Biochemistry, 150, 108008.

Phillips, R., P., Finzi, A., C., Bernhardt, E., S. 2011. Enhanced root exudation induces microbial feedbacks to N cycling in a pine forest under long-term CO_2 fumigation. Ecological Letters 14, 187-194.

Piccolo, A., Spaccini, R., Cozzolino, V., Nuzzo, A., Drosos, M., Zavattaro, L., Grignani, C., Puglisi,

E., Trevisan, M., 2018. Effective carbon sequestration in Italian agricultural soils by in situ polymerization of soil organic matter under biomimetic photocatalysis. Land Degradation and Development 29, 485-494.

Pierret, A., Maeght, J.L., Clément, C., Montoroi, J.P., Hartmann, C., Gonkhamdee, S., 2016. Understanding deep roots and their functions in ecosystems: An advocacy for more unconventional research. Annals of Botany. 118, 621-635.

Polain, K., Knox, O., Wilson, B. and Pereg, L., 2020. Subsoil microbial diversity and stability in rotational cotton systems. Soil Systems, 4, 44.

Porras, R.C., Hicks Pries, C.E., Torn, M.S., Nico, P.S., 2018. Synthetic iron (hydr)oxide-glucose associations in subsurface soil: Effects on decomposability of mineral associated carbon. Science of the Total Environment 613-614, 342-351.

Poulton, P., Johnston, J., Macdonald, A., White, R., Powlson, D., 2018. Major limitations to achieving “4 per 1000” increases in soil organic carbon stock in temperate regions: Evidence from long-term experiments at Rothamsted Research, United Kingdom. Global Change Biology 24, 2563-2584.

Powlson, D.S., Whitmore, A.P., Goulding, K.W.T., 2011. Soil carbon sequestration to mitigate climate change: A critical re-examination to identify the true and the false. European Journal of Soil Science 62, 42-55.

Preusser, S., Poll, C., Marhan, S., Angst, G., Mueller, C.W., Bachmann, J., Kandeler, E., 2019. Fungi and bacteria respond differently to changing environmental conditions within a soil profile. Soil Biology and Biochemistry 137, 107543.

Pries, C.E.H., Castanha, C., Porras, R.C. and Torn, M.S., 2017. The whole-soil carbon flux in response to warming. Science, 355, 1420-1423.

Pries, C.E.H., Sulman, B.N., West, C., O'Neill, C., Poppleton, E., Porras, R.C., Castanha, C., Zhu, B., Wiedemeier, D.B. and Torn, M.S., 2018. Root litter decomposition slows with soil depth. Soil Biology and Biochemistry, 125, 103-114.

Qin, S.Q., Chen, L.Y., Fang, K., Zhang, Q.W., Wang, J., Liu, F.T., Yu, J.C., Yang, Y.H., 2019. Temperature sensitivity of SOM decomposition governed by aggregate protection and microbial communities. Science Advances 5, eaau1218.

Ralph, J., Lundquist, K., Brunow, G., Lu, F., Kim, H., Schatz, P.E., Marita, J.M., Hatfield, R.D., Ralph, S.A., Christensen, J.H., 2004. Lignins: Natural polymers from oxidative coupling of 4-hydroxyphenyl-propanoids. Phytochemistry Reviews 3, 29-60.

Rao, S., Wu, Y.Y., Wang, R., 2019. Bicarbonate stimulates non-structural carbohydrate pools of *Camptotheca acuminate*. Physiologia Plantarum 165, 780-789.

Rasse, D.P., Mulder, J., Moni, C., Chenu, C., 2006. Carbon turnover kinetics with depth in a french loamy soil. Soil Science Society of America Journal 70, 2097.

Rasse, D.P., Rumpel, C., Dignac, M.F., 2005. Is soil carbon mostly root carbon? Mechanisms for a specific stabilisation. Plant and Soil 269, 341-356.

Ray, D.K., West, P.C., Clark, M., Gerber, J.S., Prishchepov, A.V., Chatterjee, S., 2019. Climate change has likely already affected global food production. PLOS One 14, e0217148.

Robock, A., Jerch, K., Bunzl, M., 2015. 20 reasons why geoengineering may be a bad idea. Bulletin of the Atomic Scientists 64, 14-59.

Rumpel, C., Kögel-Knabner, I., 2011. Deep soil organic matter-a key but poorly understood component of terrestrial C cycle. Plant and Soil 338, 143-158.

Rumpel, C., Kögel-Knabner, I., Bruhn, F., 2002. Vertical distribution, age, and chemical composition of organic carbon in two forest soils of different pedogenesis. Organic Geochemistry 33, 1131-1142.

Rumpel, C., Eusterhues, K., Kögel-Knabner, I., 2004. Location and chemical composition of stabilized organic carbon in topsoil and subsoil horizons of two acid forest soils. Soil Biology and Biochemistry 36, 177-190.

Rumpel, C., Baumann, K., Remusat, L., Dignac, M.F., Barré, P., Deldicque, D., Glasser, G., Lieberwirth, I. and Chabbi, A., 2015. Nanoscale evidence of contrasted processes for root-derived organic matter stabilization by mineral interactions depending on soil depth. Soil Biology and Biochemistry 85, 82-88.

Saini, R., Kapoor, R., Kumar, R., Siddiqi, T.O., Kumar. A., 2011. CO_2 utilizing microbes—a comprehensive review. Biotechnology Advances 29, 949-960.

Salminen, R., 2005. Geochemical Atlas of Europe. Forum of European Geological Surveys (FOREGS).

Salomé, C., Nunan, N., Pouteau, V., Lerch, T.Z., Chenu, C., 2010. Carbon dynamics in topsoil and in subsoil may be controlled by different regulatory mechanisms. Global Change

Biology 16, 416-426.

Sanaullah, M., Chabbi, A., Leifeld, J., Bardoux, G., Billou, D., Rumpel, C., 2011. Decomposition and stabilization of root litter in top- and subsoil horizons: What is the difference? Plant and Soil 338, 127-141.

Sanderman, J., Hengl, T., Fiske, G.J., 2017. Soil carbon debt of 12,000 years of human land use. Proceedings of the National Academy of Sciences 115, 9575-9580.

Šantrůčková, H., Kotas, P., Bárta, J., Urich, T., Čapek, P., Palmtag, J., Alves, R.J.E., Biasi, C., Diáková, K., Gentsch, N., Gittel, A., Guggenberger, G., Hugelius, G., Lashchinsky, N., Martikainen, P.J., Mikutta, R., Schleper, C., Schnecker, J., Schwab, C., Shibistova, O., Wild, B., Richter, A., 2018. Significance of dark CO_2 fixation in arctic soils. Soil Biology and Biochemistry 119, 11-21

Saunois, M., Stavert, A.R., Poulter, B., Bousquet, P., Canadell, J.G., Jackson, R.B., Raymond, P.A., Dlugokencky, E.J., Houweling, S., Patra, P.K. and Ciais, P., 2020. The global methane budget 2000–2017. Earth System Science Data, 12, 1561-1623.

Setlow, P., 2007. I will survive: DNA protection in bacterial spores. Trends in microbiology 15, 172-180.

Scanlan, C.A., Rahmani, H., Bowles, R., Bennamoun, M., 2018. Three-dimensional scanning for measurement of bulk density in gravelly soils. Soil Use and Management 34, 380-387.

Scharlemann, J.P., Tanner, E.V., Hiederer, R., Kapos, V., 2014. Global soil carbon: understanding and managing the largest terrestrial carbon pool. Carbon Management 5, 81-91.

Schiedung, M., Tregurtha, C.S., Beare, M.H., Thomas, S.M. and Don, A., 2019. Deep soil flipping increases carbon stocks of New Zealand grasslands. Global change biology.

Schlatter, D.C, Kahl, K., Carlson, B., Huggins, D.R., Paulitz, T., 2018. Fungal community composition and diversity vary with soil depth and landscape position in a no-till wheat-based cropping system. FEMS microbiology ecology 94.

Schlesinger, W.H., Andrews, J.A., 2000. Soil respiration and the global carbon cycle. Biogeochemistry 48, 7-20.

Schmidt, M.W.I., Torn, M.S., Abiven, S., Dittmar, T., Guggenberger, G., Janssens, I.A., Kleber, M., Kögel-Knabner, I., Lehmann, J., Manning, D.A.C., Nannipieri, P., Rasse, D.P., Weiner, S., Trumbore, S.E., 2011. Persistence of soil organic matter as an ecosystem property.

Nature 478, 49-56.

Schneider, F., Don, A., Hennings, I., Schmittmann, O., Seidel, S.J., 2017. The effect of deep tillage on crop yield - What do we really know? Soil and Tillage Research 174, 193-204.

Schöning, I., Kögel-Knabner, I., 2006. Chemical composition of young and old carbon pools throughout Cambisol and Luvisol profiles under forests. Soil Biology and Biochemistry 38, 2411-2424.

Schweizer, S.A., Hoeschen, C., Schlüter, S., Kögel-Knabner, I. and Mueller, C.W., 2017. Rapid soil formation after glacial retreat shaped by spatial patterns of organic matter accrual in microaggregates. Global change biology, 24, 1637-1650.

Shahzad, T., Anwar, F., Hussain, S., Mahmood, F., Arif, M.S., Sahar, A., Nawaz, M.F., Perveen, N., Sanaullah, M., Rehman, K., Rashid, M.I., 2018a. Carbon dynamics in surface and deep soil in response to increasing litter addition rates in an agro-ecosystem. Geoderma 333, 1-9.

Shahzad, T., Imtiaz, M., Maire, V., Barot, S., 2018b. Root penetration in deep soil layers stimulates mineralization of millennia-old organic carbon. Soil Biology and Biochemistry 124, 150-160.

Sharrar, A.M., Crits-Christoph, A., Méheust, R., Diamond, S., Starr, E.P. and Banfield, J.F., 2020. Bacterial secondary metabolite biosynthetic potential in soil varies with phylum, depth, and vegetation type. Mbio, 11, e00416-20.

Shaw, G., Atkinson, B., Meredith, W., Snape, C., Steven, M., Hoch, A., Lever, D., 2014. Quantifying $^{12/13}CH_4$ migration and fate following sub-surface release to an agricultural soil. Journal of Environmental Radioactivity 133, 18-23.

Sher, Y., Baker, N.R., Herman, D., Fossum, C., Hale, L., Zhang, X., Nuccio, E., Saha, M., Zhou, J., Pett-Ridge, J. and Firestone, M., 2020. Microbial extracellular polysaccharide production and aggregate stability controlled by switchgrass (Panicum virgatum) root biomass and soil water potential. Soil Biology and Biochemistry 143, 107742.

Shi, Z., Allison, S.D., He, Y., Levine, P.A., Hoyt, A.M., Beem-Miller, J., Zhu, Q., Wieder, W.R., Trumbore, S. and Randerson, J.T., 2020. The age distribution of global soil carbon inferred from radiocarbon measurements. Nature Geoscience 13, 555-559.

Siedenburg, J., Martin, A., Mcguire, S., Siedenburg, J., Martin, A., Mcguire, S., 2012. The power of “farmer friendly” financial incentives to deliver climate smart agriculture : a critical

data gap. Journal of Integrative Environmental Sciences 9, 201-217

Six, J., Bossuyt, H., Degryze, S., Denef, K., 2004. A history of research on the link between (micro)aggregates, soil biota, and soil organic matter dynamics. Soil and Tillage Research 79, 7-31.

Slessarev, E.W., Nuccio, E.E., McFarlane, K.J., Ramon, C.E., Saha, M., Firestone, M.K. and Pett-Ridge, J., 2020. Quantifying the effects of switchgrass (Panicum virgatum) on deep organic C stocks using natural abundance ^{14}C in three marginal soils. GCB Bioenergy, 12, 834-847.

Smith, P., 2016. Soil carbon sequestration and biochar as negative emission technologies. Global Change Biology 22, 1315-1324.

Smith, P., 2008. Land use change and soil organic carbon dynamics. Nutrient Cycling in Agroecosystems 81, 169-178.

Smith, P., 2004. Carbon sequestration in croplands: The potential in Europe and the global context. European Journal of Agronomy 20, 229-236.

Smith, P., Davies, C.A., Ogle, S., Zanchi, G., Bellarby, J., Bird, N., Boddey, R.M., McNamara, N.P., Powlson, D., Cowie, A. and van Noordwijk, M., 2012. Towards an integrated global framework to assess the impacts of land use and management change on soil carbon: current capability and future vision. Global Change Biology 18, 2089-2101.Smith, P., Bustamante, M., Ahammad, H., Clark, H., Dong, H., Elsiddig, E. A. et al., 2014. Climate change 2014 : mitigation of climate change : Working Group III contribution to the Fifth Assessment Report of the Intergovernmental Panel on Climate Change.

Smith, P., Smith, J.U.O., Powlson, D.S., McGill, W.B., Arah, J.R.M., Chertov, O.G., Coleman, K., Franko, U., Frolking, S., Jenkinson, D.S., Jensen, L.S., Kelly, R.H., Klein-Gunnewiek, H., Komarov, A.S., Li, C., Molina, J.A.E., Mueller, T., Parton, W.J., Thornley, J.H.M., Whitmore, A.P., Smith, P., Wattenbach, M., Zaehle, S., Hiederer, R., Jones, R.J. a, Montanarella, L., Rounsevell, M.D., Reginster, I., Ewert, F., 1997. A comparison of the performance of nine soil organic matter models using datasets from seven long-term experiments. Geoderma 81, 153-225.

Smith, P., Soussana, J.F., Angers, D., Schipper, L., Chenu, C., Rasse, D.P., Batjes, N.H., van Egmond, F., McNeill, S., Kuhnert, M. and Arias-Navarro, C., 2020. How to measure, report and verify soil carbon change to realize the potential of soil carbon sequestration for

atmospheric greenhouse gas removal. Global Change Biology 26, 219-241.

Smith, D.B.C., Woodruff, W.F., Solano, L.G., Ellefsen, F. and Karl, J., 2014b. Geochemical and mineralogical maps for soils of the conterminous United States.

Solinger, S., Park, J.-H., Michalzik, B., Matzner, E., 2000. Controls on the dynamics of dissolved organic matter in soils: a review. Soil Science 165, 277-304.

Song, X., Pan, G., Zhang, C., Zhang, L., Wang, H., 2016. Effects of biochar application on fluxes of three biogenic greenhouse gases: a meta-analysis. Ecosystem Health and Sustainability 2, e01202.

Sosa-Hernandez, M.A., Leifheit, E.F., Ingraffia, R., Rillig, M.C., 2019. Subsoil arbuscular mycorrhizal fungi for sustainability and climate-smart agriculture: A solution right under our feet? Frontiers in Microbiology 10, 744.

Sosa-Hernandez, M.A., Roy, J., Hempel, S., Rillig, M.C., 2018. Evidence for subsoil specialization in arbuscular mycorrhizal fungi. Frontiers in Ecology and Evolution 6, UNSP 67.

Spohn, M., Klaus, K., Waneka, W., Richter, A., 2016. Microbial carbon use efficiency and biomass turnover times depending on soil depth – Implications for carbon cycling. Soil Biology and Biochemistry 96, 74-81.

Springmann, M., Clark, M., Mason-D'Croz, D., Wiebe, K., Bodirsky, B.L., Lassaletta, L., De Vries, W., Vermeulen, S.J., Herrero, M., Carlson, K.M. and Jonell, M., 2018. Options for keeping the food system within environmental limits. Nature, 562, 519-525.

Stockmann, U., Adams, M.A., Crawford, J.W., Field, D.J., Henakaarchchi, N., Jenkins, M., Minasny, B., McBratney, A.B., Courcelles, V. de R. de, Singh, K., Wheeler, I., Abbott, L., Angers, D.A., Baldock, J., Bird, M., Brookes, P.C., Chenu, C., Jastrow, J.D., Lal, R., Lehmann, J., O'Donnell, A.G., Parton, W.J., Whitehead, D., Zimmermann, M., 2013. The knowns, known unknowns and unknowns of sequestration of soil organic carbon. Agriculture, Ecosystems and Environment 164, 80-99.

Stone, M.M., DeForest, J.L. and Plante, A.F., 2014. Changes in extracellular enzyme activity and microbial community structure with soil depth at the Luquillo Critical Zone Observatory. Soil Biology and Biochemistry 75, 237-247.

Suseela, V., Tharayil, N., Pendall, E., Rao, A.M., 2017. Warming and elevated CO_2 alter the suberin chemistry in roots of photosynthetically divergent grass species. AoB Plants 9, 1-

11.

Sykes, A.J., Macleod, M., Eory, V., Rees, R.M., Payen, F., Myrgiotis, V., Williams, M., Sohi, S., Hillier, J., Moran, D. and Manning, D.A., 2020. Characterising the biophysical, economic and social impacts of soil carbon sequestration as a greenhouse gas removal technology. Global Change Biology, 26, 1085-1108.

Taft, H.E., Cross, P.A., Edwards-Jones, G., Moorhouse, E.R., Jones, D.L., 2017. Greenhouse gas emissions from intensively managed peat soils in an arable production system. Agriculture Ecosystems and Environment 237, 162-172.

Taft, H.E., Cross, P.A., Jones, D.L., 2018. Efficacy of mitigation measures for reducing greenhouse gas emissions from intensively cultivated peatlands. Soil Biology and Biochemistry 127, 10-21.

Taghizadeh-Toosi, A., Christensen, B.T., Hutchings, N.J., Vejlin, J., Kätterer, T., Glendining, M., Olesen, J.E., 2014. C-TOOL: A simple model for simulating whole-profile carbon storage in temperate agricultural soils. Ecological Modelling 292, 11-25.

Tao, J.J., Bai, T.S., Xiao, R., Wang, P., Wang, F.W., Duryee, A.M., Wang, Y., Zhang, Y, Hu, S.J., 2018. Vertical distribution of ammonia-oxidizing microorganisms across a soil profile of the Chinese Loess Plateau and their responses to nitrogen inputs. Science of the Total Environment 635, 240-248.

Tassi, F., Montegrossi, G., Vaselli, O., Liccioli, C., Moretti, S., Nisi, B., 2009. Degradation of C_2-C_{15} volatile organic compounds in a landfill cover soil. Science of the Total Environment 407, 4513-4525.

Tautges, N.E., Chiartas, J.L., Gaudin, A.C., O'Geen, A.T., Herrera, I. and Scow, K.M., 2019. Deep soil inventories reveal that impacts of cover crops and compost on soil carbon sequestration differ in surface and subsurface soils. Global change biology 25, 3753-3766.

Taylor, J., Wilson, B., Mills, M., Burns, R., 2002. Comparison of microbial numbers and enzymatic activities in surface soils and subsoils using various techniques. Soil Biology and Biochemistry 34, 387-401.

Terrer, C., Phillips, R.P., Hungate, B.A., Rosende, J., Pett-Ridge, J., Craig, M.E., van Groenigen, K.J., Keenan, T.F., Sulman, B.N., Stocker, B.D. and Reich, P.B., 2021. A trade-off between plant and soil carbon storage under elevated CO_2. Nature, 591, 599-603.

Todd-Brown, K.E.O., Randerson, J.T., Post, W.M., Hoffman, F.M., Tarnocai, C., Schuur, E.A.G., Allison, S.D., 2013. Causes of variation in soil carbon simulations from CMIP5 Earth system models and comparison with observations. Biogeosciences 10, 1717-1736.

Torn, M.S., Trumbore, S.E., Chadwick, O.A., Vitousek, P.M., Hendricks, D.M., 1997. Mineral control of soil organic carbon storage and turnover. Nature 389, 170-173.

Torn, M.S., Lapenis, A.G., Timofeev, A., Fischer, M.L., Babikov, B. V, Harden, J.W., 2002. Organic carbon and carbon isotopes in modern and 100-year- old-soil archives of the Russian steppe. Global Change Biology 8, 941-953.

Tsiafouli, M.A., Thébault, E., Sgardelis, S.P., de Ruiter, P.C., van der Putten, W.H., Birkhofer, K., Hemerik, L., de Vries, F.T., Bardgett, R.D., Brady, M.V., Bjornlund, L., Jørgensen, H.B., Christensen, S., Hertefeldt, T.D., Hotes, S., Gera Hol, W.H., Frouz, J., Liiri, M., Mortimer, S.R., Setälä, H., Tzanopoulos, J., Uteseny, K., Pižl, V., Stary, J., Wolters, V., Hedlund, K., 2015. Intensive agriculture reduces soil biodiversity across Europe. Global Change Biology 21, 973-985.

Uksa, M., Schloter, M., Endesfelder, D., Kublik, S., Engel, M., Kautz, T., Kopke, U., Fischer, D., 2015. Prokaryotes in subsoil-evidence for a strong spatial separation of different phyla by analysing co-occurrence networks. Frontiers In Microbiology 6, 1269.

Uksa, M., Fischer, D., Welzl, G., Kautz, T., Kopke, U., Schloter, M., 2014. Community structure of prokaryotes and their functional potential in subsoils is more affected by spatial heterogeneity than by temporal variations. Soil Biology and Biochemistry75, 197-201.

Valbuena-Parralejo, N., Tuohy, P., Fenton, O., Burchill, W., Williams, M., Lanigan, G.J., Humphreys, J., 2019. Greenhouse gas emissions from temperate permanent grassland on clay-loam soil following the installation of artificial drainage. Agriculture Ecosystems and Environment 269, 39-50.

van de Ven, D.J., Gonzalez-Eguino, M., Arto, I., 2018. The potential of behavioural change for climate change mitigation: a case study for the European Union. Mitigation and Adaptation Strategies for Global Change 23, 853-886.

van den Berg, L.J.L., Shotbolt, L., Ashmore, M.R., 2012. Dissolved organic carbon (DOC) concentrations in UK soils and the influence of soil, vegetation type and seasonality. Science of the Total Environment 427-428, 269-276.

Van Vuuren, D.P., Bouwman, A.F. and Beusen, A.H., 2010. Phosphorus demand for the 1970–

2100 period: a scenario analysis of resource depletion. Global environmental change, 20, 428-439.

Wang, B., An, S., Liang, C., Liu, Y. and Kuzyakov, Y., 2021. Microbial necromass as the source of soil organic carbon in global ecosystems. Soil Biology and Biochemistry, 162, 108422.

Wang, C., White, P.J., Li, C.J., 2017. Colonization and community structure of arbuscular mycorrhizal fungi in maize roots at different depths in the soil profile respond differently to phosphorus inputs on a long-term experimental site. Mycorrhiza 27, 369-381.

Wang, J., Xiong, Z., Kuzyakov, Y., 2016. Biochar stability in soil: Meta-analysis of decomposition and priming effects. GCB Bioenergy 8, 512-523.

Wang, Y.Y., Li, X.X., Dong, W.X., Wu, D.M., Hu, C.S., Zhang, Y.M., Luo, Y.Q., 2018. Depth-dependent greenhouse gas production and consumption in an upland cropping system in northern China. Geoderma 319, 100-112.

Wang, Z., Van Oost, K., Lang, A., Quine, T., Clymans, W., Merckx, R., Notebaert, B. and Govers, G., 2014a. The fate of buried organic carbon in colluvial soils: a long-term perspective. Biogeosciences, 11, 873-883.

Wang, X., GCB Sampling Team, 2014b. China geochemical baselines: Sampling methodology Journal of Geochemical Exploration.

Wang, X., Fu, S., Li, J., Zou, X., Zhang, W., Xia, H., Lin, Y., Tian, Q. and Zhou, L., 2019. Forest soil profile inversion and mixing change the vertical stratification of soil CO_2 concentration without altering soil surface CO_2 Flux. Forests 10, 192.

Wen, Y., Zang, H., Ma, Q., Evans, C.D., Chadwick, D.R., Jones, D.L., 2019a. Is the 'enzyme latch' or 'iron gate' the key to protecting soil organic carbon in peatlands? Geoderma 349, 107-113.

Wen, Y., Zang, H., Freeman, B., Ma, Q., Chadwick, D.R. and Jones, D.L., 2019b. Rye cover crop incorporation and high watertable mitigate greenhouse gas emissions in cultivated peatland. Land Degradation and Development, 30, 1928-1938.

White, R.G., Kirkegaard, J.A., 2010. The distribution and abundance of wheat roots in a dense, structured subsoil - implications for water uptake. Plant, Cell and Environment 33, 133–148.

Whitmore, A.P., Kirk, G.J.D., Rawlins, B.G., 2015. Technologies for increasing carbon storage in soil to mitigate climate change. Soil Use and Management 31, 62-71.

Wiesmeier, M., Lützow, M. von, Spörlein, P., Geuß, U., Hangen, E., Reischl, A., Schilling, B., Kögel-Knabner, I., 2015. Land use effects on organic carbon storage in soils of Bavaria: The importance of soil types. Soil and Tillage Research 146, 296-302.

Wilkinson, M.T., Richards, P.J., Humphreys, G.S., 2009. Breaking ground: Pedological, geological, and ecological implications of soil bioturbation. Earth-Science Reviews 97, 257-272.

Wordell-Dietrich, P., Don, A., Helfrich, M., 2017. Controlling factors for the stability of subsoil carbon in a Dystric Cambisol. Geoderma 304, 40-48.

Wu, X.W., Cao, R., Wei, X., Xi, X.Q., Shi, P.L., Eisenhauer, N., Sun, S.C., 2017. Soil drainage facilitates earthworm invasion and subsequent carbon loss from peatland soil. Journal of Applied Ecology 54, 1291-1300.

Xiao, X., Kuang, X., Sauer, T.J., Heitman, J.L. and Horton, R., 2015. Bare soil carbon dioxide fluxes with time and depth determined by high-resolution gradient-based measurements and surface chambers. Soil Science Society of America Journal 79, 1073-1083.

Xiang, S.R., Doyle, A., Holden, P.A., Schimel, J.P., 2008. Drying and rewetting effects on C and N mineralization and microbial activity in surface and subsurface California grassland soils. Soil Biology and Biochemistry 40, 2281-2289.

Xu, Z.S., Yang, Q.Q., Feng, K., Xiong, A.S., 2019. Changing carrot color: Insertions in DcMYB7 alter the regulation of anthocyanin biosynthesis and modification. Plant Physiology 181, 195-207.

Yang, J., Kang, Y.M., Sakurai, K., Ohnishi, K., 2017. Fixation of carbon dioxide by chemoautotrophic bacteria in grassland soil under dark conditions. Acta Agriculturae Scandinavica Section B-Soil and Plant Science 67, 362-371.

Yost, J.L. and Hartemink, A.E., 2020. How deep is the soil studied–an analysis of four soil science journals. Plant and Soil 452, 5-18.

Zhalnina, K., Louie, K.B., Hao, Z., Mansoori, N., da Rocha, U.N., Shi, S., Cho, H., Karaoz, U., Loqué, D., Bowen, B.P. and Firestone, M.K., 2018. Dynamic root exudate chemistry and microbial substrate preferences drive patterns in rhizosphere microbial community assembly. Nature microbiology, 3, 470-480.

Zhang, X., Dai, G., Ma, T., Liu, N., Hu, H., Ma, W., Zhang, J.B., Wang, Z., Peterse, F. and Feng,

X., 2020. Links between microbial biomass and necromass components in the top-and subsoils of temperate grasslands along an aridity gradient. Geoderma, 379, 114623.

Zhao, Q., Poulson, S.R., Obrist, D., Sumaila, S., Dynes, J.J., McBeth, J.M., Yang, Y., 2016. Iron-bound organic carbon in forest soils: Quantification and characterization. Biogeosciences 13, 4777-4788.

Zieger, A., Kaiser, K., Guayasamín, P.R., Kaupenjohann, M., 2018. Massive carbon addition to an organic-rich Andosol increased the subsoil but not the topsoil carbon stock. Biogeosciences 15, 2743-2760.

Zomer, R.J., Bossio, D.A., Sommer, R., Verchot, L. V., 2017. Global sequestration potential of increased organic carbon in cropland soils. Scientific Reports 7, 1-8.

Chapter 3

Addition of iron to agricultural topsoil and subsoil is not an effective C sequestration strategy

Authors

Erik S. Button, David R. Chadwick, Davey L. Jones.

Publication status

This manuscript has been published in *Geoderma*.

Citation

Button, E.S., Chadwick, D.R. and Jones, D.L., 2022. Addition of iron to agricultural topsoil and subsoil is not an effective C sequestration strategy. *Geoderma*, 409, p.115646.

Author contributions

ESB, DRC and DLJ conceived the experiment. ESB conducted the experiments and wrote the manuscript. DRC and DLJ reviewed the manuscript.

Abstract

The interaction of soil organic matter (SOM) with Fe-containing minerals represents a key mechanism that promotes carbon (C) stabilisation in soil. The addition of Fe-rich industrial by-products to soil may therefore help accelerate C storage. Our understanding of the effects of exogenous Fe addition (Fe (oxy)hydroxide vs. Fe chloride) on SOM dynamics and C dynamics in agricultural soils, especially in subsoils, however, remains poor. Here, we simulate the addition of Fe in an arable soil context and assess its effectiveness based on CO_2 emissions and soil chemistry. We hypothesised that insoluble and soluble Fe would reduce the mineralization of newly added unprotected organic materials more than native SOM and that soluble Fe would cause mineralisation of native SOM. To investigate this, insoluble $Fe(OH)_3$ or soluble $FeCl_2$ (0-5 g kg^{-1}) were added to arable top- (0-10 cm) or subsoils (50-60 cm) and CO_2 emissions, pH and nutrient dynamics (e.g. P, N) measured in a laboratory incubation over a 45 d period. We also compared the effect of Fe on the turnover of native SOM and newly added C (i.e. ^{14}C-labelled glucose, citrate and crop residues) which was pre-mixed with exogenous Fe. We found that: (1) despite a reduction in P and DOC, $Fe(OH)_3$ did not suppress total CO_2 efflux; (2) high $FeCl_2$ rates induced a rapid and significant release of CO_2, which we attribute almost entirely due to $FeCl_2$-induced soil acidification increasing DOC availability and carbonate dissolution; (3) ^{14}C-substrate mineralisation was weakly suppressed by $Fe(OH)_3$ but strongly by $FeCl_2$ following the series: citrate < glucose < crop residues; and (4) Fe addition to subsoils induced a stronger C mineralisation response but weaker effect on soil solution chemistry compared to topsoil, possibly due to subsoils having a lower buffering ability and less microbial biomass. We conclude that addition of extra Fe was not effective in promoting greater C sequestration in the arable soil we tested.

Keywords: acidification, carbon cycling, enzyme-latch, ferric-ferrous, iron-gate mechanism.

3.1 Introduction

Increasing carbon (C) sequestration in soils has the potential to reduce the continued rise of atmospheric CO_2 concentrations (Lal, 2004; Minasny et al., 2017). Considering the size of the soil C stock (Jobbágy and Jackson, 2000) and that it is in constant balance between fluxes of C entering and leaving the soil, even a small increase in soil C persistence can ultimately impact the global climate (Minasny et al., 2017). Of the mechanisms controlling C persistence in soil, associations of soil organic matter (SOM) with minerals is thought to be one of the most important (Lehmann and Kleber, 2015). In particular, iron (Fe), which is ubiquitous and can form complexes with C, nitrogen (N), oxygen (O_2), sulphur (S) and phosphorus (P), is one of the most important elements for living organisms but also for regulating C dynamics in soils (Li et al., 2012; Melton et al., 2014; Wu et al., 2018).

It is well established that Fe oxides, in particular non-crystalline forms, are important in the stabilisation of SOM (Giannetta et al., 2020; Kaiser and Guggenberger, 2007, 2000; Li et al., 2012; Mikutta et al., 2006; Zhao et al., 2016). Many compounds within soil organic carbon (SOC) carry a negative charge, while most metal oxides, such as Fe hydroxide, have a positive charge and a high capacity to sorb SOC at relevant pH values (Kaiser and Guggenberger, 2007). Low molecular weight organic acids and microbial biopolymers in soil solution can be rapidly adsorbed by Fe, almost completely supressing their biodegradation (Jones and Brassington, 1998; Jones and Edwards, 1998; Porras et al., 2018; Solomon et al., 2012). In addition, Fe oxides can suppress C mineralisation by immobilising inorganic N and P through sorption and complexation reactions, making substrates required for enzyme synthesis less available to decomposers (Lalonde et al., 2012; Riedel et al., 2013). We therefore hypothesise that addition of exogenous Fe-rich materials to temperate soils with relatively low Fe contents may promote greater C storage.

In contrast to crystalline Fe, the oxidation of Fe(II) has the potential to stimulate the decomposition of SOM via the production of strong SOC-oxidising OH^- radicals (i.e. 'Fenton reaction'; Hall and Silver, 2013; Melton et al., 2014; Van Bodegom et al., 2005), and stimulate decomposition due to increases of easily-mineralised DOC made available by acidification of the soil (Hall and Silver, 2013). However, oxidation of Fe(II) to short-range-ordered Fe precipitates can preserve SOC from mineralisation (Chen et al., 2020; Wen et al., 2019) via specific C compound stabilisation (e.g. lignin; Hall et al., 2016), or via direct toxicity to the

microbial community (Hall et al., 2016). As SOC may be both stabilised and mineralised by the addition of soluble Fe, the net stabilised C is likely to be dependent on soil type, forms of C and the prevailing conditions.

At the field scale, Silva et al. (2015) found substantial sequestration (*ca.* 140 Mg C ha^{-1} y^{-1}) of C following the application of highly reactive amorphous Fe-rich biosolids to a mine remediation site. The driver of this C accumulation was largely attributed to the complexation of Fe with organic compounds which promoted aggregation and further C accrual. However, it is also possible that indirect effects of nutrient enrichment may also have promoted the accumulation of SOM. Whether Fe amendment can be used in intensively managed agricultural soils to promote greater C stabilization remains untested. However, approximately 100 million tonnes of low economic value Fe-rich sludge are produced globally as a by-product of water treatment and mining (Chen et al., 2015). The optimal application of this resource to agricultural land to improve soil quality and improve waste valorisation is therefore desirable (Collivignarelli et al., 2020).

Iron addition to topsoils may be problematic for plant development, as roots release organic acids and require nutrients, such as N and P, which may become immobilised by association with Fe. However, subsoils, which are recognised as being far from reaching C saturation and having a high sequestration potential (Kell, 2012; Schiedung et al., 2019), may be a more successful target. In addition, while the study of Fe-driven C stabilisation has increased, the focus has been almost exclusively on topsoils, when subsoils may respond differently to Fe addition (Porras et al., 2018). Furthermore, most focus has been on environments where changes in redox states occur due to regular fluctuations in O_2 and soil water, such as wetlands (van Bodegom et al., 2005; Wang et al., 2017); peatlands (Riedel et al., 2013; Wen et al., 2019); paddy soils (Sodano et al., 2017); and Fe-rich tropical soils (Coward et al., 2017; Hall and Silver, 2013). Finally, the majority of such studies often focus on a single Fe form. How the redox state of Fe differentially affect preservation of different forms of C in different depths of a more stable soil environment (i.e. freely draining temperate arable soils) has not been tested. In this laboratory study, we explored how Fe additions influence the capacity for soil C sequestration potential of arable land.

To assess what exogenous Fe forms, Fe rates, soil depths and C forms result in the best C preservation, a series of laboratory incubation studies were conducted. We investigated the

effect of different rates of insoluble and soluble Fe additions to an arable topsoil and subsoil, focusing on the turnover of native SOM and different C amendments. We hypothesised that 1) C preservation would be greatest with addition of newly added unprotected organic materials compared to native SOM in incubations with both Fe forms. We expect this because the C in native SOM may already be protected. Next, we hypothesised that 2) $Fe(OH)_3$ would sorb to and immobilise DOC and P and so limit the growth and respiration of the soil microbial community. Further, we hypothesised that 3) addition of $FeCl_2$ would induce CO_2 release via acidification driving DOC release and respiration ; finally, iv) we expect trends to be strongest in the subsoil, due to a lower SOM content possibly lowering the buffering capacity.

3.2 Materials and methods

3.2.1 Soil collection and characterisation

A sandy clay loam textured freely draining arable soil was collected from Abergwyngregyn, North Wales (53°14'29"N, 4°01'15"W) during the fallow period in October 2018 and again in March 2019 for the $Fe(OH)_3$ (insoluble Fe(III)) and $FeCl_2$ (soluble Fe(II)) incubations, respectively. Sampling occurred on 2 separate occasions to prevent the negative effects of soil storage influencing the results over successive experiments. As the soil for each incubation was collected and incubated at different times, the results from the $Fe(OH)_3$ and $FeCl_2$ incubations are not compared directly (statistically), except for in the ^{14}C study where soil was collected and incubated at the same time (March 2019).

The soil is classified as a Eutric Cambisol (WRB) or Typic Hapludalf (US Soil Taxonomy). Prior to collection, the field had been used for forage maize (*Zea mays* L.) production. Each time soil was collected, samples were taken from 4 randomly selected locations at 2 different depths; topsoil (Ah horizon; 0-10 cm) and subsoil (Bh horizon; 50-60 cm) and sieved (5 mm mesh) prior to use. These depths were chosen for studying the effects of Fe addition as contrasting representatives of the Ah and Bh horizons. A 5 mm sieve size was used as it creates minimal disturbance to the microbial community in this crumb (ca. 2 mm dia.) structured soil (Jones and Willett, 2006). Soil was stored at 4°C prior to the incubations and used within 18 d of collection. The independent samples were used as replicates (n = 4) for each sampling occasion (n = 2) in the experiments detailed below.

To determine gravimetric moisture content and water filled pore space (WFPS), samples of known volume were oven-dried (105 °C, 24 h). Soil volume was determined by repacking the soil to a known volume. Dry bulk density was determined by dividing the dry weight by the soil volume. Soil $CaCO_3$ content was determined with a FOGL Digital Soil Calcimeter (BD Inventions, Thassaloniki, Greece). Further samples of dried soil were analysed for total C and N using a TruSpec C/N analyser (Leco Corp., St Joseph, MI). Microbial biomass was determined with the $CHCl_3$ fumigation-K_2SO_4 extraction procedure of Vance et al. (1987). Briefly, field-moist soil (5 g) was fumigated with chloroform for 4 d and then extracted using 25 ml of 0.5 M K_2SO_4. Non-fumigated samples were extracted in the same way. Dissolved organic C in the extracts was determined using a Multi N/C 2100/2100 analyser (AnalytikJena AG, Jena, Germany). Total soil metal content was determined by total X-ray fluorescence (TXRF) using a S2-Picofox spectrometer (Bruker Inc., Billerica, MA). Clay and cation exchange capacity were measured using a laser diffraction particle size analyser (Beckman-Coulter Inc., Indianapolis, IN) and the sodium acetate method of Summer and Miller (1996), respectively. A summary of the initial soil properties is presented in Table 3.1.

3.2.2 Iron mineral synthesis

Our experiments investigated the effects of a common solid mineral form of Fe, namely $Fe(OH)_3$, and a soluble form of Fe, namely $FeCl_2$ on soil C dynamics. The ferric hydroxide ($Fe(OH)_3$) gel suspension was freshly prepared as described in Jones et al. (1996). Briefly, $FeCl_3.7H_2O$ (400 g) was added to 1 l of deionised water and stirred until dissolved. Concentrated NaOH was then added to the solution to raise the pH to 7.0 and induce precipitation of amorphous $Fe(OH)_3$ (i.e. poorly ordered ferrihydrite). The mineral precipitate was allowed to settle, and the supernatant removed. The remaining mineral suspension was desalted by pouring into dialysis tubing (≥12 kDa cut-off; Sigma-Aldrich, Poole, UK) and submersing in a large volume of distilled water. The distilled water was repeatedly changed until the electrical conductivity (EC) of the suspension inside the tubing was < 100 µS cm^{-1} (EC; Jenway 4520 conductivity meter; Cole-Parmer Ltd, Stone, UK). The Fe content (110 mg ml^{-1}) of the suspension was determined using a 700 Series ICP-OES (Agilent Technologies Inc., Santa Clara,CA). The pH of the final solution was 9.21 and the EC was 42 µS cm^{-1}.

Table 3.1 Properties of the topsoil and subsoil used for the study. Values are means (± SEM) and different letters indicate significant differences ($P < 0.05$) between soil depths. For all soil solution analyses and soil analyses $n = 4$, excluding moisture content, bulk density and total organic C and N, where $n = 8$. Where appropriate, values are expressed on a dry weight basis.

		Topsoil 0 – 10 cm	Subsoil 50 – 60 cm
Soil	Clay (g kg^{-1})†	209 ± 1	179 ± 0
	Moisture content (g kg^{-1})	192 ± 4[a]	164 ± 8[b]
	Dry bulk density (g cm^{-3})	0.9 ± 0.03[a]	1.1 ± 0.04[b]
	CEC ($cmol_+$ kg^{-1})†	14.8 ± 0.2	10.3 ± 1
	Total Fe* (g kg^{-1})	46.8 ± 2.6[a]	49.2 ± 1.0[a]
	Total Al* (g kg^{-1})	89.7 ± 3.6[a]	101.9 ± 2.0[b]
	Total Fe oxides** (g kg^{-1})	1.2 ± 0.05[a]	0.9 ± 0.1[a]
	Organic C (g C kg^{-1})	27.8 ± 1.3[a]	7.4 ± 1.0[b]
	Total N (g N kg^{-1})	3.4 ± 0.1[a]	1.5 ± 0.1[b]
	C:N ratio	8.1 ± 0.1[a]	4.8 ± 0.3[b]
	$CaCO_3$ (g kg^{-1})	4.7 ± 2.0	0.0 ± 0
	Soil microbial biomass (mg C kg^{-1})	74.0 ± 3.7[a]	42.9 ± 1.4[b]
Soil solution	pH	6.8 ± 0.06[a]	6.8 ± 0.03[a]
	EC (µS cm^{-1})	1198 ± 126[a]	657 ± 102[b]
	NH_4^+ (mg N l^{-1})	0.08 ± 0.02[a]	0.09 ± 0.03[a]
	NO_3^- (mg N l^{-1})	41.1 ± 6.0[a]	22.4 ± 5.2[a]
	Molybdate reactive P (mg P l^{-1})	0.2 ± 0.03[a]	0.02 ± 0.01[b]
	DOC (mg C l^{-1})	12.6 ± 1.3[a]	4.3 ± 1.8[b]
	DON (mg N l^{-1})	4.9 ± 2.1[a]	0.6 ± 0.4[b]

*measured by X-ray fluorescence

**measured by dithionite-citrate-bicarbonate extractable Fe.

†data from Sanchez-Rodriguez et al. (in prep), $n = 4$.

Ferrous chloride ($FeCl_2.4H_2O$) was added to distilled water at the required rate and stirred to allow it to dissolve entirely in aerobic conditions immediately prior to addition to

the soil. The pH at the Fe addition rates of 1, 10, 100, 1000 and 5000 mg Fe kg^{-1} was 5.2, 4.5, 3.8, 2.9 and 2.0, respectively; while the EC was 0.04, 0.26, 1.9, 13.9 and 55.5 mS cm^{-1}. Preliminary experiments were undertaken with pH neutralised $FeCl_2$ [which led to $Fe(OH)_{2(s)}$ production], however, the chemical instability of this product [rapid transformation to $Fe(OH)_{3(s)}$] was deemed unsuitable for use in an agricultural setting and was not pursued.

3.2.3 Effect of Fe addition on soil chemistry and CO_2 efflux

Field-moist top- or subsoil (400 g) was placed into replicate (*n* = 4) transparent polypropylene containers (10.1 × 10.1 cm base, 11.8 cm high; Lock and Lock Ltd., Seoul, Republic of Korea) fitted with Suba-Seal (Sigma-Aldrich, Poole, UK) rubber septa fitted in the lids (see Appendix 2, Fig. S1). These were incubated at 21.7 ± 0.02 °C (monitored using an iButton Thermochron Data Logger; Measurement Systems Ltd., Newbury, UK) in the dark for 45 d. The incubated soil was dosed with $Fe(OH)_3$ or $FeCl_2$ at addition rates of 0, 1, 10, 100, 1000 and 5000 mg Fe kg^{-1} of soil. These rates corresponded to increases to the soil Fe oxide content (Table 3.1) by approximately 0.1, 1, 10, 100 and 500%, respectively, and were chosen to represent a range for identifying the most effective rate. While the higher rates (1000 and 5000 mg Fe kg^{-1}) are unrealistic as an agricultural addition, they were chosen to aid the mechanistic understanding in the case that the lower rates did not induce a measurable effect. They were also chosen to reflect Fe addition patches in soil (i.e. mechanical injection hotspots). The $Fe(OH)_3$ and $FeCl_2$ were suspended in distilled water and added to the soil to attain a final WFPS of 60%. To maximise coverage and mimic potential field application , the Fe solutions were injected at multiple points in the soil using a pipette. The WFPS of 60% was maintained by weighing the containers weekly and adding any water lost (ca. 1-2 ml $week^{-1}$) with a pipette. Rhizon soil water samplers (Rhizosphere Research Products, Wageningen, The Netherlands), inserted at an angle of approximately 45° and a depth of ca. 5 cm in each container, were used to extract weekly soil solution samples (1-2 ml required for soil water chemical analyses). Soil CO_2 efflux was measured according to Tagesson (2006) using an EGM 5 soil respirometer (PP Systems, Amesbury, USA) 3 times a week initially, and then weekly.

3.2.4 Effect of Fe addition on ^{14}C-glucose, citrate and plant material mineralisation

Field-moist samples of topsoil or subsoil (10 g) were placed in sterile 50 ml polypropylene centrifuge tubes. The soils were dosed with a moderate (100 mg Fe kg^{-1}) and a high (5000 mg Fe kg^{-1}) dose, corresponding to a ca. 10 and 500% increase in soil Fe oxides, respectively, of $Fe(OH)_3$ or $FeCl_2$ or distilled water (control) in the same experiment and incubated overnight. The Fe added was the same as described in *2.2.* Subsequently, ^{14}C-labelled glucose (65 mg C kg^{-1}; 1.7 kBq $sample^{-1}$), citrate (65 mg C kg^{-1}; 1.3 kBq $sample^{-1}$) or plant matter (dried and ground *Zea mays* L. shoots; crop residue; 1600 mg C kg^{-1}; 1.6 kBq $sample^{-1}$) was added to the soil. The concentrations of the substrates were chosen to reflect the inputs of C if a root cell lysed and the contents were released into soil (glucose and citrate) and sufficient to induce a response in the soil microbial community (Jones et al., 2003). Glucose was chosen as a C substrate as it is ubiquitously used by soil heterotrophic microorganisms. Citrate was chosen due to its common use by soil microorganisms and its known strong interaction with Fe-containing mineral surfaces. After ^{14}C addition, a vial containing 1 M NaOH (1 ml) was placed inside the tube to trap any $^{14}CO_2$ evolved and the tubes sealed. The NaOH traps were exchanged after 0.5, 1, 2, 4, 6, 24, 48 and 72 h. For the more complex plant matter substrate, trap changes continued after 72 h at 120, 168, 264 and 336 h. This was to allow microbial decomposition of approximately 25% of ^{14}C added to occur, which took longer due to the complexity and high C:N ratio (ca. 40) of the maize shoots. At the final time point, the glucose-incubated soil was extracted with 1 M NaCl (Darrah, 1991a); the citrate-incubated soil with 0.5 M phosphate buffer (pH 6.5) (Darrah, 1991b); and the plant matter-incubated soil extracted with 0.5 M K_2SO_4 (Badalucco et al., 1992); in a 1:4 (w/v) ratio for 20 min at 200 rev min^{-1}. NaCl was used for glucose as this is not sorbed to the solid phase, K_2SO_4 was used to recover soil solution and easily exchangeable C, while phosphate buffer was used to desorb the citrate held on the solid phase. Subsequently, 1.5 ml of the extract was removed, placed into a microfuge tube and centrifuged (14,500 *g*, 5 min). An aliquot of the supernatant (1 ml) was retained for ^{14}C determination. These extracts were used to determine the amount of free and exchangeable substrate remaining (glucose, citrate) or soluble plant C (maize residues). $^{14}CO_2$ in the NaOH traps and extracts was measured via liquid scintillation counting with automated quench correction (Wallac 1404 Scintillation Counter;

PerkinElmer Life Sciences, Boston, MA) with 4 ml of Optiphase HiSafe 3 scintillation fluid (Fisher Scientific, Loughborough, UK).

3.2.5 Soil solution analyses

Soil solution ammonium (NH_4^+), nitrate (NO_3^-), molybdate reactive phosphorus (MRP) and soil dithionite-citrate-bicarbonate Fe contents were determined colorimetrically according to Mulvaney (1996), Miranda et al. (2001), Murphy and Riley (1962) and Loeppert and Inskeep (1996), respectively, with a PowerWave XS Microplate Spectrophotometer (BioTek Instruments Inc., Winooski, VT). Total dissolved N and organic C and were analysed using a Multi N/C 2100/2100 analyser. Due to chemical interference, the inorganic N data had to be excluded and so the NO_3^-, NH_4^+ and dissolved organic N of the soil solution are not reported. Soil water EC was measured using a Jenway 4520 conductivity meter and pH with a Hanna 209 pH meter (Hanna Instruments Ltd., Leighton Buzzard, UK).

3.2.6 Statistical analysis

All data analysis was done using R (version 1.1.463; R Core Team, 2017), with figures made using the R package 'ggplot2' (Wickham, 2016). Data was assessed for test assumptions by using the Shapiro-Wilk test ($p > 0.05$) for normality, and Levene's test for homoscedasticity ($p > 0.05$) as well as assessing the qqplots and the residual versus fitted plots. If the assumptions were not met, the data were either $\log_{10}$, square root or cube transformed. In the $Fe(OH)_3$ DOC and $Fe(OH)_3$ and $FeCl_2$ MRP datasets; 2, 3 and 2 outliers were removed, respectively, due to heavily skewing the distributions, as identified by qqplots. Kruskal-Wallis tests ($p < 0.05$) were used to test each factor if the assumptions were not met after transformation. The final cumulative CO_2 efflux and ^{14}C substrate mineralisation values were compared between soil depths and applied iron rates (and in the latter case, between iron forms) by 2-way ANOVAs ($p < 0.05$). All soil solution data were analysed for the effect of soil depth, time and applied iron rates with 2-way ANOVAs ($p < 0.05$). Multiple comparisons were done using the Tukey test ($p < 0.05$). The data in Table 3.1 were tested for assumptions as above, then a 2-sample unpaired Student's t-test ($p < 0.05$) was performed on topsoil versus subsoil means. In the case of failed assumptions, the Wilcoxon signed-rank test ($p < 0.05$) was used. As the assumptions for the parametric

correlation test failed, the Kendall's tau (τ) correlation test ($p < 0.05$) was performed between untransformed $Fe(OH)_3$ and $FeCl_2$ measured properties and the Fe rates applied, shown in Table 3.2.

3.3 Results

Means and standard errors for each iron rate at top- and subsoil depth in the $Fe(OH)_3$ and $FeCl_2$ incubations are summarised in Appendix 2 (Table S1).

3.3.1 Effect of Fe on cumulative CO_2 efflux from native SOM turnover

As expected, CO_2 efflux was highest in the topsoil (Fig. 3.1), with 359 and 180% greater final cumulative CO_2 efflux compared to the subsoil in both $Fe(OH)_3$ ($p < 0.001$) and $FeCl_2$ incubations ($p < 0.001$), respectively. While $Fe(OH)_3$ had no significant effect on the final cumulative CO_2 efflux ($p = 0.99$), there was a weak significant negative association between the rate of iron added and the CO_2 efflux from the subsoil (Table 2). In contrast, $FeCl_2$ addition induced a large increase in CO_2 efflux ($p = 0.013$), with the maximum rate (5,000 mg kg^{-1}) stimulating a 39 and 200% increase in topsoil and subsoil cumulative CO_2 efflux compared to the control, respectively. In the second highest $FeCl_2$ rate (1,000 mg kg^{-1}), the cumulative efflux was 133% higher in the subsoil, but interestingly, 10% lower in the topsoil compared to the control.

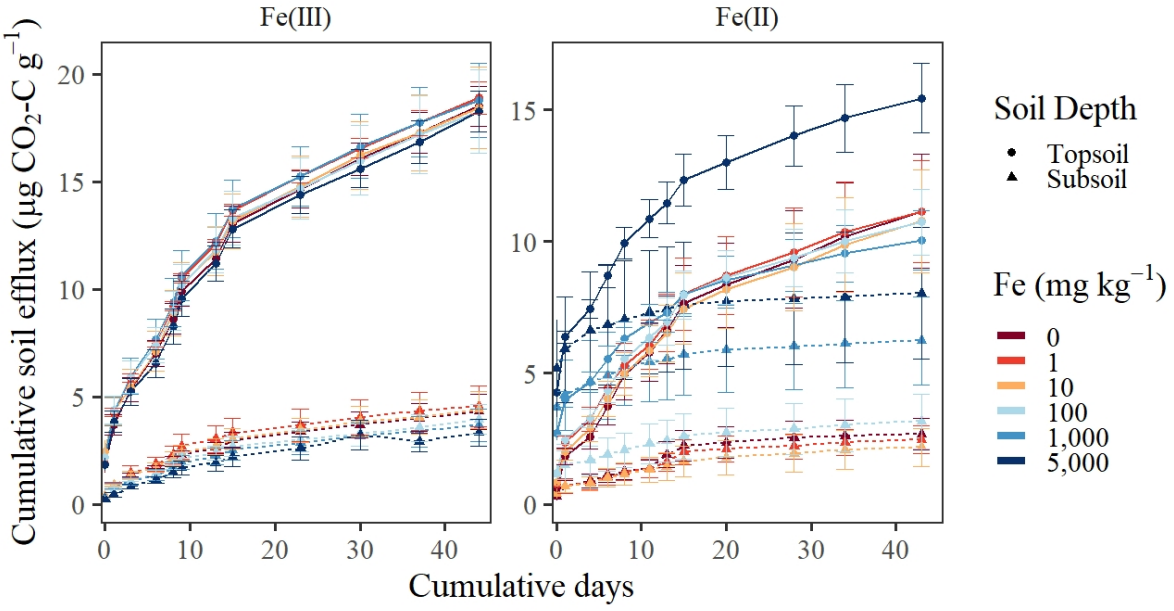

Fig. 3.1 Cumulative soil CO2 efflux from top- and subsoil (mean ± SEM) incubations (n = 4) over 45 days with the addition of different rates of Fe(III) or Fe(II). Values correspond to the g dry weight equivalent. Note different y-axis range for Fe(III) and Fe(II).

Table 3.2 Kendall tau (τ) correlations ($p < 0.05$) of measured properties with the $Fe(OH)_3$ and $FeCl_2$ rates applied across the entire incubation. Numbers in bold indicate significant relationships ($p < 0.05$).

	$Fe(OH)_3$				$FeCl_2$			
	Topsoil		Subsoil		Topsoil		Subsoil	
	τ	*p*	τ	*P*	τ	*p*	τ	*p*
CO_2 efflux	-0.022	0.61	-0.098	**0.022**	>-0.01	0.93	0.08	0.06
DOC	0.22	**<0.001**	-0.10	0.088	0.017	0.78	0.14	**0.024**
pH	0.055	0.38	0.02	0.81	-0.67	**<0.001**	-0.74	**<0.001**
EC	-0.05	0.43	<0.01	0.89	0.82	**<0.001**	0.81	**<0.001**
MRP	-0.20	**<0.001**	-0.17	**0.007**	-0.42	**<0.001**	0.072	0.31

3.3.2 Soil solution chemistry with soil depth and in response to iron addition

In the $Fe(OH)_3$ incubation, all soil properties apart from MRP differed across the 6-week period ($p < 0.001$) although these differences were greater week-to-week compared to the beginning versus the end of the incubation (Fig. 3.2). Incubated topsoil had 178% more DOC ($p < 0.001$; Fig. 3.2a); a higher pH ($p < 0.001$; Fig. 3.2b); 128% greater EC ($p < 0.001$; Fig.

3.2c); and 250% greater MRP levels ($p < 0.001$; Fig. 3.2d) than the subsoil. The rate of $Fe(OH)_3$ addition only influenced DOC and MRP. Both top- and subsoil DOC was reduced by $Fe(OH)_3$, with the highest rate driving a 24 and 40% decrease in top- and subsoil DOC compared to the control ($p < 0.001$; Fig. 3.2a) and a strong positive association between $Fe(OH)_3$ rates and DOC in the topsoil (Table 3.2). The 5,000 mg kg^{-1} $Fe(OH)_3$ rate decreased MRP in the top- and subsoil by 48 and 35% compared to the control, respectively ($p < 0.001$) and MRP was negatively associated with $Fe(OH)_3$ rates in both the topsoil and subsoil (Table 3.2).

In the incubation with $FeCl_2$, only DOC ($p = 0.02$; Fig. 3.2a) differed over the 6-week period. The topsoil had 129% more DOC ($p < 0.001$; Fig. 3.2a); a higher pH ($p = 0.007$; Fig. 3.2b); and 225% more MRP ($p < 0.001$; Fig. 3.2d), compared to the subsoil. DOC was positively associated with Fe(II) rates (Table 3.2) and $FeCl_2$ induced a 303 and 344% increase in top- and subsoil DOC ($p < 0.001$; Fig. 3.2a), respectively. However, this trend was not consistent in the 1,000 mg kg^{-1} Fe(II) rate, which increased DOC in the subsoil but decreased in the topsoil. pH decreased with increasing $FeCl_2$ rate regardless of soil depth, with 97% of the variation in pH explained by the rate of $FeCl_2$ iron added (Fig. 3.2b) and strong negative associations between Fe and pH in both top- and subsoil (Table 3.2). At the highest $FeCl_2$ rate, this corresponded to a soil solution pH of 2.5 ± 0.03 and 2.3 ± 0.02 in the top- and subsoil, respectively. Similarly, EC was also strongly associated with $FeCl_2$ addition (Table 3.2) and the rate of $FeCl_2$ explained 98% of the variation in EC. This translated to a 74, 19 and 3-fold increase in soil water EC with the 3 highest rates compared to the control ($p < 0.001$; Fig. 3.2c), respectively.

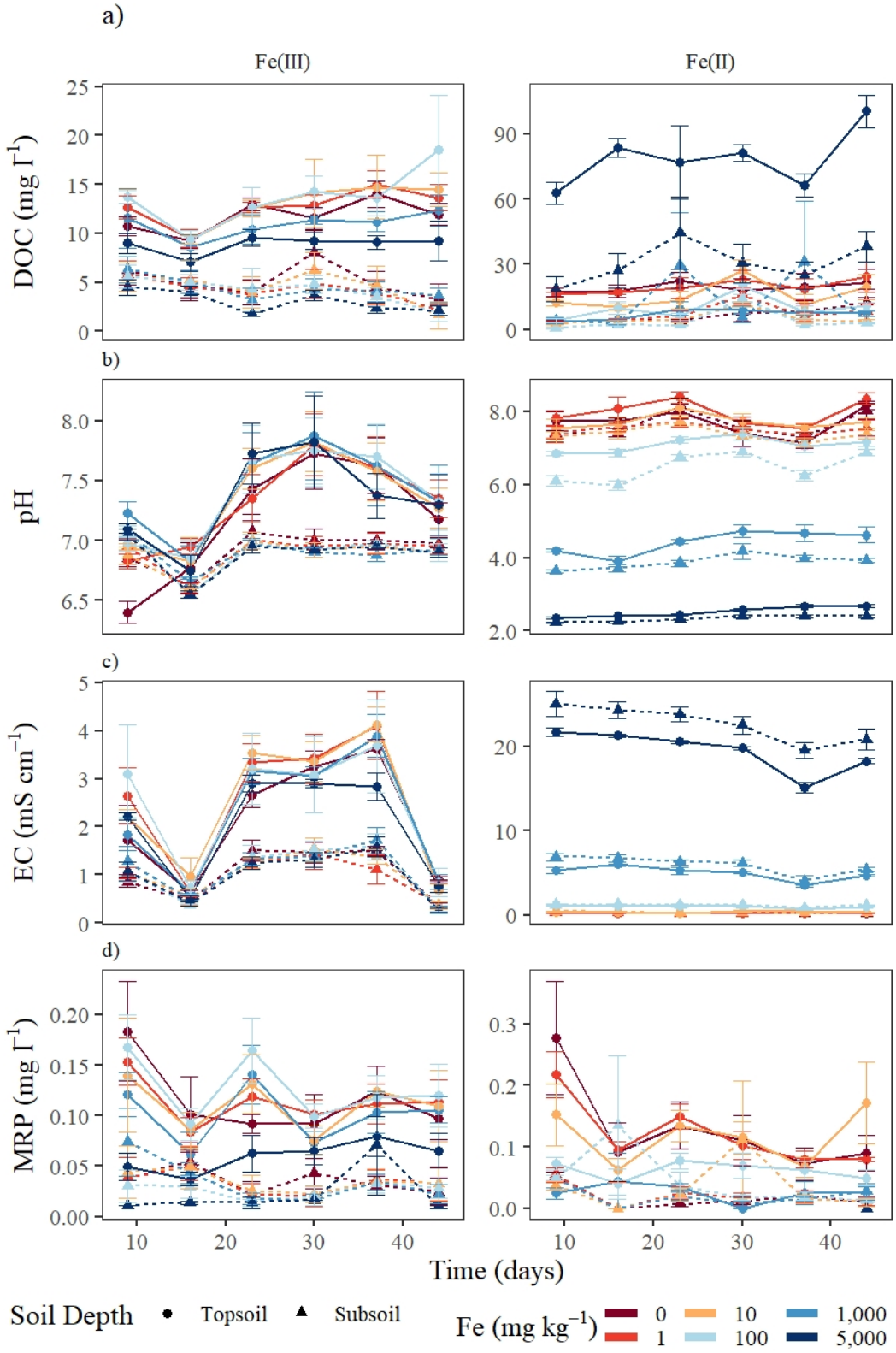

Fig. 3.2 Effect of the addition of different rates of Fe(III) or Fe(II) on soil water chemistry: (a) dissolved organic carbon (DOC), (b) soil pH, and (c) electrical conductivity (EC) and molybdate reactive phosphorus (MRP) from top- and subsoil over 45 days (mean ± SEM, *n* = 4). The highest Fe(II) rate is not displayed in panel (d) as the concentrations exceeded detectable

limits of the methodology used. Values correspond to the g dry weight equivalent. Note different y-axis range for Fe(III) and Fe(II).

3.3.3 ^{14}C-substrate mineralisation

Following the addition of the ^{14}C-labelled substrates to the topsoil, a rapid initial phase of $^{14}CO_2$ evolution was followed by a slower phase of $^{14}CO_2$ production (Fig. 3.3). This initial rapid phase was delayed in the corresponding subsoil incubations with glucose and citrate (Fig. 3.3a and b), but not in the plant matter incubation (Fig. 3.3c). Overall, both Fe forms produced similar trends of lower $^{14}CO_2$ evolution with higher iron concentration. In addition, the $FeCl_2$ treatments evolved less $^{14}CO_2$ than those incubated with $Fe(OH)_3$ [^{14}C-glucose (p = 0.044), citrate ($p < 0.001$) and plant matter ($p < 0.001$)].

Of the total ^{14}C-glucose added to the soil 18-23 and 1-22% was recovered as $^{14}CO_2$ in the $Fe(OH)_3$ and $FeCl_2$ incubations after 72 h, respectively (Appendix 2, Table S2). Only ca. 3% of the ^{14}C could be recovered from the soil water after 72 h, with the remainder assumed to remain in the soil and be immobilised in the microbial biomass. The final cumulative $^{14}CO_2$ evolution was 11 and 6% lower in the 5,000 mg kg^{-1} $Fe(OH)_3$ treatment in the topsoil and subsoil compared to the control (p = 0.047), but 38 and 91% lower in the $FeCl_2$ incubation ($p < 0.001$), respectively (Fig. 3.3a). The final cumulative $^{14}CO_2$ evolved was 87 and 138% higher in the topsoil of the $Fe(OH)_3$ (p = 0.045) and Fe(II) ($p < 0.001$) incubations compared to the subsoil, respectively.

Of the ^{14}C-citrate added to the soil, between 36-52 and 1-52% was respired in the $Fe(OH)_3$ and $FeCl_2$ treatments, respectively after 72 h (Appendix 2, Table S2). On average, 10% of the added ^{14}C was recoverable at the end of the incubation period using a phosphate buffer extractant. Final cumulative ^{14}C-citrate mineralisation was 21 and 5% lower in soil with 5,000 mg kg^{-1} of $Fe(OH)_3$ in the topsoil and subsoil compared to the control (p = 0.02), but 98 and 96% lower with $FeCl_2$ addition ($p < 0.001$), respectively (Fig. 3.3b). The final cumulative $^{14}CO_2$ evolved was 63 and 82% higher in the topsoil of the $Fe(OH)_3$ (p = 0.045) and $FeCl_2$ ($p < 0.001$) incubations compared to the subsoil, respectively. Despite a longer incubation period, the proportion of ^{14}C evolved from the plant matter was similar to that for glucose and citrate (Fig. 3.3c, Appendix 2, Table S2).

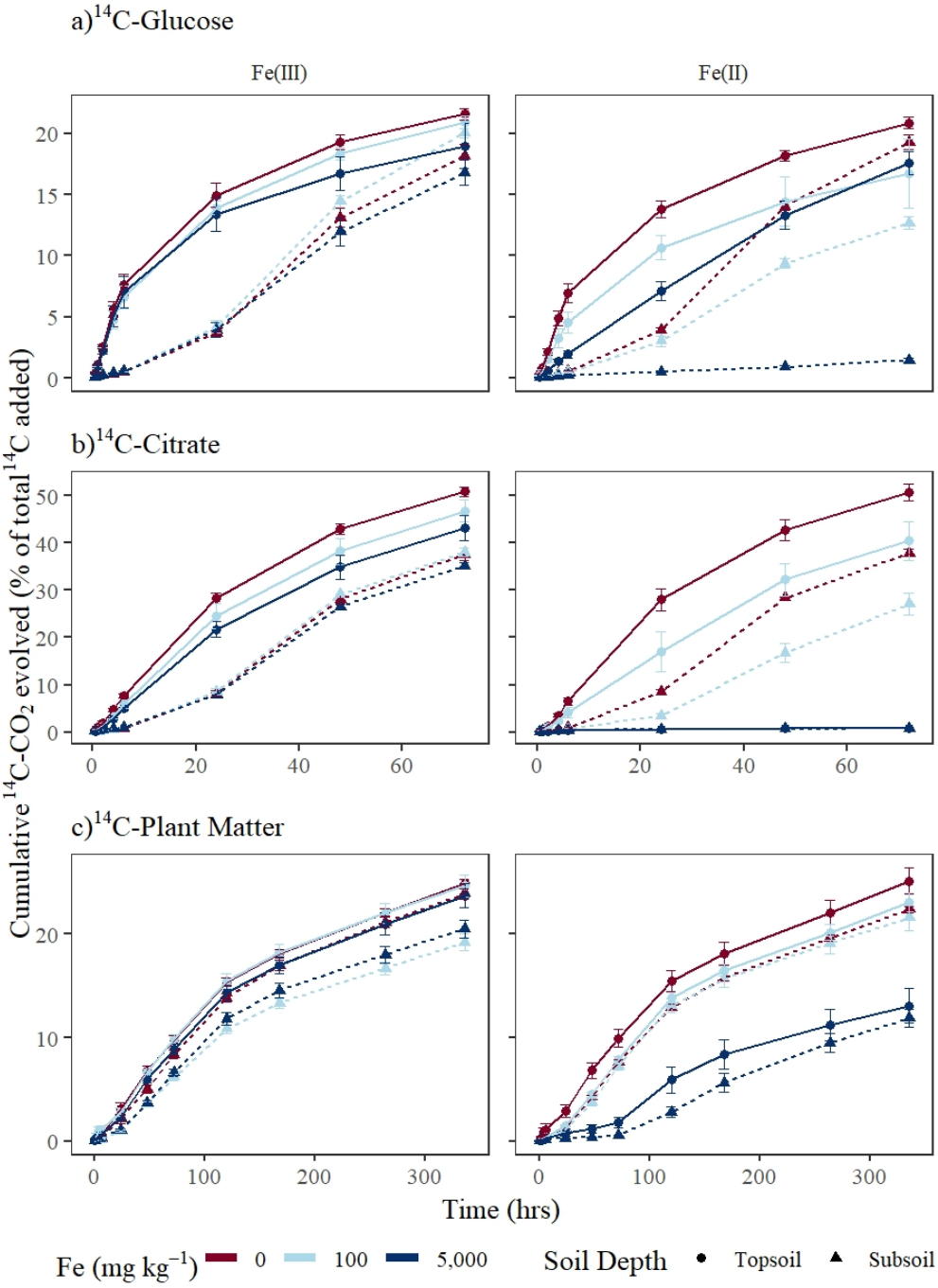

Fig. 3.3 Cumulative ^{14}C-CO_2 evolved after the addition of ^{14}C-labelled a) glucose, b) citrate, and c) *Zea mays* shoot residues incubated in top- and subsoil with different added rates of Fe(III) or Fe(II). Value are mean ± SEM (*n* = 4). Incubations were 72 h for a) and b), while c) was incubated for 336 h, before the soil was extracted.

Of the total ^{14}C-plant matter added to the soil, 19-25% and 13-25% was mineralised after 14 d in the $Fe(OH)_3$ and $FeCl_2$ incubations, respectively, with between 72 and 85% remaining in the soil (Appendix 2, Table S2). Similar to ^{14}C-glucose, the extractant at the end of the incubation period only recovered ca. 3% of the ^{14}C-plant matter. ^{14}C-plant matter

mineralisation was 6 and 16% lower in soil with 5,000 mg kg^{-1} of $Fe(OH)_3$ in the topsoil and subsoil compared to the control (p = 0.015), but 58 and 63% lower with $FeCl_2$ addition (p < 0.001), respectively. The final cumulative $^{14}CO_2$ evolved was 24% higher in the topsoil of the $Fe(OH)_3$ (p = 0.002) incubation compared to the subsoil, while there was no difference between depths in the $FeCl_2$ (p = 0.065) incubated soil.

3.4 Discussion

3.4.1 Effect of $Fe(OH)_3$ addition on CO_2 production

Although the addition of $Fe(OH)_3$ to our agricultural top- and subsoil did not result in a major reduction in CO_2 efflux, the Kendall's tau coefficients (Table 3.2) indicated that increasing rates of $Fe(OH)_3$ induced a small reduction in CO_2 efflux (albeit weakly in topsoil). There was a significant reduction in DOC and MRP with increasing $Fe(OH)_3$ addition rate (Fig. 3.2a and d), which supports our hypothesis that insoluble Fe would decrease overall CO_2 release due to DOC and P immobilisation. We attribute this to the ability of DOC to be adsorbed to $Fe(OH)_3$, which by immobilizing labile substrates can limit decomposer activity (Riedel et al., 2013). The reduction in MRP would suggest an increase in the formation of insoluble Fe-P complexes making P less available, likely causing a reduction in P for microbial growth and metabolism (e.g. ATP production) (Jones and Brassington, 1998; Li et al., 2012; Wen et al., 2019).

The hypothesis that more C would be preserved with the addition of newly added C compared to native C was confirmed in the $Fe(OH)_3$ incubation (Fig. 3.3), yet the mineralisation suppression effect was not as strong as expected with 13 and 15% less ^{14}C glucose and citrate being mineralised after 72 h at high Fe addition rates (5,000 mg kg^{-1}; Appendix 2, Table S2) compared to the control. This contrasts with Jones and Edwards (1998) who observed a 33 and 98% suppression of mineralisation of the same substrates after just 22 h following the addition of only *ca*. 150 mg kg^{-1} of $Fe(OH)_3$ to soil from the same field site. This stronger effect observed by Jones and Edwards (1998) may be due to two important differences between their study and ours: i) they used much lower concentrations of ^{14}C substrates so the binding strength to the solid surface would be much greater; and ii) they added $Fe(OH)_3$, mixed it and allowed it to equilibrate with the ^{14}C substrates prior to addition to the soil (i.e. they were exactly co-located). Importantly, the pre- addition mixing would

allow the substrates to adsorb onto the $Fe(OH)_3$ surface and become immobilized before addition to soil, while the mixing of this solution with the soil will have allowed maximum distribution of Fe in the soil. In contrast, we applied Fe in our experiments to mimic a way in which Fe-rich materials could be applied in the field (e.g. injection), resulting in a less effective soil coverage of the soil by the added Fe. Similar to Jones and Edwards (1998), Porras et al. (2018) found a 99.5% mineralisation suppression of ^{13}C-glucose pre-sorbed with $Fe(OH)_3$ after 72 h following addition to soil. This strong suppression may be due to physical protection driven by the Fe or hydrophobic interactions or adsorption of degradation products (Kögel-Knabner et al., 2008), as glucose is not predicted to sorb directly to $Fe(OH)_3$ (Jones and Edwards, 1998). When Porras et al. (2018) added glucose-free $Fe(OH)_3$, as we did in Figure 3.1, there was virtually no difference with the controls in top- or subsoil. We conclude that our method of application may have resulted in a non-uniform distribution of $Fe(OH)_3$ in the soil, limiting the impact on soil C dynamics. This heterogeneity, is however, likely to reflect real-world conditions when substances (e.g. slurry, liquid waste) are mechanically injected into the soil.

3.4.2 The effect of $FeCl_2$ on CO_2 production

The results confirmed our hypothesis that addition of soluble Fe(II) (i.e. $FeCl_2$) would induce greater CO_2 release compared to the control. The $FeCl_2$ added to the soil rapidly oxidised to form Fe oxyhydroxide. This Fe(II) oxidation to Fe(III) in the presence of O_2 drove the strong decrease in pH and increase in EC observed in this study (Fig. 3.2). At the high application rates, both the pH and EC would be toxic to some of the microbial community and plants growing in the soil (Jones et al., 2019; Kaya et al., 2003). The adding of this low pH solution is likely also the main driver of DOC solubilisation, as found by Hall and Silver (2013), who partly attributed a 270% increase in CO_2 after 24 h following $FeCl_2$ addition to tropical soil to increased DOC availability. An increase in easily-mineralisable DOC is likely to also contribute to the high cumulative CO_2 efflux observed in the high $FeCl_2$ addition rates (Fig. 3.1) in the temperate soil studied here. However, when comparing the CO_2 efflux with the results of easily-mineralised ^{14}C substrates (Fig. 3.3), this trend was not observed. While an increase in non-labelled DOC mineralisation would not be captured by our ^{14}C studies, the lack of a decrease in DOC (Fig. 3.2a) and associated increase in CO_2 efflux in the higher $FeCl_2$

addition rates throughout the 6 weeks suggests that increased DOC availability was not the primary source of the higher cumulative CO_2 evolution rates. In addition, citrate which is easily mineralised in soil, had up to 52 and 39% of the added labelled substrate mineralised in 72 h in both the top- and subsoil free from added $FeCl_2$ (Fig. 3.3; Appendix 2, Table S2). Addition of high rates of $FeCl_2$, however, reduced substrate mineralisation rather than stimulating it, confirming the hypothesis that newly added C would be preserved to a greater extent than native soil C by addition of soluble Fe. This further suggests that the higher cumulative efflux observed in Figure 3.1 is not primarily a microbial response to increased DOC availability.

Despite the higher total cumulative CO_2 efflux of the high $FeCl_2$ rates reported in the results, the difference in efflux between $FeCl_2$ rates is entirely explained by the efflux at the first sampling time-point (Appendix 2, Fig. S2), with both topsoil and subsoil contributing more to overall CO_2 efflux with increasing $FeCl_2$ at the first sampling time-point. In addition, if the efflux data from day 0 (i.e. 0-1 h after iron addition – first sampling time point) are excluded and CO_2 efflux is only considered from day 1 (Appendix 2, Fig. S4), the differences between $FeCl_2$ rates are lost, confirming that the increase in CO_2 production primarily occurred immediately (< 24 h) following iron addition.

As observed by Jones et al. (2011), the short-term increase in CO_2 production following biochar addition to soil was both biotically determined by positive priming, and abiotically driven by stimulating the dissolution of inorganic carbonates and degassing as CO_2. The strong $FeCl_2$-induced acidification of the soil (pH ≥2.3) observed here (Fig. 3.2) would convert any HCO_3^- present in the soil to CO_2, a reaction driven completely by pH and not Fe (Hall and Silver, 2013). To test whether this occurred, distilled water and HCl-amended distilled water of the same pH as the high $FeCl_2$ rates (5,000 and 1,000 mg kg^{-1}) were added to the soil and the CO_2 efflux was measured (Appendix 2). The results confirm that pH was a significant driver in the short-term (i.e. first hour following addition) production of CO_2 observed in the 5,000 mg kg^{-1} $FeCl_2$ rate (Appendix 2, Fig. S3). With small amounts of $CaCO_3$ present in the topsoil (Table 3.1), we speculate that this is potentially a source of HCO_3^- and the immediate spike in CO_2 measured in Figure 3.1.

Another mechanism that may have contributed to the intense short term CO_2 production is an increase in phenol-oxidative activity, which Hall and Silver (2013) found to increase linearly with $FeCl_2$ concentration both with and without (aerobic) tropical soil. This

enzyme activity is a product of the 'Fenton reaction', where H_2O_2 (produced by $FeCl_2$ oxidation) and $FeCl_2$ react to produce the strong SOC-oxidising hydroxyl radical (•OH). The •OH then oxidises phenolics which stimulates phenol-oxidative activity. This is likely another reaction that contributed to the short-term CO_2 production in Figure 3.1, though the low soil solution pH in this study will likely have limited phenol oxidase activity for which neutral conditions are typically optimal (Sinsabaugh, 2010). In addition, this mechanism is not as important a driver as pH which accounts for the majority of the Fe-induced increase in CO_2 in the first sampling time point (Appendix 2, Fig. S3) and reduces microbial C use efficiency at low pH (Jones et al., 2019). However, it may be a more important mechanism over longer timescales (Sinsabaugh, 2010).

Hall et al. (2016) found that despite a 21% reduction in lignin decomposition with the addition of $FeCl_2$, there was no effect on overall CO_2 production. This implies that $FeCl_2$-induced C stabilisation is specific to certain forms of C rather than bulk SOC, which, when measuring CO_2 efflux, cannot be distinguished, as we (Fig. 3.1) and Hall et al. (2016) found. This is also consistent with the ^{14}C results of this study that show different rates of mineralisation suppression depending on the form of C added (Fig. 3.3).

Co-precipitation of new DOC/Fe(III) phases following Fe(II) oxidation is an important mechanism of C preservation in soils experiencing frequent redox fluctuations (e.g. paddy soils; Sodano et al., 2017). This may have been an important mechanism suppressing CO_2 production in the Fe(II) glucose and citrate incubations (Eusterhues et al., 2011), as the suppression effect was much lower in the $Fe(OH)_3$ incubation where adsorption of DOC on added Fe(III) would be more dominant.

In this study, the addition of $FeCl_2$ to the soil drove an immediate intense CO_2 response. We ascribe this response to i) soil acidification which promoted the abiotic conversion of DIC to CO_2, ii) an increase in DOC availability and biotic respiration, (iii) a reduction in microbial C use efficiency; and to a lesser extent, iv) SOC oxidation, from increased phenol-oxidative activity resulting from the 'Fenton reaction'. However, buffering the $FeCl_2$ solution to typical soil pH values (i.e. >5.5; Jones et al., 2019) is likely to induce the rapid precipitation of $Fe(OH)_2$ which will then oxidise rapidly to $Fe(OH)_3$. This is expected to vastly reduce the intense short-term CO_2 response observed, as found by Hall and Silver

(2013), and may induce a net decrease in CO_2 production (Hall and Silver, 2013; Wen et al., 2019) and would improve microbial C use efficiency (Jones et al., 2019) .

3.4.3 CO_2 efflux and soil chemistry differences by depth

The hypothesis that the greatest reduction in C turnover would be seen in subsoil was met in the $Fe(OH)_3$ incubation, where less ^{14}C was mineralised in the subsoil compared to the topsoil. Differences in soil chemistry were primarily driven by the depth of soil rather than the rate of Fe added. In contrast, soil depth was a poorer predictor of soil properties in the $FeCl_2$ incubation. The differences between the top- and subsoil properties measured in the $FeCl_2$ incubation were smaller than those in the $Fe(OH)_3$ and, in the case of EC, there was no difference between either depth. This latter trend is attributable to the Cl^- ions produced by the oxidation of the added $FeCl_2$, which explained 98% of the variation in EC, rather than any physical, chemical or biological differences between the soil depths. Despite the $FeCl_2$ rate also being a strong predictor for pH, the lower pH in the subsoil demonstrates that its ability to buffer acidity is lower than that of topsoil – considering they started at almost identical soil solution pH levels (Table 3.1).

The $^{14}CO_2$ responses were different in the top and subsoil (Fig. 3.3) with a lag phase in $^{14}CO_2$ production present in subsoil incubations, which is consistent with Jones et al. (2018). The lack of difference in lag phases with the addition of $Fe(OH)_3$ suggest that C is not limiting microbial growth, while $FeCl_2$ addition is.

3.4.4 Opportunities and limitations

The results of this study demonstrate that while there is potential for C to be preserved by the addition of Fe-rich material to agricultural soil, the quantity, form and method of application are critical to its success. In addition, as soil texture plays an important role in the Fe and C cycles (Saidy et al., 2013), targeting sandy soils where little chemical C protection potential exists (i.e. limited clay and metal content) could prove more successful than the sandy clay loam used in this study. While surface application or conventional injection could be a viable and cheap method for shallow application, to reach the subsoil a different method of application would be needed. Injection via a deep ripper (the same way liquid manure is agriculturally injected) or surface application followed by deep soil inversion

could be a potential to increase the Fe content deep in the soil, which in the latter case could also have concomitant C sequestration benefits (Alcántara et al., 2016; Feng et al., 2020). However, this method may be less cost-effective and more difficult to convince land users to implement. Large amounts of $Fe(OH)_3$ and $Fe(OH)_2$ containing sludge can efficiently be recovered from wastewater treatment to be reused (Chen et al., 2015). In addition, large quantities of 'red mud' high in iron oxide are produced (175 M t in 2020; World Aluminium, 2021) from industry and only a small proportion is reused. Addition to soil has been studied for improved P cycling and acidity amelioration but its use for accelerated soil C sequestration has yet to be fully explored. Mixed with OM, such as slurry, these Fe sources have potential to be effective C sequestration strategies. However, as no *in situ* experiments testing Fe on agricultural soil C sequestration exist, this is yet to be determined. The net CO_2 budget as well as the cost of the strategy would need to be determined to understand if this is an effective C sequestration strategy.

3.5 Conclusions

To the best of our knowledge, this is the first experiment to test Fe application to agricultural soils specifically to promote C sequestration. The greatest preservation of C was achieved with introduced ^{14}C substrates rather than with native SOM. The decomposition suppression effect was greatest in the subsoil, indicating that the subsoil may be the most effective target for future Fe addition studies. However, $Fe(OH)_3$ had only weak C preservation effects overall, whilst $FeCl_2$ induced strong C preservation of the added substrate, but equally a strong short-term CO_2 response with native SOM. This latter CO_2 response was predominantly due to acidification-driven abiotic (loss of carbonates) and biotic (greater DOC availability and respiration) responses and is likely to outweigh any C preservation gains. Our results suggest that the addition of $Fe(OH)_3$ or $FeCl_2$ (unless buffered) to agricultural top- or subsoil at any rate up to 5 g kg^{-1} would unlikely protect a substantial amount of SOC. Therefore, from our results, we conclude that this strategy is not effective. We suggest targeting low-Fe sandy soil and adding OM pre-associated with soluble Fe for more success, as it maximises C preservation and co-location of Fe and C in the soil. Finally, repeating these experiments *in situ* and with available Fe sources (e.g. wastewater sludge,

red mud) will increase our understanding of the full potential of this strategy for C sequestration.

3.6 Acknowledgements

This work was supported by the FLEXIS (Flexible Integrated Energy Systems) programme, an operation led by Cardiff University, Swansea University and the University of South Wales and funded through the Welsh European Funding Office (WEFO). We thank Dr Lucy Greenfield for help with the radiotracer experiments and Dr Antonio Sanchez-Rodriguez for help with the soil analysis.

3.7 References

Alcántara, V., Don, A., Well, R., Nieder, R., 2016. Deep ploughing increases agricultural soil organic matter stocks. Global Change Biology 22, 2939–2956.

Badalucco, L., Gelsomino, A., Dellorco, S., Grego, S., Nannipieri, P., 1992. Biochemical-characterization of soil organic-compounds extracted by 0.5 M K_2SO_4 before and after chloroform fumigation. Soil Biology and Biochemistry 24, 569-578.

Chen, C., Hall, S.J., Coward, E., Thompson, A., 2020. Iron-mediated organic matter decomposition in humid soils can counteract protection. Nature Communications 11, 1–13.

Chen, Z., Wang, X., Ge, Q., Guo, G., 2015. Iron oxide red wastewater treatment and recycling of iron-containing Sludge. Journal of Cleaner Production 87, 558–566.

Collivignarelli, M.C., Abbà, A., Benigna, I., 2020. The reuse of biosolids on agricultural land: Critical issues and perspective. Water Environment Research 92, 11–25.

Coward, E.K., Thompson, A.T., Plante, A.F., 2017. Iron-mediated mineralogical control of organic matter accumulation in tropical soils. Geoderma 306, 206–216.

Darrah, P.R., 1991a. Measuring the diffusion coefficient of rhizosphere exudates in soil. I. The diffusion of non-sorbing compounds. Journal of Soil Science 42, 413–420.

Darrah, P.R., 1991b. Measuring the diffusion coefficients or rhizosphere exudates in soil. II. The diffusion of sorbing compounds. Journal of Soil Science 42, 421–434.

Eusterhues, K., Rennert, T., Knicker, H., Kögel-Knabner, I., Totsche, K.U., Schwertmann, U., 2011. Fractionation of organic matter due to reaction with ferrihydrite: Coprecipitation versus adsorption. Environmental Science and Technology 45, 527–533.

Feng, Q., An, C., Chen, Z., Wang, Z., 2020. Can deep tillage enhance carbon sequestration in soils? A meta-analysis towards GHG mitigation and sustainable agricultural management. Renewable and Sustainable Energy Reviews 133, 110293.

Giannetta, B., Plaza, C., Siebecker, M.G., Aquilanti, G., Vischetti, C., Plaisier, J.R., Juanco, M., Sparks, D.L., Zaccone, C., 2020. Iron speciation in organic matter fractions isolated from soils amended with biochar and organic fertilizers. Environmental Science and Technology 54, 5093–5101.

Hall, S.J., Silver, W.L., 2013. Iron oxidation stimulates organic matter decomposition in humid tropical forest soils. Global Change Biology 19, 2804–2813.

Hall, S.J., Silver, W.L., Timokhin, V.I., Hammel, K.E., 2016a. Iron addition to soil specifically stabilized lignin. Soil Biology and Biochemistry 98, 95–98.

Jobbágy, E.G., Jackson, R.B., 2000. The vertical distribution of soil organic carbon and its relation to climate and vegetation. Ecological Applications 10, 423–436.

Jones, D.L., Brassington, D.S., 1998. Sorption of organic acids in acid soils and its implications in the rhizosphere. European Journal of Soil Science 49, 447–455.

Jones, D.L., Cooledge, E.C., Hoyle, F.C., Griffiths, R.I., Murphy, D. V., 2019. pH and exchangeable aluminum are major regulators of microbial energy flow and carbon use efficiency in soil microbial communities. Soil Biology and Biochemistry 138, 0–4.

Jones, D.L., Darrah, P.R., Kochian, L. V., 1996. Critical evaluation of organic acid mediated iron dissolution in the rhizosphere and its potential role in root iron uptake. Plant and Soil 180, 57–66.

Jones, D.L., Edwards, A.C., 1998. Influence of sorption on the biological utilization of two simple carbon substrates. Soil Biology and Biochemistry 30, 1895–1902.

Jones, D.L., Magthab, E.A., Gleeson, D.B., Hill, P.W., Sánchez-Rodríguez, A.R., Roberts, P., Ge, T., Murphy, D. V., 2018. Microbial competition for nitrogen and carbon is as intense in the subsoil as in the topsoil. Soil Biology and Biochemistry 117, 72–82.

Jones, D.L., Murphy, D. V, Khalid, M., Ahmad, W., Edwards-jones, G., Deluca, T.H., 2011. Short-term biochar-induced increase in soil CO_2 release is both biotically and abiotically mediated. Soil Biology and Biochemistry 43, 1723–1731.

Jones, D.L., Willett, V.B., 2006. Experimental evaluation of methods to quantify dissolved organic nitrogen (DON) and dissolved organic carbon (DOC) in soil. Soil Biology and Biochemistry 38, 991–999.

Jones, D.L., Farrar, J., Giller, K.E., 2003. Associative nitrogen fixation and root exudation - What is theoretically possible in the rhizosphere? Symbiosis 35, 19-38.

Kaiser, K., Guggenberger, G., 2007. Sorptive stabilization of organic matter by microporous goethite : sorption into small pores vs . surface complexation. European Journal of Soil Science 58, 45–59.

Kaiser, K., Guggenberger, G., 2000. The role of DOM sorption to mineral surfaces in the preservation of organic matter in soils. Organic Geochemistry 31, 711–725.

Kaya, M.D., Ipek, A., Öztürk, A., 2003. Effects of different soil salinity levels on germination and seedling growth of safflower (*Carthamus tinctorius L.*). Turkish Journal of Agriculture and Forestry 27, 221–227.

Kell, D.B., 2012. Large-scale sequestration of atmospheric carbon via plant roots in natural and agricultural ecosystems: why and how. Philosophical Transactions of the Royal Society B: Biological Sciences 367, 1589–1597.

Kögel-Knabner, I., Guggenberger, G., Kleber, M., Kandeler, E., Kalbitz, K., Scheu, S., Eusterhues, K., Leinweber, P., 2008. Organo-mineral associations in temperate soils: Integrating biology, mineralogy, and organic matter chemistry. Journal of Plant Nutrition and Soil Science 171, 61–82.

Lal, R., 2004. Soil Carbon Sequestration Impacts on Global Climate Change and Food Security. American Association for the Advancement of Science 304, 1623–7.

Lalonde, K., Mucci, A., Ouellet, A., Gélinas, Y., 2012. Preservation of organic matter in sediments promoted by iron. Nature 483, 198–200.

Lehmann, J., Kleber, M., 2015. The contentious nature of soil organic matter. Nature 528, 60–68.

Li, Y., Yu, S., Strong, J., Wang, H., 2012. Are the biogeochemical cycles of carbon, nitrogen, sulfur, and phosphorus driven by the "FeIII-FeII redox wheel" in dynamic redox environments? Journal of Soils and Sediments 12, 683–693.

Melton, E.D., Swanner, E.D., Behrens, S., Schmidt, C., Kappler, A., 2014. The interplay of microbially mediated and abiotic reactions in the biogeochemical Fe cycle. Nature Reviews Microbiology 12, 797–808.

Mikutta, R., Kleber, M., Torn, M.S., Jahn, R., 2006. Stabilization of soil organic matter: Association with minerals or chemical recalcitrance? Biogeochemistry 77, 25–56.

Minasny, B., Malone, B.P., McBratney, A.B., Angers, D.A., Arrouays, D., Chambers, A., Chaplot, V., Chen, Z.S., Cheng, K., Das, B.S., Field, D.J., Gimona, A., Hedley, C.B., Hong, S.Y., Mandal, B., Marchant, B.P., Martin, M., McConkey, B.G., Mulder, V.L., O'Rourke, S., Richer-de-Forges, A.C., Odeh, I., Padarian, J., Paustian, K., Pan, G., Poggio, L., Savin, I., Stolbovoy, V., Stockmann, U., Sulaeman, Y., Tsui, C.C., Vågen, T.G., van Wesemael, B., Winowiecki, L., 2017. Soil carbon 4 per mille. Geoderma 292, 59–86.

Miranda, K.M., Espey, M.G., Wink, D.A., 2001. A rapid, simple spectrophotometric method for simultaneous detection of nitrate and nitrite. Nitric Oxide - Biology and Chemistry 5, 62–71.

Mulvaney, R.L.-M. of soil analysis, 1996. Nitrogen—inorganic forms. SSSA, Madison 3, pp 1123–1184.

Murphy, J., Ripely, J.P., 1962. Determination Single Solution Method For The In Natural Waters. Analytica Chimica Act 27, 31–36.

Porras, R.C., Hicks Pries, C.E., Torn, M.S., Nico, P.S., 2018. Synthetic iron (hydr)oxide-glucose associations in subsurface soil: Effects on decomposability of mineral associated carbon. Science of the Total Environment 613–614, 342–351.

Riedel, T., Zak, D., Biester, H., Dittmar, T., 2013. Iron traps terrestrially derived dissolved organic matter at redox interfaces. Proceedings of the National Academy of Sciences 110, 10101–10105.

Saidy, A.R., Smernik, R.J., Baldock, J.A., Kaiser, K., Sanderman, J., 2013. The sorption of organic carbon onto differing clay minerals in the presence and absence of hydrous iron oxide. Geoderma 209–210, 15–21.

Schiedung, M., Tregurtha, C.S., Beare, M.H., Thomas, S.M., Don, A., 2019. Deep soil flipping increases carbon stocks of New Zealand grasslands. Global Change Biology 25, 2296–2309.

Silva, L.C.R., Doane, T.A., Corrêa, R.S., Valverde, V., Pereira, E.I.P., Horwath, W.R., 2015. Iron-mediated stabilization of soil carbon amplifies the benefits of ecological restoration in degraded lands. Ecological Applications 25, 1226–1234.

Sinsabaugh, R.L., 2010. Phenol oxidase, peroxidase and organic matter dynamics of soil. Soil Biology and Biochemistry 42, 391–404.

Sodano, M., Lerda, C., Nisticò, R., Martin, M., Magnacca, G., Celi, L., Said-Pullicino, D., 2017. Dissolved organic carbon retention by coprecipitation during the oxidation of ferrous iron. Geoderma 307, 19–29.

Solomon, D., Lehmann, J., Harden, J., Wang, J., Kinyangi, J., Heymann, K., Karunakaran, C., Lu, Y., Wirick, S., Jacobsen, C., 2012. Micro- and nano-environments of carbon sequestration: Multi-element STXM-NEXAFS spectromicroscopy assessment of microbial carbon and mineral associations. Chemical Geology 329, 53–73.

Tagesson, T., 2006. Calibration and analysis of soil carbon efflux estimates with closed chambers at Forsmark and Laxemar.

Van Bodegom, P.M., Broekman, R., Van Dijk, J., Bakker, C., Aerts, R., 2005. Ferrous iron stimulates phenol oxidase activity and organic matter decomposition in waterlogged wetlands. Biogeochemistry 76, 69–83.

Vance, E.D., Brookes, P.C., Jenkinson, D.S., 1987. An Extraction Method for Measuring Soil Microbial Biomass. Soil Biology and Biochemistry 19, 703–707.

Wang, Y., Wang, H., He, J.S., Feng, X., 2017. Iron-mediated soil carbon response to water-table decline in an alpine wetland. Nature Communications 8, 1–9.

Wen, Y., Zang, H., Ma, Q., Evans, C.D., Chadwick, D.R., Jones, D.L., 2019. Is the 'enzyme latch' or 'iron gate' the key to protecting soil organic carbon in peatlands? Geoderma 349, 107–113.

Wu, B., Amelung, W., Xing, Y., Bol, R., Berns, A.E., 2018. Iron cycling and isotope fractionation in terrestrial ecosystems. Earth-Science Reviews 190, 323–352.

Zhao, Q., Poulson, S.R., Obrist, D., Sumaila, S., Dynes, J.J., McBeth, J.M., Yang, Y., 2016. Iron-bound organic carbon in forest soils: Quantification and characterization. Biogeosciences 13, 4777–4788.

Chapter 4

Impact of deep-rooting grass root exclusion on aboveground biomass and soil greenhouse gas fluxes

Authors

Erik S. Button, Antonio R. Sánchez-Rodríguez, David R. Chadwick, Davey L. Jones.

Disclaimer

The setting up of this experiment was effectively delayed by a year as the University was closed due to the COVID-19 pandemic. This meant the grass plots were not established in time for the originally planned experiment, which was to radio-label the grass with $^{14}CO_2$ and trace the carbon allocation to the roots and quantify their contribution to soil organic carbon. Presented here are preliminary results from one growing season.

Publication status

This manuscript will not be submitted.

Author contributions

ESB, DRC and DLJ conceived the experiment. ARSR conducted soil characterisation analyses. ESB set up and ran the experiment and conducted all experimental analysis and wrote the manuscript. DRC and DLJ reviewed the manuscript.

Abstract

Roots are a major source of carbon (C) to the soil, especially in deep soil layers. Use of deeper rooting crops is thought to have substantial potential to increase the amount of C entering and staying in the soil, thus removing C from the atmosphere. For their widespread adoption evidence is needed to understand 2 major areas of concerns with promoting deeper rooting; i) that an increase in resource allocation to belowground biomass does not negatively impact the harvestable aboveground biomass, and ii) that deep rooting may not be C negative as they may stimulate the mineralisation of old and stable deep C by supplying microbial communities in deep soil with easily-mineralisable substrates. To address these areas of concern, we set up a field study with deep-rooting grass (Festulolium hybrid) grown on plots with or without root-excluding nylon mesh buried at 20, 40 and 60 cm for a growing season. CO_2 and N_2O was measured from surface chambers and gas pipes installed above and below the mesh. Fresh aboveground biomass was measured throughout a growing season and subsurface fluxes were determined using the concentration gradient method (CGM). The results from this study suggest that establishment of grass roots to >30 cm can take more than a year for meaningful differences to be measured. Exclusion of grass roots from >20 cm depth reduced the aboveground biomass indicating that access to deeper soil layers is important for grass growth. The performance of the CGM in accurately estimating surface fluxes was good for CO_2 but, likely due to simultaneously and spatially heterogeneously occurring production and consumption processes, poor for N_2O. Plots with root access to 30 cm depth had 106-fold higher soil CO_2 fluxes than without root access, but this only accounted for 0.5% of surface CO_2 fluxes. These results improve our understanding of the mechanisms of deep rooting and suggest deeper rooting increases soil C without increasing net CO_2 emissions.

Keywords: subsoil; sequestration; perennialisation; rhizosphere; priming.

4.1 Introduction

Grasses cover almost half of the world's land area and the majority of agricultural land and represent important carbon (C) sinks, estimated to store more than 10% of the global terrestrial C (Jones and Donnelly, 2004). The turnover of above and belowground plant biomass are major sources of C to the soils within these ecosystems (Dodd et al., 2015; Rasse et al., 2005). In the subsoil (B horizon), roots and their products are especially important sources of C where rates of C input are lower than in surface soil (Button et al., 2022; Suseela et al., 2017). A deep rooting phenotype can have co-benefits of improved plant uptake of nutrients and water (Kell, 2012; Lynch and Wojciechowski, 2015; Pierret et al., 2016), and greater resistance to slope erosion (Dignac et al., 2017) and drought (Kell, 2011). The use of deep-rooting crops can also be readily combined with mechanical interventions to promote access to previously compacted subsoil layers (He et al., 2019) or to the deep placement of fertilisers to promote root proliferation at depth (McEwan and Johnston, 1979). Therefore, there is growing interest in understanding how deep rooting interacts with subsoils to evaluate the potential of increasing long-term deep soil C stores via deep-rooting crops and grasses (Paustian et al., 2016).

In deep soil (30-100 cm), where disturbance is limited and oligotrophic conditions prevail, C is able to reside for thousands of years (Shi et al., 2020). Mineralisation of this intrinsic C by stimulating the microbial community with a fresh supply of easily accessible C from deep roots (i.e. priming; Salomé et al., 2010) is an undesirable outcome. Shahzad et al. (2018) observed mineralisation of ~15,000-year-old C from root penetration to 80 cm, though they were not able to determine whether this had an impact on the net soil profile C stock. In general, substantial increases in C stocks have been observed when annual crops were changed for more extensively rooting perennials over multiple year/decade timescales (Dodd et al., 2015; Ledo et al., 2020; Omonode and Vyn, 2006; Slessarev et al., 2020). It should be noted, however, that limited or no net change in C stock have also been observed from conversion to perennials (Chimento et al., 2016; Ma et al., 2000). There is a lack of experimental field studies that quantify the contribution of deep roots to soil organic C and soil respiration at depth to understand the trade-off between increased 'new' C input and 'old' C loss.

As plants can allocate up to 50% of their photosynthetically fixed C to roots (Jones et

al., 2009), there is a common concern that increasing plant C allocation to roots decreases harvestable aboveground biomass (Kell, 2012; Powlson et al., 2011), which would significantly limit the application of deep-rooting in agriculture due to lower yields. A review by Kell (2012) concluded that deeper roots are unlikely to limit - but may instead promote - harvestable biomass (e.g. Lilley and Kirkegaard, 2011). Therefore, it is important to both confirm that deeper rooting traits do not negatively impact aboveground biomass and to understand where or how it may be enhanced for greater political and stakeholder support.

While studying and quantifying deep roots is recognised as being important, it is not commonly undertaken due to the often laborious and costly methods required to study them *in situ* (Mooney et al., 2012; Maeght et al., 2013). In fact, since 1989, there is strong evidence that studies are generally sampling shallower soil (Yost and Hartemink, 2020). As a result, root studies (e.g. Shahzad et al., 2018) are often undertaken in soil columns or mesocosms that do not represent field conditions very well. A 'whole plant in whole soil' perspective is needed for best understanding the potential of deep rooting advancements (Lynch et al., 2022). *In situ* studies on conversion of annual cropped fields to perennials (Ledo et al., 2020), for example, have improved our understanding of deep rooting but lack mechanistic insight into root-soil-microbial functioning. Exclusion of roots in situ (e.g. using mesh cages) provides a direct measure of how roots influence soil functioning, yet this is uncommon, possibly due to the challenge of non-destructive sampling. This can be overcome by gas sampling at depth and use of the concentration gradient method (CGM) for estimating soil fluxes with or without the presence of roots to quantify root-derived fluxes (Maier and Schack-Kirchner, 2014). To our knowledge, this approach has not been used to study deep roots in the context of C dynamics. To address the areas of uncertainties and advance this field, we established deep-rooting grass plots with or without root-excluding mesh buried at either 20, 40 or 60 cm. CO_2 and N_2O was measured from surface chambers and gas pipes installed above and below the mesh. Fresh aboveground biomass was measured throughout the growing season and subsurface fluxes were determined using the concentration gradient method. We hypothesised that, i) deeper rooting will not limit aboveground biomass, ii) deeper rooting will increase the net CO_2 and N_2O fluxes from the soil surface due to greater root access and respiration at depth, and; iii) the CGM will produce good estimates of soil fluxes as validated by the surface chamber measurements.

4.2 Materials and methods

4.2.1 Experimental site and soil characterisation

The field trial was located at the Henfaes Research Centre, Abergwyngregyn, North Wales (53°14'29"N, 4°01'15"W). The freely draining sandy clay loam textured soil is classified as a Eutric Cambisol (WRB) or Typic Hapludalf (US Soil Taxonomy). An area of ca. 100 m^2 previously grazed grass ley was applied with SAMURAI® glyphosate (6 l ha^{-1}; Monsanto UK Ltd., Cambridge, UK) on the 11th August 2020 and then scarified to remove dead grass, cultivated with a rigged tine harrow before a power harrow was used to create a level area two weeks later.

In 2018, soil from the same field was characterised extensively for chemical, biological and physical properties (mean values presented in Table 4.1). Soil samples were taken from 4 independent soil pits located ca. 50 m apart at 10 cm depth intervals to a depth of 100 cm and sieved to 5 mm. Soil texture was measured with a LS 13320 laser diffraction particle size analyser (Beckman-Coulter Inc., Indianapolis, IN). Soil pH and electrical conductivity (EC) were measured in a fresh soil 1:2.5 (w/v) distilled water suspension with a Model 209 pH meter (Hanna Instruments Ltd., Leighton Buzzard, UK) and a Jenway 4520 conductivity meter (Cole-Palmer Ltd., Stone, UK), respectively. Cation exchange capacity (CEC) was determined using the sodium acetate method of Sumner and Miller (1996). Total soil C and N were determined with a TruSpec® CN analyser (Leco Corp., St Joseph, MI). Soil subsamples (5 g) were extracted with 0.5 M K_2SO_4 (1:5 w/v; 150 rev min^{-1}, 30 min) and the supernatant recovered after centrifugation (14,000 g, 10 min). NH_4^+ and NO_3^- were determined colorimetrically according to Mulvaney (1996) and Miranda et al. (2001), respectively, on a PowerWave XS Microplate Spectrophotometer (BioTek Instruments Inc., Winooski, VT, USA). Immediately after soil collection, field-moist soil samples (25 g) were sieved (2 mm), frozen (-20 °C), freeze-dried and phospholipid-derived fatty acids (PLFA) were determined according to Bartelt-Ryser et al. (2005).

4.2.2 Experimental design

The field trial consisted of 16 plots (4.3 ± 0.1 m^2) separated by ≥1 m wide borders; see Appendix 3, Fig. S1 for plot layout). These plots were split into 4 treatments (n = 4) based on the presence and depth of a 4 m^2 nylon root excluding mesh (40 µm; Anping County Comesh

Filter Co. Ltd., Hengshui City, China). The mesh size was chosen to allow hyphae, water and gases to penetrate freely but to exclude plant roots (Paymaneh et al., 2018). See Figure 4.1 for a schematic diagram of an example plot. The location of the treatments, no mesh (i.e. control) and mesh at 20, 40 and 60 cm, were randomly allocated to the plots in the field (Appendix 3, Fig. S1). The plots were all excavated using a mechanical excavator on the 16-17th September 2020. Soil was excavated in layers (0-20, 20-40 and 40-60 cm) and put in separate piles before refilling in the original order. All plots were excavated and thus disturbed equally regardless of treatment. When excavated, the mesh and gas sampling pipes (see 4.2.3) were installed and 8m long strips of heavy-duty polythene sheets were lined along the walls of the excavated plots to exclude any root-soil interference from outside of the plots (Fig. 4.1). The height of the liners was equal to the depth of the buried mesh and 60 cm in the no mesh (control) plots. During excavation, all stones encountered greater than ca. 150 cm^3 were removed. On 21st September 2020 the plots were raked level and hand seeded at an

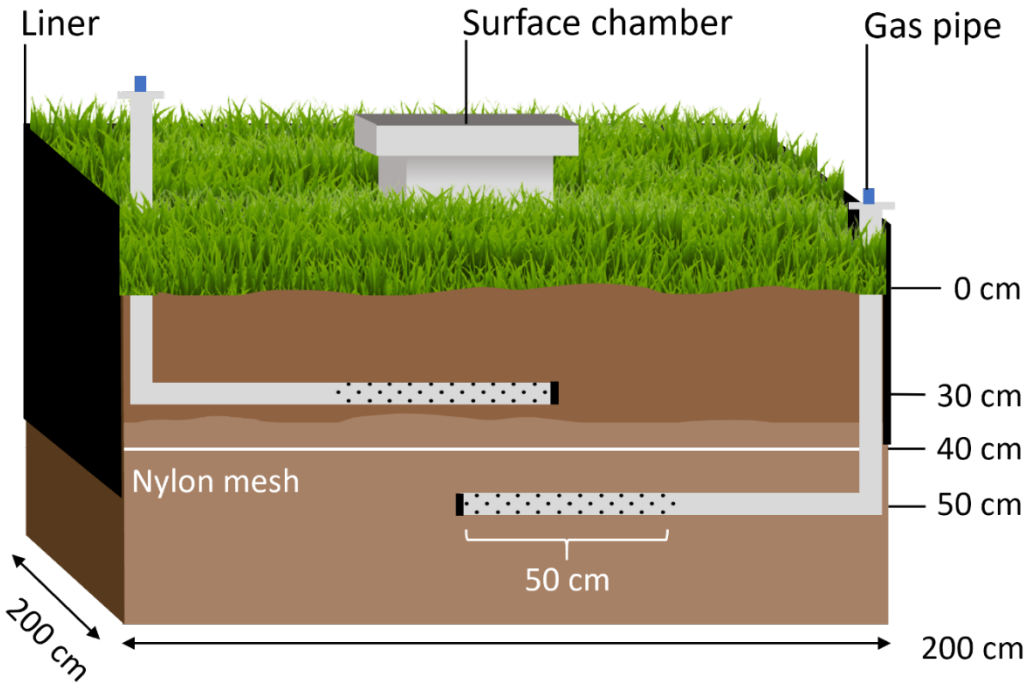

Fig. 4.1 Schematic 3D diagram of an example root exclusion plot used in this study (40 cm depth mesh shown as the exemplar). Plots had a buried mesh at either 20, 40 or 60 cm with gas sampling pipes positioned 10 cm above and below the mesh depth. The control plots (no mesh) had gas pipes at all depths (i.e. 10, 30, 50 and 70 cm). The terminal end 50 cm of the gas pipes had holes in them to enable soil air sampling at the centre of the plot. All plots had surface gas sampling chambers positioned on the top of plots and plastic liners on the walls surrounding the plots to prevent root ingress from the surrounding area. The dimensions of the plots were ca. 2 m x 2 m.

Table 4.1. Physical, chemical and biological soil properties at different depths from the field used in the study. Values (*n* = 4) are means ± SEM.

Properties	Soil depth (cm)						
	0 - 10	10 - 20	20 - 30	30 - 40	40 - 50	50 - 60	60-70
Sand (%)	62.9 ± 0.7	62.0 ± 1.3	60.3 ± 2.3	60.3 ± 3.3	62.4 ± 4.4	67.2 ± 6.5	71.9 ± 4.5
Silt (%)	16.2 ± 1.3	17.8 ± 0.6	17.8 ± 1.2	17.5 ± 1.5	17.1 ± 1.8	14.9 ± 3.1	12.1 ± 1.5
Clay (%)	20.9 ± 1.0	20.2 ± 0.9	21.9 ± 1.5	22.2 ± 2.3	20.6 ± 2.6	17.9 ± 4.1	16.0 ± 3.3
Dry bulk density (g cm^{-3})	1.4 ± 0.03	1.4 ± 0.07	1.7 ± 0.1	1.7 ± 0.2	1.8 ± 0.1	2.0 ± 0.3	1.7 ± 0.2
pH (1:2.5)	6.0 ± 0.1	6.2 ± 0.1	6.5 ± 0.1	6.6 ± 0.1	6.7 ± 0.1	6.7 ± 0.1	6.8 ± 0.1
EC (1:2.5 µS cm^{-1})	33 ± 4	32 ± 2	24 ± 1	25 ± 3	19 ± 1	23 ± 5	21 ± 2
CEC ($cmol_+$ kg^{-1})	14.8 ± 0.2	15.6 ± 0.4	12.7 ± 1.0	12.7 ± 0.5	11.1 ± 1.7	10.3 ± 1.0	9.6 ± 1.3
Soil C:N	9.7 ± 0.2	9.7 ± 0.5	8.8 ± 0.7	6.4 ± 0.4	4.9 ± 0.5	5.0 ± 0.8	4.5 ± 0.7
NH_4^+ (mg kg^{-1})	2.4 ± 0.1	1.9 ± 0.2	1.7 ± 0.1	1.6 ± 0.1	1.6 ± 0.2	1.4 ± 0.2	1.8 ± 0.2
NO_3^- (mg kg^{-1})	10.8 ± 0.7	11.6 ± 2	4.9 ± 0.4	3.3 ± 0.2	2.0 ± 0.1	2.5 ± 0.7	2.4 ± 0.3
Total PLFA biomass (nmol g^{-1})	134.2 ± 8.9	116.3 ± 4.1	57.7 ± 4.9	33.5 ± 2.5	22.9 ± 1.8	26.9 ± 8.4	14.3 ± 3.0

equivalent rate of 35 kg ha^{-1} (as per supplier recommendation) with a deep-rooting *Festulolium* variety (AberNiche; Cotswolds Seeds Ltd., Moreton-in Marsh, UK). *Festulolium* is a cross between meadow fescue (*Festuca pratensis* L.) and Italian ryegrass (*Lolium multiflorum* L.) and was developed for drought tolerance, with potential for deep-rooting (Carswell et al., 2022). A 1-2 cm layer of topsoil removed previously was placed over the seeds to facilitate germination. The plots were reseeded at the same rate the 4th March due to poor initial establishment of the grass over the winter of 2020. The plots were fertilized by hand on the 13th July 2021 with 75 kg N ha^{-1} as NH_4NO_3, 25 kg P ha^{-1} and 100 kg K ha^{-1} after the 2nd silage cut, according to the Nutrient Management Guide (AHDB, 2017).

4.2.3 Environmental and vegetation measurements

Rainfall, atmospheric pressure, soil moisture and air and soil temperature were recorded hourly at a weather station located adjacent to the research site. Due to an operational error, no data was available between Jan and 23rd of March 2021. The grass on the plots were cut by hand to 3-4 cm from the base in May, June, July, and August 2021 and again in May 2022. The fresh weight of the inside 1.8 m^2 were weighed in the field, to avoid any edge-related effects.

4.2.3 Gas measurement systems

PVC pipes (32 mm diameter) were cut to 100 and 75 cm lengths and connected by a 90° bend using solvent cement to create L-shaped pipes (Fig. 1). The 100 cm pipe buried horizontally in the soil was pre-drilled randomly with 3 mm diameter holes (n = ~50) at the terminal end 50 cm opposite to the connecting bend and the end was sealed with electrical tape (Fig. 4.1). The end of the vertical 75 cm pipe was sealed with a cemented end cap that was then drilled (14 mm diameter) and 16 mm Suba-Seal® gas sampling ports (Sigma-Aldrich Ltd., Poole, UK) were fitted. All PVC connections were further sealed with PTFE and duct tape to ensure no leaks were present or could develop with time. In total, 40 identical gas sampling pipes were made for burial at 10, 30, 50 and 70 cm. Mesh buried at 20 cm had pipes installed at 10 and 30 cm; mesh buried at 40 cm had pipes installed at 30 and 50 cm and mesh buried at 60 cm had pipes installed at 50 and 70 cm. The control (no mesh) plots had gas pipes installed at 10, 30, 50 and 70 cm. For surface-atmosphere GHG flux measurement, 16 plastic

chambers (42 cm x 42 cm x 25 cm) were installed approx. 40 cm from the edge of the plots (Fig. 1) in February 2021. These have removable lids with Suba-Seal® gas sampling ports (Sigma-Aldrich Ltd., Poole, UK) fitted in their centre for sampling via syringe.

4.2.4 Gas sampling and analysis

Gas samples were taken between 1000 and 1300 h fortnightly between April and September 2021. Using a gas-tight polypropylene syringe, air in the pipes and surface chambers was mixed by filling and emptying the syringe 3 times before a ca. 25 ml gas sample was taken and over-filled (to prevent loss of sample during storage) into a pre-evacuated 20 ml glass vial (QUMA Elektronik and Analytik GmbH, Wuppertal, Germany). For the surface chambers, this was done at t = 30 and 60 mins after chamber closure with 8 replicates of ambient air taken from random locations within the field site for t = 0. Before analysis, gas samples were brought to ambient air pressure by inserting a needle into the vials and releasing the pressure. These were then analysed for CO_2 and N_2O concentrations using a Perkin Elmer 580 Gas Chromatograph (GC), served with a Turbo Matrix 110 auto sampler (Perkin Elmer Inc., Waltham, MA). Gas samples passed through two Elite-Q mega bore columns via a split injector, with one connected to an electron capture detector (ECD) for N_2O determination, and the other to a flame ionisation detector (FID) for CO_2 determination. Gas fluxes were calculated as per the method described in Scheer et al., (2014) adjusted for differences in timepoints.

4.2.5 Concentration gradient methodology

To estimate the fluxes of gases in the soil profile and at the soil surface, the concentration gradient method (CGM) was used (Maier and Schack-Kirchner, 2014). The details of this method are presented in detail in Chapter 5. Briefly, the transport of gas through porous media in one dimension was approximated using Fick's first law, for which the concentration gradient was calculated according to Jong and Schappert (1972); and the effective diffusion coefficient of CO_2 and N_2O in the soil were calculated as described in Chapter 5. This was done by calculating the diffusion coefficient of SF_6 depletion from vessels using the Currie (1960) method. Air-filled pore space (ε) related diffusion coefficient (D_s) was calculated with the power function, $D_s = 0.0907(\varepsilon)^{3.1848}$ (R_2 = 0.99; Chapter 6). Then the

effective diffusion coefficient for CO_2 and N_2O was calculated using the free air diffusion coefficients of SF_6 and CO_2 or N_2O (0.0335, 0.0529 and 0.0515 m^2 h^{-1}, respectively; Pritchard and Currie, 1982; Rudolph et al., 1996). The surface soil-atmosphere flux was then estimated by extrapolating the fluxes from the 10 and 70 cm depths to the surface. To validate the accuracy of these, the CGM modelled fluxes were plotted against the chamber measured soil-atmosphere fluxes. The strength and gradient of the relationship was assessed to determine the reliability of the estimates at depth.

Soil temperature and moisture data was available from the weather station at 10 and 20 cm. For more accurate flux calculation below this, the data from the 10 and 20 cm depth were used to estimate the conditions at 30, 50 and 70 cm using best fits. Data from 10, 20 and 30 cm depths from 5 equivalent months in 2019 (Chapter 5) were used to determine the best fits for temperature and moisture with depth (Appendix 3, Table S1, S2). As the most variation in the 2019 temperature (R^2 = 0.84; Appendix 3, Table S1) and moisture data (R^2 = 0.66; Appendix 3, Table S2) was explained by power functions, these were used to estimate the temperature and moisture at 30, 50 and 70 cm for the CGM calculation.

4.2.6 Data and statistical analysis

All data analysis was done using R (R Core Team, 2017), with figures made using the R package 'ggplot2'(Wickham, 2016). Data was assessed for test assumptions by using the Shapiro-Wilk test (p <0.05) for normality, and Levene's test for homoscedasticity (p <0.05) as well as assessing the qqplots and the residual versus fitted plots. Fresh aboveground biomass was measured by a two-way ANOVA after the data was log-transformed to meet assumptions. CO_2 and N_2O concentrations were compared with Kruskal-Wallis rank sum tests at each individual soil depth. Differences between soil CO_2 fluxes were tested individually with the Kruskal-Wallis rank sum test by root access and depth and then by root access within each depth.

4.3 Results

4.3.1 Environmental conditions and grass biomass

The hottest month was Jul with an average monthly air temperature of 17 °C, followed by Sep > Aug > Jun > Oct > May > Nov > Apr > Dec. The average monthly air temperatures in

Apr and Dec were 8 °C, suggesting unseasonal cold weather in Apr. The monthly soil temperatures were consistently higher than in the air (Fig. 4.2a), but otherwise followed very a similar pattern. Monthly average atmospheric barometric pressure was highest in Apr (1022 mbar) followed by Jun > Nov > Sep > Aug > Jul > Oct > Dec and May (1007 mbar) (Fig. 4.2b). The low pressures experienced are partly in synchronism with the rainfall patterns, where

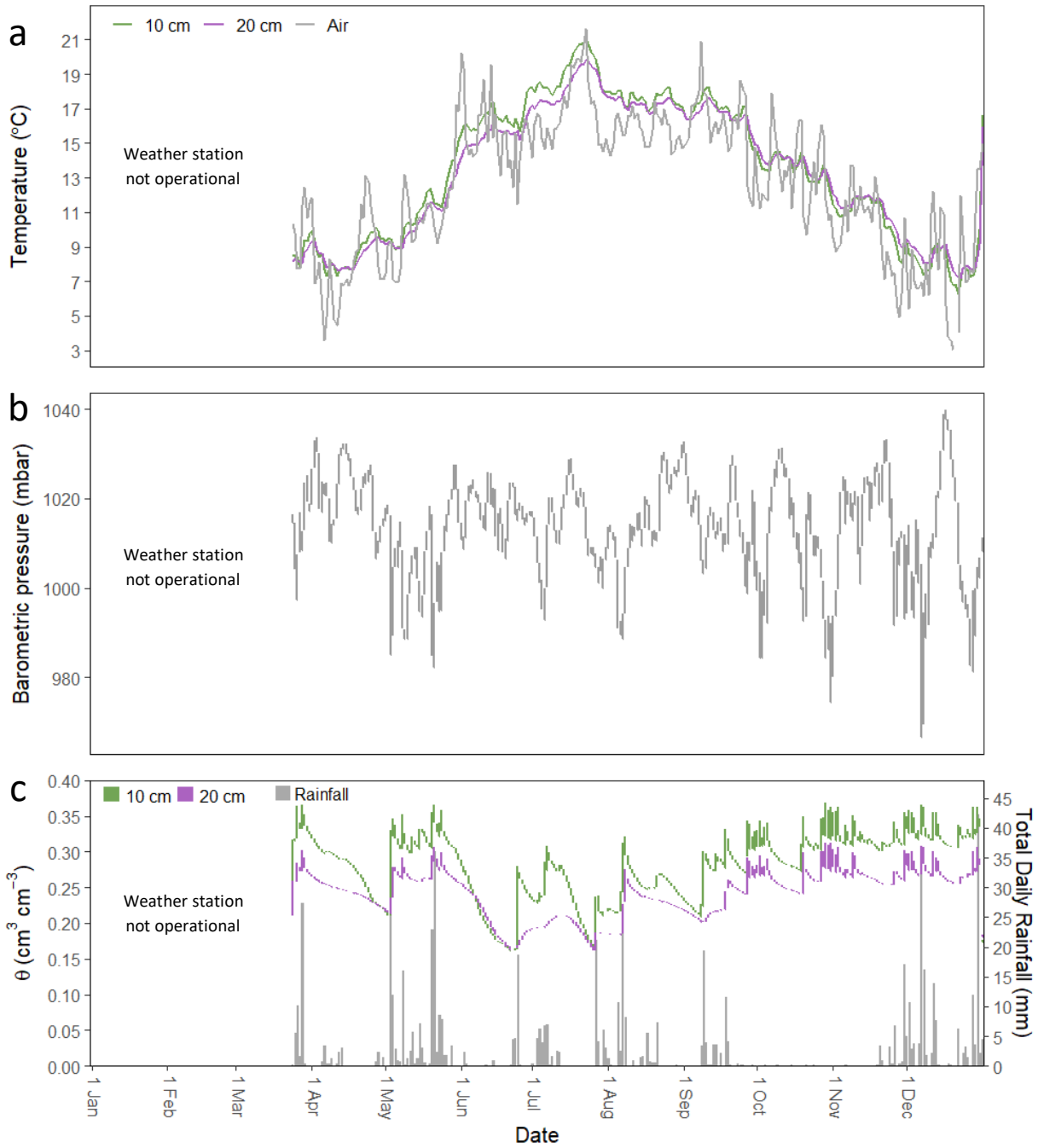

Fig. 4.2 a) Daily average air and soil temperature, b) hourly barometric pressure, and c) average volumetric soil water content (θ) and total daily rainfall for the experimental period 1st Jan – 31st Dec 2021. N.B the weather station was not operational from the 1st Jan – 23rd March due to a technical issue.

monthly total rainfall was highest in December with 174 mm, followed by May (166 mm), Jul (70 mm), Aug (65 mm), Sep (54 mm), Jun (36 mm), Nov (33 mm), Apr (17 mm) and Oct with just 1 mm of rainfall. This is also partially reflected in the soil volumetric water content (θ) at different soil depths (Fig. 4.2c). The monthly θ was highest in Dec (0.33 and 0.27 cm^3 cm^{-3}) for the 10 and 20 cm soil depths, respectively. Despite the low rainfall, Oct did not have the lowest θ. This was experienced by Jun, Jul and Aug for both depths.

The overall aboveground biomass differed between all sampling times except between May and June 2021 (p <0.001; Fig. 4.3), with Aug 2021 > June 2022 > May 2021 > June 2021 > July 2021. All treatments had higher grass biomasses than the plots with mesh installed at 20 cm (p = 0.003). The 20 cm plots had 30, 11 and 12% less biomass than the 40, 60 cm and no mesh plots, respectively, which did not differ from each other.

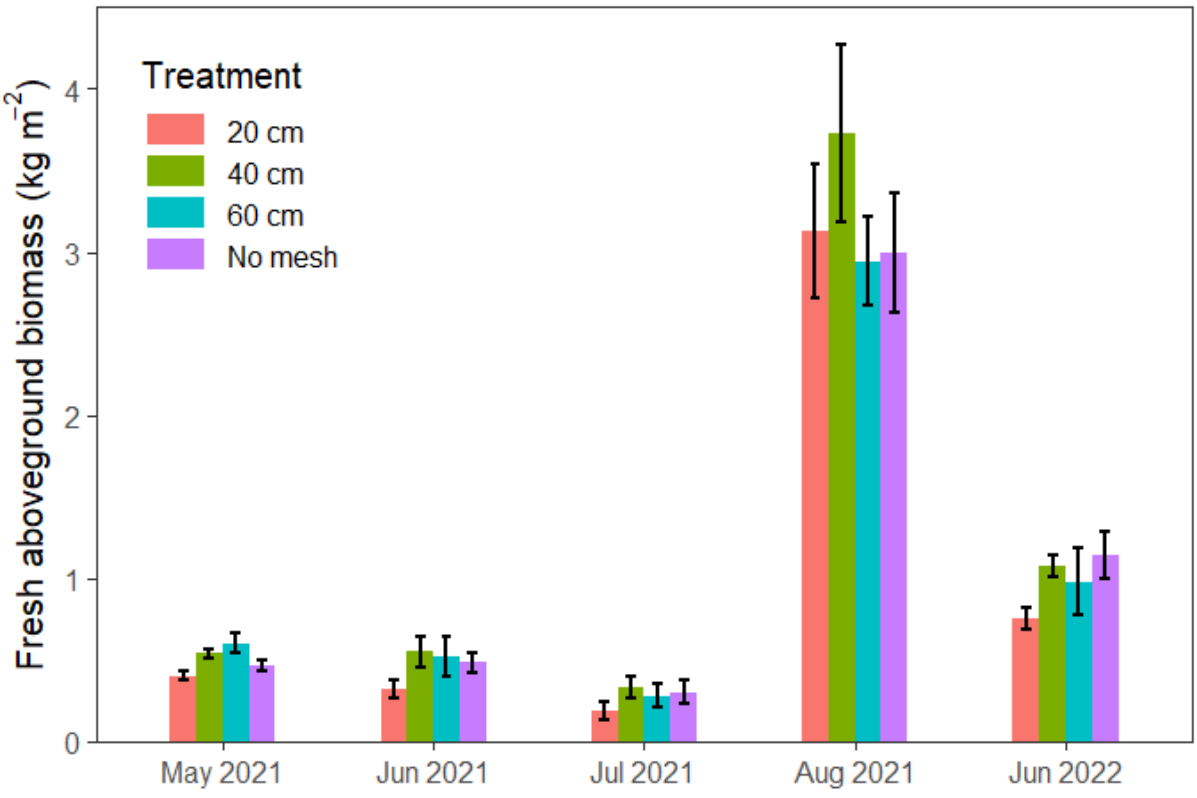

Fig. 4.3 Mean (± SEM) aboveground fresh biomass in plots (n = 4) with root-excluding mesh installed at 20, 40, 60 cm or without mesh (No mesh) at different harvesting times in 2021 and 2022. N.B. the grass was wet in the August harvest resulting in higher biomass.

4.3.3 Cumulative surface fluxes

The cumulative surface CO_2 fluxes were 9, 13 and 12% lower in the plots with root-excluding mesh at 20 cm compared to the 40 cm, 60 cm and no mesh plots (Fig. 4.4a), respectively. Despite this, mesh depth or absence did not impact cumulative soil CO_2 surface fluxes (p = 0.5). There were negative surface N_2O fluxes in all plots, but the mean cumulative flux was negative in the plots with mesh at 20 and 60 cm (Fig. 4.4b). Surface fluxes were highest in the plots absent of mesh. Yet overall, the depth or absence of root-excluding mesh had no impact on the cumulative flux of N_2O (p = 0.60).

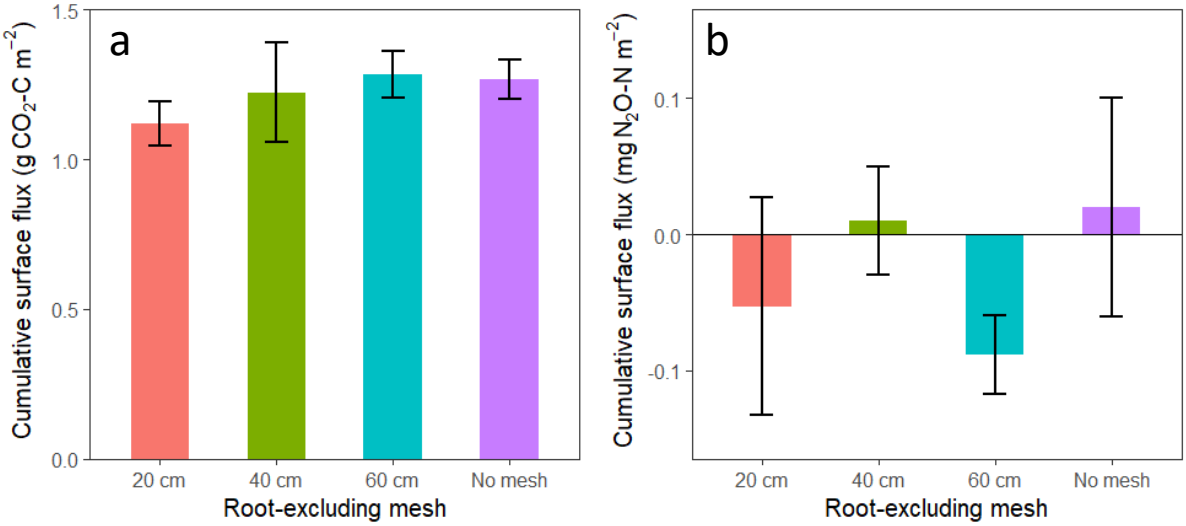

Fig. 4.4 Mean (± SEM) cumulative surface a) CO_2 and b) N_2O fluxes from deep rooting grass plots (n = 4) with or without root-excluding mesh buried at 20, 40, 60 cm depths.

4.3.4 Concentration profiles

The concentrations of CO_2 and N_2O increased exponentially and linearly with soil depth (p <0.001, p <0.001, respectively; Fig. 4.5), respectively. Differences between plots with or without root-excluding mesh at different depths were only measured at 10 and 30 cm for CO_2 concentrations. At 10 and 30 cm, the concentration of CO_2 was lower in the plots with root-excluding mesh at 20 cm than in the no mesh plots (p = 0.01; Fig. 4.5a). There were no differences in N_2O concentrations at each soil depth with plot mesh type (p >0.05; Fig. 4.5b).

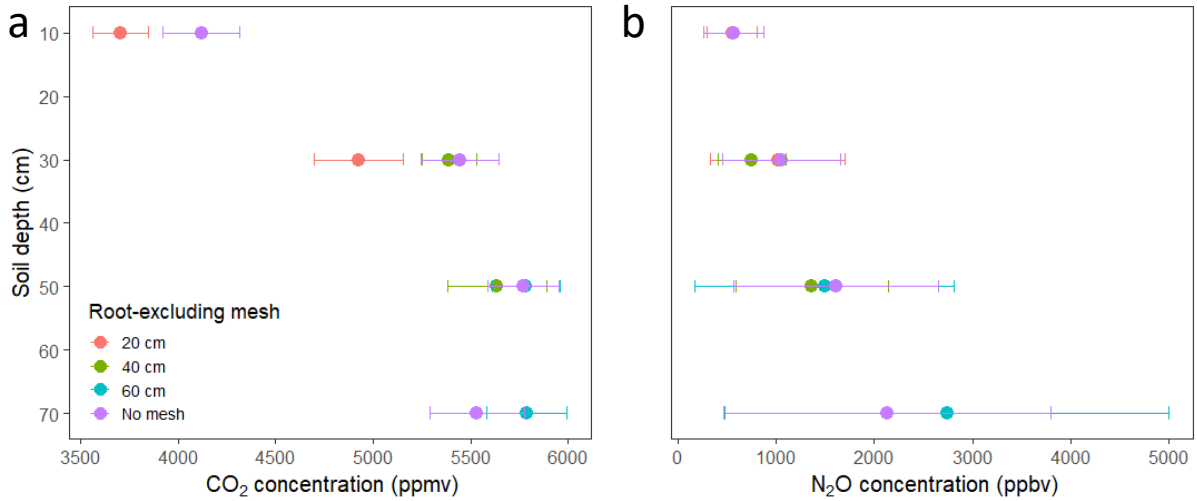

Fig. 4.5 Depth profiles of mean (± SEM) gas concentrations of a) CO_2 and b) N_2O from biweekly sampling of gas collectors installed at different soil depths (*n* = 4) between April and September 2021. Colours reflect the depth or absence of a buried root-excluding mesh.

4.3.5 CGM modelled fluxes

The fit of CGM modelled versus the chamber measured surface flux demonstrated a strong positive linear relationship for CO_2 (Fig. 4.6a). However, the fit suggests that CO_2 fluxes were overestimated by the CGM at lower measured surface fluxes and underestimates them at higher fluxes, with the intercept between the x = y and the fitted line at ca. 1.6 g C m^{-2} h^{-1}. In contrast, there was no meaningful relationship between the CGM modelled and the measured fluxes of N_2O (Fig. 4.6b). Due to the poor fit we did not believe the N_2O modelled fluxes at depth would be reflective of in situ fluxes and so did not include them.

Soil CO_2 fluxes modelled by the CGM show a decrease with increasing soil depth ($p < 0.001$; Fig. 4.7). While there was no overall impact of root access on soil CO_2 flux ($p = 0.06$), at 30 cm root access produced a 10.6-fold greater flux ($p < 0.001$). The root-derived CO_2 flux (i.e. flux with no mesh '+Roots' subtracted by flux below mesh '-Roots'; Fig. 4.7) at 30 cm was 0.58 mg C m^{-2} h^{-1}. This corresponds to 91% of the CO_2 flux at 30 cm being root-derived, which is equivalent of 0.48 and 0.53% of the mean CGM estimated and chamber measured surface CO_2 fluxes, respectively.

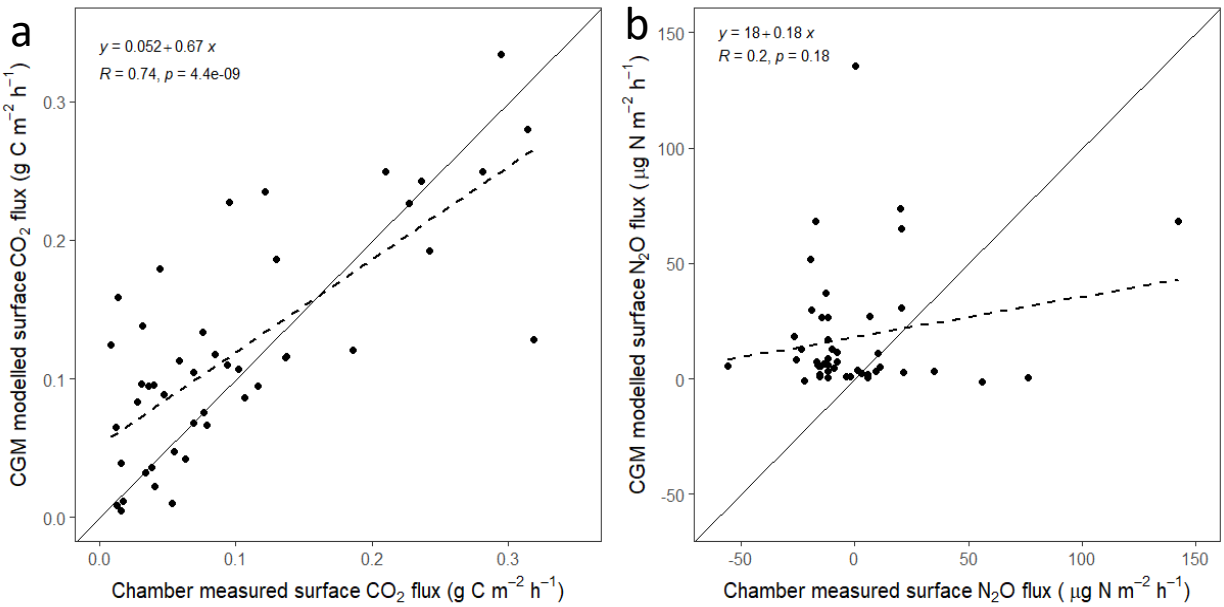

Fig. 4.6 The CGM modelled versus the chamber measured surface a) CO_2 and b) N_2O flux between April and September 2021. The straight lines are the x = y and the dashed lines are the linear fit of the data. The equation, R^2 and *p* values correspond to the fitted line of the data. Negative N_2O fluxes indicate consumption by the soil.

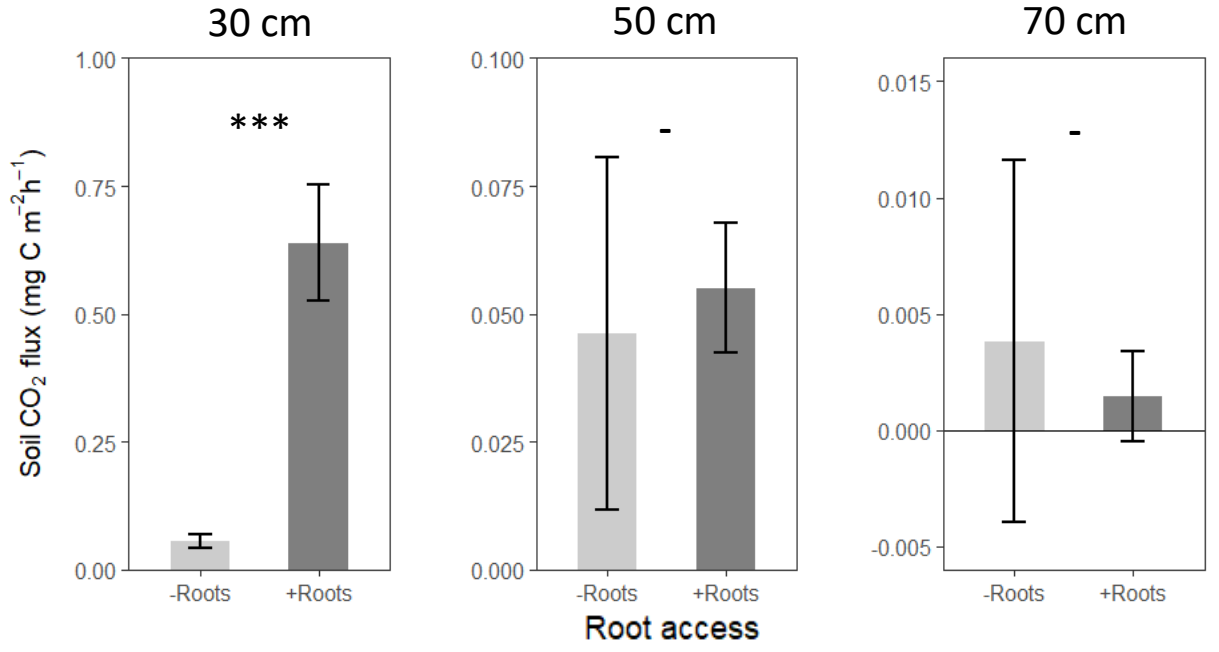

Fig. 4.7 Soil CO_2 fluxes modelled by the CGM from soil at 30, 50 and 70 cm with or without root access. In plots with no root access ('-Roots'), the gas sampling pipes were 10 cm below a root-excluding mesh installed at either 20, 40 or 60 cm. There was no mesh present in the '+Roots' plots that could limit rooting access. Asterisks represent statistical difference between soil CO_2 with root access status at *p* <0.001 (***); *p* <0.01 (**); *p* <0.05 (*) and *p* >0.05 (-)

4.4 Discussion

4.4.1 Grass rooting and aboveground biomass

Significantly less aboveground biomass was produced in the plots with root-excluding mesh at 20 cm (Fig. 4.3). This suggest that the grass roots are reaching a depth >20 cm and the presence of the mesh is affecting aboveground biomass by limiting water and nutrient uptake, for which deep roots are grown to overcome (Kell, 2011; Maeght et al., 2013). This result contrasts with the statement from Powlson et al. (2011) that suggests increasing belowground input decreases aboveground growth. However, this idea has been refuted by Kell (2012), where they argue it is implausible as below- and aboveground biomass are likely to match each other. Applying this to the results from this study would suggest that root biomass in the plots with mesh at 20 cm is lower than the other treatments and that there is no difference in rooting biomass between the plots with and without mesh at 40 or 60 cm. This is supported by a 2-year study at the same field site with the same *festulolium* grass variety which found rooting to significantly decrease in mass with every 10 cm increase in depth (Carswell et al., 2022). At depths >50 cm they found rooting mass to be between 0.4 and 0.01% of the mass measured at the 0-10 cm soil depth. Therefore, the plots with mesh at 40 and 60 cm are unlikely to cause sufficient impacts on the overall rooting mass of the grass for differences in the aboveground biomass to be measured. Therefore, these results confirm the hypothesis that deeper rooting does not limit aboveground biomass, though this only applies to rooting to or beyond 20 cm due to unconfirmed establishment of rooting at >30 cm soil depths.

Deep roots of >60 cm have been observed to establish rapidly (ca. 1 month) in tropical forage grass species grown in repacked soil columns (Huot et al., 2020). However, root growth is slower in temperate conditions and homogenous sieved and repacked soil is less limiting for root growth than more heterogenous *in situ* soil. However, excavating the plots and removing large stones during set up would have loosened and homogenised the soil to an extent allowing greater ease of root penetration. Yet, the poor initial surface establishment of grass and the need for reseeding in March 2021 suggests that establishment of substantial roots at depth (>30 cm) is unlikely to have occurred over the measurement period. This is supported by a lack of differences in the soil CO_2 fluxes at 50 and 70 cm between plots with or without root access (Fig. 4.7), surface CO_2 fluxes and CO_2 concentrations (Fig. 4.3, 4.4a,

4.5a) between the plots with no mesh or mesh at 40 or 60 cm. However, considering the low root mass at depth (>50 cm) even under conditions promoting deep rooting (i.e. drought; Carswell et al., 2022), maximum rooting depth potential may have been reached in this study but not captured by the measures mentioned above. Yet, it is likely that several years are required for greater establishment of roots at depth and the associated implications of these, as suggested by Carter and Gregorich (2010) and Ma et al. (2000) who found that tangible differences (i.e. SOC) due to deep rooting may only be apparent in the long term (5+ years).

4.4.2 Surface fluxes and root respiration

The increase in the aboveground biomass and surface CO_2 flux from the 20 cm mesh to the no mesh plots was <0.5% different, suggesting that the aboveground biomass (and the belowground biomass, assuming an equal root-shoot ratio) was relative to the surface CO_2 flux. The cumulative surface CO_2 fluxes, while not statistically different, did indicate that limiting root growth to a soil depth of 20 cm decreased surface fluxes (Fig. 4.4a). This result is consistent with Li et al. (2004), who found lower CO_2 fluxes and microbial biomass with tree root exclusion. This suggests that a lower total root biomass results in a lower relative respiration rate. This is confirmed by i) lower CO_2 concentrations at 30 cm in the plots with mesh at 20 cm (Fig. 4.5a); and, ii) lower soil CO_2 fluxes at 30 cm in the plots with no root access (Fig. 4.7). There was no difference between the surface N_2O fluxes or N_2O concentrations with or without root excluding mesh, suggesting rooting has limited impact on N_2O fluxes which is consistent with the results from Kusa et al. (2008). N_2O concentrations increased linearly with depth (Fig. 4.5b), as the gas produced in the soil accumulates near the point of production due to restriction of diffusion to the soil surface (Shcherbak and Robertson, 2019).

Root-derived (i.e. rhizosphere) CO_2 fluxes are thought to be 40% from root respiration and 60% from microbial respiration of root exudates and arbuscular mycorrhizal associations (Kuzyakov and Larionova, 2006). The fluxes at 30 cm demonstrate that the presence of roots increased soil fluxes by 106-fold (Fig. 4.7), suggesting both an increase in root respiration and microbial respiration of root exudates. However, it is likely that this large increase in CO_2 production was also stimulated by the microbial mineralisation of native soil C (Kuzyakov et al., 2000; Shahzad et al., 2018). Despite 91% of the flux at 30 cm being entirely due to the presence of roots, this corresponded to only 0.5% of the surface flux. Therefore, it is possible

that the increase in C from deeper rooting is not overshadowed by higher respiration, as supported by a lack of statistical difference between cumulative surface CO_2 fluxes (Fig. 4.4). Therefore, we reject the hypothesis that deeper rooting would increase surface fluxes.

4.4.3 CGM performance

The use of the CGM for flux estimation has been demonstrated in many pervious studies (Kusa et al., 2008; Luther-Mosebach et al., 2018; Maier and Schack-Kirchner, 2014; Wang et al., 2018; Xiao et al., 2015). In our study, the estimation of surface fluxes by the CGM compared to the chamber method was good for CO_2 with a strong positive linear relationship that explained the majority of the variation in the data (Fig. 4.6a). In addition, the results are within the range of relative accuracy (slope and R^2) of several other studies estimating CO_2 using the CGM, as summarised by Maier and Schack-Kirchner (2014). Therefore, we confirm the hypothesis in the case of CO_2, that the CGM can perform well and produce good estimates of soil fluxes at depth from gas concentrations at depth.

In the case of N_2O, performance was poor with no meaningful relationship between the modelled and measured fluxes (Fig. 4.6b), meaning the hypothesis was rejected for N_2O. These results are consistent with the findings of Maier and Schack-Kirchner (2014) who found agreement between the CGM and measured fluxes was in general better with CO_2 than with N_2O, due to simultaneously and spatially heterogeneously occurring consumption and production processes altering the fate and behaviour of N_2O at aggregate to microsite scales (Clough et al., 2005; Schlüter et al., 2018). Kusa et al. (2008) concluded that because they were not able to account for these processes occurring in the soil above the location of the sampling tube at 5 cm, an accurate CGM N_2O flux could not be obtained. In our study the shallowest gas sampling depth was 10 cm, suggesting that the reason for the poor fit between the CGM and chamber surface fluxes was primarily due to the concentrations at 10 cm not accounting for changes to the flux of N_2O above this. Therefore, this caused the extrapolation to the surface to produce inaccurate fluxes as verified by the chamber flux measurements (Fig. 4.6b). However, the CGM estimates of N_2O corresponded better with the chamber measured fluxes when at lower values (i.e. <30 µg N m^{-2} h^{-1}; Fig. 4.6b). After observing poor estimation of the CGM at high N_2O fluxes, Kusa et al. (2008) concluded that the CGM is useful for N_2O flux estimation when high fluxes (>0.6 mg N m^{-2} h^{-1}) were excluded. In our study the

ideal threshold for exclusion would be even lower, which puts into question the repeatability of using this threshold for improving the CGM fluxes.

4.5 Conclusions

Aboveground biomass and soil profile and surface gas measurements were measured throughout a growing season of deep-rooting grass in plots with root-excluding mesh installed at 3 different depths. The results from this study suggest that establishment of deep grass roots in an agricultural field may take more than a year for root exclusion related differences to be measured at depths >30 cm. Nevertheless, exclusion of grass roots from >20 cm depth reduced the aboveground biomass indicating that access to deeper soil layers is important for grass growth. Plots with root access to 30 cm depth had higher soil CO_2 fluxes than when no root access, suggesting root respiration and microbial respiration of root and soil C is a primary driver of CO_2 production in the rooted soil. However, this did not induce a difference in surface CO_2 fluxes, suggesting C input may exceed C output. The performance of the CGM was good for CO_2 but poor for N_2O, due to the complexity and heterogeneity of N_2O dynamics not captured by the CGM. The results from this study give important preliminary support for pursuing deep rooting as an approach for enhancing soil C storage without impacting harvestable biomass. To improve this study, moisture sensors installed at depth, dry aboveground biomass measurement, rooting depth quantification, isotope labelling and ^{14}C dating of soil CO_2 would enhance the insight and confidence in the mechanisms behind the observed measurements.

4.6 Acknowledgements

This work was supported by the FLEXIS (Flexible Integrated Energy Systems) programme, an operation led by Cardiff University, Swansea University and the University of South Wales and funded through the Welsh European Funding Office (WEFO). Thanks to Mark Hughes, Bleddyn, Erick R. S. Santos and Robert Brown for help establishing the field trial. Thanks also to Chris Chukwuebeka Okolo for his help with sampling.

4.7 References

AHDB, 2017. Nutrient Management Guide (RB209), Agriculture and Horticulture Development Board.

Bartelt-Ryser, J., Joshi, J., Schmid, B., Brandl, H., Balser, T., 2005. Soil feedbacks of plant diversity on soil microbial communities and subsequent plant growth. Perspectives in Plant Ecology, Evolution and Systematics 7, 27–49.

Button, E.S., Pett-ridge, J., Murphy, D. V, Kuzyakov, Y., Chadwick, D.R., Jones, D.L., 2022. Deep-C storage : Biological , chemical and physical strategies to enhance carbon stocks in agricultural subsoils. Soil Biology and Biochemistry 170, 108697.

Carswell, A., Sánchez-Rodríguez, A.R., Saunders, K., le Cocq, K., Shaw, R., Cotton, J., Zhang, Y., Evans, J., Chadwick, D.R., Jones, D.L. and Misselbrook, T., 2022. Combining targeted grass traits with red clover improves grassland performance and reduces need for nitrogen fertilisation. European Journal of Agronomy, 133, 126433.

Carter, M.R., Gregorich, E.G., 2010. Carbon and nitrogen storage by deep-rooted tall fescue (*Lolium arundinaceum*) in the surface and subsurface soil of a fine sandy loam in eastern Canada. Agriculture, Ecosystems and Environment 136, 125–132.

Chimento, C., Almagro, M., Amaducci, S., 2016. Carbon sequestration potential in perennial bioenergy crops: The importance of organic matter inputs and its physical protection. GCB Bioenergy 8, 111–121.

Clough, T.J., Sherlock, R.R., Rolston, D.E., 2005. A review of the movement and fate of N_2O in the subsoil. Nutrient Cycling in Agroecosystems 72, 3–11.

Currie, J.A., 1960. Gaseous diffusion in porous media Part 1. - A non-steady state method. British Journal of Applied Physics 11, 314–317.

Dignac, M.-F., Derrien, D., Barré, P., Barot, S., Cécillon, L., Chenu, C., Chevallier, T., Freschet, G.T., Garnier, P., Guenet, B., Hedde, M., Klumpp, K., Lashermes, G., Maron, P.-A., Nunan, N., Roumet, C., Basile-Doelsch, I., 2017. Increasing soil carbon storage: mechanisms, effects of agricultural practices and proxies. A review. Agronomy for Sustainable Development 37, 14.

Dodd, M., Rutledge, S., Mosquera-losada, R., Mosquera-losada, R., Mosquera-losada, R., Mcnally, S.R., Laughlin, D.C., Rutledge, S., Dodd, M.B., Six, J., Schipper, L.A., 2015. Root carbon inputs under moderately diverse sward and conventional ryegrass-clover pasture : implications for soi ... Related papers for soil carbon sequestration. Plant Soil 392, 289–299.

Huot, C., Zhou, Y., Philp, J.N.M., Denton, M.D., 2020. Root depth development in tropical perennial forage grasses is related to root angle , root diameter and leaf area 145–158.

Jones, D.L., Nguyen, C., Finlay, R.D., 2009. Carbon flow in the rhizosphere: Carbon trading at the soil-root interface. Plant and Soil 321, 5–33.

Jones, M.B., Donnelly, A., 2004. Carbon sequestration in temperate grassland ecosystems and the influence of management, climate and elevated CO_2. New Phytologist 164, 423–439.

Jong, E. De, Schappert, H.J., 1972. Calculation of soil respiration and activity from CO_2 profiles in the soil. Soil Science 113, 328–333.

Kell, D.B., 2012. Large-scale sequestration of atmospheric carbon via plant roots in natural and agricultural ecosystems: why and how. Philosophical Transactions of the Royal Society B: Biological Sciences 367, 1589–1597.

Kell, D.B., 2011. Breeding crop plants with deep roots: Their role in sustainable carbon, nutrient and water sequestration. Annals of Botany 108, 407–418.

Kusa, K., Sawamoto, T., Hu, R., Hatano, R., 2008. Comparison of the closed-chamber and gas concentration gradient methods for measurement of CO_2 and N_2O fluxes in two upland field soils. Soil Science and Plant Nutrition 54, 777–785.

Kuzyakov, Y. V., Larionova, A.A., 2006. Contribution of rhizomicrobial and root respiration to the CO_2 emission from soil (A review). Eurasian Soil Science 39, 753–764.

Kuzyakov, Y., Friedel, J.K., Stahr, K., 2000. Review of mechanisms and quantification of priming effects. Soil Biology and Biochemistry 32, 1485–1498.

Ledo, A., Smith, P., Zerihun, A., Whitaker, J., Vicente-Vicente, J.L., Qin, Z., McNamara, N.P., Zinn, Y.L., Llorente, M., Liebig, M., Kuhnert, M., Dondini, M., Don, A., Diaz-Pines, E.,

Datta, A., Bakka, H., Aguilera, E., Hillier, J., 2020. Changes in soil organic carbon under perennial crops. Global Change Biology 26, 4158–4168.

Li, Y., Xu, M., Sun, O.J., Cui, W., 2004. Effects of root and litter exclusion on soil CO_2 efflux and microbial biomass in wet tropical forests 36, 2111–2114.

Lilley, J.M., Kirkegaard, J.A., 2011. Benefits of increased soil exploration by wheat roots. Field Crops Research 122, 118–130.

Luther-Mosebach, J., Kalinski, K., Gröngröft, A., Eschenbach, A., 2018. CO_2 fluxes in subtropical dryland soils—a comparison of the gradient and the closed-chamber method. Journal of Plant Nutrition and Soil Science 181, 21–30.

Lynch, J.P., Wojciechowski, T., 2015. Opportunities and challenges in the subsoil: Pathways to deeper rooted crops. Journal of Experimental Botany 66, 2199–2210.

Ma, Z., Wood, C.W., Bransby, D.I., 2000. Soil management impacts on soil carbon sequestration by switchgrass. Biomass and Bioenergy 18, 469–477.

Maeght, J.-L., Rewald, B., Pierret, A., 2013. How to study deep roots—and why it matters. Frontiers in Plant Science 4, 1–14.

Maier, M., Schack-Kirchner, H., 2014. Using the gradient method to determine soil gas flux: A review. Agricultural and Forest Meteorology 192–193, 78–95.

Miranda, K.M., Espey, M.G., Wink, D.A., 2001. A rapid, simple spectrophotometric method for simultaneous detection of nitrate and nitrite. Nitric Oxide - Biology and Chemistry 5, 62–71.

Mooney, S.J., Pridmore, T.P., Helliwell, J. and Bennett, M.J., 2012. Developing X-ray computed tomography to non-invasively image 3-D root systems architecture in soil. Plant and soil, 352, 1-22.

Mulvaney, R.L.-M. of soil analysis, 1996. Nitrogen—inorganic forms. SSSA, Madison 3, pp 1123–1184.

Omonode, R.A., Vyn, T.J., 2006. Vertical distribution of soil organic carbon and nitrogen under warm-season native grasses relative to croplands in west-central Indiana, USA. Agriculture, Ecosystems and Environment 117, 159–170.

Paustian, K., Lehmann, J., Ogle, S., Reay, D., Robertson, G.P., Smith, P., 2016. Climate-smart soils. Nature 532, 49–57.

Paymaneh, Z., Gryndler, M., Konvalinková, T., Benada, O., Borovička, J., Bukovská, P., Püschel, D., Řezáčová, V., Sarcheshmehpour, M. and Jansa, J., 2018. Soil matrix determines the outcome of interaction between mycorrhizal symbiosis and biochar for *Andropogon gerardii* growth and nutrition. Frontiers in Microbiology *9*, 2862.

Pierret, A., Maeght, J.L., Clément, C., Montoroi, J.P., Hartmann, C., Gonkhamdee, S., 2016. Understanding deep roots and their functions in ecosystems: An advocacy for more unconventional research. Annals of Botany 118, 621–635.

Powlson, D.S., Whitmore, A.P., Goulding, K.W.T., 2011. Soil carbon sequestration to mitigate climate change: A critical re-examination to identify the true and the false. European Journal of Soil Science 62, 42–55.

Pritchard, D.T., Currie, J.A., 1982. Diffusion of coefficients of carbon dioxide, nitrous oxide, ethylene and ethane in air and their measurement. Journal of Soil Science 33, 175–184.

R Core Team, 2017. A language and environment for statistical computing. R.

Rasse, D.P., Rumpel, C., Dignac, M.F., 2005. Is soil carbon mostly root carbon? Mechanisms for a specific stabilisation. Plant and Soil 269, 341–356.

Rudolph, J., Rothfuss, F., Conrad, R., 1996. Flux between soil and atmosphere, vertical concentration profiles in soil, and turnover of nitric oxide: 1. Measurements on a model soil core. Journal of Atmospheric Chemistry 23, 253–273.

Salomé, C., Nunan, N., Pouteau, V., Lerch, T.Z., Chenu, C., 2010. Carbon dynamics in topsoil and in subsoil may be controlled by different regulatory mechanisms. Global Change Biology 16, 416–426.

Scheer, C., Rowlings, D.W., Firrel, M., Deuter, P., Morris, S., Grace, P.R., 2014. Impact of nitrification inhibitor (DMPP) on soil nitrous oxide emissions from an intensive broccoli production system in sub-tropical Australia. Soil Biology and Biochemistry 77, 243–251.

Schlüter, S., Henjes, S., Zawallich, J., Bergaust, L., Horn, M., Ippisch, O., Vogel, H.J., Dörsch, P., 2018. Denitrification in soil aggregate analogues-effect of aggregate size and oxygen diffusion. Frontiers in Environmental Science 6, 1–10.

Shahzad, T., Imtiaz, M., Maire, V., Barot, S., 2018. Root penetration in deep soil layers stimulates mineralization of millennia-old organic carbon. Soil Biology and Biochemistry 124, 150–160.

Shcherbak, I., Robertson, G.P., 2019. Nitrous oxide (N_2O) emissions from subsurface soils of agricultural ecosystems. Ecosystems 22, 1650-1663.

Shi, Z., Allison, S.D., He, Y., Levine, P.A., Hoyt, A.M., Beem-Miller, J., Zhu, Q., Wieder, W.R., Trumbore, S., Randerson, J.T., 2020. The age distribution of global soil carbon inferred from radiocarbon measurements. Nature Geoscience.

Slessarev, E.W., Nuccio, E.E., McFarlane, K.J., Ramon, C.E., Saha, M., Firestone, M.K., Pett-Ridge, J., 2020. Quantifying the effects of switchgrass (Panicum virgatum) on deep organic C stocks using natural abundance ^{14}C in three marginal soils. GCB Bioenergy 12, 834–847.

Sumner, M.E., Miller, W.P., 1996. Cation Exchange Capacity and Exchange Coefficients, Methods of soil analysis: Part 3 Chemical methods, 5, 1201-1229.

Suseela, V., Tharayil, N., Pendall, E., Rao, A.M., 2017. Warming and elevated CO_2 alter the suberin chemistry in roots of photosynthetically divergent grass specfile. AoB PLANTS 9, 1–11.

Wang, Y., Li, X., Dong, W., Wu, D., Hu, C., Zhang, Y., Luo, Y., 2018. Depth-dependent greenhouse gas production and consumption in an upland cropping system in northern China. Geoderma 319, 100–112.

Wickham, H., 2016. Elegant Graphics for Data Analysis. ggplot2.

Xiao, X., Kuang, X., Sauer, T.J., Heitman, J.L., Horton, R., 2015. Bare Soil Carbon Dioxide Fluxes with Time and Depth Determined by High-Resolution Gradient-Based Measurements and Surface Chambers. Soil Science Society of America Journal 79, 1073.

Yost, J.L., Hartemink, A.E., 2020. How deep is the soil studied – an analysis of four soil science journals. Plant and Soil.

Chapter 5

Greenhouse gas production, diffusion and consumption in a soil profile under maize and wheat production

Authors

Erik S. Button, Miles Marshall, Antonio R. Sánchez-Rodríguez, Aimeric Blaud, Maïder Abadie, David R. Chadwick, Davey L. Jones.

Publication status

This manuscript is under review in *Geoderma*.

Citation

Button, E.S., Marshall, M., Sánchez-Rodríguez, A.R., Blaud, A., Abadie M., Chadwick, D.R. and Jones, D.L., 2022. Greenhouse gas production, diffusion and consumption in a soil profile under maize and wheat production. Under review in Geoderma.

Author contributions

ESB, DRC and DLJ conceived the experiment. ESB conducted the experiments, with technical support from MM, and wrote the manuscript. ARS, AB and AM provided data and reviewed the manuscript. DRC and DLJ reviewed the manuscript.

Abstract

Agricultural soil emissions are a balance between sinks and sources of greenhouse gases (GHGs). The fluxes of GHGs from soils are complex and spatially and temporally heterogenous. While the soil surface is the exchange site with the atmosphere and is commonly where GHG fluxes are measured, it is important to consider processes occurring throughout the soil profile. To reduce emissions and improve agricultural sustainability we need to better understand the drivers and dynamics (production, consumption, diffusion) of these gases within the soil profile. Due to the heterogeneous nature of GHG processes at small to large scales, it is important to test how these processes differ with depth in different systems. In this study, we measured in situ CO_2, N_2O and CH_4 concentration gradients as a function of soil depth over subsequent maize and wheat growing seasons with active gas samplers inserted into an arable field at 10, 20, 30 and 50 cm depths. We found N_2O and CH_4 concentrations increased with depth, but only CO_2 concentrations differed with depth between growing seasons due likely to differences in soil diffusivity driven by soil conditions. Using the concentration gradient method (CGM), the CO_2 fluxes at each depth and their contribution to the surface flux were calculated and validated against a chamber measured surface flux. We found the GM estimated surface CO_2 flux was only 6% different in the wheat, but 28% lower than the surface measured flux in the maize growing season, due to drought conditions reducing the accuracy of the GM. Finally, we measured fluxes of CO_2, N_2O and CH_4 in ambient and highly concentrated headspaces in laboratory mesocosms over a 72 h incubation period. We provide evidence of depth-dependent CH_4 oxidation and N_2O consumption and possibly CO_2 fixation. In conclusion, our study provides valuable information on the applicability of the GM and further evidence of the GHG production, consumption and diffusion mechanisms that occur deeper in the soil in a temperate arable context.

Keywords: Fick's law, depth dependent, subsoil, diffusion coefficient, denitrification, dark CO_2 fixation.

5.1 Introduction

Agricultural soils represent significant sources of CO_2, CH_4 and N_2O to the atmosphere. However, they can also act as greenhouse gas (GHG) sinks (Chapuis-Lardy et al., 2007; Johnston et al., 2009). Net emissions of GHGs from the soil are therefore a balance between production and consumption processes that occur simultaneously in soil. As the pool of soil organic matter (SOM), the principal soil sink of CO_2, grows or shrinks, the potential for microbial decomposition and the resulting net CO_2 flux increases or decreases (Johnston et al., 2009). The net soil-atmosphere flux of N_2O, on the other hand, is dynamically governed by the availability of N, soil conditions and the soil microbial processes that underpin the production and consumption of N_2O in the soil (Chapuis-Lardy et al., 2007). Finally, the CH_4 flux depends almost entirely on O_2 availability when C is not limiting and the temperature is not too low (Le Mer and Roger, 2001). The fluxes of these important agricultural GHGs are complex and spatially and temporally heterogenous, but to improve agricultural sustainability through reduction of GHG emissions, the drivers and dynamics need to be better understood.

Quantifying the differences between surface and soil profile fluxes and their drivers is important as agricultural practices (e.g. tillage, nitrogen inputs, organic matter amendments) influence and drive GHG production throughout the soil. While we have a good understanding of soil-to-air GHG fluxes from surface measurements (e.g. closed chamber and eddy-covariance methods; Dossa et al., 2015; Kusa et al., 2008), these do not capture information concerning GHG-related processes occurring deeper in the soil (Wang et al., 2018). In addition, they largely assume that the emissions of GHGs are instantaneous and disregard the possibility of changes in the C and N pools in the soil (Wang et al., 2018). Finally, the soil-to-air flux is not necessarily representative of GHG fluxes in the whole soil profile (Boon et al., 2014; Clark et al., 2001). To capture more information on GHG processes that lead to the surface-atmosphere flux different methods are required.

The concentration gradient method (CGM) is an approach that uses the soil profile gas concentration gradient to estimate soil fluxes, which are difficult to measure in situ, and extrapolates from this gradient to determine the surface flux. TheCGM contributes to greater understanding of GHG dynamics at different soil depths, which is essential to better predict movements of C and N in ecosystems (Maier and Schack-Kirchner, 2014). This is especially important in the light of climate change and the increasing interest (e.g. '4 per 1000' initiative)

and urgent need for sequestering C in soil and subsoil. The method requires concentration gradient data which we aim to produce for CO_2, CH_4 and N_2O, which only a few studies have done simultaneously (Wang et al., 2018) and fewer still across different crops (Dong et al., 2013). Typically, concentrations of N_2O and CO_2 in the soil profile are much greater than in the overlying air, while an opposite trend is often found for CH_4 in oxic soils (Dong et al., 2013; Li and Kelliher, 2005; Maier and Schack-Kirchner, 2014; Wang et al., 2018; Xiao et al., 2015). However, how these concentration profiles may differ across multiple soils, climates and crop rotations is poorly studied.

For the utility of the CGM in furthering the understanding of the GHG dynamics to be realised, the modelled fluxes need to be reliable. As the performance of the CGM is influenced by many factors, including the target GHG, sampling frequency and the method for determining the diffusion coefficient (D_s), it is important to test the limits and opportunities of the method for determining the most effective use of the method (Maier and Schack-Kirchner, 2014). An aim of this study was to test the performance of the CGM in modelling CO_2 fluxes across multiple growing seasons and crop rotations at low temporal resolution with a measured D_s against a surface chamber method.

While it is well documented that GHG fluxes differ with depth (Davidson et al., 2004; Dong et al., 2013; Wang et al., 2018), the net GHG flux is a result of a balance between consumption and production processes. For CO_2, CH_4 and N_2O, the consumption process is known as dark CO_2 fixation (Akinyede et al., 2020); methanotrophy (i.e. CH4 oxidation; Le Mer and Roger, 2001); and N_2O consumption (i.e. final stage of denitrification) (Maier and Schack-Kirchner, 2014; Neftel et al., 2007), respectively. While these processes have been measured in different systems, how their rates differ with depth is not fully understood. A further aim of this study was to quantify GHG consumption rates, with an expectation that consumption of GHG would be depth dependent as consuming microbes and the conditions that support these processes differ with soil depth.

In this study, we measured in situ CO_2, N_2O and CH_4 concentration gradients from 10 to 50 cm over a maize and a subsequent wheat growing season. We hypothesised that maize and wheat crops would result in measurable differences in GHG concentration profiles due to their differing rooting architectures. We also hypothesised that the CGM would be a reliable method in the estimation of CO_2 fluxes despite low temporal resolution, different growing

seasons and crops. To address the hypothesis that production and consumption of GHGs is depth dependent, a laboratory soil incubation study was also undertaken to measure net production and consumption of CO_2, N_2O and CH_4 at different soil depths under different concentrated headspaces.

5.2 Materials and methods

5.2.1 Experimental site and soil characterisation

The study site was a lowland (<10 m.a.s.l.) arable field located at the Henfaes Research Centre, Abergwyngregyn, North Wales (53°14'29"N, 4°01'15"W) drilled with maize (*Zea mays L.*, cv. Emmerson) on the 6th of May 2018 and sown with winter wheat (*Triticum aestivum L.*, Mulika) on the 26th of March 2019. The freely draining sandy clay loam textured soil is classified as a Eutric Cambisol (WRB) or Typic Hapludalf (US Soil Taxonomy; Soil Survey Staff, 2014). The field received no N fertilizer in 2018 as the soil mineral N content was already high (34 ± 0.1 mg N kg^{-1} soil, *n* = 8), but received 2 rates of N fertilizer as ammonium nitrate in 2019: High (150 kg ha^{-1}) and Medium (75 kg ha^{-1}). Plots were established within a randomised block design with 4 blocks and 3 treatment plots per block. The plots receiving Medium and High fertilizer rates both received 40 kg ha^{-1} of N fertilizer on the 7th May, and then a further 35 or 110 kg ha^{-1} on the 30th of May 2019, respectively. The soil was conventionally ploughed both years to a depth of 30 cm at the beginning of the growing seasons in March. As the soil was undisturbed thereafter for >2 months before the first gas samples were taken, the soil was considered to have settled. This is supported by Fiedler et al. (2015) who found soil respiration to return to pre-tillage levels 36 d after tillage.

In 2018, soil from the same field was characterised extensively for chemical, biological and physical properties (mean values presented in Table 5.1). Soil samples were taken from 4 independent soil pits located ca. 50 m apart at 10 cm depth intervals to a depth of 100 cm and sieved to 5 mm. Soil texture was measured with a LS 13320 laser diffraction particle size analyser (Beckman-Coulter Inc., Indianapolis, IN). Soil pH and electrical conductivity (EC) were measured in a fresh soil 1:2.5 (w/v) distilled water suspension with a Model 209 pH meter (Hanna Instruments Ltd., Leighton Buzzard, UK) and a Jenway 4520 conductivity meter (Cole-Palmer Ltd., Stone, UK), respectively. Cation exchange capacity (CEC) was determined using the sodium acetate method of Sumner and Miller (1996). Total soil C and N were determined

with a TruSpec® CN analyser (Leco Corp., St Joseph, MI). Soil subsamples (5 g) were extracted with 0.5 M K_2SO_4 (1:5 w/v; 150 rev min^{-1}, 30 min) and the supernatant recovered after centrifugation (14,000 g, 10 min). NH_4^+ and NO_3^- were determined colorimetrically according to Mulvaney (1996) and Miranda et al. (2001), respectively, on a PowerWave XS Microplate Spectrophotometer (BioTek Instruments Inc., Winooski, VT, USA). Dissolved organic C (DOC) in the extracts was measured with a Multi N/C 2100/2100 analyser (AnalytikJena AG, Jena, Germany). Soil microbial biomass C (MBC) was measured using the $CHCl_3$ fumigation-K_2SO_4 extraction procedure of De-Polli et al. (2007) using a KEC extraction efficiency value of 0.45 (Vance et al., 1987). Immediately after soil collection, field-moist soil samples (25 g) were sieved (2 mm), frozen (-20 °C), freeze-dried and phospholipid-derived fatty acids (PLFA) were determined according to Bartelt-Ryser et al. (2005). Finally, quantitative PCR (qPCR) analyses of N cycling gene abundance (*nirK, nirS, nosZ*) were processed at the same time following the methods described in de Sosa et al. (2018).

5.2.2 Environmental and crop measurements

Soil volumetric water content (θ) and temperature were measured using 18 Acclima TDT Soil-Water-Temperature-BEC sensors (Acclima, Inc., Meridian, ID, USA), installed at 10, 20, and 30 cm depths (50 cm in 2018 only). Rainfall, atmospheric pressure, and air temperature were recorded hourly at a weather station located at the research site. Normalised Difference Vegetation Index (NDVI) was measured weekly using a handheld GreenSeeker® crop sensor (Trimble Inc., Sunnyvale, CA, USA) held ca. 40 cm above the crop canopy. The crop height (base of plant to the tallest part) was also measured weekly, or more frequently, on 10 randomly selected plants per plot.

To characterise changes in inorganic N during the growing seasons, 5 g fresh soil samples were collected weekly from 0-5 cm depth and immediately extracted with 25 ml of 0.5 M K_2SO_4, shaken at 200 rev min^{-1} for 30 mins and centrifuged at 12,000 g for 5 mins before the supernatant was removed and analysed for NO_3^--N and NH_4^+-N as described above.

The maize and wheat fields were harvested on the 12th September 2018 and 2nd of September 2019, respectively. For maize, 4 plants per plot were randomly selected and oven dried (80°C, 72 h). For wheat, 1 m strips of the 4 central rows from each plot where harvested and oven dried (80°C, 72 h). On the 24th October 2018 and between the 2nd and 12th of July

Table 5.1 Physical, chemical and biological soil properties at different depths and root properties from the maize and wheat plots in 2018 and 2019. Where appropriate, the data are expressed on a soil dry weight basis. Values are means ± SEM. Unless stated otherwise, *n* = 4.

Properties		Soil depth (cm)				
		0 - 10	10 - 20	20 - 30	30 - 40	40 - 50
Sand (%)		62.9 ± 0.7	62.0 ± 1.3	60.3 ± 2.3	60.3 ± 3.3	62.4 ± 4.4
Silt (%)		16.2 ± 1.3	17.8 ± 0.6	17.8 ± 1.2	17.5 ± 1.5	17.1 ± 1.8
Clay (%)		20.9 ± 1.0	20.2 ± 0.9	21.9 ± 1.5	22.2 ± 2.3	20.6 ± 2.6
Dry bulk density (g cm^{-3})		1.4 ± 0.03	1.4 ± 0.07	1.7 ± 0.1	1.7 ± 0.2	1.8 ± 0.1
Porosity (%)		66 ± 2.0	69 ± 1.1	67 ± 1.0	63 ± 1.2	59 ± 1.8
pH (1:2.5)		6.0 ± 0.1	6.2 ± 0.1	6.5 ± 0.1	6.6 ± 0.1	6.7 ± 0.1
EC (1:2.5 µS cm^{-1})		33 ± 4	32 ± 2	24 ± 1	25 ± 3	19 ± 1
DOC (mg C kg^{-1})		82.3 ± 4	76.8 ± 4	57.0 ± 7	52.0 ± 10	47.1 ± 9
CEC ($cmol_+$ kg^{-1})		14.8 ± 0.2	15.6 ± 0.4	12.7 ± 1.0	12.7 ± 0.5	11.1 ± 1.7
NH_4^+ (mg kg^{-1})		2.4 ± 0.1	1.9 ± 0.2	1.7 ± 0.1	1.6 ± 0.1	1.6 ± 0.2
NO_3^- (mg kg^{-1})		10.8 ± 0.7	11.6 ± 2	4.9 ± 0.4	3.3 ± 0.2	2.0 ± 0.1
Total PLFA biomass (nmol g^{-1})		132 ± 9	116 ± 4	58 ± 5	34 ± 3	23 ± 2
nirK gene (x10^8 copies g^{-1})		4.8 ± 0.4	4.5 ± 0.3	2.3 ± 0.3	1.1 ± 0.1	0.7 ± 0.08
nirS gene (x10^6 copies g^{-1})		6.9 ± 0.7	4.9 ± 0.5	1.6 ± 0.4	0.6 ± 0.1	0.2 ± 0.04
nosZ gene (x10^7 copies g^{-1})		5.3 ± 0.3	4.2 ± 0.4	1.3 ± 0.2	0.4 ± 0.07	0.2 ± 0.05
Root density (mg DW cm^{-3})	Maize*	5.4 ± 1.1	0.15 ± 0.02	0.2 ± 0.09	0.1	0.009
	Wheat‡	2.1 ± 0.7	0.09 ± 0.03	0.06 ± 0.01	0.03 ± 0.01	0.04 ± 0.02
Root length (cm cm^{-3})	Maize*	1.9 ± 0.3	0.9 ± 0.1	0.7 ± 0.1	0.7 ± 0.2	0.6 ± 0.2
	Wheat‡	2.1 ± 0.2	0.3 ± 0.05	0.2 ± 0.07	0.1	0.2

*data collected 24th October 2018; 171 days after sowing, *n* = 4, 4, 3, 1, 1;

‡data collected between the 2-12th July 2019; 98-108 days after sowing, *n* = 4, 4, 3, 2, 1

2019, when the crops were fully established, soil cores (ca 80 cm deep x 50 mm diameter) were taken from each plot for root analysis using a percussion corer. Cores were cut into 10 cm sections (soil vol. ca. 196 cm^3) and washed to separate the roots from the soil. Roots were

arranged on a plastic tray in water and scanned and analysed using the 2019 WinRhizoTM software (Regent Instruments Inc., Québec, Canada) to estimate total root length, before oven drying (70°C, 24 h) to determine root biomass. The results are displayed in Table 5.1.

5.2.3 Greenhouse gas measurement systems

PVC pipes (3 cm diameter) of differing lengths (10, 20, 30 and 50 cm) were fitted with Suba-Seal® gas sampling ports at the top (Sigma-Aldrich Ltd., Poole, UK). The final 3 cm region at the base of the pipe was perforated (0.8 mm diameter; ca. 20 holes) to allow gas ingress and the monitoring of GHGs at specific depths. The inside of this 3 cm section was lined with 1 mm nylon mesh to prevent soil entering the pipe and the base of the pipe was sealed with electrical tape (Appendix 4, Fig. S1). In July 2019, the gas collecting pipes were fitted with plastic 2-way (4 × 1.2 × 2.3 cm) valves, where one end was sealed into a drilled hole in the headspace of the pipes and the other end had a 5 cm piece of silicon tubing attached to it (Appendix 4, Fig. S1) for non-syringe gas sampling. In total, 8 pipes were made for each of the 4 depths (n = 32) and were inserted vertically to the desired depth by pushing them carefully into pre-cored holes (slightly smaller diameter). If the required depth was not reached by pushing alone, they were lightly tapped with a rubber mallet. These pipes were installed in mid-June 2018 when the field was under maize and sampled weekly until October 2018, after which they were carefully removed and maintained before re-inserting at the beginning of May 2019 for the wheat growing season. In 2019, 4 pipes of each depth were located in the High (150 kg ha^{-1}) and Medium (75 kg ha^{-1}) N fertilizer-applied blocks (n = 4).

The surface-atmosphere CO_2 flux was measured hourly with 12 in situ LI-COR LI-8100A automated soil CO_2 flux system with infrared gas analysis (LI-COR Biosciences, Inc., Lincoln, NE, USA) from 3rd of July to 7th of September 2018 and the 16th of May to the 30th of July and then from the 22nd of August until the 19th of September 2019. The gap in measurements in 2019 was due to equipment failure.

5.2.4 Gas sampling and analysis

Gas sampling occurred 1-3 times weekly from the 22nd of June to the 19th of September in 2018 and from the 22nd of May to the 19th of September in 2018 between 1000 and 1300

h. Using a gas-tight polypropylene syringe, air in the pipes was mixed by filling and emptying the syringe into the pipe 3 times before a ca. 25 ml gas sample was taken and over-filled (to prevent loss of sample during storage) into a pre-evacuated 20 ml glass vial (QUMA Elektronik and Analytik GmbH, Wuppertal, Germany). Before analysis, the samples were brought to ambient air pressure by inserting a needle into the vials and releasing the pressure. These were then analysed for CO_2, CH_4 and N_2O concentrations using a Perkin Elmer 580 Gas Chromatograph (GC), served with a Turbo Matrix 110 auto sampler (Perkin Elmer Inc., Waltham, MA). Gas samples passed through two Elite-Q mega bore columns via a split injector, with one connected to an electron capture detector (ECD) for N_2O determination, and the other to a flame ionisation detector (FID) for CO_2 and CH_4 determination.

5.2.5 Modelled CO_2 flux estimation

To estimate the fluxes of gases in the soil profile and at the soil surface, the concentration gradient method (GM) was used (Maier and Schack-Kirchner, 2014). The transport of gas through porous media in one dimension was approximated using Fick's first law:

$$F_z = -D_s \frac{dC}{\mathrm{dz}} \tag{1}$$

where F is the gas flux (g CO_2 m^{-2} h^{-1}) at soil depth z (m), D_s is the effective gas diffusion coefficient of the gas in soil (m^2 h^{-1}) and C is the concentration of the gas species (mg m^{-3}). As the direction of the concentration is decreasing, the given sign is negative (which can be ignored for the purposes of calculation). The concentration gradient (dC/dz) was calculated according to De Jong and Schappert (1972). The gas concentrations were converted from ppm to mg m^{-3} using Equation 2, by multiplying the concentration by the molecular weight (M_w) of CO_2 (44.01 g mol^{-1}) and then dividing by the molar volume M_v (calculated by Avogadro's Law) of the gas:

$$C = \frac{M_w C'}{\left(\frac{R \cdot T}{p}\right)} \tag{2}$$

where C is the gas concentration in mg m^{-3}, C' is the gas concentration in ppmv, R is the universal gas constant (0.08206 L atm K^{-1} mol^{-1}), T is soil temperature (K) and p is pressure (atm).

The D_s was measured in February 2020 using a modified Currie method (Currie, 1960) and DENitrification Incubation System (DENIS; Cárdenas et al., 2003) vessels. The methodology of the incubations is described in detail in Chapter 6. Briefly, SF_6 was used as a conservative tracer gas to determine the rate of diffusion through 104 cm^3 intact soil cores (n = 6) from the same field as in this study at depth intervals of 0-10 and 50-60 cm, at 0.3 and 0.5 air-filled porosities (ε). This resulted in a mean D_s of 0.0022 and 0.011 m^2 h^{-1} in the 0.3 and 0.5 ε across all depths (the depths were not different from each other). Field ε (cm^3 cm^{-3}) was estimated by subtracting the volumetric water content (ϑ; cm^3 cm^{-3}) from the total porosity of the soil as in Equation 3, where B_d is dry bulk density (g cm^{-3}) and P_d is the particle density (assumed to be 2.65 g cm^{-3}).

$$\varepsilon = \left(1 - \frac{B_d}{P_d}\right) - \theta \tag{3}$$

Then, ε-related Ds was estimated from the relationship between mean D_s and ε. This was best explained at low ε (<50%) by the power function: $D_s = 0.0907(\varepsilon)^{3.1848}$ (R^2 = 0.99). The effective diffusion coefficient for CO_2 was determined from the D_s of SF_6 by Equation 4:

$$D_s = D'_s \frac{D_0}{D'_0} \tag{4}$$

Where D'_s is the ε-related SF_6 diffusion coefficient, D'_0 is the diffusion coefficient of SF_6 in air (0.0335 m^2 h^{-1}; Rudolph et al., 1996), and D_0 is the diffusion coefficient of CO_2 in air (0.0529 m^2 h^{-1}). These were compared with the mean fluxes from the surface instruments between 1000 and 1300 h. The surface soil-atmosphere flux was estimated by extrapolating the fluxes from the 10 and 50 cm depths to the surface using Equation 5, where F_s is the surface flux and Fn (calculated using Eq. 1) is the flux at depth zn:

$$F_s = \frac{z_2 F_1 - z_1 F_2}{z_2 - z_0} \tag{5}$$

5.2.6 Gas consumption in laboratory mesocosms

In September 2019, ca. 50 g of soil was collected from each depth (10, 20, 30 and 50 cm) at 4 different sites within the same field (as the maize and wheat) and sieved to 5 mm. Subsequently, 2 g replicates of field-moist soil were placed into 20 ml glass vials (*n* = 4) and mechanically sealed with a butyl septum (QUMA Elektronik and Analytik GmbH, Wuppertal, Germany) using a crimper. Two different gas mixes (GC standards) were injected into the vials: an ambient-approximate mix: 490 ppm of CO_2, 2 ppm of CH_4 and 310 ppb of N_2O; and a high-concentrated mix; 2800 ppm of CO_2, 32 ppm of CH_4 and 5500 ppb of N_2O. Both gas mixes were made up in 21% O_2. This was done by flushing the vials with the gas mix for ca. 15 s at >100 ml min^{-1} with a needle while another needle allowed the purged headspace gas to escape. This same method was done with empty vials (*n* = 4), which confirmed the effectivity in replacing the headspace with the gas mix without loss of concentration. Three sets of identical vials containing four replicates from four soil depths at the two headspace concentrations were sampled at three different timepoints. After 24, 48 and 72 h incubating in the dark at room temperature (ca. 23 °C), 1 ml of gas was taken with a syringe from the headspaces of a set of vials and immediately filled into a new pre-evacuated vial. The new vials were then filled with 19 ml of N_2 gas (1:20 dilution) and analysed by gas chromatography (CO_2, CH_4 and N_2O), as described above. The gas fluxes were calculated on a dry weight basis according to the equations described by Comeau et al. (2018).

5.2.7 Data processing and statistical analysis

Zeros were removed from CH_4 dataset due to being below the detection limit of the GC (limit of detection: ca. 1.42 ppm – see Appendix 4, S1), resulting in the removal of 74 and 36% of the maize and wheat CH_4 concentration data. In addition, the maize gas pipe GHG dataset from 2018 required selective removal of data, due to containing impossibly high values or zeros due to data far below or exceeding the concentrations of the analytical standards (see Appendix 4, S2 for more detail). As the 2019 wheat dataset was of higher quality (see Appendix 4, S2), this was used to inform and validate outlier removals in the 2018 maize dataset. Removing data that exceeded the single highest datapoints in 2019 and zeros, resulted in 19 and 9% of the N_2O and CO_2 measurements being removed from the 2018 maize dataset, respectively.

All statistical data analysis was done on R (version 1.1.463; R Core Team, 2017). Before further analysis, as there were no differences between the concentrations at different depths with 2 rates of N fertilizer (two-way ANOVA), GHG concentration gradient data in 2019 were pooled (i.e. n = 8). One-way ANOVAs were used on the environmental measures with depth and Kruskal-Wallis rank sum tests were performed on the GHG concentration, CGM flux means, soil temperature, and diffusivity data by depth, as they did not meet the assumptions for the equivalent parametric test following transformation (log, square root and cube). Mean GHG concentrations were compared between the maize and wheat growing seasons (equal-sized dataset of 10 weeks from 25th June to 5th September) by Welch's t-test. Two-way ANOVAs (Tukey's HSD) were performed on the GHG fluxes of the mesocosms by depth and headspace concentration. Trend lines were drawn for each wheat and maize GHG concentration gradient depth profile using Affinity Designer (Serif Europe Ltd., Nottingham, UK).

5.3 Results

5.3.1 Environmental and crop conditions

The mean air temperature between the 1st May and 20th September in 2018 was 15.4 ± 0.06°C with highest average daily temperatures of 20.6 on the 26th of June and lowest of 10°C on the 8th of May. In the soil, average temperatures were 15, 12 and 8% higher than in the air in the 10, 30 and 50 cm depths (p < 0.001), respectively. In 2019, the average air temperature was only 2% lower than in 2018 (15.1 ± 0.3°C), but experienced higher maximum and minimum daily average temperatures of 25.2°C on 27th June and a 7.5°C on 3rd May (Fig. 5.1a), respectively. Similar to 2018, mean soil temperatures in 2019 were 13, 12 and 11% higher than in the air than at 10, 20 and 30 cm (p < 0.001), respectively.

The total precipitation for the 1st May - 20th September period was 208 mm in 2018 and 83% greater in 2019 (381 mm; Fig. 5.1b), demonstrating that 2018 was an exceptionally dry year (p < 0.001) (Turner et al., 2021). The wettest months in this period in 2018 were September > August > July > May > June, where the entirety of June had only 2 mm of rainfall. In stark comparison, June was 54-fold wetter and the wettest month in the same period in 2019 with 115 mm followed by August > July > September > May. Interestingly, in 2018 soil

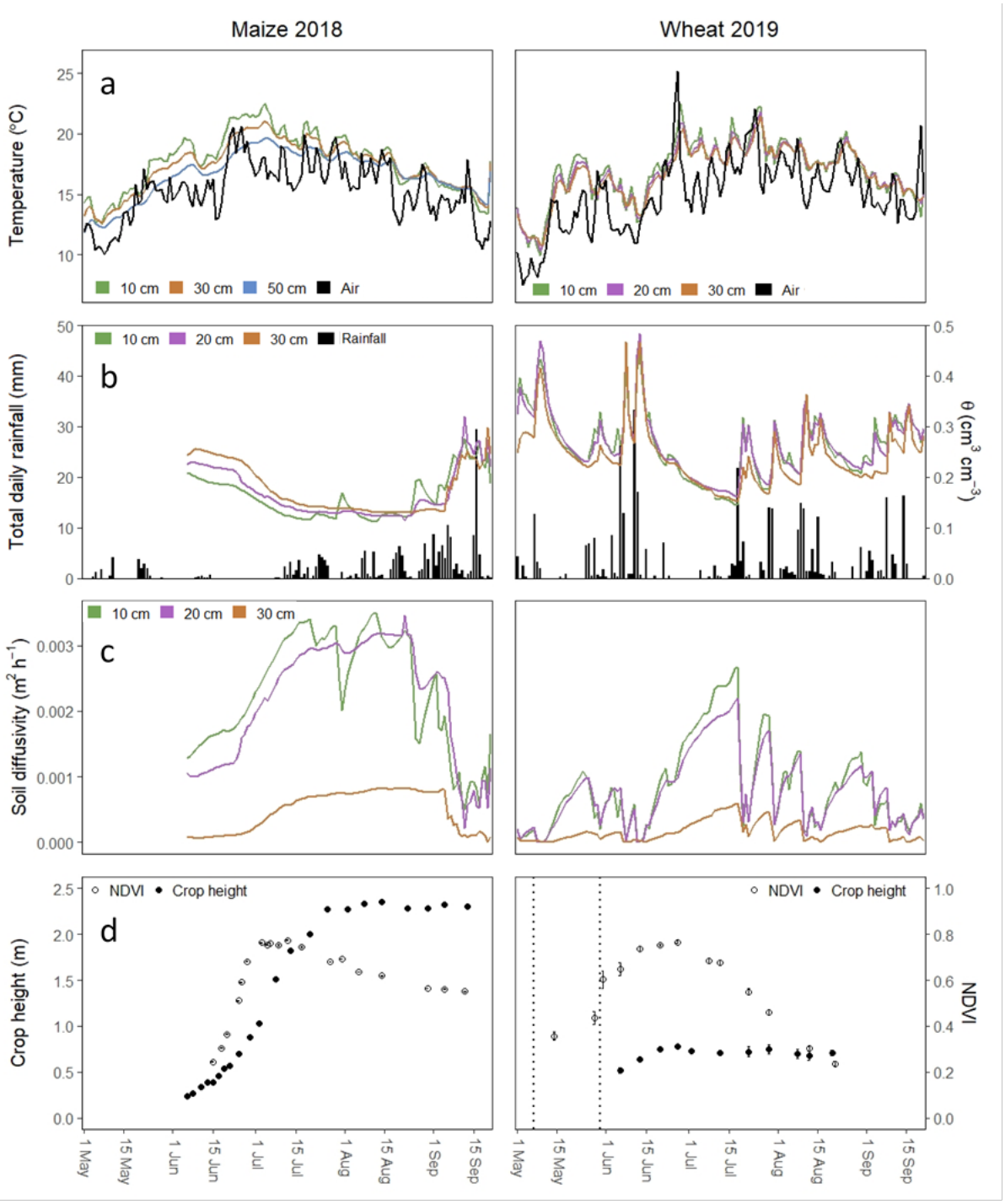

Fig. 5.1 Daily average a) air and soil temperature; b) total daily precipitation and average volumetric water content (θ); c) estimated diffusivity of SF_6 through the soil of different depths; and d) mean (± SEM) crop height (n = 10) and NDVI (n = 4) during the 2018 and 2019 growing seasons (1st May – 20th Sep). Colours reflect different measurement depths. The vertical dotted lines are the dates when ammonium nitrate fertilizer was applied in 2019, where 40 kg ha^{-1} was applied on the 7th May and 110 kg ha^{-1} on the 30th May.

water content increased and in 2019 decreased with depth. Mean volumetric water content (θ) was the same in 2019 in the 10 and 20 cm depths (0.26 cm^3 cm^{-3}) and slightly lower at 30 cm (0.24 cm^3 cm^{-3}). In 2018, between the 6th June and the 20th September mean θ was 0.16, 0.17 and 0.18 cm^3 cm^{-3} in the 10, 20 and 50 cm depths, respectively. With the lower water content in the soil profile throughout 2018, the mean estimated diffusivity of SF_6 (low solubility; 0.0017 m^2 h^{-1}) was 1.7-fold higher in all depths, compared to 2019 ($p < 0.001$; Fig. 5.1c). Mean diffusivity decreased with depth similarly in both years ($p < 0.001$), with 5-7 and 79% lower diffusivity at 20 and 30 cm respectively compared to the diffusivity of the soil at 10 cm.

In 2018, the highest mean NDVI was measured as 0.77 ± 0.01 on the 12th July, while the highest plant height of 2.4 m ± 0.02 was measured >1 month later on the 14th August. Peak plant productivity in 2019 likely occurred during the week of the 27th June, which was the warmest week of the season and when both the highest mean NDVI (0.77 ± 0.01) and crop heights (0.78 m ± 0.01) were measured (Fig. 5.1c). The largest increase in NDVI in 2019 was following N fertilizer addition on the 31st May. Approaching peak NDVI, the increase in the maize was faster (slope of 0.02) compared to the wheat (0.01), but after peak NDVI in the wheat, the linear decrease was steeper (-0.01) than in the maize (-0.004).

5.3.2 GHG concentrations at depth

Across both growing seasons, the concentrations of CO_2 and N_2O in the gas pipes were consistently higher than atmospheric concentrations and increased with soil depth, while the opposite trend was observed with CH_4 concentrations (Fig. 5.2). The mean CO_2 concentrations were greater under wheat compared to maize at all depths (Fig. 5.2a; $p < 0.001$). Under maize, 3 to 7-fold higher CO_2 concentrations were measured in the soil depths compared to ambient CO_2 concentration ($p < 0.001$), whereas under wheat, CO_2 concentrations increased by 9 to 16-fold with depth compared to the ambient concentration ($p < 0.001$). There was no difference in mean N_2O concentrations at the soil depths between the maize and wheat growing seasons (Fig. 5.2b; $p = 0.11$). Both the maize and wheat N_2O concentrations were greater with depth, with 2 to 12-fold higher concentrations compared to the ambient N_2O concentration ($p < 0.001$). The mean CH_4 concentrations across the soil profile were not different between the maize and wheat growing seasons (Fig. 5.2c; $p = 0.23$). The decrease in

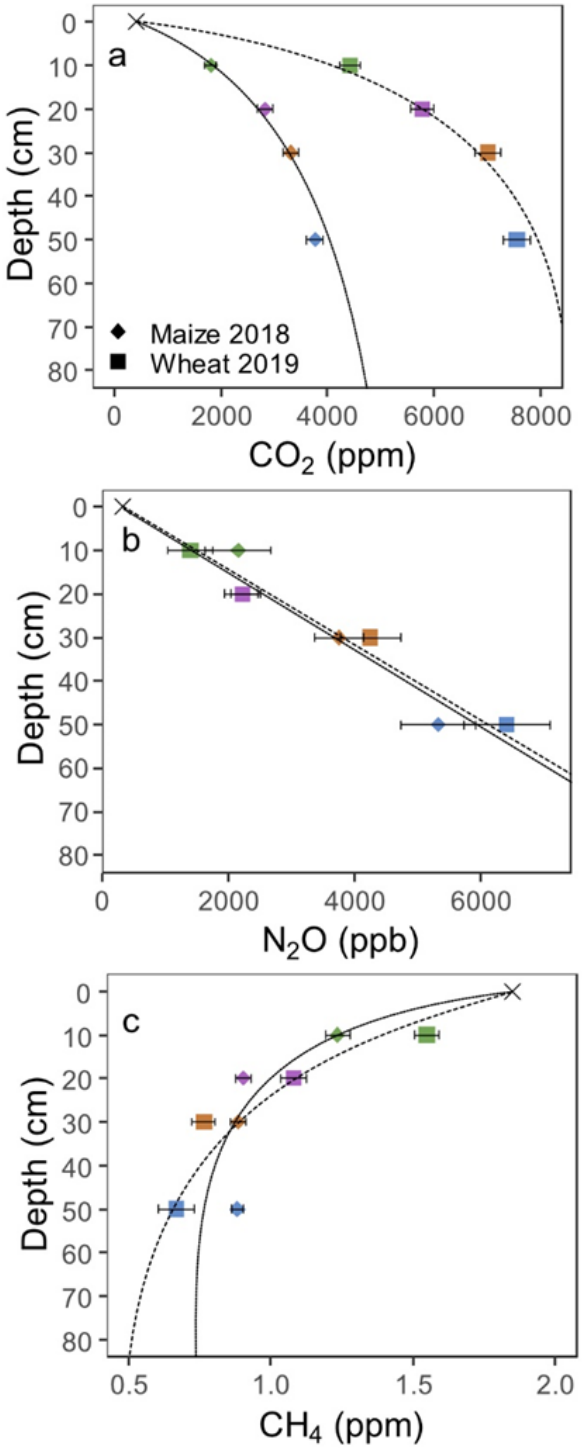

Fig. 5.2 Depth profiles of mean (± SEM) gas concentrations of a) CO_2; b) N_2O; and c) CH_4 from weekly sampling of gas collectors installed at different soil depths (*n* = 8) in a field under maize in 2018 (22 Jun 2018 – 19 Sep 2018; *N* = 644) and wheat in 2019 (22 May 2019 – 5 Sep 2019; *N* = 533). Colours reflect different sampling depths. Solid and dotted lines represent the maize and wheat, respectively. The 'X' at 0 cm depth represents the approximate ambient levels of the respective gases (CO_2, 420 ppm; N_2O, 330 ppb; CH_4, 1.85 ppm, respectively). The curves were forced to intercept the x-axis (0 cm) at the aforementioned concentrations.

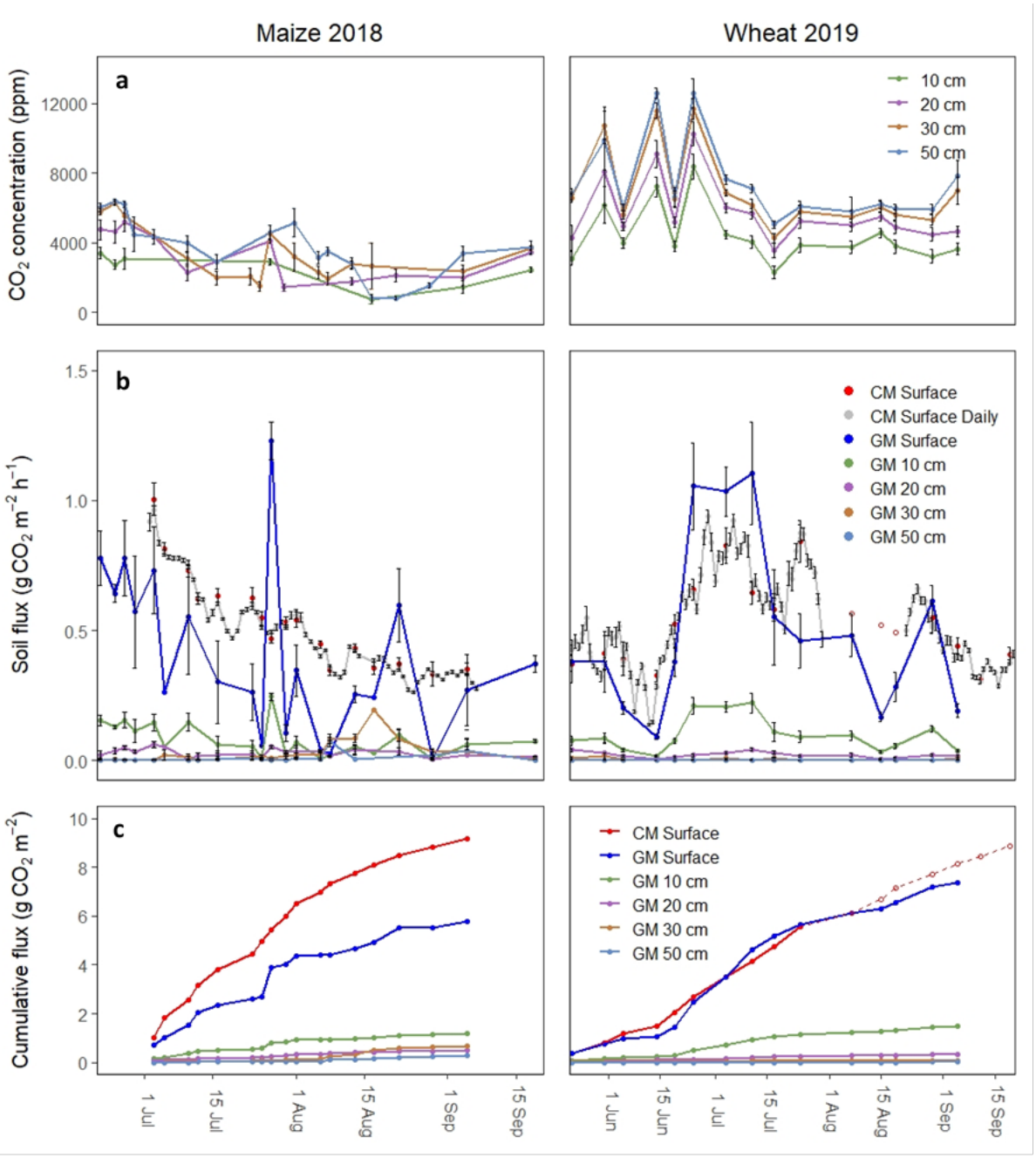

Fig. 5.3 The a) mean (± SEM) CO_2 concentrations from the gas collectors installed at different depths (n = 8); b) measured (CM) and modelled estimates (GM) of CO_2 fluxes (mean ± SEM) at different depths in the soil profile (n = 8); and c) cumulative CO_2 flux of the mean measured and estimated fluxes from different depths. 'CM Surface Daily' is the mean 24 h surface CO_2 flux, while 'CM Surface' is the mean surface flux between 1000 and 1300 h - the same sampling times and days as for the gas collector sampling. The 3 sampling times in 2019 (7th, 14th and 19th Aug) in b) had no surface CO_2 flux measurements, so these were estimated from 58 CO_2 flux sampling points before and after the missing dates via the best fit (exponential; R^2 = 0.76).

CH_4 concentration with soil depth was not significant under maize (p = 0.14), but CH_4 concentrations were 24-80% lower in the soil depths compared to ambient concentration in the wheat season (p < 0.001).

5.3.3 Measured and estimated CO_2 fluxes with soil depth

The concentration of CO_2 (Fig. 5.3a) in the gas collection pipes increased with greater soil depth (p < 0.001) and differed across growing season (p < 0.001) under both the maize and wheat.

The extrapolation of the GM estimates of the soil depth fluxes produced a good estimate of the soil surface flux in the wheat 2019 season (Fig. 5.3b and c), demonstrated by only 6% difference between the measured surface flux (0.52 ± 0.05 g CO_2 m^{-2}- h^{-1}) and the GM surface flux (p = 0.72). In the maize season, the mean measured surface flux (0.54 ± 0.08 g CO_2 m^{-2} h^{-1}) was 28% higher than the GM estimated surface flux (p = 0.004; Fig. 5.3b and c) in 2018. When comparing the modelled GM CO_2 fluxes with those that were measured, the maize linear fit only explained 10% of the variation in the data with a line slope below 1 (of the 1:1 line) of 0.62, while 46% of the variation in the data was explained by the 1.02 slope of the wheat season linear correlation (Fig. 5.4).

In the 2018 maize growing season (Fig. 5.3b), the overall mean estimated CO_2 flux was 6, 17, 17 and 54-fold lower in the 10, 20, 30 and 50 cm depths than measured at the soil surface (0.52 ± 0.07 g CO_2 m^{-2} h^{-1}), respectively. This corresponds to a contribution of 21, 9, 11 and 0.05% to the estimated cumulative surface flux (5.79 g CO_2 m^{-2}) from the 10, 20, 30 and 50 cm depths (Fig. 5.3c), respectively, suggesting that these depths contributed ca. 41% to the surface flux. The CO_2 fluxes in the 2019 wheat growing season were 4, 23, 105 and 1365-fold lower in the 10, 20, 30 and 50 cm depths than measured at the surface (0.54 ± 0.08 g CO_2 m^{-2} h^{-1}), respectively. The contribution to the estimated cumulative surface flux (7.37 g CO_2 m^{-2}) of the 10, 20, 30 and 50 cm depths was therefore lower with 20, 4, 1 and 0.08%, respectively, or a total of 26% (Fig. 5.3c).

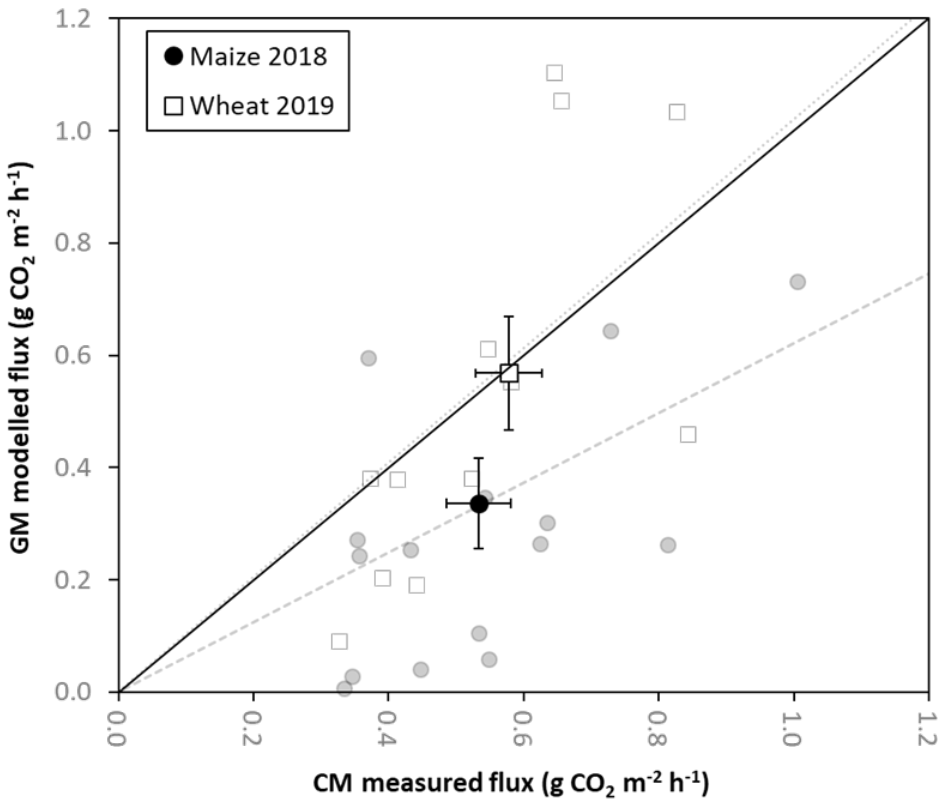

Fig. 5.4 The mean surface chamber measured (CM) versus concentration gradient modelled (GM) CO_2 flux (± SEM) in a field under maize (*n* = 12) or wheat (*n* = 16) production. The grey symbols points represent the raw data while the transparent dashed line is the linear correlation for maize (y = 0.62x, R^2 = 0.10) and the transparent dotted line is the corresponding correlation for wheat (y = 1.02x, R^2 = 0.46). The trend lines are forced through 0 at the y-intercept. The solid line is the 1:1 line (y = x).

5.3.3 Production and consumption of GHGs in laboratory mesocosms

In the vials where an ambient gas mix was added, the fluxes of all gases showed an increase in gas production from the soil during the 3-d incubation (Fig. 5.5). However, following the addition of the highly concentrated gas mix a decrease in all gas fluxes was observed, apart from CO_2 in the shallow depths. The mean fluxes of the ambient treatments were significantly greater than those of the highly concentrated headspace treatments in all gases ($p < 0.001$). The gas concentrations in the no-soil blanks remained stable over the 72 h period, confirming that there were no leaks.

Both soil depth and headspace gas concentration had a significant effect on the fluxes of the GHGs, but the added headspace concentration had the stronger effect (Fig. 5.5). The flux of CO_2 production in ambient concentrated CO_2 headspace was significantly higher at soil depth ≥20 cm ($p < 0.001$). Similarly, in the highly concentrated headspace, the production flux

was higher in the ≥ 10 cm soil depths ($p < 0.001$; Fig. 5.5), whereas the 30 and 50 cm depths were sinks of CO_2. As CH_4 was produced in the ambient headspace, the flux was greater than in the high concentration headspace ($p < 0.001$) but was not different with depth ($p = 0.4$). In contrast, in the highly concentrated headspace, the CH_4 flux was depth dependent ($p < 0.001$). The flux in the 10 and 20 cm depths was only 6% different, but 27-57% lower than the 30 and 50 cm fluxes, respectively. Finally, more N_2O was produced in the ambient headspace incubation ($p < 0.001$) than in the high concentration headspace, but the flux of N_2O was not different between depths in the ambient gas treatment ($p = 0.06$). In the high concentration headspace, 22-34% more N_2O was consumed at 10 and 20 cm compared to 30 and 50 cm depths ($p < 0.001$).

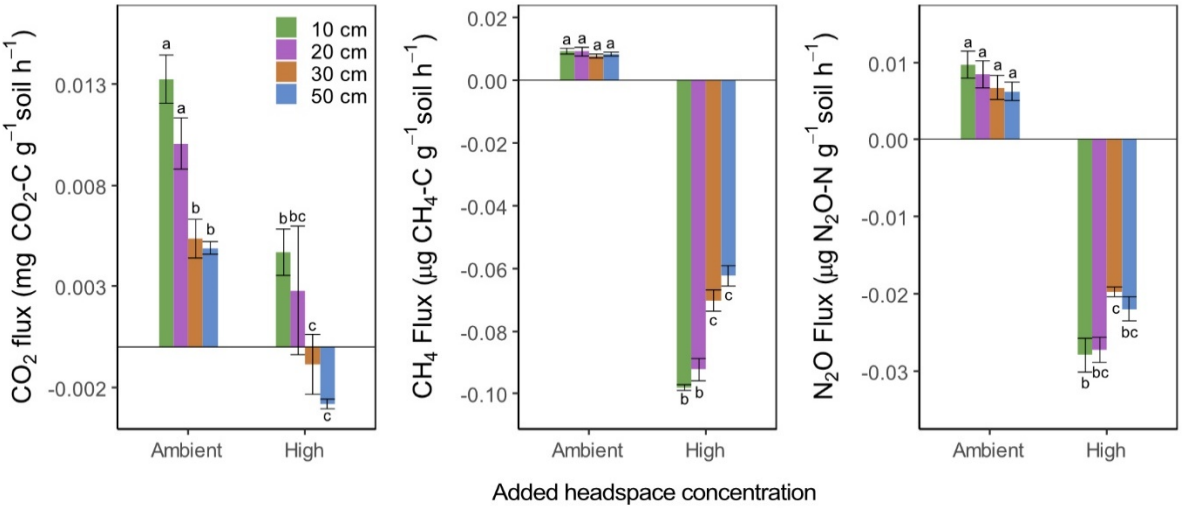

Fig 5.5 Net fluxes (means ± SEM) of CO_2, CH_4, and N_2O of destructively sampled ($n = 4$) soil of different depths incubated for 72 h with added headspace gas concentrations: Ambient (490 ppm CO_2; 2 ppm CH_4; 310 ppb of N_2O) and High (2800 ppm CO_2; 32 ppm CH_4; 5500 ppb N_2O). Different letters indicate significant differences between the gas concentrations of the soil depths and headspace concentrations for each GHG at p <0.05 (Tukey). Positive values indicate production and negative values indicate consumption.

5.4 Discussion

5.4.1 Soil CO_2 concentrations, fluxes and GM estimations

The convex-shaped depth profiles of CO_2 concentrations are consistent with other studies in tropical forest (Davidson et al., 2004) and semi-arid arable (Dong et al., 2013; Wang et al., 2018) systems. The CO_2 concentrations were significantly higher in all depths in the

wheat growing season compared to those under maize (Fig. 5.3a). While this is as hypothesised, it is unlikely due to crop-related root respiration as the rooting density was highest under maize (Table 5.1). Therefore, it is more likely explained by environmental factors driven by the differences in climatic conditions experienced in 2018 versus those in 2019. Compared to 2019, the 2018 growing season had 84% less precipitation and the soil water content was a third lower, resulting in a 170% increase in soil diffusivity (Fig. 5.1). As CO_2 retention in the soil profile is primarily influenced by the diffusivity of the soil (Risk et al., 2002), a reduction in the soils capacity to retain CO_2 means the accumulation of CO_2 in the soil is limited. In addition, the formation of large cracks and macropores in the field due to the drought will have created heterogeneity in soil diffusion and a more rapid escape of CO_2 from depth (Deurer et al., 2009). This is also supported by observations of Kochiieru et al. (2018) who demonstrated the importance of macropores in moderating soil surface CO_2 fluxes, albeit for topsoils. The drier conditions under maize may also have affected the seal of the gas collection pipes with the surrounding soil, resulting in dilution of the samples with less concentrated atmospheric air which diffuses into the soil (as the pipes are vertically installed; Appendix 4, Fig. S1). However, if this made a significant contribution, the CH_4 and N_2O concentrations may be expected to also be lower in the 2018 growing season which they were not, meaning either atmospheric dilution of the samples is unlikely to have been the main reason for the lower concentrations; or, if there was dilution, other factors prevented the concentrations to differ in the CH_4 and N_2O concentration profiles (i.e. higher production, lower diffusion).

While the CO_2 fluxes of the wheat growing season were estimated reliably by the CGM, as hypothesised, the maize growing season fluxes were underestimated (Fig. 5.4). This suggests that the CGM is unreliable in estimating fluxes under drought conditions experienced in 2018. However, differences in pore and soil structure driven by drought were unaccounted for in the measured Ds, which has strong influence over the CGM results. In situ measurement of the Ds alongside the gas profile measurements would give the best GM estimations (Maier and Schack-Kirchner, 2014) and may have prevented underestimation.

The large overestimations of the CGM fluxes, most notably on the 27th July 2018 (Fig. 5.4b), is likely due to an increase in CO_2 concentrations measured at shallower soil depths (i.e. 20 and 30 cm; Fig. 5.4a) causing the CGM to extrapolate the surface flux inaccurately. High

CO_2 concentrations close to the surface can occur following precipitation after a sustained period of warm dry weather causing a bidirectional concentration gradient (Pingintha et al., 2010). This pulse of CO_2 production is called the 'Birch' effect (Barnard et al., 2020) and considering the drought conditions and increase in precipitation from mid-July (Fig. 5.1), this could explain the flux overestimations. This scenario represents a potential weakness in the accuracy of the CGM that needs to be considered.

In this study, the 10, 20, 30 and 50 cm depths in the 2019 growing season were estimated to contribute 20, 4, 1 and 0.08% to the surface flux, respectively. As the 2018 estimated fluxes are underestimated (Fig. 5.4), their contributions to the surface flux are likely to be greater than the 21, 9, 11 and 0.05% estimated for the 10, 20, 30 and 50 cm depths, respectively. The decrease in CO_2 production with depth was consistent with the lower root distribution of wheat and maize down the soil profile (Table 5.1). The 2019 flux contributions correspond well with both Xiao et al. (2015) and Wang et al. (2018) who estimated the 0–5 cm layer to contribute 70-90% and only around 2% below a soil depth of 15 cm. The 2018 growing season had a greater contribution from the 20 and 30 cm depths, which could be due to fine root mortality at depth and subsequent decomposition (Davidson et al., 2004). The higher water content at depth throughout most of the 2018 growing season (Fig. 5.1) supports the idea that decomposition conditions were relatively enhanced deeper in the soil compared to soil near the surface.

The laboratory-based ambient headspace incubation demonstrated that CO_2 was produced across the 72 h incubation period and was significantly higher in the shallower soil depth (Fig. 5.5). The fluxes from this incubation fall within the range of mean CO_2 production estimated by the CGM in the field both years at the same depths (i.e. 0.38 – 82 CO_2 m^{-2} h^{-1}). The rate of CO_2 consumption differed with depth in the highly concentrated headspace incubation (Fig. 5.5). While a decrease in CO_2 production with depth is well established and supported by data from this study (Fig. 5.3 and 5.5), the biotic consumption of CO_2 remains relatively understudied. Microbial dark CO_2 fixation is a process reported to decrease with depth in temperate soil (Akinyede et al., 2020), increase with greater CO_2 concentration (Spohn et al., 2020) and be optimal close to 25 °C (Nel and Cramer, 2019). The rates we measured agree with the range measured (0.2 – 4.8 mg CO_2 m^{-2} h^{-1}) in a short (30 mins) incubation of agricultural surface soil by Shimmel (1987) and at the lower end of the range

(2.8 – 36.5 mg CO_2 m^{-2} h^{-1}) of longer (21 d) temperate field and forest topsoil incubations (Santruckova et al., 2005). The net fluxes measured in this incubation will be a balance between the production and fixation of CO_2. The net negative fluxes in the high CO_2 concentration headspace in the 30 and 50 cm depths (Fig. 5.5) suggests the fixation rate was greater than the production rate. While the higher than *in situ* temperatures in the incubation would have enhanced both rates (Nel and Cramer, 2019; Risk et al., 2002), the 'high' CO_2 concentration added as headspace (ca. 2800 ppm) is lower than the average CO_2 concentrations at all depths under normal growing conditions (2019; Fig. 5.2). Using higher CO_2 headspace concentrations would likely have increased the fixation rate but may have been cancelled out using lower in situ temperatures. In addition, as CH_4 oxidation produces CO_2, this could have accounted for a small percentage of the net CO_2 flux of the shallow soil in the high headspace gas concentration treatment. Without disentangling the origins and processes of the CO_2, measured, it is not possible to confirm whether dark CO_2 fixation is depth-dependent in this arable soil. We suggest measuring dark fixation via $^{14}CO_2$ as this method is much more sensitive and predominantly measures unidirectional influx over short labelling periods.

5.4.2 Soil N_2O concentrations and fluxes

N_2O concentrations increased with depth in a linear trend and the mean values were not different between the growing seasons (Fig. 5.3), which is not what we hypothesised. It is consistent with the N_2O concentration profiles across 2 maize growing seasons reported by Wang et al. (2018). However, considering the differences in soil temperature, water content and soil diffusivity between 2018 and 2019 in this study (Fig. 5.1), a difference in N_2O concentrations would be expected. While higher soil water content under wheat means greater retention, it also means slower diffusion and higher potential for N_2O reduction with the greater residence time in the soil (Clough et al., 2005; Neftel et al., 2007). In addition, C released from roots is expected to stimulate microbial respiration causing localised O_2 depletion , which can drive N_2O consumption. While wheat root density and length were 60 and 40% lower than in the maize at 0-50 cm (Table 5.1), respectively, wheat roots release a greater amount of exudates per gram of dry root weight (Vančura et al., 1977). Finally, NO_3^- concentrations were greater in the 2018 year (Appendix 4, Fig. S2) which leads to higher N_2O

concentrations in the profile (Dong et al., 2013). Therefore, we conclude that the N_2O concentrations in the wheat growing seasons are not greater than those in the maize due to lower production resulting from low NO_3^- concentrations and possibly also due to higher rates of N_2O consumption.

Despite the rates of N_2O production not statistically differing with soil depth in the mesocosm incubation (Fig. 5.5), the trend in means clearly show a decrease in production with depth. The data does demonstrate significantly greater N_2O consumption in shallower soil (10 and 20 cm; Fig. 5.5) as hypothesised. Despite the evidence of depth-dependent N_2O consumption, we concede that using only 2 g of soil from one point in time and incubated at higher temperatures at ambient O_2 concentration is unlikely to capture the full extent of consumption and production fluxes observed in situ. Especially as N_2O production, consumption and movement may be more complex than that of CO_2 and CH_4, partly due to N_2O fluxes having greater spatial and temporal variability in soil (Mosier et al., 1998; Wang et al., 2018).

5.4.3 Soil CH_4 concentrations and fluxes

Despite no expected difference between the overall CH4¬ concentrations with crop, they did decrease with depth (Fig. 5.2) which is consistent with other studies (Dong et al., 2013; Wang et al., 2018). As anaerobic conditions are required for methanogenesis, production of CH_4 is likely to be very low within the soil profile and while anaerobic (micro)sites may occur and produce CH_4 in the soil profile, this can be almost completely oxidised in aerated soil zones (Le Mer and Roger, 2001). The ambient atmospheric concentration of CH_4 is consistently higher than in the profile, suggesting that oxidation of CH_4 by methanotrophs occurs throughout the soil profile (Dong et al., 2013; Wang et al., 2018). This is supported by the results shown in figure 5.5, where CH_4 is oxidised at all soil depths included. Therefore, the lack of a difference between the maize and wheat CH_4 concentrations was more likely due to the similar soil microbial community rather than differences in crop root structure.

As expected, consumption of CH_4 was depth-dependent with greater consumption occurring in shallower soil. This agrees with the results of Wang et al. (2018), who found CH_4 consumption to decrease with soil depth. As temperature is not a major controlling factor in

CH_4 oxidation in the non-extreme environment in this study (Le Mer and Roger, 2001), the rates measured at a higher temperatures in the incubation are likely reasonably representative of those in situ.

5.5 Conclusion

Here we provide GHG concentration profiles and further proof of concept of the CGM in a lowland arable context with low resolution (weekly) data over an extended period (2 y). A good GM extrapolation of the surface CO_2 flux from soil gas collectors under normal growing conditions was achieved despite low temporal resolution. Drought conditions caused significant CGM underestimation of the surface flux, due to the greater soil diffusivity associated with lower soil moisture unaccounted for by the D_s. This likely also caused the CO_2 concentration depth profile to be different between growing seasons. The N_2O concentration profile was only marginally affected by soil inorganic N concentration. Finally, we provide evidence of depth-dependent CH_4 oxidation, N_2O consumption and possibly CO_2 fixation. The results of this study improve our understanding of the opportunities and limitations of the CGM and of GHG dynamics in the soil profile of a temperate arable system.

5.6 Acknowledgements

This work was supported by the FLEXIS (Flexible Integrated Energy Systems) programme, an operation led by Cardiff University, Swansea University and the University of South Wales and funded through the Welsh European Funding Office (WEFO). This work was also supported by the UK-China Virtual Joint Centre for Agricultural Nitrogen (CINAg, BB/N013468/1), which is jointly supported by the Newton Fund, via UK BBSRC and NERC, and the Chinese Ministry of Science and Technology. The authors would also like to thank the lab and farm technicians for their valuable help and advice.

5.7 References

Akinyede, R., Taubert, M., Schrumpf, M., Trumbore, S., Küsel, K., 2020. Rates of dark CO_2 fixation are driven by microbial biomass in a temperate forest soil. Soil Biology and Biochemistry 150, 107950.

Barnard, R.L., Blazewicz, S.J., Firestone, M.K., 2020. Rewetting of soil: Revisiting the origin of soil CO_2 emissions. Soil Biology and Biochemistry 147, 107819.

Bartelt-Ryser, J., Joshi, J., Schmid, B., Brandl, H., Balser, T., 2005. Soil feedbacks of plant diversity on soil microbial communities and subsequent plant growth. Perspectives in Plant Ecology, Evolution and Systematics 7, 27–49.

Boon, A., Robinson, J.S., Chadwick, D.R., Cardenas, L.M., 2014. Effect of cattle urine addition on the surface emissions and subsurface concentrations of greenhouse gases in a UK peat grassland. Agriculture, Ecosystems and Environment 186, 23–32.

Cárdenas, L.M., Hawkins, J.M.B., Chadwick, D., Scholefield, D., 2003. Biogenic gas emissions from soils measured using a new automated laboratory incubation system. Soil Biology and Biochemistry 35, 867–870.

Chapuis-Lardy, L., Wrage, N., Metay, A., Chotte, J.L., Bernoux, M., 2007. Soils, a sink for N_2O? A review. Global Change Biology 13, 1–17.

Clark, M., Jarvis, S., Maltby, E., 2001. An improved technique for measuring concentration of soil gases at depth in situ. Communications in Soil Science and Plant Analysis 32, 369–377.

Clough, T.J., Sherlock, R.R., Rolston, D.E., 2005. A review of the movement and fate of N_2O in the subsoil. Nutrient Cycling in Agroecosystems 72, 3–11.

Comeau, L.P., Lai, D.Y.F., Cui, J.J., Hartill, J., 2018. Soil heterotrophic respiration assessment using minimally disturbed soil microcosm cores. MethodsX 5, 834–840.

Currie, J.A., 1960. Gaseous diffusion in porous media Part 1. - A non-steady state method. British Journal of Applied Physics 11, 314–317.

Davidson, E.A., Ishida, F.Y., Nepstad, D.C., 2004. Effects of an experimental drought on soil emissions of carbon dioxide, methane, nitrous oxide, and nitric oxide in a moist tropical forest. Global Change Biology 10, 718–730.

De-Polli, H., Costantini, A., Romanik, R., Pimentel, M.S., 2007. Chloroform fumigation-extraction labile C pool (microbial biomass C “plus”) shows high correlation to microbial biomass C in Argentinian and Brazilian soils. Ciencia del Suelo 25, 15–22.

de Sosa, L.L., Glanville, H.C., Marshall, M.R., Williams, A.P., Abadie, M., Clark, I.M., Blaud, A., Jones, D.L., 2018. Spatial zoning of microbial functions and plant-soil nitrogen dynamics across a riparian area in an extensively grazed livestock system. Soil Biology and Biochemistry 120, 153–164.

Deurer, M., Grinev, D., Young, I., Clothier, B.E., Müller, K., 2009. The impact of soil carbon management on soil macropore structure: A comparison of two apple orchard systems in New Zealand. European Journal of Soil Science 60, 945–955.

Dong, W., Wang, Y., Hu, C., 2013. Concentration profiles of CH_4, CO_2 and N_2O in soils of a wheat–maize rotation ecosystem in North China Plain, measured weekly over a whole year. Agriculture, Ecosystems and Environment 1, 260–272.

Dossa, G.G.O., Paudel, E., Wang, H., Cao, K., Schaefer, D., Harrison, R.D., 2015. Correct calculation of CO_2 efflux using a closed-chamber linked to a non-dispersive infrared gas analyzer. Methods in Ecology and Evolution 6, 1435–1442.

Fiedler, S.R., Buczko, U., Jurasinski, G., Glatzel, S., 2015. Soil respiration after tillage under different fertiliser treatments - implications for modelling and balancing. Soil Tillage Research, 150, 30–42.

Johnston, A.E., Poulton, P.R., Coleman, K., 2009. Soil Organic Matter. Its Importance in Sustainable Agriculture and Carbon Dioxide Fluxes. Advances in Agronomy, 101, 1–57.

Jong, E. De, Schappert, H.J., 1972. Calculation of soil respiration and activity from CO_2 profiles in the soil. Soil Science, 113, 328–333.

Kochiieru, M., Lamorski, K., Feiza, V., Feizienė, D., Volungevičius, J., 2018. The effect of soil macroporosity, temperature and water content on CO_2 efflux in the soils of different genesis and land management. Zemdirbyste 105, 291–298.

Kusa, K., Sawamoto, T., Hu, R., Hatano, R., 2008. Comparison of the closed-chamber and gas concentration gradient methods for measurement of CO_2 and N_2O fluxes in two upland field soils. Soil Science and Plant Nutrition, 54, 777–785.

Le Mer, J., Roger, P., 2001. Production, oxidation, emission and consumption of methane by soils: A review. European Journal of Soil Biology, 37, 25–50.

Li, Z., Kelliher, F.M., 2005. Determining nitrous oxide emissions from subsurface measurements in grazed pasture: A field trial of alternative technology. Australian Journal of Soil Research, 43, 677–687.

Maier, M., Schack-Kirchner, H., 2014. Using the gradient method to determine soil gas flux: A review. Agricultural and Forest Meteorology, 192–193, 78–95.

Miranda, K.M., Espey, M.G., Wink, D.A., 2001. A rapid, simple spectrophotometric method for simultaneous detection of nitrate and nitrite. Nitric Oxide – Biology and Chemistry 5, 62–71.

Mosier, A., Kroeze, C., Nevison, C., Oenema, O., Seitzinger, S., van Cleemput, O., 1998. Closing the global N_2O budget: nitrous oxide emissions through the agricultural nitrogen cycle. Nutrient Cycling in Agroecosystems 52, 225–248.

Mulvaney, R.L.-M. of soil analysis, 1996. Nitrogen—inorganic forms. Methods of soil analysis: Part 3 Chemical methods, 5, 1123-1184.

Neftel, A., Flechard, C., Ammann, C., Conen, F., Emmenegger, L., Zeyer, K., 2007. Experimental assessment of N_2O background fluxes in grassland systems. Tellus B: Chemical and Physical Meteorology 59, 470–482.

Nel, J.A., Cramer, M.D., 2019. Soil microbial anaplerotic CO_2 fixation in temperate soils. Geoderma 335, 170–178.

Pingintha, N., Leclerc, M.Y., Beasley, J.P., Zhang, G., Senthong, C., 2010. Assessment of the soil CO_2 gradient method for soil CO_2 efflux measurements: Comparison of six models in the calculation of the relative gas diffusion coefficient. Tellus B: Chemical and Physical Meteorology 62, 47–58.

Risk, D., Kellman, L., Beltrami, H., 2002. Carbon dioxide in soil profiles: Production and temperature dependence. Geophysical Research Letters 29, 1–4.

Rudolph, J., Rothfuss, F., Conrad, R., 1996. Flux between soil and atmosphere, vertical concentration profiles in soil, and turnover of nitric oxide: 1. Measurements on a model soil core. Journal of Atmospheric Chemistry 23, 253–273.

Santruckova, H., Bird, M.I., Elhottová, D., Novák, J., Picek, T., Šimek, M., Tykva, R., 2005. Heterotrophic fixation of CO_2 in soil. Microbial Ecology 49, 218–225.

Shimmel, S.M., 1987. Dark fixation of carbon dioxide in an agricultural soil. Soil Science 144, 20–23.

Spohn, M., Müller, K., Höschen, C., Mueller, C.W., Marhan, S., 2020. Dark microbial CO_2 fixation in temperate forest soils increases with CO_2 concentration. Global Change Biology 26, 1926–1935.

Staff, S.S., 2014. Keys to Soil Taxonomy, 12th ed, USDA. Resources Conservation Services, Washington, DC.

Sumner, M.E., Miller, W.P., 1996. Cation Exchange Capacity and Exchange Coefficients, Methods of soil analysis: Part 3 Chemical methods, 5, 1201-1229.

Tagesson, T., 2006. Calibration and analysis of soil carbon efflux estimates with closed chambers at Forsmark and Laxemar.

Turner, S., Barker, L.J., Hannaford, J., Muchan, K., Parry, S., Sefton, C., 2021. The 2018/2019 drought in the UK: a hydrological appraisal. Weather 76, 248–253.

Vance, E.D., Brookes, P.C., Jenkinson, D.S., 1987. An Extraction Method for Measuring Soil Microbial Biomass. Soil Biology and Biochemistry 19, 703–707.

Vančura, V., Přikryl, Z., Kalachová, L., Wurst, M., 1977. Some Quantitative Aspects of Root Exudation. Soil Organisms as Components of Ecosystems 25, 381–386.

Wang, Y., Li, X., Dong, W., Wu, D., Hu, C., Zhang, Y., Luo, Y., 2018. Depth-dependent greenhouse gas production and consumption in an upland cropping system in northern China. Geoderma 319, 100–112.

Xiao, X., Kuang, X., Sauer, T.J., Heitman, J.L., Horton, R., 2015. Bare Soil Carbon Dioxide Fluxes with Time and Depth Determined by High-Resolution Gradient-Based Measurements and Surface Chambers. Soil Science Society of America Journal 79, 1073.

Chapter 6

Separating production and consumption of N_2O in intact agricultural soil cores at different depths and moisture contents using the ^{15}N-N_2O pool dilution method

Authors

Erik S. Button, Karina A. Marsden, Phil D. Nightingale, Elizabeth R. Dixon, David R. Chadwick, David L. Jones, Laura M. Cárdenas

Publication status

This manuscript is under review in the *European Journal of Soil Science*.

Citation

Button, E.S., Marsden, K.A., Nightingale, P.D., Dixon, E.R., Chadwick, D.R., Jones, D.L., Cárdenas, L.M., 2022. Separating production and consumption of N_2O in intact agricultural soil cores at different depths and moisture contents using the ^{15}N-N_2O pool dilution method. Under review in the *European Journal of Soil Science*.

Author contributions

ESB, LMC, DRC and DLJ conceived the experiment. ESB conducted the experiments and wrote the manuscript, with technical support from PDN and ERD. KAM supported with the pool dilution calculations. DRC, LMC, KAM and DLJ reviewed the manuscript.

Abstract

Agricultural soils are a major source of the potent greenhouse gas and ozone depleting substance, N_2O. To implement management practices that minimise microbial N_2O production and maximise its consumption (i.e. complete denitrification) we must understand the interplay between simultaneously occurring biological and physical processes, especially how this changes with soil depth. Meaningfully disentangling these processes is challenging and typical N_2O flux measurement techniques provide little insight into subsurface mechanisms. Additionally, denitrification studies are often conducted on sieved soil in altered O_2 environments which relate poorly to *in situ* field conditions. Here, we use a novel dual headspace system with field-relevant O_2 concentrations to incubate intact sandy clay loam textured agricultural topsoil (0-10 cm) and subsoil (50-60 cm) cores for 3-4 d at 50 and 70% water filled pore space (WFPS), respectively. ^{15}N-N_2O pool dilution and an SF_6 tracer were used to determine the relative diffusivity (D_s/D_0) and the net N_2O emission and gross N_2O emission and consumption rates. The relationship between calculated fluxes from the below- and above- soil core headspaces confirmed that the system performed well. We found no difference in D_s/D_0 between soil depth fractions, which was probably because of the preservation of preferential flow pathways in intact cores. Both gross N_2O emissions and uptake were not different with depth but were higher in the 50% WFPS, contrary to expectation. We attribute this to aerobic denitrification and simultaneously occurring denitrification and nitrification for the gross consumption and emission of N_2O, respectively. Here, we developed a novel system that allows careful control of conditions and, with a headspace below and above a soil core, a more realistic reconstruction of *in situ* gas dynamics. We provide further evidence of substantial N_2O consumption in drier soil and without net negative N_2O emissions. The results from this study are important for the future application of the ^{15}N-N_2O pool dilution method and N budgeting and modelling, as required for improving management to minimise N_2O losses.

Keywords: diffusion coefficient; denitrification; sulphur hexafluoride; isotope pool dilution; nitrogen cycling.

6.1 Introduction

Nitrous oxide (N_2O) exchange between the soil and atmosphere has received significant attention in recent decades due to its prominent role in climate change and atmospheric ozone depletion (e.g. Jia et al., 2019). More than half of global agricultural emissions are from N_2O, resulting from N inputs to soil, including fertiliser and manure application (direct) and leaching and atmospheric deposition of nitrogen (N; indirect) (Clough et al., 2005; Jia et al., 2019). The production of atmospheric N_2O is primarily governed by microbial denitrification in the soil, where N_2O is produced from nitrate (NO_3^-) under partially anaerobic conditions (Diba et al., 2011). Nitrification, although considered less important than denitrification in generating N_2O in most agricultural soils , can be the dominant N_2O producing process (e.g. North China Plain; Zhang et al., 2016) and can produce N_2O in tandem with denitrification (Bateman and Baggs, 2005). However, denitrifiers are also able to consume N_2O to produce inert dinitrogen (N_2) gas (Diba et al., 2011), which constitutes 78% of the Earth's atmosphere. This process is often masked by greater production rates and is mostly only measured when the consumption rate exceeds the production rate (i.e. net negative emissions; Chapuis-lardy et al., 2007; Schlesinger, 2013). Measuring the consumption of N_2O directly (e.g. by N2 flux) is challenging against a very high atmospheric background (Clough et al., 2006; Wen et al., 2016; Yang et al., 2011). Yet, accurately measuring N_2O consumption is important for modelling and prediction of future N budgets and N_2O emissions from soils, which are poorly constrained by inaccuracies (Almaraz et al., 2020; Blagodatsky and Smith, 2012; Boyer et al., 2006).

The balance between gross production and consumption of N_2O in agricultural soil is influenced by a range of environmental factors (temperature, moisture, O_2 content; Chapuis-lardy et al., 2007), soil characteristics (pH, mineral N content, porosity, organic matter content, soil depth; Clough et al., 2005; Stuchiner and von Fischer, 2022; Chapuis-lardy et al., 2007) and management practices (fertilizing regime, tillage, irrigation; Khalil et al., 2002; Wang et al., 2018). This complexity has meant that N_2O consumption does not always occur as expected and so making a clear definition of a set of N_2O promoting conditions is not possible (Chapuis-lardy et al., 2007). For example, N_2O consumption is generally thought to be stimulated by high moisture and low mineral N content (Chapuis-lardy et al., 2007), but it has also been found to coincide with low water-filled pore space (WFPS) in fertilized (<50%

WFPS; Khalil et al., 2002) and unfertilised soil (5-20% WFPS; Wu et al., 2013). In addition, both lower (Donoso et al., 1993) and higher (Yamulki et al., 1995) temperatures have been observed to enhance N_2O consumption. Despite these uncertainties and exceptions, there are also well-known facts. N_2O consumption relies on anaerobic conditions, which occur more extensively in waterlogged soils, hence why peat- and wetlands represent the greatest N_2O sinks globally (Schlesinger, 2013). Anaerobic conditions can also exist in microsites heterogeneously distributed throughout the soil profile of free-draining soils, within soil aggregates (even in dry aerobic soil; Sexstone et al., 1985) or can be caused by localised respiration hot spots that deplete O_2 (Clough et al., 1999; Hill and Cardaci, 2004; Van Cleemput, 1998). Therefore, N2O produced in the soil is not necessarily consumed in the same location but may diffuse to another site in the soil, may be lost to the atmosphere or groundwater (Shcherbak and Robertson, 2019), or become entrapped in the soil (Clough et al., 1999). In addition, aerobic consumption of N_2O is possible, where N_2O is used as an electron acceptor when nitrate (NO_3^-) is limited (Chapuis-Lardy et al., 2007; Wang et al., 2018). To understand these processes in a meaningful way, the physical diffusion and the gross N_2O production and consumption rates need to be separated from each other.

N_2O processes occurring deeper in the soil have received less attention but are important in understanding the balance between N_2O production and consumption (Almaraz et al., 2020; Clough et al., 2005; Jahangir et al., 2012). The movement of N_2O to the soil surface is predominantly via passive diffusion through air-filled pores in the soil. The concentration of N2O at depth is frequently higher than near the soil surface due to lower diffusivity (Balaine et al., 2013; Currie, 1984; Fujikawa and Miyazaki, 2005) causing a build-up of N2O concentration with depth (Davidson et al., 2004; Dong et al., 2013; Laughlin and Stevens, 2002; van Bochove et al., 1998; Van Groenigen et al., 2005; Wang et al., 2018; Zona et al., 2013). This lag between production and surface emission is supported by a ^{15}N-labelled experiment by Clough et al. (1999), where it took 11 d for N_2O produced at 80 cm to first reach the soil surface and 6% remained in the soil even after 38 d (i.e. entrapment). Soil conditions restricting N_2O diffusion, thereby increasing its residence time in the soil, can increase its consumption (Chapuis-lardy et al., 2007; Clough et al., 2005; Neftel et al., 2007). The generally higher rate of N_2O consumption and production in the topsoil is a reflection of the greater microbial abundance and activity (Van Beek et al., 2004; van Bochove et al., 1998;

Wang et al., 2018) compared to subsoils, but considerable N_2O production and consumption can also occur in the subsoil if conditions allow (Clough et al., 1999; Shcherbak and Robertson, 2019). In addition, understanding of the relation between diffusion and N_2O emissions is lacking (Balaine et al., 2013), especially in intact deep soil (Chamindu Deepagoda et al., 2019). Therefore, understanding the balance of N_2O production and consumption between topsoil and subsoil depths at different soil conditions and their relation to diffusion is needed to best predict N2O surface emissions for modelling the global N budget (Almaraz et al., 2020; Blagodatsky and Smith, 2012; Boyer et al., 2006).

In addition to underpin more accurate modelling and N budgeting, understanding N_2O mechanisms in the soil is important to support emerging attempts to minimise N_2O losses from soil, where the ideal scenario is to be able to implement management practices that limit production and potentially enhance N_2O consumption. Chamindu Deepagoda et al. (2019) found a range of relative gas diffusivity rates which lowered N_2O emissions that could be monitored and maintained by land users. Stuchiner and von Fischer (2022) recently demonstrated a case of increased N_2O consumption and decreased N_2O emissions (coined ICDE) via promotion of anoxia from relieving the C-limitation to the microbial community.

To address these areas of uncertainty and support future work, we asked: does the balance between soil N_2O production and consumption differ between soil depths and moisture contents in intact agricultural soil cores? To answer this, we used a novel dual headspace system with field relevant O_2 concentrations to incubate intact sandy clay loam agricultural top- and subsoil cores. Following the ^{15}N-N_2O pool dilution (Wen et al., 2016; Yang et al., 2011) and Currie method (Currie, 1960) with SF_6 as a conservative tracer, the relative diffusivity (D_s/D_0) and the net N_2O emission and gross N_2O emission and uptake rates were measured. We hypothesised that, i) the rate of diffusion would decrease with soil depth and wetness due to greater soil density and lower porosity; ii) despite higher N_2O and lower O_2 concentrations deeper in the soil, consumption of N_2O will be greater in the more microbially-active topsoil; iii) A WFPS above the critical level (ca. ≥60%; Bateman and Baggs, 2005) will increase N_2O consumption, whereas at a lower WFPS, N_2O consumption will be minimal.

6.2 Materials and methods

6.2.1 Soil collection and characterisation

Sandy clay loam textured freely draining arable soil was collected from Abergwyngregyn, North Wales (53°14'29"N, 4°01'15"W) in February 2020. The soil is classified as a Eutric Cambisol (WRB) or Typic Hapludalf (US Soil Taxonomy) and has a crumb structure due to high levels of earthworm bioturbation. Prior to collection, the field had been used for winter wheat (*Triticum aestivum*) production. Soil was collected from 6 randomly selected locations within the field from the topsoil (0 - 10 cm) and subsoil (50 – 60 cm), which were retained as 6 independent replicates. The latter soil depth was from below the plough layer and the field had no history of subsoiling. Two disturbed soil samples and 3 intact soil cores (using stainless steel rings of 53 mm outside diameter x 50 mm height, 104 cm^3 volume; steel from Complete Stainless Ltd., Glasgow, UK) were collected from each hole at each depth, not including spare cores used for soil characterisation. The soil cores were placed in plastic bags (but not sealed) in the field and stored at <5°C prior to use.

One of the set of 3 soil cores per depth and hole were removed from their metal core rings, weighed and oven-dried (105°C, 24 h) immediately after collection. Dry bulk density was determined by dividing the dry weight by the soil volume. Water-filled pore space (WFPS) was determined using the volumetric water content, particle density (assumed at 2.65 g cm^{-3}) and dry bulk density. In addition, 5 g replicates of soil were extracted using 0.5 M K_2SO_4 at a ratio of 1:5 (w/v) on the same day the soil was collected. These were shaken at 200 rpm for 30 mins and then centrifuged (14,000 g, 10 min). The supernatant was then removed and frozen for later ammonium (NH_4^+) and nitrate (NO_3^-) content determination by colourimetry, according to Mulvaney (1996) and Miranda et al. (2001), respectively, with a PowerWave XS Microplate Spectrophotometer (BioTek Instruments Inc., Winooski, VT). Dissolved organic C and N in the extracts was determined using a Multi N/C 2100/2100 analyser (AnalytikJena AG, Jena, Germany). Dissolved organic N was determined by subtracting inorganic N (NO_3^- and NH_4^+) from the total N. Soil EC and pH in water were determined in a 1:5 ratio (w/v) using a Jenway 4520 conductivity meter and a Hanna 209 pH meter (Hanna Instruments Ltd., Leighton Buzzard, UK), respectively. A summary of the initial soil properties is presented in Table 6.1.

Table 6.1. Properties of the Eutric Cambisol topsoil (0-10 cm) and subsoil (50-60 cm) used for the study. Values represent means ± SEM (n = 4) and weight values are expressed as dry soil weight equivalents.

Properties	Topsoil	Subsoil
	0 – 10 cm	50 – 60 cm
Sand (%)†	62.9 ± 0.7	67.2 ± 6.5
Silt (%)†	16.2 ± 1.3	14.9 ± 3.1
Clay (%)†	20.9 ± 1.0	17.9 ± 4.1
Dry bulk density (g cm^{-3})	1.11 ± 0.06	1.26 ± 0.04
Porosity (%)	55.7 ± 0.8	53.0 ± 3.5
Organic C (g C kg^{-1})	27.8 ± 1.3	7.4 ± 1.0
Total N (g N kg^{-1})	3.4 ± 0.1	1.5 ± 0.1
C:N ratio	8.1 ± 0.1	4.8 ± 0.3
pH_{H2O}	6.8 ± 0.06	6.8 ± 0.03
EC (µS cm^{-1})	1198 ± 126	657 ± 102
Extractable NH_4^+ (mg N l^{-1})	0.08 ± 0.02	0.09 ± 0.03
Extractable NO_3^- (mg N l^{-1})	41.1 ± 6.0	22.4 ± 5.2
Dissolved organic C (mg C l^{-1})	12.6 ± 1.3	4.3 ± 1.8
Dissolved organic N (mg N l^{-1})	4.9 ± 2.1	0.6 ± 0.4
Soil microbial biomass (mg C kg^{-1})	74.0 ± 3.7	42.9 ± 1.4

†data from Sanchez-Rodriguez et al., (in prep), *n* = 4.

6.2.2 Experimental system

A specialised gas-flow-soil-core incubation system (DENitrification Incubation System (DENIS); Cárdenas et al., 2003), allowing controlled environmental condition control (including O_2 concentration and temperature), was adapted for this study using custom made lids used by Boon et al. (2013). The system, with 12 large individual stainless-steel chambers (2120 ml), was modified to hold 53 mm wide soil cores with a lid and septum for direct gas application and sampling from a small headspace (77.2 ml) with a 3 m (4.8 mm ID, 53.4 ml) sampling tube (Fig. 6.1). Details of the DENIS modification and a photograph are provided in the Appendix 5 (S1, Fig. S1).

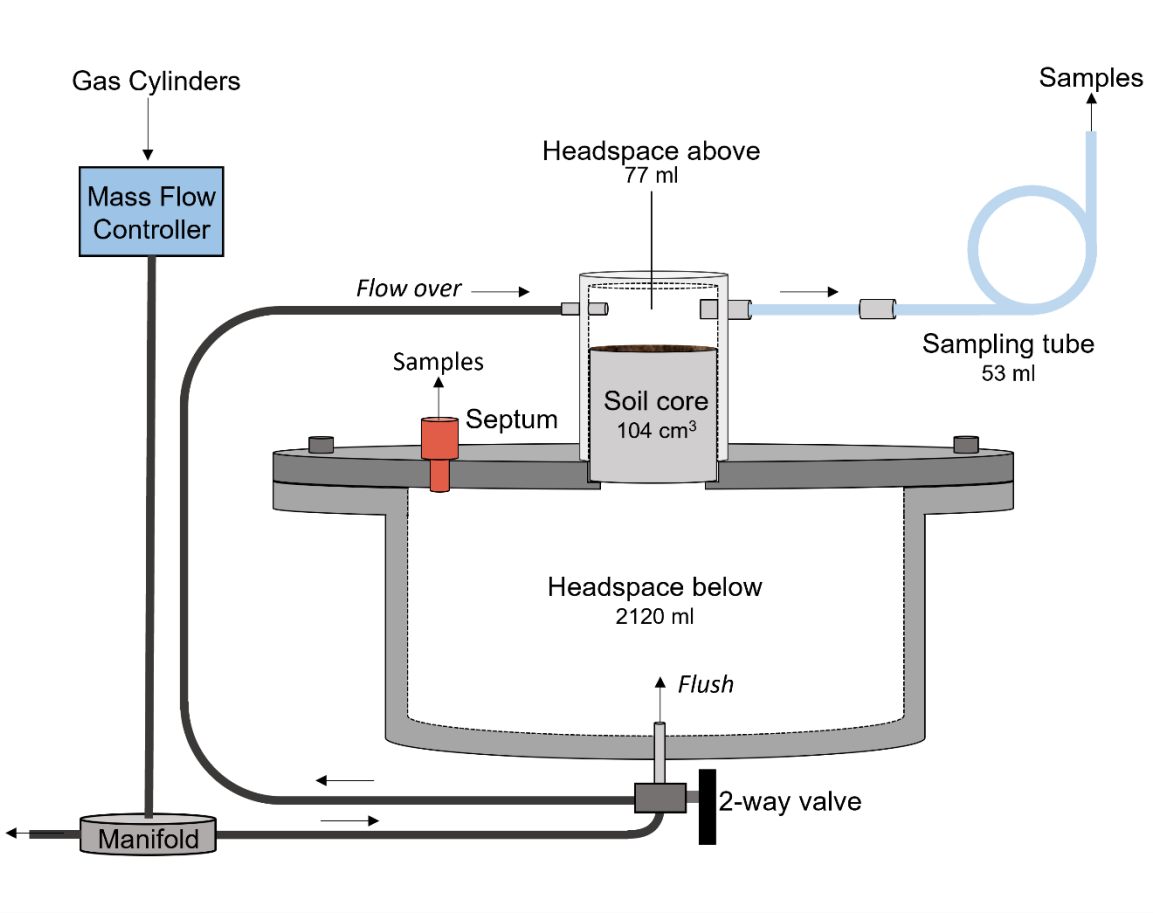

Fig. 6.1 The dual-headspace system used for incubating the soil cores in this study. The system can be placed in 2 different modes, 'flush' and 'flow over'. The former is where air flow from the gas cylinders is directed to enter via the headspace below the core, while the latter directs this air via the headspace above the soil core. Specific dimensions and materials can be found in the Appendix 5 (S1).

Gas flow from O_2 and N_2 cylinders into the system could be adjusted via mass flow controllers (MFC) to achieve the desired flow rate and O_2 concentration, and then split via a manifold evenly to each of the 12 incubation vessels. A valve (Fig. 6.1) enabled flow to be either directed to enter the large headspace below the intact soil cores ('flush mode') or to enter the small headspace on top of the intact soil cores ('flow over mode'). In both modes the gas exited via the sampling tube. The MFC was calibrated for all gases used in the experiment by measuring the flow 5 times at 10 flow rate settings with a bubble meter.

In this study, 2 gas cylinders were used: an ECD-Grade N_2 cylinder and a grade zero O_2 cylinder (BOC; Linde plc, Guildford, UK). The N_2 cylinder and a compressed air line that was used for the 'flow over mode' both had SF_6 concentrations below atmospheric levels (i.e. <10 ppt). During pilot studies, we discovered that the SF_6 concentration in the O_2 cylinder was

surprisingly high (ca. 6 ppb), which is about three orders of magnitude greater than the concentration of atmospheric SF_6 (10.6 ppt). We, therefore, decided to use this as our source of SF_6 for the incubations.

^{15}N labelled N_2O was generated specifically for this experiment using the ammonium sulphate method described by Laughlin et al. (1997). This generates N_2O and N_2 at the same ^{15}N enrichment as the ammonium sulphate. The generated N_2O and N_2 were collected in evacuated exetainers (Labco Ltd., Lampeter, UK). N_2 was removed using the cryotrapping loops in a Sercon trace gas analyser (TG2, Sercon Ltd., Crewe, UK) so that the N_2O was trapped while the N_2 was flushed to waste. Once the N_2 had been removed, N_2O was collected in a Tedlar® gas sample bag from the outlet of the TG2. The contents of the Tedlar® bag were analysed for N_2O and N_2 concentration and enrichment using a Sercon trace gas analyser and Sercon 20:22 isotope ratio mass spectrometer (Sercon Ltd., Crewe, UK).

6.2.3 Soil core preparation and installation

Soil cores from both depths were brought to either 50 or 70% WFPS for the incubation experiment. These WFPS were chosen as they are either side of the 60% WFPS threshold for N_2O production and N_2O produced is likely to be underpinned by different processes (Bateman and Baggs, 2005). Soil cores were brough to the desired weight for attaining a WFPS of 50 or 70% (n = 6 each) by adding distilled water (70% WFPS) or air-drying the field moist soil (50% WFPS). Cores that had not lost enough weight after air-drying overnight to meet the required WFPS were further dried in an incubator at 40°C (see Appendix 5, S3, for more information). Once all the cores had attained the target WFPS, they were randomly installed in the system (Fig. 6.1). The inside edges of the top of the soil cores (ca. 2-4 mm) were carefully sealed with silicone grease to ensure no edge related diffusion effects. This was also done on the bottom of the soil cores, where drying had caused cores to slightly (<1 mm) shrink away from the metal core ring. A circular nylon mesh was placed in the lid groove before installing the cores to prevent soil from falling into the large headspace. The inside walls of the small headspace chambers and where they met the large headspace lids were also greased with silicone to ensure an airtight fit. This was confirmed by measuring gas flow through all 12 cores using a bubble flow meter.

6.2.4 Soil core incubations

Soil cores were incubated in the dark and the temperature in the laboratory was kept constant at 22°C for the 4-5 day incubation (depending on soil depth). As an acclimatisation period, the soil cores were put into 'flush mode' at a flow rate of 5 ml min^{-1} $core^{-1}$ for ca. 18 h with an SF_6-containing (see 2.2) O_2:N_2 mixture. This mix was 20.9:100 and 13:100 O_2:N_2 for the 0-10 and 50-60 cm cores, respectively. The O_2 content of the mix was chosen by a fitted trend of a similar soil profile (Fig. S3). The acclimatisation period was to allow air-filled pore space to attain the air mix representative of the soil core depths and for the accumulation of a reservoir of SF_6 tracer gas in the headspace below the soil core.

After the 'flush mode', the gas flow was momentarily stopped and the (high SF_6) O_2 cylinder was exchanged for a (ambient-SF6) compressed air cylinder and the flow adjusted to maintain the same O_2:N_2 ratio. The flow was changed to 'flow over mode' by switching the valve below the large headspace to divert the gas to flow over the small headspace (Fig. 1) and resumed at the same rate (ca. 5 ml min^{-1} $vessel^{-1}$) for the rest of the experiment. The vessels were left for ca. 4 h to allow the small headspace SF_6 concentrations to return to background levels. 60 ml of 30 atom% containing 85 and 100 ppm ^{15}N-isotopically labelled N_2O was then syringe-injected into the 0-10 cm and 50-60 cm core large headspace vessels (below the intact soil cores) via the septum (Fig. 1), to attain a $^{15}N_2O$ headspace concentration below the soil core of 2.4 and 2.8 ppm, respectively. These represent the in situ concentrations of N_2O at the same field site between the two depths (ca. 30 cm; Chapter 5, Fig. 5.2b). The flow rate was tested daily 3 times per core after sampling using a bubble meter and these specific flow rates were used to calculate fluxes.

6.2.5 Gas sampling and analysis

Approximately 30 mins after injection of the $^{15}N_2O$ into the headspace below the intact soil cores, the large headspace was assumed to be mixed and the initial '*t = 0*' SF_6 (10 ml) and mass spectrometry (duplicate 12 ml) samples were taken using separate gas-tight 20 ml polypropylene syringes. Samples were assumed to be representative of the large headspace by filling and emptying the syringe 3 times into the headspace before a gas sample was taken. SF_6 samples were analysed immediately, while the duplicate samples for mass

spectrometry were injected directly into 12 ml pre-evacuated (flushed with Helium and doubly evacuated) Exetainers® (Labco Ltd., Lampeter, UK). Large headspace samples were taken daily for SF_6 analysis. Samples from the headspace below the soil core for mass spectrometry were taken at the start (day 1) and end of the incubation (day 3 or 4). A total of 4% of the volume of gas in the headspace below the soil core was removed for analysis across the incubation period and this was factored in the calculations of the gas concentrations. Headspace above the core were sampled (via the sampling tube) for SF_6 and mass spectrometry (duplicate) analysis daily, with these always taken before headspace below the soil core samples. This was done by disconnecting the sampling tube (see Fig. 6.1) from the headspace (to avoid creating negative pressure in the system and turbulent mixing with ambient air) and then connecting a syringe to the tube and taking samples before re-connecting the sampling tube. The volume of the sampling tube (53.4 ml) was sufficient to take 2 samples (maximum of 24 ml) without diluting with ambient air, as was tested (Appendix 5; S2, Fig. S2).

One of the two duplicate samples was analysed for N_2O and N_2 concentration and enrichment using a Sercon trace gas analyser and Sercon 20:22 isotope ratio mass spectrometer (Sercon Ltd., Crewe, UK), while the other was spare in case of analysis failure. Samples were stored for 8 months before analysis due to COVID-19 related restrictions and delays. At the same time 12 ml N_2O standards (5 ppm ; n = 15) were stored with the samples to track any loses of concentration across the storage period. After this period, the mean standard concentration of this stored 5 ppm standard was 4.34 ppm ± 0.07. The analysed concentrations were adjusted to compensate for losses during storage.

For the analysis of SF_6, the 10 ml samples were used to flush and fill a 1 ml loop that was then injected directly into a Shimadzu GC-8A (Shimadzu KK, Kyoto, Japan) equipped with an Electron Capture Detector (ECD) and adapted for the rapid and precise analysis of SF_6 in either the gas or water phase (Law et al., 1994). Separation of SF_6 from O_2 and N_2O was achieved by a 3 m by 1/8 ” stainless steel column packed with molecular sieve 5A. The system was calibrated daily using a six-point calibration curve to cover the large range of concentrations observed between the two gas reservoirs. Analytical precision was typically better than 1% and the detection limit was close to 2 pptv.

6.2.6 Diffusion coefficient (D_s) calculation

The natural logs of SF_6 concentration depletion in the vessels were plotted against time for each WFPS treatment and soil depth. The diffusion coefficient (D_s) was then calculated from the gradient of the depletion curve using Equation 1.

$$C = \frac{2h \exp(-D_s a_1^2 t/\varepsilon)}{L(a_1^2 + h^2) + h} \quad (1)$$

Where, C is the concentration of gas in the chamber (g m^{-3}); ε is total air-filled porosity (m^3 of air m^{-3} soil); L is the depth of the soil core (m); t is time (h); $h = \varepsilon(a\varepsilon_c)$, where $\varepsilon_c = 1$, is the air content of the chamber (m^3 of air m^{-3} chamber); a is the volume of the chamber per area of soil (m^3 of air m^{-2} soil). A plot of lnC against time becomes linear with slope $-D_s a_1^2 t/\varepsilon$ for sufficiently large t. By finding the product of hL, the value of $a1$, the positive root of (aL)tan(aL) = hL, can be found using the table in (Rolston and Moldrup, 2002) and the root derivatives of $a1L$. The relative diffusion (D_s/D_0) of gas was calculated using the diffusion rate of SF_6 in air, D_0, (0.093 m^2 s^{-1}; Rudolph et al., 1996).

6.2.7 ^{15}N-N_2O pool dilution calculation

The calculation of gross production and consumption of N_2O was done using the modified (Wen et al., 2017, 2016) ^{15}N-N_2O pool dilution method developed by Yang et al. (2011) from von Fischer and Hedin (2002):

$$[^{14}N_2O]_t = \frac{F_{14} \cdot P}{k_{14} + k_l} - \left(\frac{F_{14} \cdot P}{k_{14} + k_l} - [^{14}N_2O]_0\right) \cdot e\left(-(k_{14} + k_l) \cdot (t - t_0)\right) \quad (2)$$

$$[^{15}N_2O]_t = \frac{F_{15} \cdot P}{k_{15} + k_l} - \left(\frac{F_{15} \cdot P}{k_{15} + k_l} - [^{15}N_2O]_0\right) \cdot e\left(-(k_{15} + k_l) \cdot (t - t_0)\right) \quad (3)$$

Where the concentration of $^{14}N_2O$ at time t ($[^{14}N_2O]_t$) is calculated as the product of the N_2O concentration (ppb) and the ^{14}N-N_2O atom% (i.e. 100 - ^{15}N-N_2O atom%); $[^{15}N_2O]_t$ is the concentration of $^{15}N_2O$ at time t, calculated as the product of the N_2O concentration (ppb) and the ^{15}N-N_2O atom% excess (assuming a ^{15}N isotope composition of background N_2O of 0.3688 atom%; Yang et al., 2011); F_{14} and F_{15} are the $^{14}N_2O$ (0.997) and $^{15}N_2O$ (0.003) mole fractions of emitted N_2O, respectively; k_{14} and k_{15} are the first-order rate constants of $^{14}N_2O$

and $^{15}N_2O$ reduction to N_2, respectively, calculated using Equation 4 and the average literature value (α = 0.9924 ± 0.0036; Yang et al., 2011) for the stable N isotopic fractionation factors defined as $\alpha = k_{15}/k_{14}$; k_l is the first-order exponential decay constant for SF_6 concentrations over time and represents physical loss via diffusion and/or advection (von Fischer and Hedin, 2002), calculated using Equation 4; t is the time (hours) when the headspace was sampled. The gross N_2O emission (ppb h^{-1}), P, was calculated as the sum of Equations 2 and 3 relative to their mole fractions, solved using MATLAB (MathWorks, Version R2022a, USA).

The first-order rate constants for $^{15}N_2O$ (k_{15}) and SF_6 (k_l) were calculated using the following equation:

$$k = -\frac{ln\left(\frac{C_t}{C_0}\right)}{t} \quad (4)$$

Where k is the first-order rate constant; C_t and C_0 are the concentrations (ppb) of the gas at sampling time t (hours) and at $t = 0$, respectively. The rate constant for $^{14}N_2O$, k_{14}, was calculated by solving $\alpha = k_{15}/k_{14}$, as described above.

The net N_2O emission from the flow-through small headspace was calculated as:

$$F = t \cdot f \cdot (C_{out} - C_{in}) \quad (5)$$

Where F is the flux (ppb h^{-1}); t is the time (h) the sample is representative of; f is the flow rate of air through the headspace (l h^{-1}) and C_{out} and C_{in} are the concentrations of N_2O leaving and entering the headspace (ppb). The results from Equation 5 were then averaged and divided by the total incubation time to give a net flux (ppb h^{-1}) per incubation vessel.

The net emission (Equation 5) and gross production (Equation 4 and 5) N_2O rates were then converted to µg N kg^{-1} h^{-1} using Equation 6.

$$F_E = \frac{F \cdot V_h}{10^{12}} \cdot \frac{p}{R \cdot (T + 273)} \cdot \frac{28}{W_d} \cdot 10^9 \quad (6)$$

Where F_E is either the net emission or gross production of N_2O (µg N kg^{-1} h^{-1}), F is the net or gross emission of N_2O flux in ppb h^{-1}; V_h is the headspace volume (l); R is the ideal gas constant (8.314 J K^{-1} mol^{-1}); p is the pressure (Pa); T is the incubation temperature (°C) and 273 is the conversion constant to Kelvin; 28 is the molecular weight of N in N_2O (g mol^{-1}); W_d is the dry weight of the soil cores (g); 10^{12} and 10^9 are unit conversion factors. Gross N_2O consumption

was then calculated as the difference between the gross N_2O production and net N_2O emission (Yang et al., 2011).

6.2.8 Statistical analysis

All data analysis was done using R (R Core Team, 2017), with figures made using the R package 'ggplot2'(Wickham, 2016). Data were assessed for test assumptions by using the Shapiro-Wilk test (p >0.05) for normality, and Levene's test for homoscedasticity (p <0.05) as well as assessing the qqplots and the residual versus fitted plots. The difference in mean SF_6 fluxes from the headspace above versus below the soil cores was tested with a Welch Two Sample t-test. Differences in relative diffusivity were tested individually by depth and WFPS with a Welch Two Sample t-test. Difference in fluxes with depth and WFPS were tested by 2-way ANOVAs. Data that did not meet assumptions were log or square root transformed to pass the Shapiro-Wilk and Levene's tests.

6.3 Results

6.3.1 Relative diffusivity

As a test to ensure the SF_6 flux results from the small headspace and the depletion of SF_6 from the large headspace corresponded with each other, the fluxes were plotted against each other (Fig. 6.2). The proximity of the data to the x = y line demonstrate that they correspond well with each other. This is confirmed by a lack of statistical difference between the fluxes from the small and large headspaces (p = 0.62). The linear trendline (y = 1.26x – 0.29) explained most of the variation in the data (R^2 = 0.96) but its deviation from the x = y line highlights that the mean measured headspace below the soil core flux was overall 16.3% lower than that measured in the headspace above the soil core. While the cores at 70% WFPS (R^2 = 0.55; y = 0.92x + 0.46) more closely aligned with the x=y 1:1 line, substantially more variation was explained by the line for the 50% WFPS cores (R^2 = 0.98; y = 1.21x + 0.54).

The differences in relative diffusivity (D_s/D_0) of the soil cores were driven by the WFPS rather than the depth of the soil (Fig. 6.3). Relative diffusivity was 383 and 436% higher in the 0-10 and 50-60 cm cores at 50% WFPS compared to the 70% WFPS (p = 0.002), respectively. While the 50-60 cm cores did have 12 and 21% lower relative diffusivities than the 0-10 cm cores at 50 and 70% WFPS, respectively, these differences were not significant (p = 0.54).

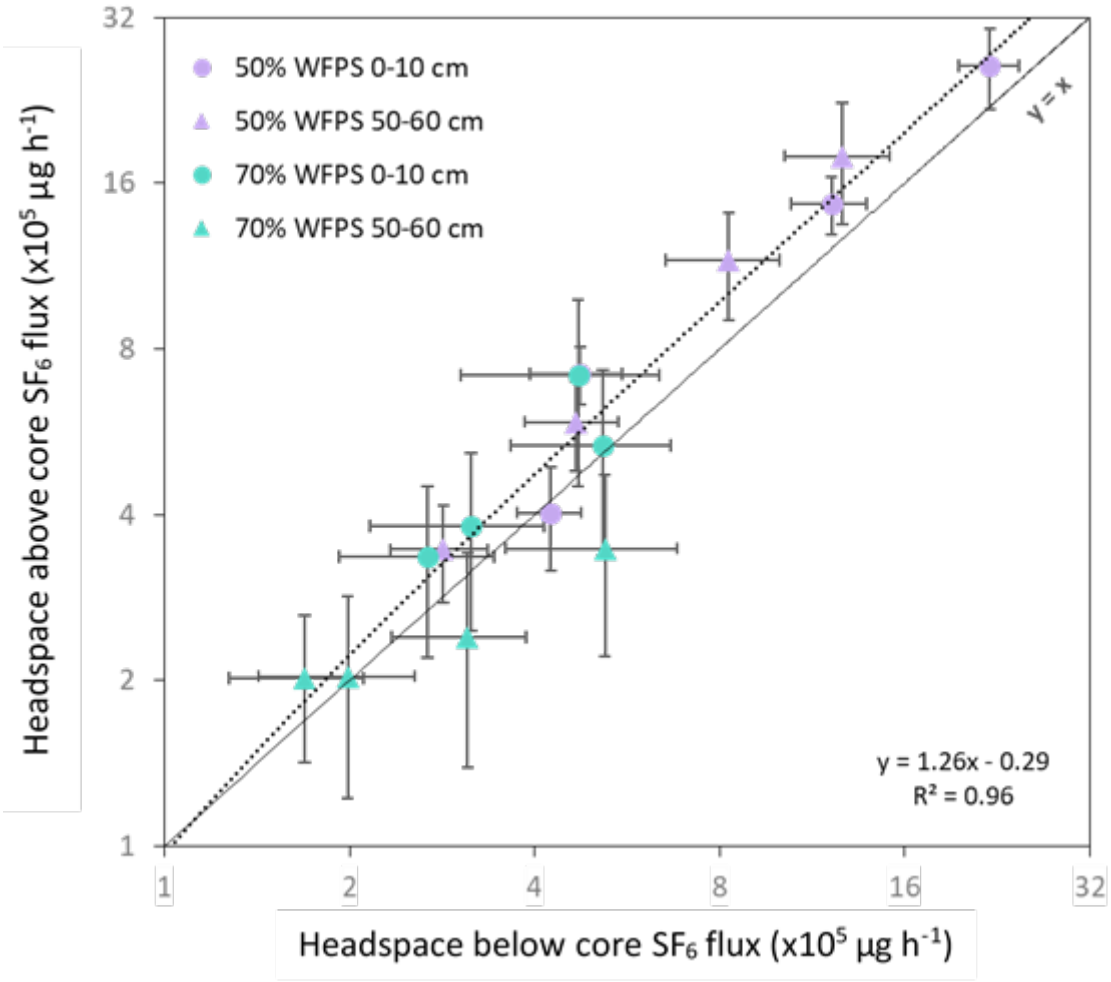

Fig. 6.2 The fluxes of SF_6 (means ± SEM; n = 6) from the headspace above and below the incubated soil core from the 0-10 and 50-60 cm soil depths at 50 and 70% WFPS. The depletion of SF_6 from the headspace below was calculated as a The dashed line represents the best fit for the flux data (R^2 = 0.96; y = 1.26x – 0.29) and the solid line represents the y = x. Note that the axes are logarithmic.

6.3.2 Gross N_2O emission and uptake

Soil cores at 50% WFPS produced 189 and 69% more gross N_2O than at 70% WFPS in the 0-10 and 50-60 cm soil core depths (p = 0. 028; Fig. 6.4a), respectively. The 0-10 cm cores produced 75% more gross N_2O than the 50-60 cm cores, though this was not significant (*p* = 0.70). This was primarily driven by differences between the 50% WFPS cores from the different depths, as there was only a 2% difference in gross N_2O production between the depths at 70% WFPS. Similar to the gross production of N_2O, 221 and 71% more N_2O was taken up in the soil at 50% WFPS than at 70% in the 0-10 and 50-60 cm soil cores, respectively (p = 0.036; Fig. 6.4b). There was only a 4% difference in gross N_2O uptake between the depths

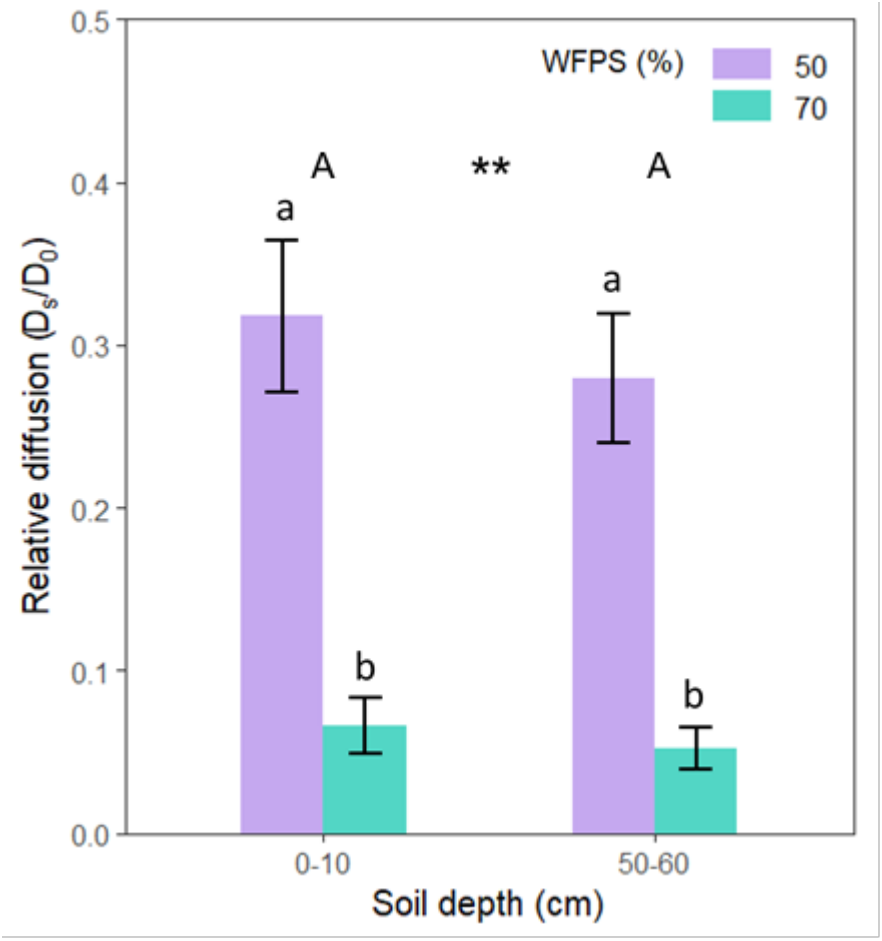

Fig. 6.3 The mean (± SEM) relative diffusivity (D_s/D_0) of intact top- and subsoil cores at 2 different levels of water-filled pore space (WFPS, %; *n* = 6). Different letters represent statistical difference of means between soil depths (upper-case) and between soil depth and WFPS (lower-case) at p < 0.05. Asterisks represent statistical difference in overall WFPS means at $p < 0.001$ (***); $p < 0.01$ (**); $p < 0.05$ (*) and $p > 0.05$ (-).

at 70% WFPS, whereas 80% more N_2O was taken up by the 0-10 cm soil cores compared to the 50-60 cm cores at 50% WFPS. Despite this, there was no overall effect of soil depth on gross N_2O uptake ($p = 0.97$).

6.3.3 Net N_2O emission

Overall, the 0-10 cm soil cores had a higher net N_2O emission (50% WFPS, 0.045 ± 0.002; 70% WFPS, 0.048 ± 0.008 µg N kg^{-1} h^{-1}) compared to the deeper soil cores (50% WFPS, 0.044 ± 0.002; 70% WFPS, 0.029 ± 0.002 µg N kg^{-1} h^{-1};) ($p = 0.014$; Fig. 6.4c). Net emissions of N_2O were higher in the cores at 50% WFPS than at 70% ($p = 0.042$). This difference was not driven by the 4% higher net N_2O emissions from the 50% WFPS 0-10 cm cores compared to the 50-60 cm cores, but the 40% lower emissions from the 70% cores at 50-60 cm. In the 50-

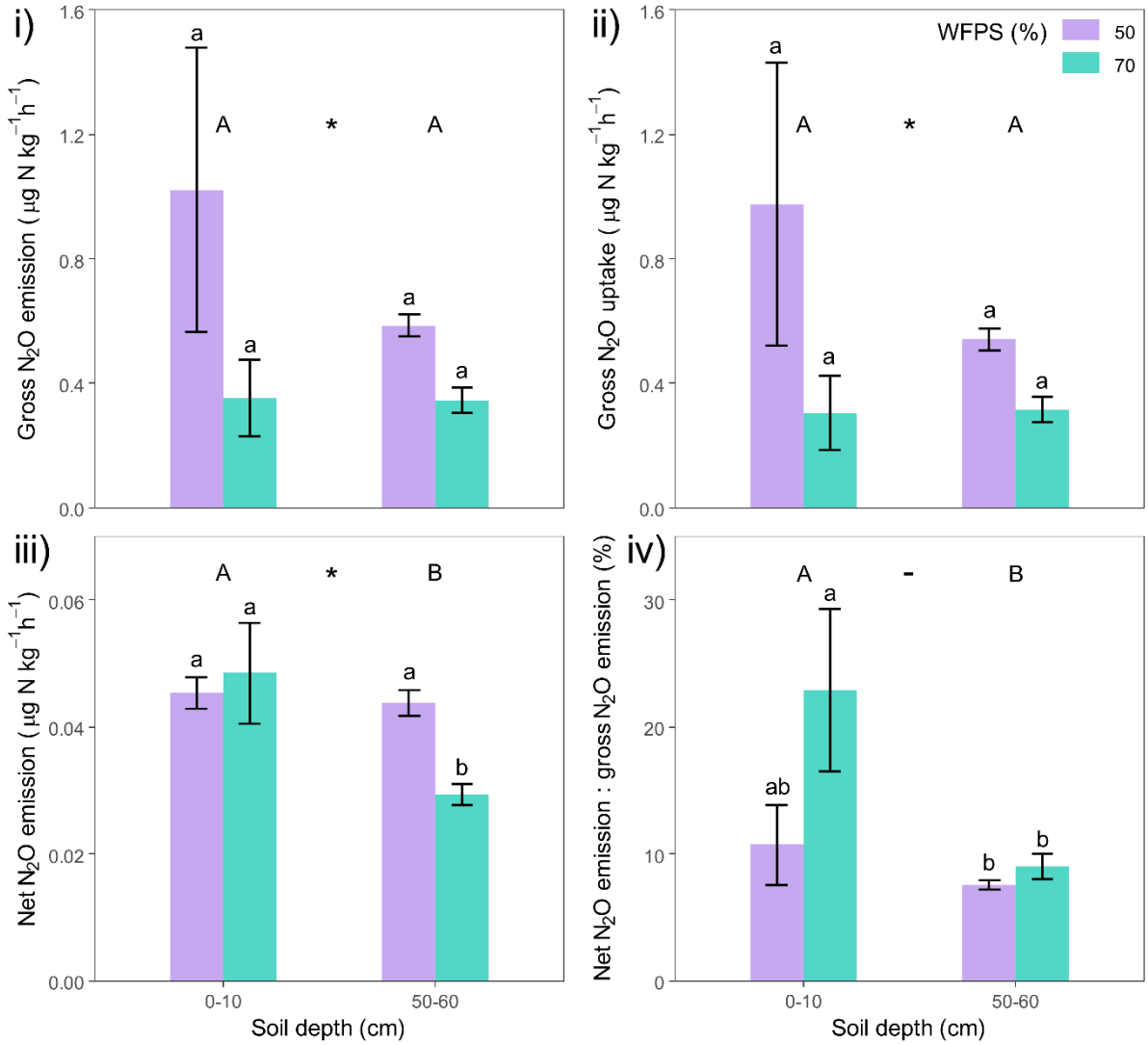

Fig. 6.4 The gross N_2O emission i); gross N_2O uptake ii); Net N_2O emission iii); and the ratio between the net and gross N_2O emission iv) (means ± SEM; n = 6) in intact 0-10 and 50-60 cm soil cores at 50 and 70% WFPS measured by the ^{15}N-N_2O pool dilution method. Different letters represent statistical difference of means between soil depths (upper-case) and between soil depth and WFPS (lower-case) at $p < 0.05$. Asterisks represent statistical differences in overall WFPS means at $p < 0.001$ (***); $p < 0.01$ (**); $p < 0.05$ (*) and $p > 0.05$ (-).

60 cm cores, the emissions from the 50% WFPS treatment were 50% higher than in the 70% WFPS treatment, but 5% lower than from the 70% WFPS cores. The ratio between net and gross N_2O emission was greatest in the 0-10 cm cores (p = 0.028; Fig. 6.4d). The ratio in the 0-10 cm 50% WFPS cores was 42% higher than in the subsoil cores at the same WFPS. At 70% WFPS, the 0-10 cm cores had a 154% higher ratio than the 50-60 cm cores. Within the soil core depths, ratios were 114 and 20% higher in the 70 than the 50% WFPS in the 0-10 and 50-

60 cm soil core depths, respectively. Despite these differences, there was no overall impact of WFPS on the ratio between net and gross N_2O emissions (p = 0.071).

6.4 Discussion

In this study we successfully utilised a novel sampling set-up alongside the $^{15}N_2O$ isotope pool dilution method to explore gross and net N_2O emissions and N_2O uptake within intact soil cores of different depths and moisture contents.

6.4.1 Soil diffusivity

While the agreement between the small and large headspace SF_6 fluxes was good (Fig. 6.2), we attribute the overall higher fluxes in the headspace above the core compared to the headspace below the core to be likely due to several potential technical factors. Of the discrepancy between the two headspaces, 4% can be attributed to volume of gas removed from sampling across each incubation. At every sampling timepoint the removal of 0.5-1.6% of the total below core headspace would have caused a slight negative pressure that is likely to have been equalised by the dilution of gas from the low SF_6 air (<10 ppt) flowing over the soil cores. In addition, considering the exponential depletion of SF_6 from the headspace below the cores, samples from the headspace above the cores that were taken 1-2 h before the ones below them would translate to higher fluxes. Therefore, we believe the difference between the calculated fluxes is predominantly due to the delay in above core headspace samples and in part due to the dilution of the headspace below the core from some air flow into the bottom headspace. We believe the nature of the fit to be within an acceptable range of error for the relationship between the small and large headspaces to produce meaningful results from the ^{15}N-N_2O pool dilution.

The relative diffusivity values in Figure 6.2 (0.024 – 0.480) are consistent with the expected values for the exponential increase in D_s/D_0 with increasing air-filled pore porosity for soils with different overall pore architectures (Hashimoto and Komatsu, 2006) and using different measuring techniques (Allaire et al., 2008) . The hypothesis that soil diffusion would be reduced by both increasing depth and WFPS was only partly confirmed (Fig. 6.3). As expected, the higher WFPS in the soil reduced the diffusivity of the soil substantially, but the different inherent physical soil characteristics (bulk density, porosity, texture; Table 6.1) of

the cores did not affect the D_s/D_0 of the soil when at the same WFPS. Fujikawa and Miyazaki (2005) found D_s/D_0 to increase with higher bulk density which they attributed to lower total porosity via the change in shape and size of pores which can be assumed to restrict gas movement, consistent with other studies (Balaine et al., 2013; Currie, 1984). However, these studies were all done on sieved and repacked soil which would create a more homogenous soil pore structure and can cause significant errors in determining the 'true' D_s/D_0 (Allaire et al., 2008). The inherent pore structure and preferential flow pathways (i.e. macropores, soil pipes and cracks) were preserved in the cores (though edge related diffusion was avoided by sealing these) and this heterogeneity is a primary factor driving gas flow and is very important for studying gas diffusion (Allaire et al., 2008; Chamindu Deepagoda et al., 2019; Guo and Lin, 2018). However, no difference in D_s/D_0 between intact soil cores at a range of depths, bulk densities and porosities has also been observed (Chamindu Deepagoda et al., 2019). We attribute this lack of difference between depths to the presence of natural macropores, pipes and preferential flow paths that create similarities in the diffusivity of gas through the soil and the differences in soil physical properties was not sufficient to drive differences in D_s/D_0.

6.4.2 Gross N_2O uptake

Evidence for N_2O consumption by soils is extensive in the literature literature (see review by Chapuis-lardy et al., 2007). In our study, we report gross N_2O-N uptake rates ranging from 0.03 – 2.79 µg N kg^{-1} h^{-1} (Fig. 6.4b) which is a similar range to that measured by others in similar agricultural soils (Clough et al., 2006; Luo et al., 2022; Wen et al., 2016). N_2O consumption rates, in our study, correlated closely with production rates, which is consistent with other studies (Wen et al., 2016; Yang et al., 2011; Yang and Silver, 2016), suggesting that consumption increased proportionally with N_2O production (Fig. 6.4a, b). These results uncovered a high potential for N_2O uptake that would have been masked by higher N_2O production had only the latter been measured.

The hypothesis that the uptake of N_2O would be greater in the more microbially-active topsoil compared to the subsoil was rejected (Fig. 6.4b). While the uptake rate was highest in the topsoil cores at 50% WFPS, there was no statistical difference between depths. In fact, considering the lower soil microbial biomass and abundance of denitrification (*nirK*, *nirS*) and complete denitrification (*nosZ*) gene copies in the subsoil (Table S1), the uptake of N_2O

relative to the size and denitrification potential of the soil microbial community was much greater in the subsoil compared to the topsoil (though this does not mean the denitriers were active). This result is supported by the findings that reduction of N_2O to N_2 can be considerable in the subsoil, dependent on a combination of inherent soil characteristics (C, NO_3^-) and physical conditions (WFPS, O_2 concentration, diffusivity) (Clough et al., 2005, 1999; Semedo et al., 2020). The cores in this study were incubated at an O_2 content similar to their *in situ* levels - which was 20.9 and 13% in the topsoil and subsoil incubations. Due to 38% less O_2 in the subsoil cores, the formation of semi-anaerobic and full anaerobic conditions required for N_2O production and consumption would be more easily achieved. This is supported by others that found increased denitrification when O_2 was restricted (Patureau et al., 1996; Schlüter et al., 2018), which would explain the lack of difference in gross N_2O uptake between soil depths.

Higher WFPS decreases the diffusion of N_2O produced in the soil to the surface and increases its residence time allowing for higher potential of complete denitrification of N_2O to N_2 (Balaine et al., 2013; Chamindu Deepagoda et al., 2019). While the diffusion rate did decrease with greater WFPS (Fig. 6.3), this did not produce a difference between the N_2O uptake rates of the soil cores incubated at different WFPS levels. In fact, the 50% WFPS cores had higher consumption rates. We therefore reject our final hypothesis, that N_2O uptake would be higher with increasing WFPS.

N_2O consumption is generally expected to occur under conditions of low N availability and high soil moisture (Chapuis-lardy et al., 2007). While there is extensive literature that suggests there is a high WFPS 'critical threshold' at which consumption predominantly takes place (ca. >60-80%; Bateman and Baggs, 2005; Chamindu Deepagoda et al., 2019; Davidson, 1991), there are studies that have found no differences or even an increase in N_2O uptake with lower WFPS (Goldberg and Gebauer, 2009; Khalil et al., 2002; Rosenkranz et al., 2006; Wu et al., 2013) and low N (Wang et al., 2018). A possible explanation for N_2O consumption in drier soil is greater diffusivity allowing N_2O present in air or headspace to diffuse to the denitrification site, where in the absence of NO_3^-, N_2O may be used as an electron acceptor for denitrification (Chapuis-Lardy et al., 2007). Bazylinski et al. (1986) demonstrated this in isolated denitrifier growth using only N_2O as an electron acceptor. An alternative pathway is the microbial reduction of NO_3^- in aerobic conditions, which is suggested to be an

underappreciated sink (Roco et al., 2016). Therefore, substantial N_2O consumption in our study may be driven by aerobic rather than anaerobic denitrification processes (Wang et al., 2018; Wu et al., 2013). If this is the case and anaerobic microsites were not an important location for denitrification in this study, the calculated gross N_2O production and consumption rates may be more accurate. This is because the ^{15}N-N_2O pool dilution method does not allow for accurate measurement of gross production and consumption of N_2O in situations most likely to be occurring within anaerobic microsites. These are when i) N_2O produced is immediately consumed within the cells of denitrifiers, and ii) produced N_2O diffuses out of denitrifiers and is taken up by other microbes without mixing with the $^{15}N_2O$ label during the measurement period (Wen et al., 2016). Due to the 58% smaller volumes of the cores in this study compared to Wen et al. (2016), these processes may have been less likely to occur due to shorter diffusion distances reducing the time N_2O spent in the soil and therefore the potential for its consumption in microsites.

6.4.3 Gross N_2O emission

Gross N_2O emission rates varied from 0.056 to 2.83 µg N kg^{-1} h^{-1} (Fig. 6.4a), which is within the range of measurements reported in other studies (Clough et al., 2006; Luo et al., 2022; Wen et al., 2016). These rates may be low as N_2O can be lost rapidly (hours) after wetting (Barrat et al., 2022; Smith and Tiedje, 1979). As the cores were brought to the desired WFPS ca. 18 h before the incubation, they may have already lost substantial soil N prior to incubation.

N_2O production is driven by microbial denitrification and nitrification in the soil under partially anaerobic and aerobic conditions (Chapuis-Lardy et al., 2007; Diba et al., 2011). The dominating process has been found to change from nitrification to denitrification at WFPS of 60-70% (Bateman and Baggs, 2005; Pihlatie et al., 2004). This would suggest that the N_2O produced in the 50 and 70% WFPS cores was predominantly from nitrification or denitrification, respectively. However, these may occur in the soil simultaneously (Bateman and Baggs, 2005; Pihlatie et al., 2004). Denitrification is a common source of N_2O in many agricultural soils , which the close coupling between gross emission and uptake of N_2O in this study (Fig. 6.4a, b) would suggest this is due to (Chapuis-Lardy et al., 2007; Wen et al., 2016). N_2O 60% WFPS) as nitrification and denitrification rates are comparable sources of N_2O

occurring simultaneously. Therefore, a higher gross N_2O emission in the soil cores at 50% WFPS could be explained by simultaneous denitrification and nitrification producing N_2O.

Gross emission rates were not different with depth in this study (Fig. 6.4a). Emission rates of N_2O have been observed to be higher in subsoil than in topsoil under certain conditions (Goldberg et al., 2008; Müller et al., 2004; Shcherbak and Robertson, 2019). This may be due to denser deeper soils more quickly becoming anaerobic as a result of a restriction in diffusivity and lower pore volume (Berisso et al., 2013). As the subsoil cores were incubated with almost 38% less O_2 than the topsoil, the formation of semi-anaerobic and full anaerobic conditions required for N_2O production would be more easily achieved. Therefore, despite higher biological N_2O production potential in the topsoil (Table 6.1), it would suggest that physical N_2O-promoting conditions in the subsoil can match this potential.

6.4.4 Net N_2O emission

Net emissions from the soil cores varied between 0.025-0.084 µg N kg^{-1} h^{-1} (Fig. 6.4c). This low emission rate is expected from an unfertilized, low N arable soil (Table 1; Wen et al., 2016). The net N_2O emission decreased with soil depth which is primarily due to the low rate from the 70% WFPS 50-60 cm cores (Fig. 6.4c). This trend reflects the gross N_2O uptake and emission in the soil, as the net emission is the gross consumption subtracted from the gross emission.

The ratios between the net N_2O emissions and gross production of 66-79% measured by others (Wen et al., 2016; Yang et al., 2011; Yang and Silver, 2016) were substantially higher than in this study (2-47%; Fig. 6.4d). This discrepancy casts doubt on whether a general ratio would yield accurate gross N_2O emission and uptake estimates based on more easily measured net N_2O emissions, as suggested by Wen et al. (2016). However, the mean ratios from this study (8-23%) are within the range measured by the gas flow soil core method (5-28%) by Wen et al. (2016). This might suggest that due to anaerobic microsites not playing an important role in the production or consumption of N_2O as argued above, the rates were not underestimated and so the ratios were more accurate.

6.5 Conclusions

Using a novel dual-headspace system for soil core incubation, we demonstrated that this method is reliable for measuring fluxes both above and below a soil core at controlled O_2 concentration and for applying the ^{15}N-N_2O pool dilution method. We believe this novel dual headspace approach is likely to better replicate soil profile gas diffusion dynamics, compared to using a single headspace. The dual headspaces rates measured all fall within previously measured ranges measured in the field. We provide evidence that the relative diffusivity of gas within intact soil cores does not differ with soil depth, likely due to the preservation of preferential flow pathways. This contrasts with studies that use sieved and repacked cores which allow for more equal mixing of labelled and non-labelled isotope pools, but do not represent or measure true soil diffusivity. Gross N_2O production and consumption rates did not differ with depth but were higher in the 50% WFPS cores. We attribute this to aerobic denitrification and simultaneous denitrification and nitrification for N_2O consumption and production, respectively. We contribute further evidence challenging the hypothesis that only wet soils play a crucial role in N_2O production, consumption and net emissions. In addition, we challenge the notion that only soils with net negative emissions experience substantial N_2O consumption rates. The results from this study provide a novel application of the ^{15}N-N_2O pool dilution method and important evidence of N_2O production and consumption fluxes in low-N status, arable soil at different depths.

6.6 Acknowledgements

This work was supported by the FLEXIS (Flexible Integrated Energy Systems) programme, an operation led by Cardiff University, Swansea University and the University of South Wales and funded through the Welsh European Funding Office (WEFO). Rothamsted Research is supported by the Biotechnology and Biological Sciences Research Council (BBSRC, grants BBS/E/C/000I0310 and BBS/E/C/000I0320). The authors would like to thank Plymouth Marine Laboratory for the loan of the SF_6 GC. Sincere thanks also to Alan Jones for his excellent engineering advice and work; Lucy Greenfield for helping with the fieldwork; Nadine Loick and Neil Donovan for their technical support; Alex Boon for his help with the diffusion calculations and Marife Corre for her help with the pool dilution calculations.

6.7 References

Allaire, S.E., Lafond, J.A., Cabral, A.R., Lange, S.F., 2008. Measurement of gas diffusion through soils: Comparison of laboratory methods. J. Environ. Monit. 10, 1326–1336.

Almaraz, M., Wong, M.Y., Yang, W.H., 2020. Looking back to look ahead: a vision for soil denitrification research. Ecology 101, 1–10.

Balaine, N., Clough, T.J., Beare, M.H., Thomas, S.M., Meenken, E.D., Ross, J.G., 2013. Changes in Relative Gas Diffusivity Explain Soil Nitrous Oxide Flux Dynamics. Soil Sci. Soc. Am. J. 77, 1496–1505.

Barrat, H.A., Clark, I.M., Evans, J., Chadwick, D.R., Cardenas, L., 2022. The impact of drought length and intensity on N cycling gene abundance, transcription and the size of an N_2O hot moment from a temperate grassland soil. Soil Biol. Biochem. 168, 108606.

Bateman, E.J., Baggs, E.M., 2005. Contributions of nitrification and denitrification to N_2O emissions from soils at different water-filled pore space. Biol. Fertil. Soils 41, 379–388.

Bazylinski, D.A., Soohoo, C.K., Hollocher, T.C., 1986. Growth of Pseudomonas aeruginosa on nitrous oxide. Appl. Environ. Microbiol. 51, 1239–1246.

Berisso, F.E., Schjønning, P., Keller, T., Lamandé, M., Simojoki, A., Iversen, B. V., Alakukku, L., Forkman, J., 2013. Gas transport and subsoil pore characteristics: Anisotropy and long-term effects of compaction. Geoderma 195–196, 184–191.

Blagodatsky, S., Smith, P., 2012. Soil physics meets soil biology: Towards better mechanistic prediction of greenhouse gas emissions from soil. Soil Biol. Biochem. 47, 78–92.

Boon, A., Robinson, J.S., Nightingale, P.D., Cardenas, L., Chadwick, D.R., Verhoef, A., 2013. Determination of the gas diffusion coefficient of a peat grassland soil. Eur. J. Soil Sci. 64, 681–687.

Boyer, E.W., Alexander, R.B., Parton, W.J., Li, C., Butterbach-Bahl, K., Donner, S.D., Skaggs, R.W., Del Grosso, S.J., 2006. Modeling denitrification in terrestrial and aquatic ecosystems at regional scales. Ecol. Appl. 16, 2123–2142.

Cárdenas, L.M., Hawkins, J.M.B., Chadwick, D., Scholefield, D., 2003. Biogenic gas emissions from soils measured using a new automated laboratory incubation system. Soil Biol. Biochem. 35, 867–870.

Chamindu Deepagoda, T.K.K., Jayarathne, J.R.R.N., Clough, T.J., Thomas, S., Elberling, B., 2019. Soil-Gas Diffusivity and Soil-Moisture effects on N_2O Emissions from Intact Pasture Soils . Soil Sci. Soc. Am. J. 83, 1032–1043.

Chapuis-lardy, L., Wrage, N., Metay, A., Chotte, J.L., Bernoux, M., 2007. Soils, a sink for N_2O? A review. Glob. Chang. Biol. 13, 1–17.

Chapuis-Lardy, L., Wrage, N., Metay, A., Chotte, J.L., Bernoux, M., 2007. Soils, a sink for N2O? A review. Glob. Chang. Biol. 13, 1–17.

Clough, T.J., Jarvis, S.C., Dixon, E.R., Stevens, R.J., Laughlin, R.J., Hatch, D.J., 1999. Carbon induced subsoil denitrification of 15N-labelled nitrate in 1 m deep soil columns. Soil Biol. Biochem. 31, 31–41. h

Clough, T.J., Kelliher, F.M., Wang, Y.P., Sherlock, R.R., 2006. Diffusion of ^{15}N-labelled N_2O into soil columns: a promising method to examine the fate of N_2O in subsoils. Soil Biol. Biochem. 38, 1462–1468.

Clough, T.J., Sherlock, R.R., Rolston, D.E., 2005. A review of the movement and fate of N_2O in the subsoil. Nutr. Cycl. Agroecosystems 72, 3–11.

Currie, J.A., 1984. Gas diffusion through soil crumbs: the effects of wetting and swelling. J. Soil Sci. 34, 217–232.

Currie, J.A., 1960. Gaseous diffusion in porous media Part 1. - A non-steady state method. Br. J. Appl. Phys. 11, 314–317.

Davidson, E.A., 1991. Fluxes of nitrous oxide and nitric oxide from terrestrial ecosystems. Microb. Prod. Consum. Greenh. Gases Methane, Nitrous Oxide, Halomethanes 219–235.

Davidson, E.A., Ishida, F.Y., Nepstad, D.C., 2004. Effects of an experimental drought on soil emissions of carbon dioxide, methane, nitrous oxide, and nitric oxide in a moist tropical forest. Glob. Chang. Biol. 10, 718–730.

Diba, F., Shimizu, M., Hatano, R., 2011. Effects of soil aggregate size, moisture content and fertilizer management on nitrous oxide production in a volcanic ash soil. Soil Sci. Plant Nutr. 57, 733–747.

Dong, W., Wang, Y., Hu, C., 2013. Concentration profiles of CH_4, CO_2 and N_2O in soils of a wheat–maize rotation ecosystem in North China Plain, measured weekly over a whole year. Agric. Ecosyst. Environ. 1, 260–272.

Donoso, L., Santana, R., Sanhueza, E., 1993. Seasonal variation of N_2O fluxes at a tropical savannah site: Soil consumption of N_2O during the dry season. Geophys. Res. Lett. 20, 1379–1382.

Fujikawa, T., Miyazaki, T., 2005. Effects of bulk density and soil type on the gas diffusion coefficient in repacked and undisturbed soils. Soil Sci. 170, 892–901.

Goldberg, S.D., Gebauer, G., 2009. Drought turns a Central European Norway spruce forest soil from an N2O source to a transient N_2O sink. Glob. Chang. Biol. 15, 850–860.

Goldberg, S.D., Knorr, K.H., Gebauer, G., 2008. N_2O concentration and isotope signature along profiles provide deeper insight into the fate of N_2O in soils. Isotopes Environ. Health Stud. 44, 377–391.

Guo, L., Lin, H., 2018. Addressing Two Bottlenecks to Advance the Understanding of Preferential Flow in Soils, 1st ed, Advances in Agronomy. Elsevier Inc.

Hashimoto, S., Komatsu, H., 2006. Relationships between soil CO_2 concentration and CO_2 production, temperature, water content, and gas diffusivity: Implications for field studies through sensitivity analyses. J. For. Res. 11, 41–50.

Hill, A.R., Cardaci, M., 2004. Denitrification and Organic Carbon Availability in Riparian Wetland Soils and Subsurface Sediments. Soil Sci. Soc. Am. J. 68, 320–325.

Jahangir, M.M.R., Khalil, M.I., Johnston, P., Cardenas, L.M., Hatch, D.J., Butler, M., Barrett, M., O, V., Richards, K.G., 2012. Denitrification potential in subsoils : A mechanism to reduce nitrate leaching to groundwater. "Agriculture, Ecosyst. Environ. 147, 13–23.

Jia, G., Shevliakova, Elena, Artaxo, Paulo, De Noblet-Ducoudré, Nathalie, Houghton, Richard, Anderegg, W., Bernier, P., Carlo Espinoza, J., Semenov, S., Xu, X., Shevliakova, E, Artaxo, P, De Noblet-Ducoudré, N, Houghton, R, House, J., Kitajima, K., Lennard, C., Popp, A., Sirin, A., Sukumar, R., Verchot, L., 2019. Land-climate interactions. Clim. Chang. L. an IPCC Spec. Rep. Clim. Chang. Desertif. L. Degrad. Sustain. L. Manag. food Secur. Greenh. gas fluxes Terr. Ecosyst. 131–248.

Khalil, M.I., Rosenani, A.B., Van Cleemput, O., Fauziah, C.I., Shamshuddin, J., 2002. Nitrous Oxide Emissions from an Ultisol of the Humid Tropics under Maize-Groundnut Rotation. J. Environ. Qual. 31, 1071–1078.

Laughlin, R.J., Stevens, R.J., 2002. Evidence for Fungal Dominance of Denitrification and Codenitrification in a Grassland Soil. Soil Sci. Soc. Am. J. 66, 1540–1548.

Laughlin, R.J., Stevens, R.J., Zhuo, S., 1997. Determining Nitrogen-15 in Ammonium by Producing Nitrous Oxide. Soil Sci. Soc. Am. J. 61, 462.

Law, C.S., Watson, A.J., Liddicoat, M.I., 1994. Automated vacuum analysis of sulphur hexafluoride in seawater: derivation of the atmospheric trend (1970-1993) and potential as a transient tracer. Mar. Chem. 48, 57–69.

Li, Z., Kelliher, F.M., 2005. Determining nitrous oxide emissions from subsurface measurements in grazed pasture: A field trial of alternative technology. Aust. J. Soil Res. 43, 677–687.

Luo, J., Beule, L., Shao, G., Veldkamp, E., Corre, M.D., 2022. Reduced Soil Gross N_2O Emission Driven by Substrates Rather Than Denitrification Gene Abundance in Cropland Agroforestry and Monoculture. J. Geophys. Res. Biogeosciences 127, 1–16.

Müller, C., Stevens, R.J., Laughlin, R.J., Jäger, H.J., 2004. Microbial processes and the site of N2O production in a temperate grassland soil. Soil Biol. Biochem. 36, 453–461.

Neftel, A., Flechard, C., Ammann, C., Conen, F., Emmenegger, L., Zeyer, K., 2007. Experimental assessment of N_2O background fluxes in grassland systems. Tellus, Ser. B Chem. Phys. Meteorol. 59, 470–482.

Patureau, D., Bernet, N., Moletta, R., 1996. Effect of oxygen on denitrification in continuous chemostat culture with Comamonas sp SGLY2. J. Ind. Microbiol. Biotechnol. 16, 124–

Pihlatie, M., Syväsalo, E., Simojoki, A., Esala, M., Regina, K., 2004. Contribution of nitrification and denitrification to N_2O production in peat, clay and loamy sand soils under different soil moisture conditions. Nutr. Cycl. Agroecosystems 70, 135–141.

R Core Team, 2017. A language and environment for statistical computing. R.

Roco, C.A., Bergaust, L.L., Shapleigh, J.P., Yavitt, J.B., 2016. Reduction of nitrate to nitrite by microbes under oxic conditions. Soil Biol. Biochem. 100, 1–8.

Rolston, D.E., Moldrup, P., 2002. 4.3 Gas Diffusivity, in: Methods of Soil Analysis: Part 4 Physical Methods. pp. 1113–1139.

Rosenkranz, P., Bruggemann, N., Papen, H., Xu, Z., Seufert, G., Butterbach-Bahl, K., 2006. N_2O, NO and CH_4 exchange, and microbial N turnover over a Mediterranean pine forest soil. Environ. Res. 121–133.

Rudolph, J., Rothfuss, F., Conrad, R., 1996. Flux between soil and atmosphere, vertical concentration profiles in soil, and turnover of nitric oxide: 1. Measurements on a model soil core. J. Atmos. Chem. 23, 253–273.

Schlesinger, W.H., 2013. An estimate of the global sink for nitrous oxide in soils. Glob. Chang. Biol. 19, 2929–2931.

Schlüter, S., Henjes, S., Zawallich, J., Bergaust, L., Horn, M., Ippisch, O., Vogel, H.J., Dörsch, P., 2018. Denitrification in soil aggregate analogues-effect of aggregate size and oxygen diffusion. Front. Environ. Sci. 6, 1–10.

Semedo, M., Wittorf, L., Hallin, S., Song, B., 2020. Differential expression of clade i and II N_2O reductase genes in denitrifying Thauera linaloolentis 47LolTunder different nitrogen conditions. FEMS Microbiol. Lett. 367, 1–6.

Sexstone, A.J., Revsbech, N.P., Parkin, T.B., Tiedje, J.M., 1985. Direct Measurement of Oxygen Profiles and Denitrification Rates in Soil Aggregates. Soil Sci. Soc. Am. J. 49, 645–651.

Shcherbak, I., Robertson, G.P., 2019. Nitrous Oxide (N_2O) Emissions from Subsurface Soils of Agricultural Ecosystems. Ecosystems 22, 1650–1663.

Smith, M.S., Tiedje, J.M., 1979. Phases of denitrification following oxygen depletion in soil. Soil Biol. Biochem. 11, 261–267.

Stuchiner, E.R., von Fischer, J.C., 2022. Using isotope pool dilution to understand how organic carbon additions affect N_2O consumption in diverse soils . Glob. Chang. Biol. 0–2.

Van Beek, C.L., Hummelink, E.W.J., Velthof, G.L., Oenema, O., 2004. Denitrification rates in relation to groundwater level in a peat soil under grassland. Biol. Fertil. Soils 39, 329–336.

van Bochove, E., Bertrand, N., Caron, J., 1998. In Situ Estimation of the Gaseous Nitrous Oxide Diffusion Coefficient in a Sandy Loam Soil. Soil Sci. Soc. Am. J. 62, 1178–1184.

Van Cleemput, O., 1998. Subsoils: Chemo- and biological denitrification, N2O and N2 emissions. Nutr. Cycl. Agroecosystems 52, 187–194.

Van Groenigen, J.W., Zwart, K.B., Harris, D., Van Kessel, C., 2005. Vertical gradients of δ15N and δ18O in soil atmospheric N_2O - Temporal dynamics in a sandy soil. Rapid Commun. Mass Spectrom. 19, 1289–1295.

von Fischer, J.C., Hedin, L.O., 2002. Separating methane production and consumption with a field-based isotope pool dilution technique. Global Biogeochem. Cycles 16, 8-1-8–13.

Wang, Y., Li, X., Dong, W., Wu, D., Hu, C., Zhang, Y., Luo, Y., 2018. Depth-dependent greenhouse gas production and consumption in an upland cropping system in northern China. Geoderma 319, 100–112.

Wen, Y., Chen, Z., Dannenmann, M., Carminati, A., Willibald, G., Kiese, R., Wolf, B., Veldkamp, E., Butterbach-Bahl, K., Corre, M.D., 2016. Disentangling gross N_2O production and consumption in soil. Science Reports 6, 1–8.

Wen, Y., Corre, M.D., Schrell, W., Veldkamp, E., 2017. Gross N_2O emission and gross N_2O uptake in soils under temperate spruce and beech forests. Soil Biol. Biochem. 112, 228–236.

Wickham, H., 2016. Elegant Graphics for Data Analysis. ggplot2.

Wu, D., Dong, W., Oenema, O., Wang, Y., Trebs, I., Hu, C., 2013. N_2O consumption by low-nitrogen soil and its regulation by water and oxygen. Soil Biol. Biochem. 60, 165–172.

Yamulki, S., Goulding, K.W.T., Webster, C.P., Harrison, R.M., 1995. Studies on NO and N_20 fluxes from a wheat field. Atmos. Environ. 29, 1627–1635.

Yang, W.H., Silver, W.L., 2016. Net soil-atmosphere fluxes mask patterns in gross production and consumption of nitrous oxide and methane in a managed ecosystem. Biogeosciences 13, 1705–1715.

Yang, W.H., Teh, Y.A., Silver, W.L., 2011. A test of a field-based ^{15}N-nitrous oxide pool dilution technique to measure gross N_2O production in soil. Glob. Chang. Biol. 17, 3577–3588.

Zhang, Y., Mu, Y., Zhou, Y., Tian, D., Liu, J., Zhang, C., 2016. NO and N_2O emissions from agricultural fields in the North China Plain: Origination and mitigation. Sci. Total Environ. 551–552, 197–204.

Zona, D., Janssens, I.A., Gioli, B., Jungkunst, H.F., Serrano, M.C., Ceulemans, R., 2013. N2o fluxes of a bio-energy poplar plantation during a two years rotation period. GCB Bioenergy 5, 536–547.

Chapter 7

Discussion and conclusions

7.1 Introduction

Discussion of the findings from each chapter are described in detail within the individual experimental thesis Chapters (2 to 6). In this Chapter, the results from the experimental Chapters are discussed in relation to each other and their limitations, their wider implications and the priorities for future research that have evolved from the research.

7.2 Discussion of findings and limitations

The research in this thesis has highlighted the importance of including subsoils in soil studies, as they have been found to: be good targets for C sequestration (Chapters 2 and 3); gain insight into the processes governing surface-atmosphere gas exchange (Chapters 4, 5 and 6); and, experience different rates of microbial processes compared to their topsoil counterparts (Chapters 5 and 6). While deeper soil study creates more samples to be processed and is often more challenging and costly, the results from this thesis stand to argue that the insights that are gained outweigh these costs.

The subsoil environment is difficult to study *in situ* and so many studies, including studies in this thesis (Chapters 3, 5 and 6), are based on laboratory incubations. While these can produce valuable insights, it is important to also recognise their limitations. By removing and sieving deep soil, the physical structure is destroyed and the prevailing (commonly oligotrophic) conditions of the soil change during incubation. These limitations were present in the laboratory incubations in Chapters 3 and 5. In a bid to minimise these impacts, intact soil cores were taken in Chapter 6 and incubated at a O_2 level similar to *in* situ levels to better replicate the physical structure and the environmental conditions in the subsoil, respectively. In addition, by allowing gas to travel from a below core to an above core headspace, the movement of gas through the soil was better replicated. These additions to the incubation may partly explain why the N_2O consumption rates in the soil incubated in Chapter 5 showed evidence of depth-dependency, but not in Chapter 6. It is suggested that attempting to preserve more of the *in situ* characteristics is best for producing results that are more field relevant.

Apart from the data from the meta-analysis in Chapter 2, a limitation to the findings of this body of work is that they are all based on one soil type from one field. For example, the study in Chapter 3, if repeated on a sandier textured soil, is expected to produce different

results. As such, the applicability of results from this thesis to other places and soils is limited. This narrow focus does allow for greater understanding of the mechanisms and processes important in a particular soil and for comparison between similar studies on different soils. In this case, focussing on one soil has allowed the precise measurement of the diffusion coefficient in Chapter 6 to be used as an input variable for the CGM estimation of subsurface CO_2 fluxes in Chapters 4 and 5. In addition, the results presented in this thesis have value in their own right and can be a valuable reference for future research.

The improved design in soil gas sampling systems from the vertical pipes in Chapter 5 to the L-shaped pipes in Chapter 4, likely allowed for greater accuracy of GHG data collection as i) the surface area perforated for gas entry was much larger and so more representative of the soil layer; ii) the gas in the pipes was less prone to mixing with atmospheric air from surface soil cracking; and, iii) the pipes were of the same volume for all depths so the equilibration of soil gas was equal regardless of insertion depth. This is possibly best evidenced by the closer fit between the measured and estimated surface CO_2 fluxes with the L-shaped pipes (Fig. 4.6) compared to the vertical pipes (Fig. 5.4) – though this is a crude indicator as the estimated fluxes are influenced by many other factors (i.e. environmental CGM inputs). However, the disadvantage of the L-shaped design is that it requires greater disturbance of the soil to install the pipes. While disturbance in *in situ* studies should be avoided at all opportunities, the trade off between reliable data and preserving realistic field conditions is difficult to overcome. However, given enough time after installation of the L-shaped pipes, the disturbance driven CO_2 emissions should return to pre-disturbance levels (as observed 36 d following tillage by Fielder et al., 2015). Nevertheless, the similarities in trends between the depth profiles of CO_2 and N_2O in Chapters 4 and 5 suggest that both techniques are of value. Therefore, it is concluded that for long-term studies the L-shaped design is most likely to produce reliable data, whereas the vertical pipes are a less invasive alternative better suited for shorter sampling campaigns.

Finally, it is important to emphasise that the subsoil-targeting C sequestration strategies tested and discussed in this thesis are considered part of a greater swathe of improved agricultural practices. Applying conservation and regenerative agricultural practices is likely to have great concomitant benefits to the environmental, economic and social aspects of sustainable food production. Unlike the principles of conservation agriculture, subsoil

specific sequestration strategies are unlikely to be appropriate everywhere as the outcome of a sequestration method is highly context dependent. Therefore, conservation agriculture practices in conjunction with a subsoil C sequestration strategy - if the context and evidence base supports it - is suggested for meeting agricultural C sequestration potential throughout the soil profile.

7.3 Wider implications

The global scientific community agrees that our planet is facing a climate emergency, however, addressing this relies on much more than just science (Ripple et al., 2019). As global economics, religion, culture, history, politics, society, food, energy and security are all relevant and important to this crisis, solving it must be an interdisciplinary task. While reducing C emissions at their sources is fundamental to any successes, there is opportunity for scientific findings to support the necessary transition to a low/neutral C society. As such, C sequestration for climate change mitigation has received growing attention in the scientific community and in the media. Our manged soils that have in many cases been depleted of C for millennia are clearly capable of sequestering further C by a range of improved management practices (e.g. conservation and regenerative agriculture). Yet, claims have been made that most to all anthropogenic C emissions can be offset by C sequestration in soils. A reliance on C sequestration as a sole solution is dangerous and promotes inaction in all the other important areas mentioned above. In addition, C sequestration is reversible, and soils can also become large sources of GHGs which can counteract any C gains made (e.g. in response to extreme events and land use change).

At best, C sequestration can provide substantial gains in C at low cost with co-benefits to soil fertility, agricultural productivity and the delivery of other ecosystem services. At worst, it can be expensive and have little to no long-term effect on net C storage. Importantly, any C gains made by land management need to be maintained, otherwise they can be rapidly lost. By targeting deeper soil for C sequestration, the thought is that the added C will be less vulnerable and more stable in the long term. The results in Chapter 2 support this to an extent, though context was found to be very important in achieving success. This Chapter has made important contributions and advancements to this emerging field. It will be fundamental in future development and optimisation of subsoil C sequestration strategies. In addition, a

strong case for (continued) sampling of deeper soil is made, which is critical to developing our understanding, including subsoils in modelling, and harnessing this environment for C sequestration efforts. In addition, this work will allow the general public, policymakers and soil stakeholders to gain an overview of the current evidence on deep C sequestration and make informed decisions.

Globally, mining and wastewater treatment industries produce approximately 100 million tonnes of low economic value Fe-rich sludge as a by-product (Chen et al., 2015). Therefore, valorisation of this resource as an agricultural amendment would be ideal (Collivignarelli et al., 2020). The potential of adding Fe as a C sequestration strategy was tested in Chapter 3. While potential was found, the quantity, form and method of Fe application were determined as critical to its success. In addition, its best application is suggested to be in conjunction with a C source and in low Fe-containing soils. As a pioneering piece of work, a valuable base for this concept to further develop was built. If optimised, this strategy could contribute to the stabilisation of large amounts of C.

The promotion of deeper rooting, via deeper rooting crops, phenotypes, and perennialization is seen as a cheap win-win C sequestration strategy that has received a lot of attention. However, answers to ancillary questions regarding the impact of deeper rooting on soil respiration and harvestable biomass are less known. In Chapter 4, preliminary evidence of a win-win scenario was found, which makes its adoption more attractive to policymakers and farmers. However, for the actual adoption of such co-beneficial strategies more thought on the psychology, culture and behaviour of farmers is needed to overcome the scepticism of research innovation that has become the norm amongst farmer communities in the UK (Moran et al., 2013; Hyland et al., 2016).

The CGM is a valuable tool for gaining greater insight into soil GHG behaviour and fate in deep soil that more common flux measurement methods are not able to capture. However, due to the surface flux being modelled with the CGM, it is important to assess the reliability of the estimates across different climates, soils, and configurations to understand the limitations of the method. In Chapter 4 and 5, the existing knowledge of the CGM was built on and the results support the further use of it for CO_2 fluxes under 'normal' climactic conditions, for which validation against surface chamber measurements would not have been needed. However, the work also highlights scenarios where this method performed poorly.

This information is valuable in the interpretation of results from the CGM and for the future optimisation of the method.

How N_2O emissions, a large contributor to climate change, are produced in the soil relies on different processes that depend on a complex array of factors. In Chapter 6, a novel approach to disentangle these processes was devised in a controlled and meaningful way. The method includes a headspace both above and below the soil, representing the atmospheric and deeper soil gas exchange sites, respectively. This dual headspace approach is likely to better replicate soil profile gas diffusion dynamics, compared to how others have applied the pool dilution method (e.g. Yang et al., 2011; Wen et al., 2016). The results from this Chapter further suggest that the predominating processes producing and consuming N_2O can vary with relatively small differences in moisture contents, suggesting a possibility for devising a land management practice for minimising N_2O production and maximising its consumption.

7.4 Future research

Research presented in this thesis provides crucial insight into the potential of subsoil C sequestration and the behaviour and fate of GHGs in the subsoil. The results herein address critical knowledge gaps, make scientific advancements, and raise additional research questions that are worthy of investigation and would further the field. Here, the main areas of potential future research that have emerged from the Chapters in this thesis are summarised.

The research conducted on C sequestration potential in agricultural subsoils in Chapter 2 highlighted areas where improving our understanding would be of great benefit to the future direction of this field. The greatest challenge with this field is that the mechanisms that regulate C stabilization in subsoils and the factors driving long C residence times are still not well known (Chabbi et al., 2009; Rumpel and Kögel-Knabner, 2011; Wordell-Dietrich et al., 2017). While extensive study has improved our understanding of subsoils, as discussed in detail in Chapter 2, specific mechanisms occurring in the subsoil remain poorly understood. For example, many aspects of root tissue (e.g. suberin) chemistry is not well understood, despite its importance in root functioning (McCormack et al., 2015) and SOC persistence (Suseela et al., 2017), especially in deeper soil (Rasse et al., 2005). In addition, microbial products and necromass are thought to be important contributors to SOC in deep soil (Dove

et al., 2020; Wang et al., 2021), but how this is affected by soil chemistry, microbial properties and microbial stoichiometry (Wang et al., 2021) or compares with root derived C is not known. The importance of microbial products and necromass to long term SOC also depends on the poorly known necromass production processes and the spatial organisation of microbial communities in relation to soil C (Buckeridge et al., 2022).

In Figure 2.5, the response of mineral subsoils to elevated CO_2, waterlogging and drought was predicted based on the current literature and speculation (Chapter 2). However, the truth is that much of the vulnerability of subsoils to climate change remains to be fully understood. Subsoil chemistry seems to be critical in the outcome of increased temperatures on the decomposition of subsoil SOC (Possinger et al., 2021). As soil chemistry is important for the stabilisation of subsoil C (Rumpel and Kögel-Knabner, 2011), elevated temperatures could stimulate the mineralisation of large quantities of soil C and subsoils seem to be more vulnerable than topsoils to this (Soong et al., 2021). However, increased rooting and exudates from elevated CO_2 levels could counteract this loss, though greater concomitant microbial turnover of C can negate this (Philips et al., 2011). Therefore, understanding the response of subsoils and the vulnerability of C stabilisation mechanisms to short-term extreme weather events and long-term climate change is extremely important, especially as subsoil C sequestration success relies on the long-term stability of subsoil C. Finally, this lack of understanding also contributes to the uncertainty in model predictions of soil responses to climate change (Bradford et al., 2016).

While the title from Chapter 3, 'Addition of iron to agricultural topsoil and subsoil is not an effective C sequestration strategy' is in reference to the Fe forms, soil type and method of application in the study, it is yet to be determined whether this may be different in other contexts. As significant C sequestration with Fe addition has been observed (Silva et al., 2015), the context may be fundamental to the outcome of this C sequestration strategy. For example, targeting soils with low Fe contents and low capacities for mineral stabilisation of C (e.g. sandy soils) and adding C pre-associated with soluble Fe could have more success, as seen by Porras et al. (2018). However, the true test of this method is to investigate the potential of the large available sources of Fe (i.e. Fe-rich mining and wastewater by-product; Chen et al., 2015) as these are our best Fe sources for this strategy and would be beneficial to valorise (Collivignarelli et al., 2020).

Root access to deeper soil increased C respiration in Chapter 4, however, whether this C was predominantly root-derived or derived from native SOC was not determined. There has been evidence of the mineralisation of millennia old C from deep rooting (Shazhad et al., 2018), though the impact of deeper rooting on the trade-off between fresh C supply and old C loss is not well understood (Chenu et al., 2019; Tiefenbacher et al., 2021). In addition, understanding root architecture and distribution within the soil is important for C sequestration strategies aiming to enhance these, yet, due to being notoriously difficult to study they are not well understood (Mooney et al., 2012; Hou et al., 2022). X-ray computed micro-tomography is a fast-growing method in its application to disentangling the complex relationship between roots and soil (Mooney et al., 2012; Kravchenko and Guber, 2017). Further, the importance of arbuscular mycorrhizas and their role in C stabilization is still very uncertain and requires further work, particularly in conjunction with deeper rooting plant species.

The CGM, used in Chapters 4 and 5, is a valuable tool that can help understand the behaviour and fate of GHGs in the soil. In Chapter 4, this tool was applied to assess a C sequestration method for the first time, which gained valuable insight other more commonly used methods would not capture (i.e. chamber and eddy covariance methods). Therefore, it is important that use of the CGM continues with further validation and testing of its limitations across different soil and climatic contexts. This can also build a larger database for comparison and inclusion in modelling.

The novel application of the pool dilution method with dual headspaces in Chapter 6 produced compelling evidence. However, the dual headspace approach needs to be experimentally compared to the single headspace approach to decipher which method is best for replicating *in situ* processes and is worthy of recommendation. In addition, the results from Chapter 6 suggested that agricultural soil can have a large potential for both high N_2O production and consumption. If we can manage soil to induce higher consumption and reduced production of N_2O, this could be another land management tool that could contribute towards climate change mitigation. Application of this concept has been attempted recently by Stuchiner and von Fischer (2022), who by relieving the soils C limitation attained the ideal N_2O management scenario of increased N_2O consumption and decreased N_2O emissions (ICDE), which they measured by isotope pool dilution. However, the authors

did not measure whether the ICDE they observed was offset or complemented by CO_2 and CH_4 emissions. Therefore, an opportunity exists to test the net outcome following the addition of a C source to C-limited microbial communities.

For the best chances of farm scale interventions to be implemented, a robust evidence base covering a diverse range of soil types and climates is needed. The 'gold standard' in evidence is long term (>20 y) field experiments, as effects may only be apparent in the long term (Poulton, 1995). However, as understanding gained from field trials following set up takes years to decades to enter the scientific literature (and even longer into policy), we need faster methods to increase the amount of reliable evidence of C sequestration strategies generated. There are opportunities that can save valuable time needed for gathering evidence. For example, space-for-time substitutions have been found to result in data with relatively high accuracy (Yang et al., 2022) in less time, though their use is dependent on the context (Pickett, 1989). In addition, long on-going field trials can be valuable for modern studies, as demonstrated by Alcántara et al. (2016), who took advantage of an old management technique (deep inversion ploughing) practiced at a long-term trial 35-50 years prior to assess its effect on soil C. Alternative methods to time intensive direct measurements to assess the success of C sequestration attempts are described by Smith et al. (2020).

To summarise, the main future research priorities that have emerged from this thesis can be summarised by the following areas:

1. Determine the mechanisms that regulate C stabilization and the specific factors driving long C residence times in subsoils and quantify their relative importance.
2. Determine the vulnerability of subsoil C to climate change and extreme events.
3. Determine the potential for Fe addition for C sequestration using mining and wastewater treatment by-products.
4. Quantify the net outcome of deep rooting on soil C, harvestable biomass and GHG emissions.
5. Continue using and refining the CGM for insight into subsoil GHG behaviour and fate.
6. Test the net potential of increased N_2O consumption and decreased N_2O emissions management practices.

Take advantage of alternative study techniques to speed up long term evidence gathering.

7.5 Concluding remarks

In this thesis, crucial research questions on the potential of subsoil C sequestration and the behaviour and fate of subsoil GHGs were addressed. Using a diverse range of research methodologies and techniques, robust evidence was collected which advances our understanding of these subjects. Agricultural subsoils and the strategies that target them were found to have considerable potential for C sequestration. Further evidence was added to this base by experimentally testing two different strategies from novel perspectives. Finally, GHG measuring, tracing, and modelling methods were applied to improve our understanding of soil GHG behaviour and fate in the soil profile. A new approach to an emerging technique was developed that could improve its accuracy. Assessing the reliability and limitations of these different methodologies is important for scientific progress, but also adds to a valuable database needed for comparisons. Finally, soil GHG consumption processes were measured that may hold further potential for climate change mitigation if they can be managed, though further investigation is required.

7.6 References

Bradford, M.A., Wieder, W.R., Bonan, G.B., Fierer, N., Raymond, P.A. and Crowther, T.W., 2016. Managing uncertainty in soil carbon feedbacks to climate change. Nature Climate Change 6, 751-758.

Buckeridge, K.M., Creamer, C. and Whitaker, J., 2022. Deconstructing the microbial necromass continuum to inform soil carbon sequestration. Functional Ecology 36, 1396–1410.

Chabbi, A., Kögel-Knabner, I. and Rumpel, C., 2009. Stabilised carbon in subsoil horizons is located in spatially distinct parts of the soil profile. Soil Biology and Biochemistry 41, 256-261.

Chen, Z., Wang, X., Ge, Q., Guo, G., 2015. Iron oxide red wastewater treatment and recycling of iron-containing sludge. Journal of Cleaner Production 87, 558–566.

Chenu, C., Angers, D.A., Barré, P., Derrien, D., Arrouays, D. and Balesdent, J., 2019. Increasing organic stocks in agricultural soils: Knowledge gaps and potential innovations. Soil and Tillage Research 188, 41-52.

Collivignarelli, M.C., Abbà, A., Benigna, I., 2020. The reuse of biosolids on agricultural land: Critical issues and perspective. Water Environment Research 92, 11–25.

Dove, N.C., Arogyaswamy, K., Billings, S.A., Botthoff, J.K., Carey, C.J., Cisco, C., DeForest, J.L., Fairbanks, D., Fierer, N., Gallery, R.E. and Kaye, J.P., 2020. Continental-scale patterns of extracellular enzyme activity in the subsoil: an overlooked reservoir of microbial activity. Environmental Research Letters, 15, 1040.Eilers, K.G., Debenport, S., Anderson, S., Fierer, N., 2012. Digging deeper to find unique microbial communities: The strong effect of depth on the structure of bacterial and archaeal communities in soil. Soil Biology and Biochemistry 50, 58-65.

Fiedler, S.R., Buczko, U., Jurasinski, G., Glatzel, S., 2015. Soil respiration after tillage under different fertiliser treatments - implications for modelling and balancing. Soil Tillage Research, 150, 30–42.

Hou, L.H., Gao, W., Weng, Z.H., Doolette, C.L., Maksimenko, A., Hausermann, D., Zheng, Y., Tang, C., Lombi, E. and Kopittke, P.M., 2022. Use of X-ray tomography for examining root architecture in soils. Geoderma 405, 115405.

Hyland, J.J., Jones, D.L., Parkhill, K.A., Barnes, A.P., Williams, A.P., 2016. Farmers' perceptions of climate change: identifying types. Agriculture and Human Values 33, 323-339.

Kravchenko, A.N. and Guber, A.K., 2017. Soil pores and their contributions to soil carbon processes. Geoderma 287, 31-39.

McCormack, M.L., Dickie, I.A., Eissenstat, D.M., Fahey, T.J., Fernandez, C.W., Guo, D., Helmisaari, H.S., Hobbie, E.A., Iversen, C.M., Jackson, R.B. and Leppälammi-Kujansuu, J., 2015. Redefining fine roots improves understanding of below-ground contributions to terrestrial biosphere processes. New Phytologist 20, 505-518.

Mooney, S.J., Pridmore, T.P., Helliwell, J. and Bennett, M.J., 2012. Developing X-ray computed tomography to non-invasively image 3-D root systems architecture in soil. Plant and soil 352, 1-22.

Moran, D., Lucas, A. and Barnes, A., 2013. Mitigation win–win. Nature Climate Change 3, 611-613.

Phillips, R., P., Finzi, A., C., Bernhardt, E., S. 2011. Enhanced root exudation induces microbial feedbacks to N cycling in a pine forest under long-term CO_2 fumigation. Ecological Letters 14, 187-194.

Pickett, S.T., 1989. Space-for-time substitution as an alternative to long-term studies. In Long-term studies in ecology, 110-135. Springer, New York, NY.

Porras, R.C., Hicks Pries, C.E., Torn, M.S., Nico, P.S., 2018. Synthetic iron (hydr)oxide-glucose associations in subsurface soil: Effects on decomposability of mineral associated carbon. Science of the Total Environment 613, 342–351.

Possinger, A.R., Weiglein, T.L., Bowman, M.M., Gallo, A.C., Hatten, J.A., Heckman, K.A., Matosziuk, L.M., Nave, L.E., SanClements, M.D., Swanston, C.W. and Strahm, B.D., 2021. Climate effects on subsoil carbon loss mediated by soil chemistry. Environmental Science and Technology 55, 16224-16235.

Poulton, P.R., 1995. the importance of long-term trials in understanding sustainable farming systems: The Rothamsted Experience. Australian Journal of Experimental Agriculture 35, 825–834.

Rasse, D.P., Rumpel, C. and Dignac, M.F., 2005. Is soil carbon mostly root carbon? Mechanisms for a specific stabilisation. Plant and Soil 269, 341-356.

Ripple, W., Wolf, C., Newsome, T., Barnard, P., Moomaw, W. and Grandcolas, P., 2019. World scientists' warning of a climate emergency. BioScience, Oxford University Press.

Rumpel, C. and Kögel-Knabner, I., 2011. Deep soil organic matter—a key but poorly understood component of terrestrial C cycle. Plant and Soil 338, 143-158.

Shahzad, T., Rashid, M.I., Maire, V., Barot, S., Perveen, N., Alvarez, G., Mougin, C. and Fontaine, S., 2018. Root penetration in deep soil layers stimulates mineralization of millennia-old organic carbon. Soil Biology and Biochemistry 124, 150-160.

Silva, L.C.R., Doane, T.A., Corrêa, R.S., Valverde, V., Pereira, E.I.P., Horwath, W.R., 2015. Iron-mediated stabilization of soil carbon amplifies the benefits of ecological restoration in degraded lands. Ecological Applications 25, 1226–1234.

Smith, P., Soussana, J.F., Angers, D., Schipper, L., Chenu, C., Rasse, D.P., Batjes, N.H., Van Egmond, F., McNeill, S., Kuhnert, M. and Arias-Navarro, C., 2020. How to measure, report and verify soil carbon change to realize the potential of soil carbon sequestration for atmospheric greenhouse gas removal. Global Change Biology 26, 219-241.

Soong, J.L., Castanha, C., Hicks Pries, C.E., Ofiti, N., Porras, R.C., Riley, W.J., Schmidt, M.W. and Torn, M.S., 2021. Five years of whole-soil warming led to loss of subsoil carbon stocks and increased CO_2 efflux. Science Advances 7, p.eabd1343.

Stuchiner, E.R. and von Fischer, J.C., 2022. Using isotope pool dilution to understand how organic carbon additions affect N_2O consumption in diverse soils. Global Change Biology 28, 4163-4179.

Suseela, V., Tharayil, N., Pendall, E., Rao, A.M. and Volder, A., 2017. Warming and elevated CO_2 alter the suberin chemistry in roots of photosynthetically divergent grass species. AoB Plants, 9.

Tiefenbacher, A., Sandén, T., Haslmayr, H.P., Miloczki, J., Wenzel, W. and Spiegel, H., 2021. Optimizing carbon sequestration in croplands: a synthesis. Agronomy 11, 882.

Wang, B., An, S., Liang, C., Liu, Y. and Kuzyakov, Y., 2021. Microbial necromass as the source of soil organic carbon in global ecosystems. Soil Biology and Biochemistry, 162, 108422.

Wen, Y., Chen, Z., Dannenmann, M., Carminati, A., Willibald, G., Kiese, R., Wolf, B., Veldkamp, E., Butterbach-Bahl, K. and Corre, M.D., 2016. Disentangling gross N_2O production and consumption in soil. Scientific Reports 6, 1-8.

Wordell-Dietrich, P., Don, A. and Helfrich, M., 2017. Controlling factors for the stability of subsoil carbon in a Dystric Cambisol. Geoderma 304, 40-48.

Yang, R.M., Zhu, C.M., Zhang, X. and Huang, L.M., 2022. A preliminary assessment of the space-for-time substitution method in soil carbon change prediction. Soil Science Society of America Journal 86, 423-434.

Yang, W.H., Teh, Y.A. and Silver, W.L., 2011. A test of a field-based ^{15}N–nitrous oxide pool dilution technique to measure gross N_2O production in soil. Global Change Biology 17, 3577-3588.

Appendix 1 – Supplementary Material for Chapter 2

S1.1. Systematic review and data exportation for Figure 1 and 2

We conducted a systematic review on the 12th October 2020 to obtain studies that measured different soil properties in top- and subsoils. We used Web of Science as the database and used the search string 'TS= (propert* AND ("deep soil" OR subsoil$ OR "B horizon"))' (see Table S1 for search term strategy). Studies were selected using predetermined criteria (Table S3) and in total, 211 studies met the criteria for inclusion (Fig. S1. PRISMA diagram). Once these studies were selected, we exported data on soil depth and/or horizon, soil properties, soil order, location coordinates, and land use type into an Excel spreadsheet. Each soil property measurement was converted into common units where possible. From the 211 individual studies collected, there were 1833 individual soil profile measurements (Table S2), 665 in the A and 1097 in the B horizon (Fig. S2).

Conversion of soil orders between soil classification systems were done using conversion tables from Landon (1984) and FAO (1990). The breakdown of the soil orders covered by the included studies are reported in Table S3. We used a topsoil-subsoil (A-B horizon) boundary of 30 cm when categorising the measurements unless the authors defined the boundary within the study. Where depth intervals crossed the 30 cm boundary (e.g. 25-50 cm), we relied on the author's own classification of the soil depths whether this would be best described as the A or B horizon. Where this was absent, we classified depth ranges based on whether the average of the range was <30 cm as A horizon (e.g. 25-50 cm interval = (25+50)/2 = 37.5 cm .: B horizon). Averaged ranges exceeding 30 cm and any beginning at ≥30 cm were classified as B horizons. Measurements were excluded when their soil depths were defined as C horizon or any depth ranges beginning at ≥100 cm, where the horizon was not specified.

If no location coordinates were given, the coordinates of the closest identifiable place related to the study were taken (e.g. affiliated university or institution). The location of the individual studies, the soil orders measured, and the number of soil profile measurements are presented in Figure S3.

S1.2. Statistical analysis of data included in Figure 1

The data was tested for homoscedasticity with the Fisher's F-Test before the data from the A and B horizons was compared with a student's 2-sample t-test or a Welch's Test, if the variance test was failed (i.e. $p<0.05$). For datasets that were $n<30$, a Shapiro-Wilk Test was performed, and a Mann-Whitney U Test used in cases where $p<0.05$.

References

Landon, J.R., 1984. A Handbook for soil survey and agricultural land evaluation in the tropics and subtropics. London and New York: Longman, p. 238-239.

Food and Agriculture Organisation (FAO), 1990. World Reference Base for Soil Resources, Rome Italy.

Table S1. Search term strategy for Web of Science systematic search. The final search term in italic was selected.

Criteria	Included
Agricultural soil (i.e. arable, pasture, agricultural grassland, agroforestry, vineyard or orchard)	✓
Non-agricultural soil	✗
≥1 soil property measured (of those we were interested in) in appropriate or convertible units	✓
Soil properties modelled or estimated	✗
Soil type stated	✓
Soil type not stated or not convertible to WRB or USDA classification systems	✗
Topsoil measurement only	✗
Measurement of topsoil and subsoil or only subsoil	✓
No treatment free soil profile was measured	✗
Measurements from meta-analysis or review	✗
Unobtainable study	✗
Manuscript not in English	✗
Fewer than 5 studies for any soil order	✗

Table S2. Selection criteria of studies for use in the systematic review.

Search term	Results	Comments
TS = (Soil AND depth? OR subsoil OR deep)	784,365	too many
TS = (Soil AND Propert* AND depth? OR subsoil OR deep)	772,325	too many
TS = (soil* NEAR/5 (depth? OR deep) OR subsoil? AND Propert*)	19,077	too many/unrelated topics
TS = (soil depth? OR deep soil? OR subsoil? AND Propert*)	20,371	too many/unrelated topics
TS = (deep soil? OR subsoil? AND Propert*)	292	too few/unrelated topics
TS = (deep soil? OR subsoil?)	12,314	too many/unrelated topics
TS = ("deep soil" OR subsoil?)	3,888	too many unrelated topics
TS = ("deep soil" OR subsoil? OR "B horizon")	4,747	too many unrelated topics
TS = ("deep soil" OR "subsoil" OR "B horizon")	12,115	too many
TS= (propert AND ("deep soil" OR subsoil$ OR "B horizon"))*	*2,863*	*Relevant and realistic quantity*

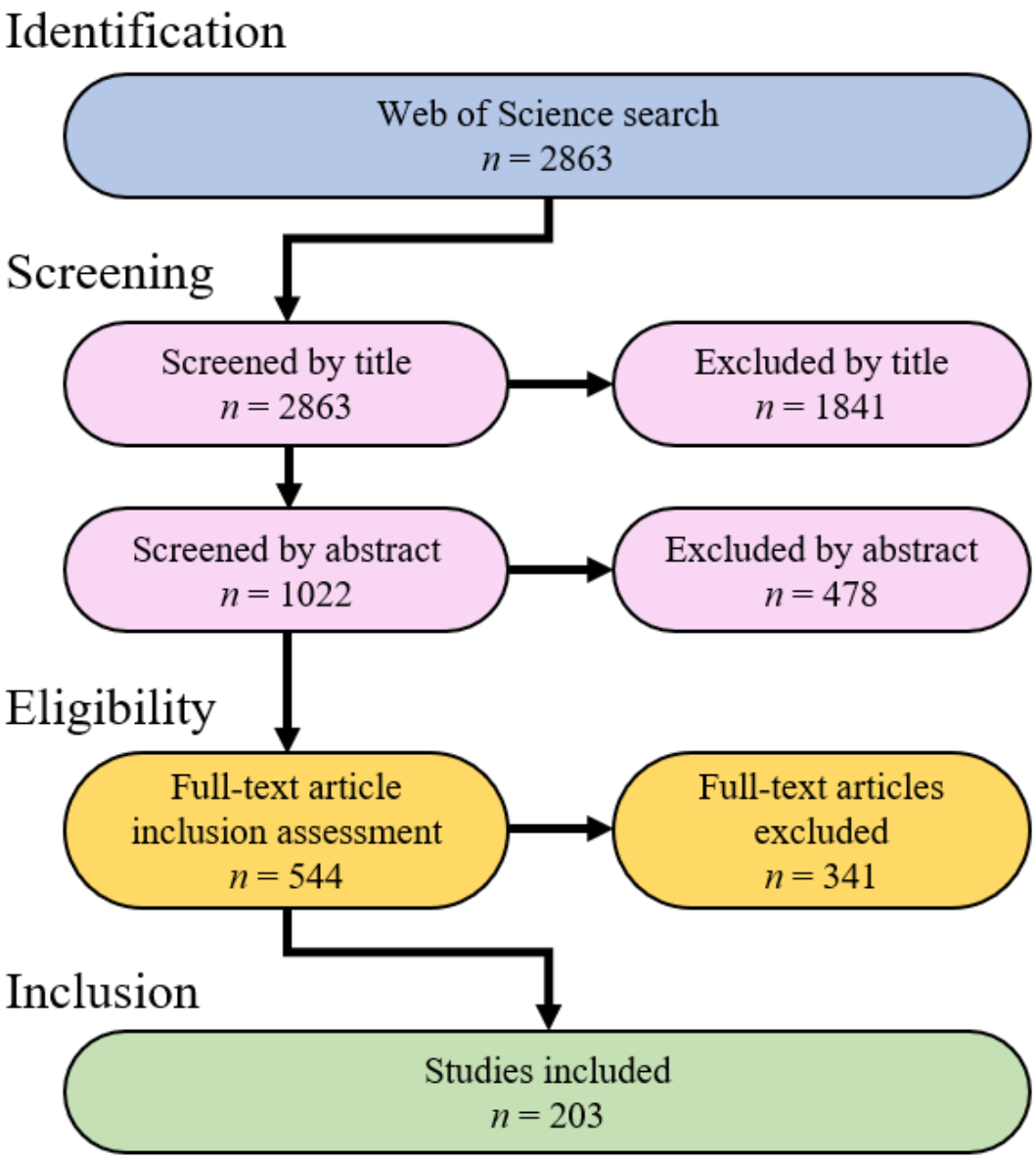

Fig. S1 PRISMA diagram of the systematic literature review process.

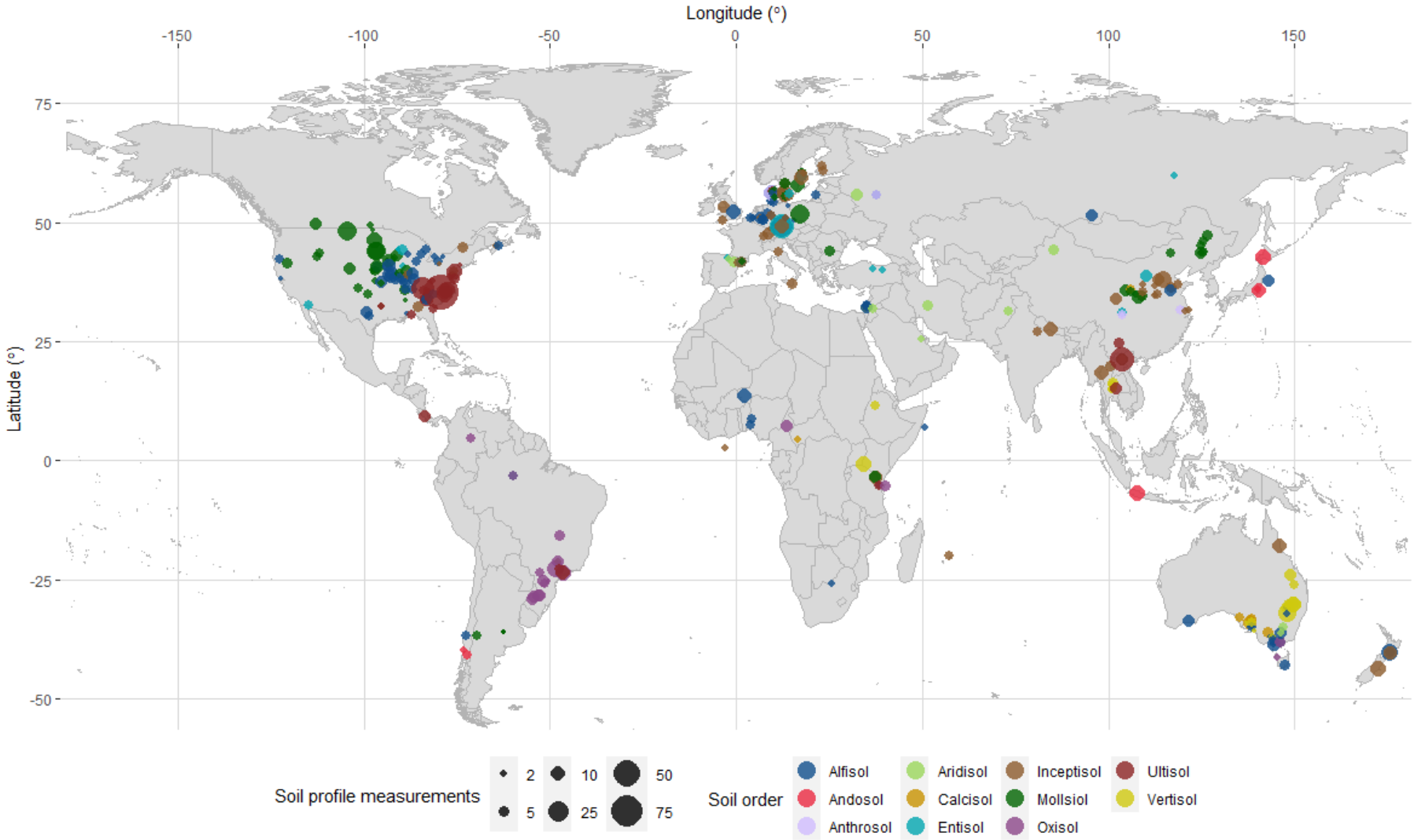

Fig. S2 Map of the 11 soil orders included in the review from 203 individual studies and the number of soil profile measurements made at each geographical location (*n* = 1762).

Table S3. Breakdown of the soil orders and soil profile measurements in the included studies. Soil orders are ranked based on the number of studies.

Soil order (USDA; unless stated otherwise)	**Studies** (#)	**Soil profile measurements** (#)
Inceptisol	59	310
Alfisol	57	382
Mollisol	40	300
Entisol	18	95
Ultisol	16	303
Vertisol	16	126
Oxisol	16	105
Aridisol	11	40
Calcisol*	6	34
Anthrosol*	6	27
Andosol	5	42
Totals 11	203[†]	1762

*no appropriate conversion from WRB to USDA classification identified

[†] studies that included measurements of more than one soil order were not counted more than once.

S2. Subsoil C sequestration strategy systematic search and data exportation for Figure 4

Due to the lower frequency of relevant studies compared to S1.1, the title and abstract screening stages (Fig. S1) were skipped and full-text eligibility was assessed before data was extracted. Search terms (Table S4) were chosen to generate data of 10 or more relevant studies for each sequestration strategy. Unfortunately, this target was not met in 4 of 7 strategies due to the low amount or absence of studies meeting the inclusion criteria. We attribute this primarily to the studies not existing, although we do concede that the search terms chosen may not have captured every relevant accessible study.

Differences between the rates of C storage between the different C sequestration strategies across the whole soil profiles were tested with a 2-way ANOVA and Tukey multiple comparisons test ($p<0.05$).

Table S4. Systematic search of literature (Web of Science) for subsoil-specific C sequestration strategies and their sequestration rates. All studies included are *in situ* and on agricultural (arable, pasture, vineyard, agroforestry) soil. Subsoil is defined as B horizon or >30 cm, unless otherwise stated in the individual study. Search terms were chosen for highest number of relevant results for inclusion of ≥10 studies. Web of Science searches conducted in May 2021. OM, organic matter; GHG, greenhouse gases.

Sequestration strategy	**Search terms** (Web of Science)	**Search results** (# studies)	**Inclusion criteria**	**Included studies** (#)	**Individual measurements** (#)	**Comments**
Deep ploughing	(TS=(carbon AND (sequest* OR storage OR "organic") AND "deep" NEAR/5 ("plough*" OR "tillag*" OR "flip*") AND ("crop*" OR "arable" OR "pasture" OR "agricultur*")))	164	Infrequent (>10 years) full inversion tillage to a depth below the topsoil layer.	6	87	5 studies excluded – measured <10 years apart
OM burial	(TS=(carbon AND (sequest* OR storage OR "organic") AND ("deep" OR "subsoil" OR "B horizon") AND ("organic matter" OR "OM" OR "straw" OR "mulch" OR "pellet*" OR "manure" OR "slurry" OR "biosolid*" OR "residue*" OR "compost") NEAR/18 ("return*" OR "incorporat*" OR "buri*" OR "add*" OR "inject*" OR "ameliorat*") AND ("crop*" OR "arable" OR "pasture" OR "agricultur*")))	202	OM source introduced into the subsoil.	10	53	-
Biochar burial	(TS=(carbon AND (sequest* OR storage OR "organic") AND ("deep" OR "subsoil" OR "B horizon"OR "subsurface") AND ("black c*" OR pyroli*" OR "biochar* " OR "charcoal*" OR "bio-char" OR "carbonise*" OR "bio char" OR "char" OR "charred") AND ("crop*" OR "arable" OR "pasture" OR "agricultur*")))	74	Pyrolysed OM (i.e. biochar) introduced into the subsoil layer.	-	-	Biochar commonly added to surface or incorporated into topsoil, not subsoil.
Deep rooting	(TS=(carbon AND (sequest* OR storage OR organic) AND "root*" NEAR/5 ("subsoil" OR "B* horizon" OR "deep") AND ("arable" OR "pasture" OR "crop" OR "agricultur*")))	130	C measured below topsoil layer where agricultural plant roots have penetrated to.	12	171	-
Fe addition	(TS=(carbon AND (sequest* OR storage OR organic OR biosolid*) AND ("deep" OR "subsoil" OR "B horizon") AND ("red mud" OR "iron*" OR "Fe" OR "ferric*" OR ferrous*") AND (crop OR "arable" OR "pasture" OR "agricultur*")))	130	Any form of Fe added to subsoil for C sequestration.	-	-	No studies found that match the criteria.
Clay addition	(TS=(carbon AND ("deep" OR "subsoil" OR "B horizon" OR "subsurface")AND ("clay*" OR "kaolin*" OR "smectit*" OR illit*) NEAR/25 ("amend*" OR "applicat*" OR "buried" OR "bury" OR "incorporat*" OR "buri*" OR "add*" OR "ameliorat*" OR "plough*" OR tillage) AND ("crop" OR "arable" OR "pasture" OR "agricultur*")))	104	Addition of clay to subsoil for C sequestration.	2	20	Clay commonly added to ameliorate sandy topsoils, but rarely to subsoils.
Water table management	(TS=(carbon AND ("deep" OR "subsoil" OR "B horizon") AND ("water table" OR "water-table" OR "watertable" OR "aquifer" OR "water level") NEAR/25 ("tile" OR "free drain*" OR "manage*" OR "drain*" OR "artificial*" OR "raise*" OR "lower*" OR "drawdown") AND ("arable" OR "pasture" OR "agricultur*")))	32	Water table managed to enhance C sequestration or reduce C loss.	-	-	GHG fluxes commonly measured, no studies met inclusion criteria.

Appendix 2 – Supplementary Material for Chapter 3

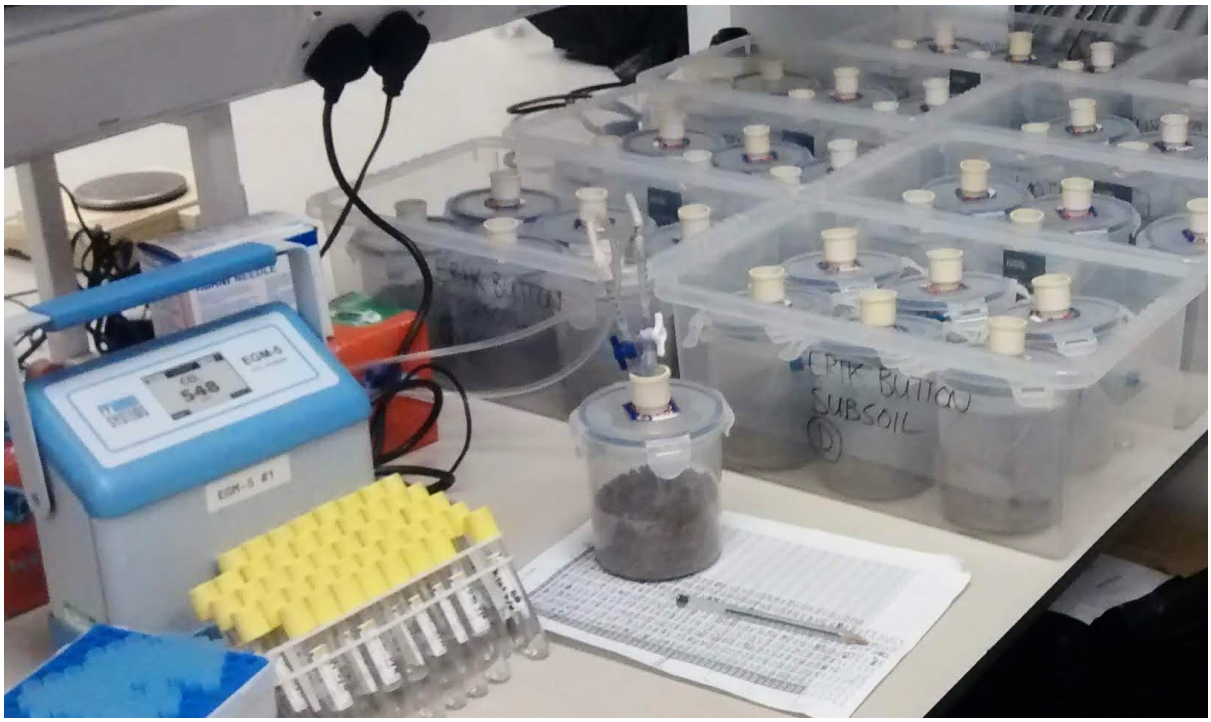

Fig. S1 Photograph of the soil mesocosms (transparent polypropylene containers) used in the experiment and the operation of the EGM 5 soil respirometer (grey and blue instrument).

Table S1. Cumulative and mean values (SEM) of the measured soil properties at different Fe application rates in top- and subsoils across the 45 d incubation (*n* = 4). *Below limit of detection

		$Fe(OH)_3$ application rate (mg kg^{-1})						$FeCl_2$ application rate (mg kg^{-1})					
Measurement	**Soil Depth**	**0**	**1**	**10**	**100**	**1,000**	**5,000**	**0**	**1**	**10**	**100**	**1,000**	**5,000**
Cumul. CO_2 efflux (ug CO_2-C g^{-1})	Topsoil	18.5 (0.9)	18.9 (0.8)	18.4 (1.9)	18.3 (2.0)	18.8 (1.7)	18.3 (1.0)	11.1 (2.2)	11.1 (1.9)	10.8 (1.9)	10.7 (1.3)	10.1 (1.1)	15.4 (1.3)
	Subsoil	4.3 (0.8)	4.6 (1.0)	4.4 (0.8)	4.0 (0.7)	3.7 (0.8)	3.3 (0.6)	2.7 (0.6)	2.5 (0.5)	2.2 (0.7)	3.2 (1.0)	6.2 (0.7)	8.0 (2.5)
DOC (mg l^{-1})	Topsoil	11.7 (0.5)	12.7 (0.5)	13.2 (0.9)	13.7 (1.1)	10.9 (0.7)	8.9 (0.5)	19.5 (1.7)	19.7 (1.7)	15.7 (1.9)	9.8 (1.3)	6.9 (0.8)	78.5 (4.0)
	Subsoil	5.1 (0.7)	4.2 (0.5)	4.6 (0.7)	4.2 (0.5)	4.4 (0.5)	3.1 (0.3)	6.7 (1.4)	7.4 (1.2)	5.1 (0.7)	4.1 (1.0)	12.8 (6.1)	30.7 (3.9)
pH	Topsoil	7.2 (0.1)	7.3 (0.1)	7.7 (0.08)	7.4 (0.1)	7.4 (0.1)	7.4 (0.1)	7.7 (0.1)	8.0 (0.1)	7.7 (0.08)	7.1 (0.06)	4.4 (0.08)	2.5 (0.03)
	Subsoil	6.9 (0.05)	6.9 (0.04)	7.4 (0.06)	6.9 (0.04)	6.9 (0.03)	6.9 (0.04)	7.6 (0.1)	7.5 (0.06)	7.4 (0.1)	6.5 (0.09)	3.9 (0.06)	2.3 (0.02)
EC (mS cm^{-1})	Topsoil	2.1 (0.3)	2.5 (0.3)	2.5 (0.3)	2.4 (0.4)	2.2 (0.3)	2.0 (0.2)	0.3 (0.01)	0.3 (0.01)	0.4 (0.03)	1.1 (0.04)	5.0 (0.2)	19.4 (0.5)
	Subsoil	1.0 (0.1)	0.9 (0.1)	1.0 (0.1)	1.0 (0.1)	1.1 (0.1)	1.0 (0.1)	0.3 (0.01)	0.3 (0.01)	0.4 (0.02)	1.2 (0.04)	5.9 (0.3)	22.6 (0.6)
MRP (mg l^{-1})	Topsoil	0.1 (0.01)	0.1 (0.008)	0.1 (0.01)	0.1 (0.01)	0.1 (0.009)	0.06 (0.006)	0.1 (0.02)	0.01 (0.01)	0.1 (0.02)	0.06 (0.007)	0.03 (0.008)	*
	Subsoil	0.04 (0.006)	0.03 (0.006)	0.03 (0.007)	0.03 (0.004)	0.3 (0.007)	0.02 (0.009)	0.02 (0.004)	0.02 (0.005)	0.03 (0.02)	0.05 (0.02)	0.02 (0.004)	*
Cumul. ^{14}C-Glucose (% of tot. ^{14}C added)	Topsoil	9.2 (1.4)	-	-	8.5 (1.4)	-	8.1 (1.3)	8.5 (1.4)	-	-	6.5 (1.2)	-	5.3 (1.2)
	Subsoil	4.5 (1.2)	-	-	5.0 (1.3)	-	4.3 (1.1)	4.8 (1.3)	-	-	3.3 (0.8)	-	0.4 (0.09)
Cumul. ^{14}C-Citrate (% of tot. ^{14}C added)	Topsoil	17.3 (3.5)	-	-	15.1 (3.2)	-	13.6 (3.0)	16.7 (3.5)	-	-	12.2 (2.8)	-	0.4 (0.04)
	Subsoil	9.5 (2.5)	-	-	9.7 (2.6)	-	9.0 (2.3)	9.6 (2.5)	-	-	6.1 (1.8)	-	0.4 (0.04)
Cumul. ^{14}C-Plant Matter (% of tot. ^{14}C added)	Topsoil	8.4 (1.3)	-	-	8.5 (1.2)	-	7.9 (1.3)	8.6 (1.3)	-	-	7.4 (1.2)	-	3.6 (0.7)
	Subsoil	7.7 (1.3)	-	-	6.0 (1.0)	-	6.4 (1.1)	7.1 (1.2)	-	-	6.9 (1.2)	-	2.6 (0.6)

Table S2. C-partitioning (% of total label added) in top- and subsoil following the addition of ^{14}C-labelled glucose, citrate or plant matter with different rates of Fe(III) or Fe(II) iron. Values are means of four replicates. Different letters represent significant differences (p<0.05) between iron rates of both depths for each ^{14}C pool and Fe form.

Fe	Fe rate	Evolved (%)		Extracted* (%)		Remainder (%)	
	(mg kg^{-1})	Topsoil	Subsoil	Topsoil	Subsoil	Topsoil	Subsoil
		----------Glucose----------					
$Fe(OH)_3$	0	23^{a}	19^{a}	3^{a}	3^{a}	74^{a}	78^{a}
	100	22^{a}	21^{a}	3^{a}	3^{a}	75^{a}	76^{a}
	5,000	20^{a}	18^{a}	3^{a}	3^{a}	77^{a}	79^{a}
$FeCl_2$	0	22^{a}	21^{a}	3^{a}	3^{a}	75^{a}	76^{a}
	100	18^{ab}	14^{b}	3^{ab}	3^{b}	79^{a}	83^{b}
	5,000	19^{ab}	1^{c}	3^{ab}	4^{c}	78^{a}	95^{c}
		----------Citrate----------					
$Fe(OH)_3$	0	52^{a}	38^{cd}	7^{a}	12^{b}	41^{a}	50^{b}
	100	48^{ab}	38^{cd}	10^{ab}	11^{b}	42^{a}	50^{b}
	5,000	44^{bc}	36^{d}	11^{b}	14^{b}	45^{a}	51^{b}
$FeCl_2$	0	52^{a}	39^{b}	9^{a}	12^{b}	40^{a}	49^{b}
	100	41^{ab}	27^{c}	8^{a}	12^{b}	51^{b}	61^{c}
	5,000	1^{d}	1^{d}	4^{c}	4^{c}	95^{d}	95^{d}
		----------Plant matter----------					
$Fe(OH)_3$	0	25^{a}	24^{ab}	3^{a}	3^{ab}	72^{a}	73^{ab}
	100	25^{a}	19^{c}	3^{a}	3^{c}	72^{a}	77^{c}
	5,000	24^{ab}	21^{b}	3^{ab}	3^{bc}	73^{ab}	76^{bc}
$FeCl_2$	0	25^{a}	22^{a}	3^{a}	3^{a}	72^{a}	74^{a}
	100	23^{a}	21^{a}	3^{a}	3^{a}	74^{a}	75^{a}
	5,000	13^{b}	12^{b}	4^{b}	4^{b}	83^{b}	85^{b}

*^{14}C remaining in solution extracted by 1 M NaCl (glucose), 0.5 M phosphate buffer at pH 6.5 (citrate) and 0.5 M K_2SO_4 (plant matter).

S1. Sampling time point contributions to total soil CO_2 efflux

While there was no difference in the t = 1 – 43 average contributions to the overall CO_2 efflux in the topsoil (Fig. S1), the contributions at t = 0 increased with Fe rate with the 1,000 and 5,000 mg kg^{-1} rates contributing over 3 times more to the total cumulative soil CO_2 efflux than the control (d.f. = 5, F = 19.7, p < 0.001). In the subsoil, the 100, 1,000 and 5,000 mg Fe kg^{-1} rates contributed 3, 4.8 and 5.2 times more to the overall efflux compared to the control (d.f. = 5, F = 2.6, p = 0.037), respectively. As in the topsoil, the t = 1 – 43 average contributions to the overall efflux in the subsoil did not differ.

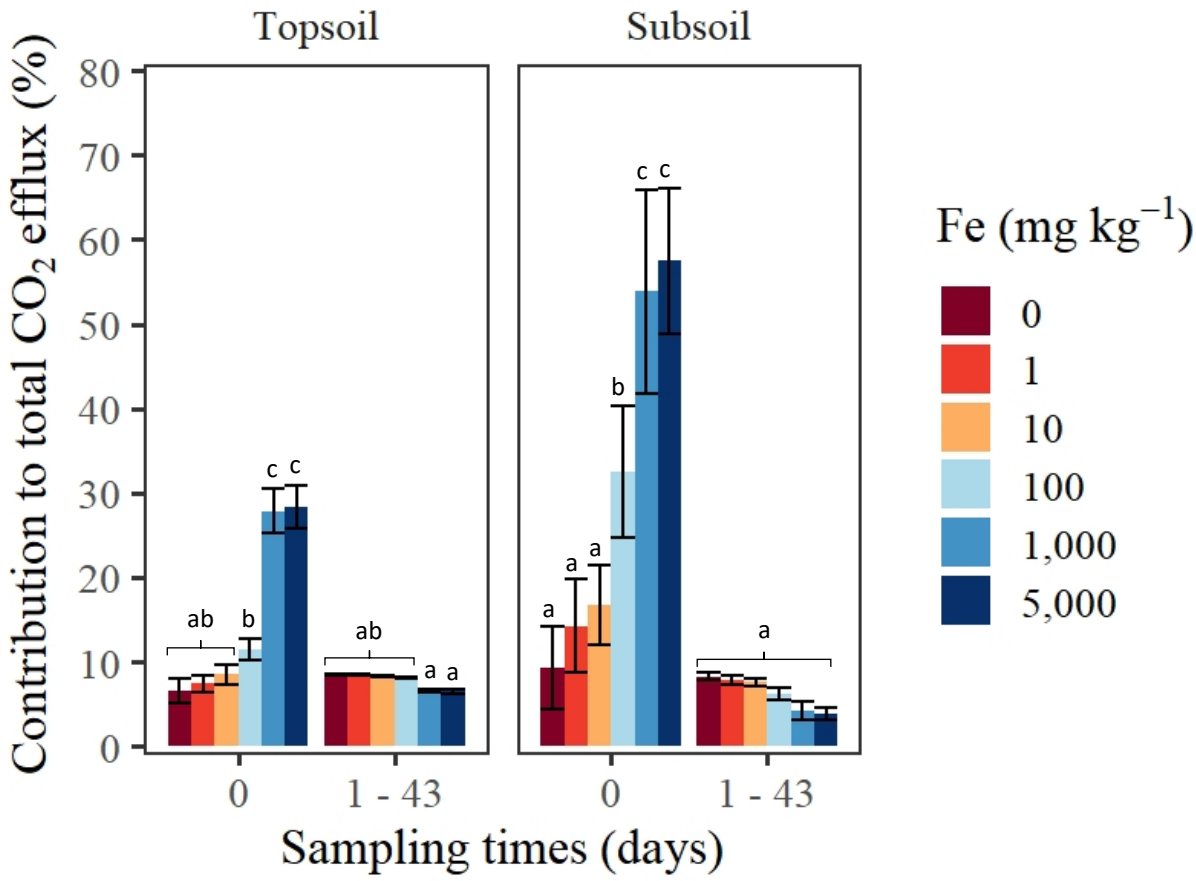

Fig. S2 Contribution (%) of the t = 0 and the average of the t = 1 – 43 sampling time points (11) to the total cumulative soil CO_2 efflux from top- and subsoil (mean ± SEM) incubations (n = 4) with the addition of different rates of Fe(II) iron. Different letters correspond to significant differences (p < 0.05) between iron rates and sampling times.

S2. pH driven CO_2 production

The addition of Fe(II) induces a shift in soil pH. To test whether the initial high rate of CO_2 production shown in Figure S1 was partly driven independent of Fe(III) *per se* (i.e. was due to a change in pH), a short incubation was undertaken to mimic the main incubation of this study without any Fe addition but in which pH was manipulated. To do this, HCl was added to soil at pH values equivalent to the 1,000 and 5,000 mg Fe kg^{-1} treatments (i.e. pH 2.9 and 2.0). This was done by amending distilled water with 1 M HCl until the desired pH was reached. Unamended distilled water (pH ca. 6.3) was added as the 0 mg Fe kg^{-1} rate (control). 400 g top- and subsoil replicates (n = 3) were sampled with an EGM-5 (as performed in the main incubation experiment) at t = 0, 6, 24, 30 and 48 h after the addition of the HCl treatments. At the initial t = 0, a 93 and 123% higher CO_2 efflux was measured in the top- (d.f. = 2, F = 3.6, p = 0.044) and subsoil (d.f. = 2, F = 6.7, p = 0.005) following the pH-amended water equivalent to the 5,000 mg kg^{-1} rate compared to the control (Fig. S2), respectively. A lower increase of 27 and 28% was observed in the 1,000 mg kg^{-1} pH-equivalent rate in the top- and subsoil compared to the control. After t = 6 h onwards, pH has no effect on soil CO_2 efflux.

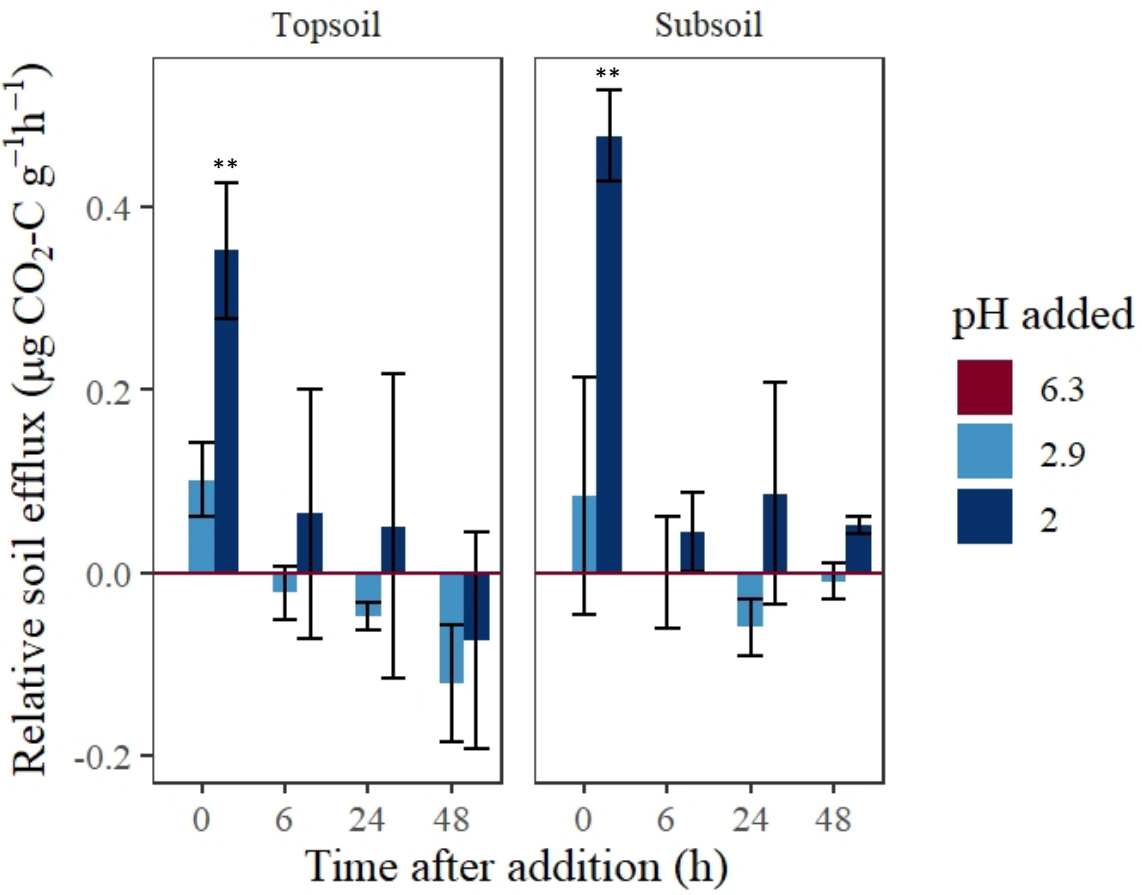

Fig. S3 Soil CO_2 efflux from top- and subsoil (mean ± SEM) incubations (n = 3) over 2 days with the addition of distilled water amended with HCl to the pH-equivalent of 1,000 and 5,000 mg Fe kg^{-1} of Fe(II) addition (as in Fig. 1). CO_2 efflux is graphed relative to the control (pH 6.3) for each time point. Stars represent the level of significance between the low pH additions (2 and 2.9) and the control at: *** $p < 0.001$; ** $p < 0.01$; * $p < 0.05$ within the soil depth.

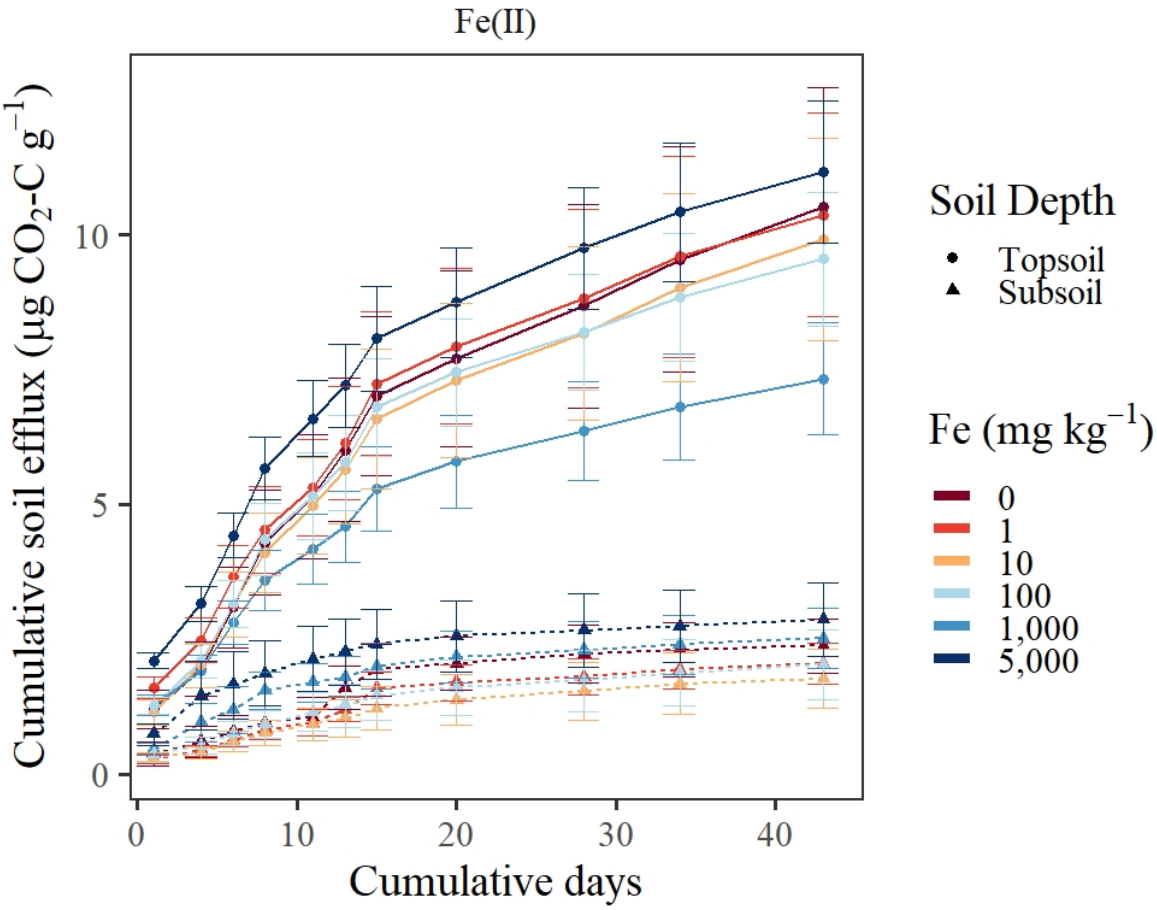

Fig. S4 Cumulative soil CO_2 efflux from top- and subsoil (mean ± SEM) incubations (*n* =4) over 45 days with the addition of different rates of Fe(II). Day 0 data are excluded, and CO_2 efflux is cumulated from day 1. Values correspond to the g dry weight equivalent.

Appendix 3 – Supplementary Material for Chapter 4

Table S1. The best fits of different trend line types for mean soil temperatures of different months and depths in 2019. Bold numbers represent the greatest mean variation explained.

	Mean soil temperature (°C)			Variation explained (R^2)			
	10 cm	20 cm	30 cm	Linear	Expon.	Log.	Power
May	14.8	14.5	14.3	0.96	1.00	0.97	1.00
Jun	16.7	16.3	16.1	0.97	1.00	0.97	1.00
Jul	19.3	19.0	18.8	0.98	1.00	0.98	1.00
Aug	18.3	18.3	18.2	1.00	0.97	1.00	0.97
Sep	15.6	15.8	15.7	0.34	0.24	0.34	0.24
Mean				0.85	**0.842**	0.852	**0.842**

Table S2. The best fits of different trend line types for mean soil moisture of different months and depths in 2019. The value in bold represents the greatest mean variation explained.

	Mean soil moisture ($cm^3\ cm^{-3}$)			Variation explained (R^2)			
	10 cm	20 cm	30 cm	Linear	Expon.	Log.	Power
May	31.1	30.7	27.4	0.83	0.80	0.82	0.80
Jun	27.9	28.3	27.2	0.39	0.45	0.39	0.46
Jul	19.6	20.2	18.4	0.41	0.48	0.42	0.49
Aug	25.4	25.5	23.1	0.71	0.72	0.71	0.73
Sep	28.9	28.1	24.9	0.89	0.84	0.88	0.84
Mean				0.646	0.658	0.644	**0.664**

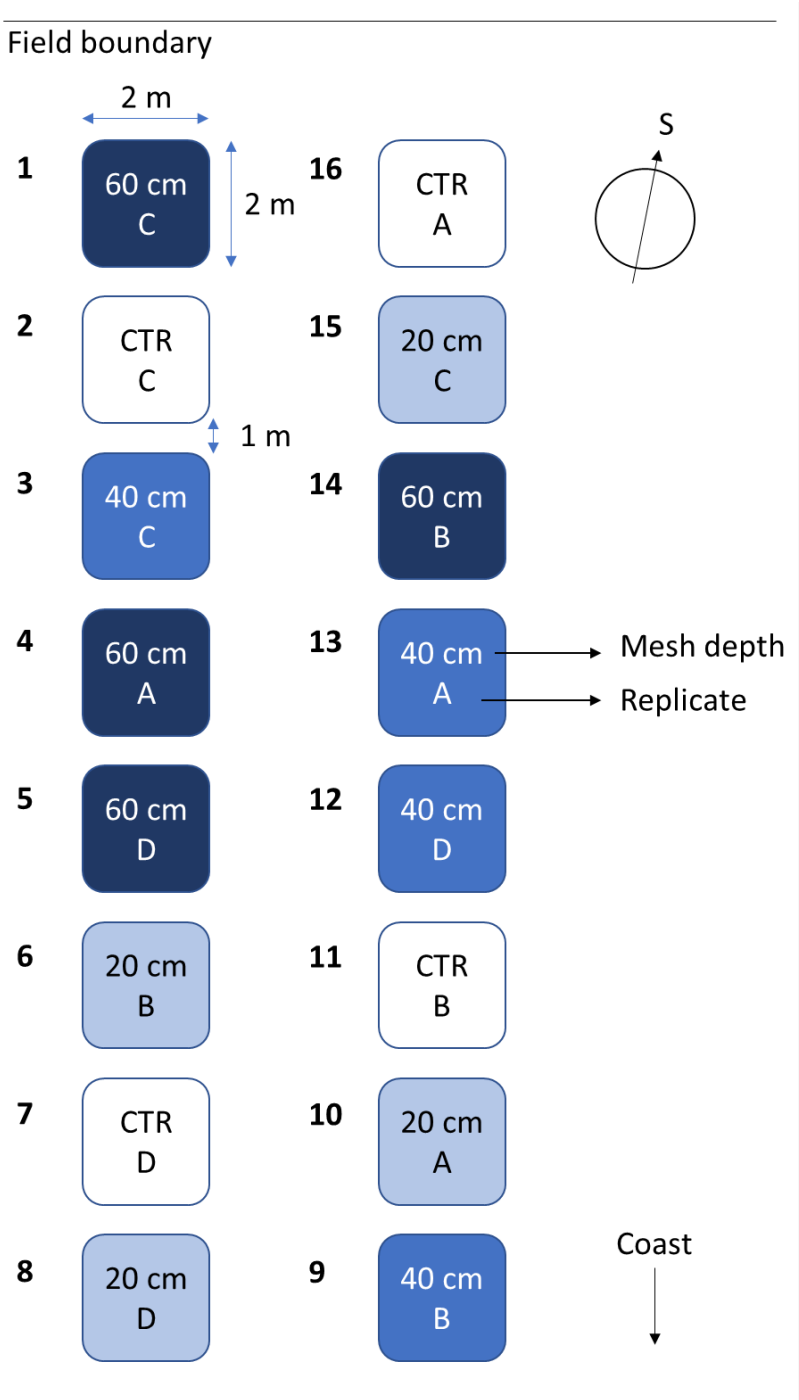

Fig. S1 Layout of the randomly distributed experimental plots used for this study.

Appendix 4 – Supplementary Material for Chapter 5

S1. Erroneous GHG data

The erroneous GHG data in the 2018 maize growing season dataset was most likely due to failed GC analysis (i.e. settings not appropriately sensitive, saturation of the peaks, drift). Concentrations far outside of the range of the standards used (CH_4: 1.42 - 25.8 ppm; N_2O: 310 - 4900 ppb; CO_2: 258.5 - 2504 ppm) were less likely to be accurate and in some cases would result in zeros or impossibly high concentrations. In addition, poor sealing of the vials (faulty vial crimper) and/or extended storage may have contributed to this, which was avoided in 2019 with more appropriate GC settings, a new crimper and shorter storage time.

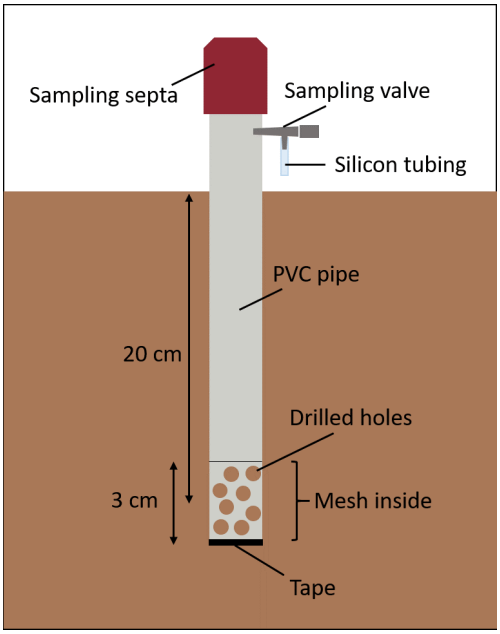

Fig. S1 Schematic diagram of a gas collection pipe (20 cm depth) used in the trial.

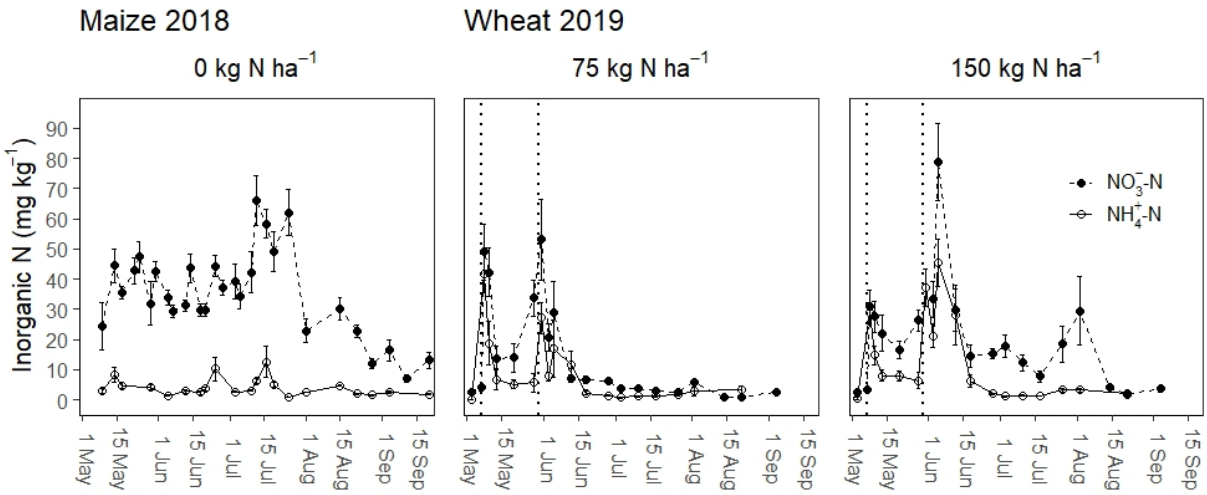

Fig. S2 Soil NH_4^+-N and NO_3^--N (mean ± SEM) content (per dry weight of soil) in the 0-5 cm layer of field plots under either maize (*n* = 12, no fertiliser) or wheat (*n* = 4; 75 and 150 kg N ha^{-1}) production. The vertical dotted lines represent the fertiliser application dates, where 40 kg ha^{-1} ammonium nitrate was applied on the 7th May and 35 and 110 kg ha^{-1} were applied on the 31st May to the 75 and 150 kg ha^{-1} fertilised plots in the wheat field, depending on the N treatment.

References

Allaire, S.E., Lafond, J.A., Cabral, A.R., Lange, S.F., 2008. Measurement of gas diffusion through soils: Comparison of laboratory methods. Journal of Environmental Monitoring 10, 1326–1336.

Li, Z., Kelliher, F.M., 2005. Determining nitrous oxide emissions from subsurface measurements in grazed pasture: A field trial of alternative technology. Australian Journal of Soil Research 43, 677–687.

Maier, M., Schack-Kirchner, H., 2014. Using the gradient method to determine soil gas flux: A review. Agricultural and Forest Meteorology 192–193, 78–95.

Rolston, D. E., and Moldrup, P. (2002). 4.3 Gas Diffusivity. Methods of soil analysis: Part 4 physical methods, 5, 1113-1139.

Wang, Y., Li, X., Dong, W., Wu, D., Hu, C., Zhang, Y., Luo, Y., 2018. Depth-dependent greenhouse gas production and consumption in an upland cropping system in northern China. Geoderma 319, 100–112.

Xiao, X., Kuang, X., Sauer, T.J., Heitman, J.L., Horton, R., 2015. Bare Soil Carbon Dioxide Fluxes with Time and Depth Determined by High-Resolution Gradient-Based Measurements and Surface Chambers. Soil Science Society of America Journal 79, 1073.

Appendix 5 – Supplementary Material for Chapter 6

S1. Incubation system specifications

The headspace chamber was made of an 83 mm x 60 mm Delrin® rod (polyoxymethylene; Gilbert Curry Industrial Plastics Co Ltd., Coventry, UK) with the inside 53 mm bored out (Fig. 6.1). Stainless steel 3.18 mm and 6.35 mm Swagelok connectors (Swagelok Company, Solon, OH) connected the headspace with a 3.18 mm stainless steel and a 6.35 mm Teflon tube (a.k.a. polytetrafluoroethene; Context Pneumatic Supplies Ltd., Bolton, UK), respectively. A 3 m long 6.35 mm diameter Teflon sampling tube (53.4 ml) was connected to the headspace tube via 6.35 mm Swagelok union. This tube was tested against 3 other sampling approaches using a known concentration of standard N_2O gas and was chosen as the most effective sampling option (Fig. S1 and Fig. S2). Silicone grease, applied in the joint between the core and the lid and between the headspace chamber and core, prevented any gas leakages (tested using a helium leak test). A fine nylon mesh placed on the underside of the core prevented any soil loss into the vessel throughout the incubation. A rubber septum (Hilltop Ltd., Warrington, UK) in the lid allowed for syringe application to or sampling from the vessels.

Fig. S1. Photograph of the incubation system used in the study.

S2. Testing of different sampling methods

Different sampling vessels were tested to determine the most effective one for evaluating gas sample quality. These were as follows:

1. 'Tubing': Samples from a sampling tube (53.4 ml) were taken by disconnecting the sampling tube from the standard gas flush and then connecting a syringe to the tube and taking 20 ml of gas, removing the syringe and reconnecting the sampling tube.
2. 'Tank Open': A sampling tank (150 ml) was disconnected from the standard gas flush, a syringe was attached, and a sample was taken. The valves remained in the open positions and the tank was reconnected.
3. 'Tank Closed': A sampling tank (150 ml) was disconnected from the standard gas flush, a syringe was attached, and the valve on the opposite side of the tank was closed before a sample was taken. The valve was opened after the sample was taken and the tank was reconnected.

4. ‘Syringe’: A 60 ml syringe without a plunger was connected to the standard gas flush and the plunger was carefully inserted and the syringe disconnected. After inserting the sample, the plunger was removed from the syringe and the syringe was reconnected.

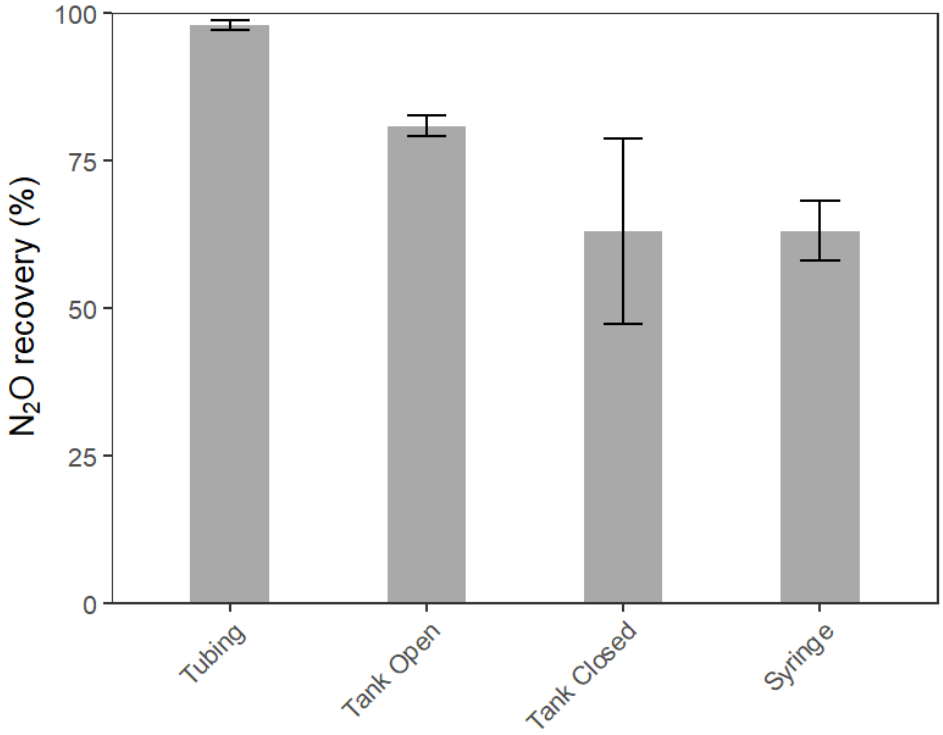

Fig. S2 Test of N_2O recovery of a standard gas (i.e. 100% represents complete recovery) of different sampling methods. Bars are means ± SEM. The sampling receptacles were flushed for > 5 mins with a flow of approximately 100 ml min^{-1} of 100 ppm N_2O standard gas before a syringe sample was taken (*n* = 6, except ‘Syringe’, where *n* = 3) and 10 ml analysed on a GC. From these results, it was decided that the ‘Tubing’ was the most effective sampling method.

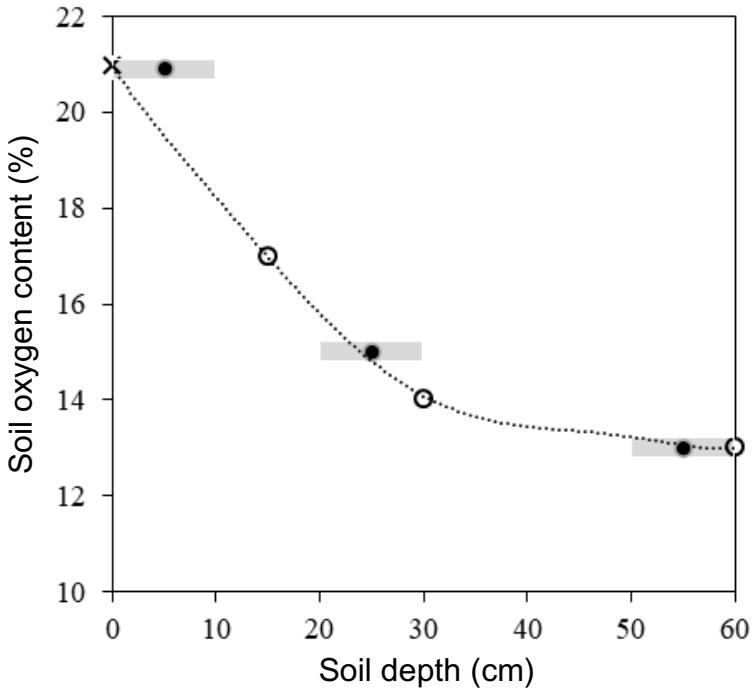

Fig. S3 Soil oxygen concentration choice for the core incubations at different depths. White points represent O_2 data from a similar soil (Smith and Dowdell, 1974), while the 'X' represents the atmospheric concentrations (21%). The fitted line (polynomial; $R^2 = 0.99$) was used to calculate the average oxygen concentration at the 3 depths the cores were extracted from (black points). These were 19.5% for the 0 - 10 cm, 15% for the 20 - 30 cm and 13% for the 50 - 60 cm cores, respectively. However, as the MFC is unreliable at low flow rate settings, it was decided that for the cores where low settings would be needed (0 – 10 cm cores) an ambient atmospheric O_2 (i.e. 20.9 %) concentration was used instead. The horizontal grey bars show the depth range that the cores represent.

Table S1. Mean ± SEM (n = 4) gene abundances (*nirK, nirS, nosZ*) in the top- and subsoil of the soil used in this study. These were analysed by quantitative PCR, processed at the same time of sampling and following the methods described in de Sosa et al. (2018).

Properties	Topsoil 0 – 10 cm	Subsoil 50 – 60 cm
nirK gene (x10^8 copies g^{-1})	4.8 ± 0.4	0.9 ± 0.5
nirS gene (x10^6 copies g^{-1})	6.9 ± 0.7	0.4 ± 0.2
nosZ gene (x10^7 copies g^{-1})	5.3 ± 0.3	0.4 ± 0.3

S3. Incubation of soil cores for drying

While it could be argued that drying the soil cores at 40°C would alter the microbial community, no systematic differences in those which were dried at 40°C and those which were not were observed. In addition, following the drying the cores were kept at room temperature overnight and a further 18 h in the acclimatisation period before the sampling began. Therefore, we conclude that the microbial community was not altered by the drying in the 40°C enough to induce differences in the N-related processes.

References

Smith, K.A. and Dowdell, R.J., 1974. Field studies of the soil atmosphere: I. Relationships between ethylene, oxygen, soil moisture content, and temperature. Journal of Soil Science, *25*, 217-230.

de Sosa, L.L., Glanville, H.C., Marshall, M.R., Williams, A.P., Abadie, M., Clark, I.M., Blaud, A., Jones, D.L., 2018. Spatial zoning of microbial functions and plant-soil nitrogen dynamics across a riparian area in an extensively grazed livestock system. Soil Biology and Biochemistry 120, 153–164.